

## RCA ENGINEER Staff

W. O. Hadlock ..... Editor  
E. R. Jennings ..... Associate Editor  
Mrs. J. S. Carter ..... Editorial Secretary  
J. L. Parvin ..... Art Director

### Consulting Editors

C. A. Meyer, Technical Publications  
Administrator,  
Electronic Components and Devices  
C. W. Sall, Technical Publications  
Administrator, RCA Laboratories  
H. H. Spencer, Technical Publications  
Administrator, Electronic Data Processing  
F. D. Whitmore, Technical Publications  
Administrator, Defense Electronic Products

### Editorial Advisory Board

A. D. Beard, Chief Engineer  
Electronic Data Processing  
E. D. Becken, Vice President and Chief Engineer,  
RCA Communications, Inc.  
J. J. Brant, Staff Vice President,  
Personnel Administration  
C. C. Foster, Mgr., RCA REVIEW  
M. G. Gander, Mgr., Consumer Product  
Administration, RCA Service Co.  
Dr. A. M. Glover, Division Vice President  
Technical Programs,  
Electronic Components and Devices  
C. A. Gunther, Division Vice President,  
Technical Programs, DEP and EDP  
E. C. Hughes, Administrator, Technical  
Committee Liaison,  
Electronic Components and Devices  
E. O. Johnson, Mgr., Engineering,  
Technical Programs,  
Electronic Components and Devices  
G. A. Kiessling, Manager, Product Engineering  
Professional Development  
L. R. Kirkwood, Chief Engineer,  
RCA Victor Home Instruments Division  
W. C. Morrison, Chief Engineer, Broadcast and  
Communications Products Division  
H. E. Roys, Chief Engineer,  
RCA Victor Record Division  
D. F. Schmit, Staff Vice President,  
Product Engineering  
Dr. H. J. Watters, Division Vice President,  
Defense Engineering  
J. L. Wilson, Director, Engineering  
National Broadcasting Co., Inc.

### OUR COVER

In the main photo, Dr. F. J. F. Osborne, Director of the Microwave and Plasma Physics Laboratory of the RCA Victor Co. Ltd. Research Laboratories, Montreal, Canada, observes an experiment with gaseous plasma. The inset photos show a few of the many other plasma experiments carried out in various RCA activities: In the top inset, Dr. Osborne is shown with Dr. M. P. Bachynski, Director, RCA Victor Co. Ltd. Research Laboratories, Montreal. In the next inset, M. Toda, a scientist from Laboratories RCA Inc., Tokyo, Japan, is shown with a solid-state-plasma experiment. The bottom two insets show laboratory setups at RCA Laboratories, Princeton, N.J. In addition to the laboratories in Montreal, Tokyo, and Princeton, important efforts in plasma research and effects are carried on in other RCA activities such as: Applied Research, Camden; Astro-Electronics Division, Princeton; and Missile and Surface Radar Division, Moorestown. The impressive scope and depth of this work in RCA is emphasized by the 19 papers published herein.

## Plasma Research

Here is a collection of papers describing RCA's participation in the present and substantial world-wide research effort on plasmas.

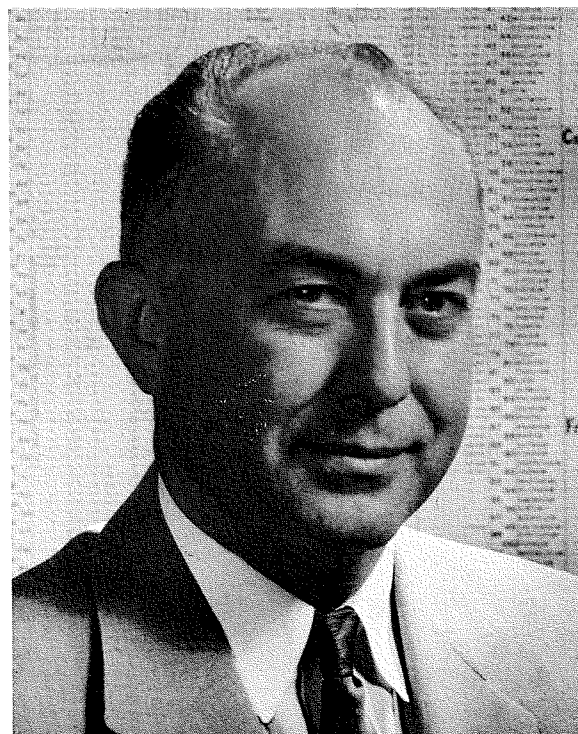
The term *plasma* was first applied by Langmuir to a region in a gas discharge where there are about equal numbers of interacting charged particles of opposite sign and the particles of at least one sign are mobile. In gas plasmas, both electrons and positive ions are mobile. Plasmas have some remarkable properties: they conduct electric current, propagate electromagnetic waves at exceptionally high frequencies, and under some circumstances even generate such waves.

The aurorae, lightning discharges, ionosphere, Van Allen belts, sun, and stars are examples of gas plasmas that occur in nature. Man-made gas plasmas are in fluorescent lamps, thyratrons, thermionic energy converters, atmospheric sheaths around missiles, and research chambers in which dense gases are superheated in attempts to produce nuclear fusion. Plasma effects are observed also in some man-made solid materials, such as semimetals and semiconductors, even at temperatures well below room temperature. In solids, electrons and positive holes are mobile, while ionized atoms remain stationary.

The number and quality of the papers published herein are indicative of the response of RCA researchers to the challenge of increasing our ability to produce, control, study, understand, and use plasmas. Looking beyond today's exploration of the great variety of plasma materials, operating conditions, and phenomena, we anticipate more beneficial uses of plasmas in RCA's future.

*Humboldt W. Severenz*

H. W. Leverenz  
Associate Director  
RCA Laboratories





VOL. 11, NO. 4  
DEC. 1965-JAN. 1966

CONTENTS

PAPERS

The Engineer and the Corporation: An Introduction to Plasma Phenomena .....Dr. M. P. Bachynski 2

Microwave Measurements of Plasmas .... Dr. M. P. Bachynski, Dr. F. J. F. Osborne, Dr. A. I. Carswell, B. W. Gibbs, and C. Richard 7

Application of the Transport Coefficients in a Plasma .....Dr. I. P. Shkarofsky 12

Comparative Studies of Plasma Diagnostics .....C. C. Peterson and J. F. Dienst 18

Laser Measurement of Electron Density in Dense, High-Temperature Plasma ..A. Boornard, L. J. Nicastro, and Dr. J. Vollmer 26

Laboratory Simulation of Reentry Plasma .....Dr. A. I. Carswell 31

Interaction of Electromagnetic Waves with Ionized Rocket Exhausts .... A. Boornard 36

Effects on Radar of Plasma Produced by High-Altitude Nuclear Detonations .....Dr. K. Sittel 41

Guided Waves in Gaseous Plasmas .....Dr. T. W. Johnston 46

Plasma-Coated Surface as a Waveguide .....Dr. L. W. Zelby 50

Resonances in the Ionosphere  
Magnetoplasma .....Dr. T. W. Johnston and Dr. I. P. Shkarofsky 52

Laboratory Simulation of Geophysical Phenomena ..Dr. F. J. F. Osborne, Dr. M. P. Bachynski, J. V. Gore, and M. A. Kasha 56

Instabilities in Solid State Plasmas .....Dr. M. C. Steele and Dr. B. Vural 60

Alfven Waves in Bismuth Plasma .....Dr. B. W. Faughnan 64

Microwave Emission from Solid State Plasmas .....Dr. R. D. Larrabee, W. A. Hicinbothem, Jr., and J. J. Thomas 67

Propagation in Solid State Plasma Waveguides—Nonreciprocal Devices .....Dr. R. Hirota and M. Toda 70

Solid State Plasma Delay Lines .....Y. Kuniya and Dr. M. Glicksman 73

Electric Propulsion for Spacecraft ..... T. J. Faith, Jr. and Dr. H. W. Hendel 76

Plasma-Anodized Lanthanum Titanate Dielectric Thin Films .....R. E. Whitmore and J. L. Vossen 81

NOTES

General Three-Resonator Filters .....R. M. Kurzrok 84

Asynchronously Multiplexed Channel Capacity .....R. C. Sommer 85

DEPARTMENTS

Pen and Podium—A Subject-Author Index to RCA Technical Papers ..... 86

Patents Granted ..... 91

Professional Activities—Dates and Deadlines ..... 92

Engineering News and Highlights ..... 93

A TECHNICAL JOURNAL PUBLISHED BY **RADIO CORPORATION OF AMERICA**, PRODUCT ENGINEERING 2-8, CAMDEN, N. J.

- To disseminate to RCA engineers technical information of professional value.
- To publish in an appropriate manner important technical developments at RCA, and the role of the engineer.
- To serve as a medium of interchange of technical information between various groups at RCA.
- To create a community of engineering interest within the company by stressing the interrelated nature of all technical contributions.
- To help publicize engineering achievements in a manner that will promote the interests and reputation of RCA in the engineering field.
- To provide a convenient means by which the RCA engineer may review his professional work before associates and engineering management.
- To announce outstanding and unusual achievements of RCA engineers in a manner most likely to enhance their prestige and professional status.

An index to RCA ENGINEER articles appears annually in the April-May issue.

Copyright 1966  
Radio Corporation of America  
All Rights Reserved

Because of the importance and scope of plasma physics, a number of research and engineering groups in RCA are actively investigating plasma properties and their applications. These efforts include theoretical studies of the geophysical and astrophysical environments by laboratory simulation experiments and by interpretation of satellite data. Of interest to systems designers are studies of the plasma generated by reentry vehicles and their effect on communications and radar detection, and the use of plasma for rocket propulsion. Much RCA effort in plasmas is oriented towards devices, including structures for guiding electromagnetic waves (both gaseous and solid-state) and techniques (primarily solid-state) for generation, amplification, and control of high-frequency waves. Finally, because of the exploratory nature of plasma physics, a considerable effort has to be devoted to methods for measuring plasma properties (diagnostic techniques) and to a theoretical understanding of the basic behavior of a plasma, particularly its transport properties. The papers published herein reflect these areas of RCA interest and activity, with this first paper standing as a basic tutorial introduction to plasma phenomena for the general engineering readership.

will not be a gas but, since this energy is sufficient to remove one or more electrons from each of the neutral particles, a mixture of free electrons and free positive ions will result. When the number of free charged particles are sufficiently large so that their properties influence in an essential way the properties of the state of matter under consideration, then we have a *plasma*. Plasma can thus be considered as a *fourth state of matter*.

#### FUNDAMENTAL PROPERTIES OF A PLASMA

From what has been said above, we can thus consider a plasma as a collection of free charged particles (there may be neutral particles as well) so that the net charge in any macroscopic volume is small compared with the charge of either sign. The net ensemble is thus electrically neutral. Thus if  $n_-$  represents the charge density/unit volume of negative charge carriers and  $n_+$  the charge density per unit volume of positive charge carriers we have in a plasma:

$$n_- \simeq n_+ = n \quad (1)$$

The charged particles comprising a plasma are constrained to move more or less together, since if they tended to separate, then large electrostatic forces due to the charge separation would build up to prevent this. We can get an estimate of the maximum allowable separation of charges (i.e. a characteristic length) in the following way: (In this discussion we will neglect numerical constants of order unity which depend on the exact shape of the volume of plasma under consideration.) Suppose that all the charges were removed from a volume of plasma whose minimum dimension is  $l$ . The space charge field built up by this removal of charge would be  $E_s \sim \rho l / \epsilon_0$  where  $\rho = nq$  is the charge density,  $q$  being the charge on a given particle and  $\epsilon_0$  the permittivity of free space. The potential energy of a charged particle of charge  $q$  in this electrostatic potential is then  $q \int E_s \cdot dl \simeq (nql^2 / \epsilon_0) q$ . The kinetic energy of this charged particle will be on the average given by  $\kappa T$  where  $\kappa$  is Boltzman's constant and  $T$  absolute temperature. At some dimension of  $l$  given by  $l_D$  the kinetic energy about equals the potential energy so that:

$$l_D = \left( \frac{\epsilon_0 \kappa T}{nq^2} \right)^{1/2} \quad (2)$$

The quantity  $l_D$  is known as the *Debye length*, and marks the maximum distance over which a plasma can produce noticeable charge separation, since the kinetic energy of the charged particles of the plasma will be insufficient. The Debye length is thus a measure of the *minimum* size of a system in which collective effects dominate over individual particle effects.

The previous discussion is valid provided the number of charged particles  $n_D$  in a volume whose radius is a Debye length is large, i.e.:

$$n_D = \left( \frac{4\pi}{3} l_D^3 \right) n \gg 1 \quad (3)$$

This condition for a plasma implies that the potential energy density in the plasma is small compared to the kinetic energy density and permits the plasma to be described in terms of fluid or continuum theory.

Since the displacement of charge in a plasma results in large electrostatic forces, then if we displace say  $n$  charges per unit volume, each of magnitude  $q$  by an amount  $\delta$  in an infinite plasma (see Fig. 1) the resulting electrostatic field  $E_s$  would try to restore these charges to their equilibrium position. If we now release the charges and permit them to move

## The Engineer and the Corporation

### AN INTRODUCTION TO PLASMA PHENOMENA

Dr. M. P. BACHYNSKI, Director  
Research Laboratories  
RCA Victor Company, Ltd., Montreal, Canada

In the earliest days of the physical sciences (400 to 500 BC) Empedocles described all elements in terms of four—earth, water, air and fire. With the discovery in recent years of over one hundred elements and the almost infinite number of combinations in which they can occur we, even today, still choose to group their physical properties into relatively few "states". Thus we have come to associate matter as in the solid, liquid, or gaseous state. Indeed, the same matter can exist in all three states—the determining factor being the *energy* of that state. Thus, by the addition of energy we can change both the kinetic energy or temperature of the particles comprising matter and the potential energy, or state. To change the state of a solid to a liquid, or a liquid to a gas, requires the addition of energy of approximately  $10^{-2}$  electron volt per particle. (The removal of an equivalent amount of energy will cause the reverse change of state.)

If, instead of adding  $10^{-2}$  electron volt per particle to a state of matter, we add 1 to 30 electron volts per particle, the result

*Final manuscript received August 18, 1965.*

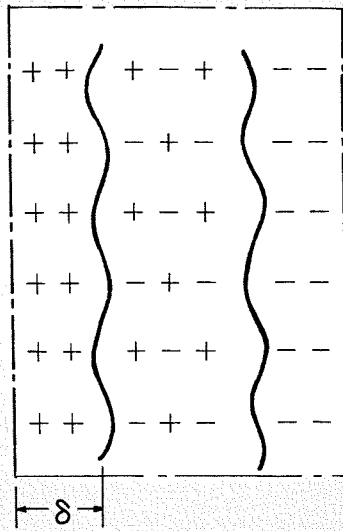


Fig. 1—Displacement of the charged particles of one sign by an amount  $\delta$  creates a space charge force which if the particles are released causes the plasma to oscillate at a characteristic frequency  $\omega_p$ .

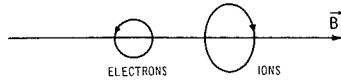


Fig. 2a—Charged particles execute circular orbits under the influence of a uniform magnetic field.

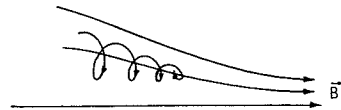


Fig. 2b—Charged particles are reflected from a magnetic barrier created by a converging magnetic field.

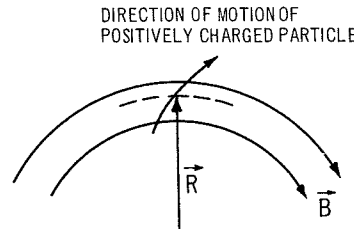


Fig. 2c—A curved magnetic field exerts an additional force on charged particles which causes them to move across the magnetic field. Charged particles of different sign move in opposite directions resulting in a net current.

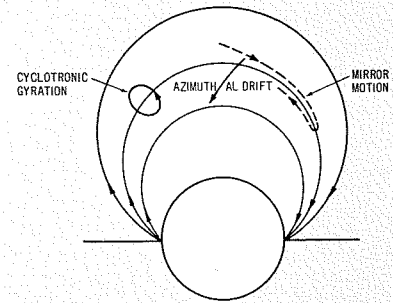


Fig. 3—In a magnetic field in the configuration of a dipole the charged particle motion is composed of: (a) a circular gyration about the magnetic line of force (b) a motion along the field lines being reflected back and forth between regions of strongly converging magnetic fields (c) an azimuthal drift across the magnetic field lines.



DR. MORREL P. BACHYNSKI graduated in 1952 from the University of Saskatchewan with the degree of B.Eng. in Engineering Physics. He was awarded the Professional Engineers of Saskatchewan prize for the highest scholastic standing amongst the graduating class. In the following year he obtained his M.Sc. degree in physics at the University of Saskatchewan in the field of radar investigations of the aurora. He then joined the Eaton Electronics Research Laboratory, McGill University where he was awarded a Ph.D. degree in 1955 with a thesis on aberrations in microwave lenses. After obtaining his Ph.D. degree, Dr. Bachynski remained at the Eaton Laboratory carrying out research on the imaging properties of non-uniformly illuminated microwave lenses. In October 1955, he joined the newly created Research Laboratories of RCA Victor Company, Ltd., became Director of the Microwave and Plasma Physics Laboratories in 1958 and Director of Research in 1965. Since this time he has conducted research on electromagnetic wave propaga-

tion, microwave and plasma physics. Dr. Bachynski is a senior member of the Institute of Electrical and Electronics Engineers, a member of the professional group on Antennas and Propagation, a member of the American Physical Society, the American Geophysical Union and the Canadian Association of Physicists, and an Associate Fellow of the Canadian Aeronautics and Space Institute. He is Chairman of Commission VI of the Canadian National Committee of the International Scientific Radio Union (URSI), a member of the AIAA Technical Committee on Plasma Dynamics and a member of the National Research Council of Canada Associate Committees on Radio Science and Plasma Physics. He is also listed in American Men of Science and has been associated with McGill University teaching classes in antennas, electromagnetic theory and plasma physics. In 1963 he was awarded the David Sarnoff Award for Outstanding Individual Achievement in Engineering.

individually under the influence of the space charge field, the charges would oscillate about their equilibrium value. The equation of motion for the charges of mass  $m$  is:

$$m\ddot{\delta} = -qE_s = -nq^2\delta/\epsilon_0$$

This is the equation of simple harmonic motion with a characteristic frequency,  $\omega_p$ :

$$\omega_p = \left(\frac{nq^2}{m\epsilon_0}\right)^{1/2} \quad (4)$$

where  $\omega_p$  is known as the *plasma frequency* and represents a resonant frequency of the system of charged particles.

A *characteristic velocity* of a charged particle in a plasma must be the mean square thermal velocity in a given direction given by:

$$v_t^2 = \frac{\kappa T}{m} = l_D^2 \omega_p^2 \quad (5)$$

We thus see that a thermal particle travels a Debye length in about a plasma period. The above expression simply relates

the characteristic velocity to the characteristic length and characteristic time or frequency.

Although plasmas and plasma effects are principally to be found in ionized gases, they also occur in solids such as metals and semiconductors. In the case of a solid, the charge carriers are generally electrons and holes which are highly mobile in a uniform ionic background. All the above ideas apply to a plasma in a solid as well as a gaseous plasma. (*Quantum or degenerate plasmas* can occur in solids. For such plasmas the Debye length can be obtained from Eq. 5 provided the average of the squared Fermi velocity is used instead of the thermal velocity.) In the solid plasma, we need only replace the mass by the effective mass of the electron or hole respectively. Also the permittivity or dielectric constant is no longer that of free space ( $\epsilon_0$ , as for an ionized gas) but that of the medium ( $\epsilon_0 \epsilon$ ) in which the plasma finds itself. The dielectric constant may exceed 100 in a solid plasma. Thus, for a plasma in a solid:

$$m \rightarrow m_{eff} \quad \epsilon_0 \rightarrow \epsilon_0 \epsilon$$

The interesting feature of plasmas in solids is that the effective mass of both the negative and positive charge carriers

(electrons and holes) are approximately equal. Hence, negative and positive charged particle effects are to be found over similar ranges of parameters (and therefore in the same experimental setup). In gaseous plasmas, because of the large discrepancy in mass between the electrons and ions, the effects due to each of the different charged particles will occur over ranges of parameters which differ by at least three orders of magnitude.

#### INTERACTION WITH ELECTRIC AND MAGNETIC FIELDS

Since a plasma contains charged particles, it will be acted upon by electric and magnetic fields. An electric field  $E$  simply creates a force  $\vec{F}_e = q\vec{E}$  which directly accelerates the charged particle. On the other hand, the force  $\vec{F}_m = (q\vec{v} \times \vec{B})$  due to a magnetic field (where  $\vec{v}$  is the velocity of the charged particle and  $B$  the magnetic field value) causes the charged particle to gyrate about the magnetic field lines (Fig. 2a). The gyration or cyclotron frequency is given by:

$$\omega_c = \frac{q}{m} B \quad (6)$$

The gyration frequency depends on the mass of the charged particle. As well, particles of opposite sign gyrate in opposite directions. A magnetic field thus introduces a second characteristic frequency for a plasma.

A combined electric and magnetic field can profoundly influence the motion of a plasma. In crossed electric and magnetic fields, for example, the charged particles (in addition to the cyclotronic gyrations) drift together in a direction perpendicular to both the electric field and the magnetic field. This so-called  $\vec{E} \times \vec{B}$  drift produces a mass motion of a plasma at a velocity of  $\vec{E} \times (\vec{B}/B^2)$ .

If the magnetic field is nonuniform in time or space, then very complicated particle behaviour can result. An important case is a converging magnetic field. In such a configuration (Fig. 2b) a charged particle will execute tighter orbits as it finds itself in stronger and stronger magnetic fields until it reverses direction (i.e. is reflected) and moves again into regions of weaker field. This is the principle of the so-called *magnetic bottle* or *magnetic mirror*, whereby plasma can be trapped in a magnetic field. Another case of interest is curved magnetic field lines (Fig. 2c). A charged particle in such a field is forced to drift in a direction normal to both the magnetic-field direction and the radius of curvature of the field line. Particles of different sign drift in opposite directions, and hence a current flows in plasmas permeated by curved magnetic field lines.

If we consider a particle in a curved converging magnetic field (as in the case of the earth's dipole), then a complicated trajectory combining all three of the above motions is present (Fig. 3). The particle gyrates around the magnetic field lines, "mirrors" back-and-forth between the strong field ends, and at the same time progresses in an azimuthal direction around the magnetic dipole configuration—resulting in a flow of current.

Again because of the charged particles, a plasma can be a medium of very high electrical conductivity. When this is the case, a moving plasma can interact strongly with a magnetic field. Many types of interaction are possible: the moving plasma can exert a force thereby compressing a magnetic field, the magnetic field can be linked to the plasma and move

along with it, or the magnetic field can diffuse through the plasma.

We thus see that intricate and complex interactions can occur in plasmas in the presence of electric and magnetic fields. The challenge of understanding these interactions has attracted the attention of numerous research workers for many years now.

#### COLLISIONS BETWEEN PLASMA CONSTITUENTS

Thus far, we have considered the free charges in a plasma as if there was only space charge force interaction between them. In reality, collisions between *all* the charged particles in the plasma are possible. For an electron-ion plasma in a neutral background, we can have *electron-neutral*, *electron-ion*, *electron-electron*, *ion-neutral*, and *neutral-neutral* encounters. Since the electrons are the most mobile of the charge carriers, they usually dominate the transport properties of a plasma—and, usually, only electron collisions with the other species need be considered. (In many cases, electron-electron collisions can also be neglected, since they serve primarily to thermalize the plasma.) The number of collisions a charged particle experiences per unit time (i.e. the collision frequency  $\nu$ ) is determined by the velocity of the particle and the mean-free-path (i.e. the average distance travelled between encounters). We can therefore write:

$$\nu = \frac{v}{l_c} = vNQ(v) \text{ seconds}^{-1} \quad (7)$$

where  $l_c$  is the mean free path,  $N$  is the total number of particles to collide with, and  $Q$  is the collision cross-section. The collision frequency is a strong function of particle temperature  $T$ , as can readily be seen. In collisions between electrons and ions, the collision cross-section varies as  $T^{-2}$ , and since particle velocity is proportional to the square-root of particle temperature:

$$\nu_{ei} \propto T^{1/2} T^{-2} = T^{-3/2}$$

For electron-neutral collisions, if the collision cross-section is independent of temperature, then:

$$\nu_{en} \propto T^{1/2}$$

The total collision frequency is the sum of the electron-ion and electron-neutral collision frequencies, and hence can be a complicated function of temperature depending on the relative values of  $\nu_{ei}$  and  $\nu_{en}$  (i.e. the degree of ionization). In practice, even for plasmas with degrees of ionization as low as 0.1% coulomb collisions begin to become important.

In the simplest case, the influence of collisions is to decrease the drift velocity of the charged particles in a plasma. Considering only elastic collisions, this decrease in particle velocity is taken into account by a viscous, or friction force which depends upon the frequency at which a complete change of the particle momentum due to collisions takes place. Although this friction force can vary in time and space and may also depend on particle velocity, the time ensemble average of this effect is considered as a damping force proportional to drift velocity. This proportionality is taken to be a constant and can physically be considered as the *collision frequency for momentum transfer*. The collision frequency is, of course, different for the different kinds of elastic particle encounters. Collisions between like particles do not count since such an encounter does not change the average momentum of that species. With this simple model, the force equa-

tion for the velocity of an average particle in electric and magnetic fields would be written:

$$m\dot{\vec{v}} = q(\vec{E} + \vec{v} \times \vec{B}) + \eta m\vec{v} \quad (8)$$

where the dot denotes the time derivative. This Eq. 8 is the starting point in describing mathematically the properties of a plasma in terms of the hydrodynamic or average particle model. From Eq. 8, the simple concepts of mobility, conductivity and resistivity of charged particles in a plasma can be obtained. More accurate descriptions of the effect of collisions on the properties of a plasma can only be obtained from a statistical description of the kinetics of the particle interaction such as afforded by the Boltzmann and Fokker-Planck equations.<sup>1</sup>

The effect of collisions between the charged particles in the plasma affects not only the transport properties of the plasma but also the interaction of the plasma with electric and magnetic fields. For instance, examples of the influence of increasing collisions are: to increase the electrical resistivity (decrease the conductivity) of a plasma; charged particle cyclotron orbits are interrupted by collisions and the magnetic field is permitted to diffuse through the plasma, etc.

#### WAVES AND SMALL AMPLITUDE PERTURBATIONS IN PLASMA

The presence of electromagnetic fields in a plasma will cause currents to flow in sufficient quantity to affect the electromagnetic fields. In the absence of a static magnetic field, the electromagnetic properties change markedly depending whether the angular frequency of the electromagnetic wave is greater or less than the plasma frequency. For radio frequencies above the plasma frequency, a plasma behaves more or less as a dielectric, the lossiness being determined by the collision frequency. At frequencies well below the plasma frequency, the plasma acts like a very good conductor, while at frequencies around the plasma frequency "cutoff", or very high attenuation and reflection occur so that the wave cannot penetrate to any great depth into the plasma.

In the presence of a static magnetic field, the plasma becomes *anisotropic* (doubly refracting), and the interaction with electromagnetic fields not only depends on the strength of the static magnetic field but also on the angle between the direction of propagation and the magnetic field. For a lossless plasma, conditions exist whereby the refractive index of the plasma is infinite (i.e., there is a "pole" in the expression for the refractive index). Under these conditions, the phase velocity of an electromagnetic wave in the plasma is zero. This "resonance" condition corresponds to a very high value (infinite in the limiting case) of the conduction current in the plasma and is associated with strong absorption of electromagnetic energy in the plasma.

Conditions for a lossless plasma also exist whereby the refractive index of the plasma can be zero (i.e., there is a "zero" in the expression for the refractive index). The phase velocity of a wave in the plasma is then infinite. At such "cutoff" conditions the conduction current is just canceled by the displacement current. This condition corresponds to a strong reflection of the electromagnetic fields from such a medium.

Thus, when the plasma parameters and the frequency are varied, the refractive index  $u$  (and hence the wave velocity given by  $c/u$  where  $c$  is the velocity of light) will vary through these values. In the case where collisions are present, the resonances and cutoffs are not as sharp as for the lossless case. The refractive index (and phase velocity) in the presence of collisions may, however, pass near the zero and infinite

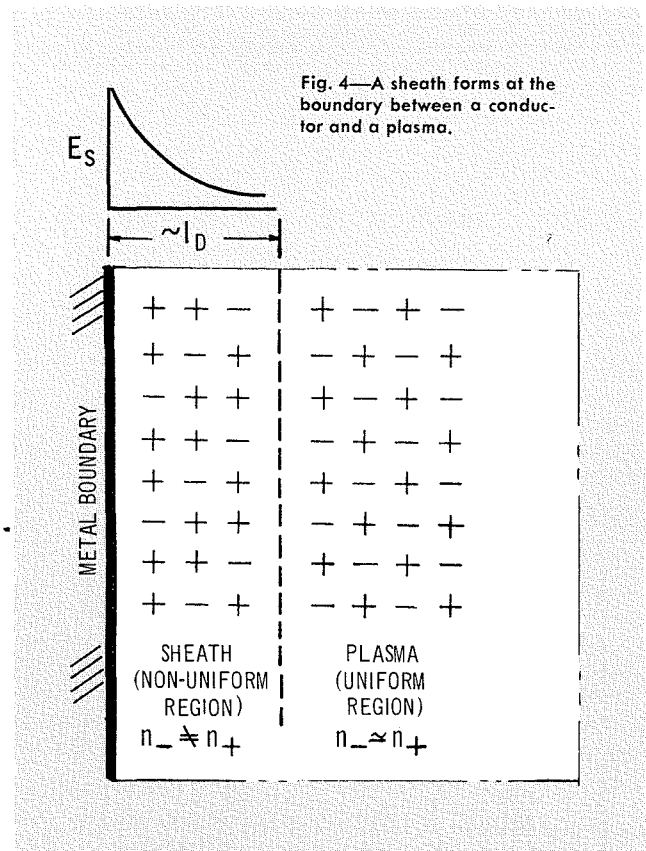


Fig. 4—A sheath forms at the boundary between a conductor and a plasma.

values as the plasma parameters and frequency are varied. When the collision frequency is high ( $\nu \sim \omega_p$ ) most of this behavior is obscured by high attenuation.

When the magnetic field is strong and collisional effects negligible, hydromagnetic type wave propagation is possible in a plasma. This can be considered as either a normal electromagnetic wave in the high dielectric constant plasma or as a vibration of a line of magnetic force with which under these conditions the plasma moves. Such waves, named *Alfven waves* (after their discoverer) travel with a phase velocity  $V_A$  given by:

$$V_A = \frac{B}{\mu_0 \rho}$$

where  $\mu_0$  is the permeability of free space and  $\rho$  the mass density of the plasma.

When the thermal energies of the charged particles in a plasma are not negligible (warm plasmas), then field disturbances moving at sound velocities in the plasma are possible. Under certain conditions it is also possible for the electromagnetic fields to interact with charged particles having directed streaming velocities and to extract energy from the streaming particles resulting in an amplification of the electromagnetic fields.

#### SHEATHS

Finally, if a plasma borders on a boundary which is a good collector of charged particles such as an electrode, then the light charge carriers (usually electrons)—which have a higher mobility than the heavier charge carriers—come into contact with and are absorbed by the electrode at a greater rate than the heavier charges. As a result, a space charge field is set up near the boundary (Fig. 4) which equalizes the migration of charged particles of both signs. In this nonuniform region, charge neutrality is not achieved and thus a *sheath* is created.

This transition region, or sheath, is of the order of a Debye length. Thus, if a plasma is bounded by an external boundary, it must be at least several Debye lengths thick in order that charge neutrality be achieved and we have a true plasma.

The above ideas apply equally if a conductor (say a probe) is immersed in a plasma—i.e. we find a sheath formed about the conductor.

#### CURRENT INTEREST IN PLASMA

Until recently, the people most interested in plasmas were the astrophysicists. This is not surprising if one looks at the amount of plasma in the geophysical and astrophysical environment.<sup>2,3</sup> These are summarized in Table I along with the pertinent plasma parameters. We thus see that the ionosphere, the interplanetary medium, the sun and its environment, and even interstellar space are principally composed of plasma. Hence it is readily seen that more than 99.9% of the matter in our Universe is comprised of plasma.

Although a plasma in the form of an ionized gas has readily been created in the laboratory for many years now, such investigations were not pursued very actively—since they appeared to bear little relation to phenomena of importance to man on earth except for the well established engineering uses of plasma such as electric switches, rectifiers, and discharge lamps. But, two recent developments have created a host of problems involving plasmas: 1) the possibility of generating energy by the fusion of nuclei of the light elements and 2) the capability of propelling vehicles at high velocities and into outer space.

In the first instance, the fusion reaction can only occur at high temperatures—attainable only in fully ionized gases consisting of ions and free electrons, i.e. a plasma. Thermonuclear fusion research is thus concerned with the confinement, heating, and diagnosis of a very high temperature plasma. The high rocket thrust now attainable has affected the investigations of plasmas in three ways: First, man now sends measuring instruments (and even man) right into the plasma surrounding the earth. Secondly, the high speed vehicles as they reentered the earth's atmosphere are surrounded by a shock-induced envelope of ionized gas. This layer of ionized gas, or *plasma sheath*, can have a profound influence on communication and telemetry to and from the vehicle. In many cases, radio blackout occurs, when the radio signal can not penetrate the plasma sheath. Also, the plasma surrounding the vehicle is swept into the wake, resulting in a long trail of ionization following the vehicle. This huge wake provides a formidable target from which to reflect radar signals, and hence ballistic missile detection has been primarily concerned with the identification of such plasma-enhanced scattering cross-sections. (In much the same way, a rocket on launch generates a large plasma in its plume or exhaust.) Third, the achievement of placing vehicles into orbit around the earth has lifted man's hopes to go even further—flights to other planets, etc. To travel from a space platform in orbit around the earth to the orbit of another planet would not require a high-thrust device, but rather one with a high specific impulse (the ratio of thrust to propellant mass flow rate). This has led to the consideration of plasmas and neutralized

TABLE I—Plasma Parameters Found in Nature

Location	$n, \text{cm}^{-3}$	$T, \text{°K}$	$B, \text{gauss}$	$l_D, \text{cm}$	$\omega_p, \text{sec}^{-1}$	$\omega_b, \text{sec}^{-1}$ electrons
Earth		$3 \times 10^2$	0.5			$0.9 \times 10^7$
Ionosphere	$10^5$	$3 \times 10^2$	$10^{-1}$	$1.3 \times 10^{-2}$	$1.8 \times 10^7$	$1.8 \times 10^6$
Interplanetary Space	$10^1$	$10^5$	$10^{-5}$	$6.9 \times 10^2$	$1.8 \times 10^5$	$1.8 \times 10^2$
Solar Corona	$10^8$	$10^6$	$10^0$	0.7	$5.6 \times 10^8$	$1.8 \times 10^7$
Solar Photosphere	$10$	$10^4$	$10^0$	$3 \times 10^{-4}$	$5.6 \times 10^{10}$	$1.8 \times 10^7$
Interstellar Space	$10^{-3}$	$10^2$	$10^{-5}$	$10^3$	$\sim 10^4$	$1.8 \times 10^2$

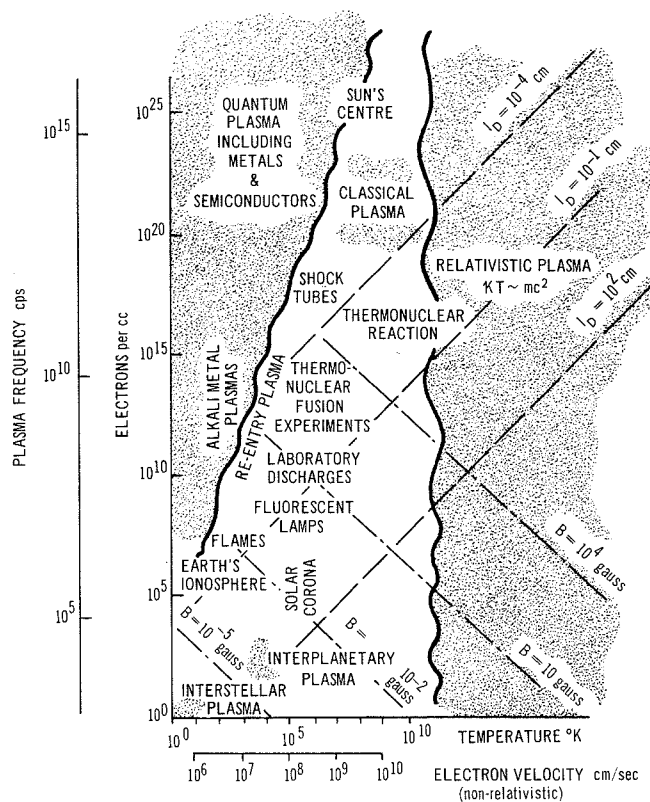


Fig. 5—Various plasmas in terms of electron density, temperature and Debye length.

beams of ions and electrons propelled by means of magnetic or electric fields as possible rocket motors.

The reawakened interest in plasmas and the closer look at some of the interactions involved has also had the result of attempting to find uses on earth for plasma-like devices. Among the potential applications using plasma, one can include microwave amplifying and circuit devices, solid-state devices, thermionic energy converters, magnetohydrodynamic electric generators, and many others.

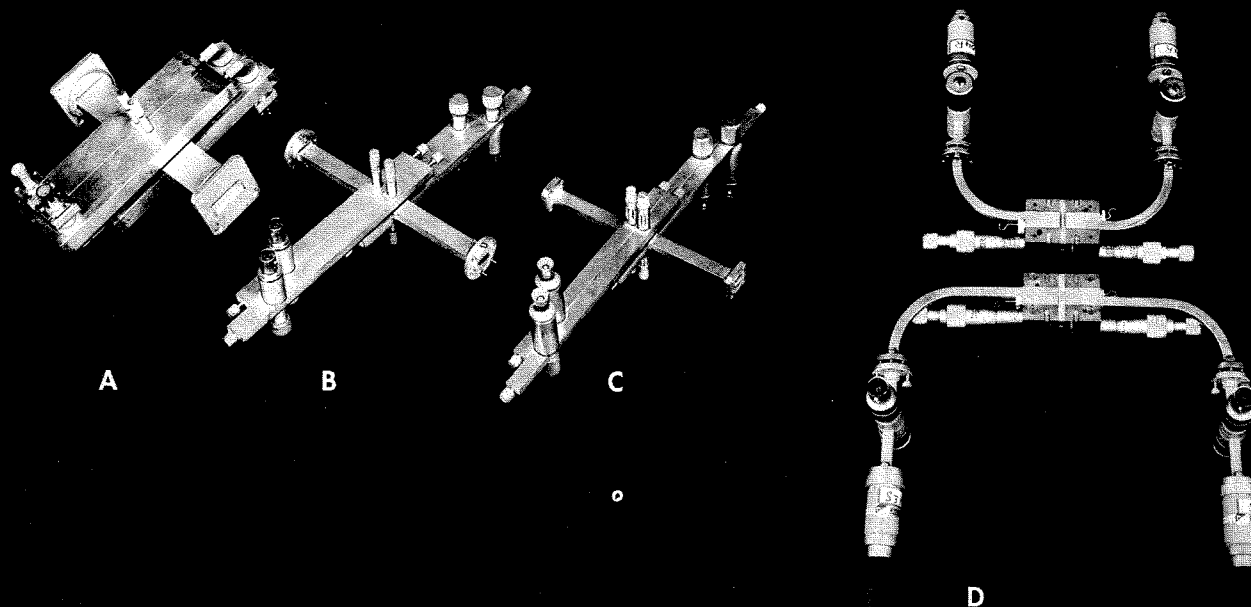
Finally, man's desire for a knowledge of the fundamental aspects of matter has stimulated him to study plasmas, and considerable work in the laboratory and in theoretical deduction are being devoted towards this end. If we take, for example, the case of solid-state plasmas, their study has two complementary purposes: to learn more about the structure of solids, and to learn more about the plasma state.

The various plasmas of importance and their basic plasma parameters (electron density, Debye length, and electron temperature) are summarized in Fig. 5 on a log-log plot of electron density vs temperature. Included as well are loci of magnetic field, such that the magnetic field energy density ( $B^2/2\mu_0$ ) is equal to the plasma energy ( $2n\kappa T$ ). Magnetic fields smaller than those given by this value will not move the plasma much, while larger fields will not be greatly affected by the plasma. The diagram is loosely subdivided into quantum plasmas, classical plasmas and relativistic plasma.

#### BIBLIOGRAPHY

- I. P. Shkarofsky, T. W. Johnston, and M. P. Bachynski (RCA Victor Res. Labs, Montreal): *The Particle Kinetics of Plasmas*, Addison-Wesley Publishing Co., Reading, Mass. (1966).
- M. P. Bachynski (RCA Victor Res. Labs, Montreal): "Plasma Physics—An Elementary Review," *Proc. IRE* 49, pp. 1751-1766; 1961. (Essentially identical to Ref. 3, with addition of a reference Bibliography.)
- M. P. Bachynski (RCA Victor Res. Labs, Montreal): "Plasma Physics: Part I—Natural Phenomena and Thermonuclear Fusion; Part II—Communications, Propulsion, and Devices" *RCA ENGINEER* 6-5, Feb.-Mar. 1961 and 6-6, April-May 1961.

Fig. 1—Multiple-probe sections operating at center frequencies a) 9.2 Gc/s, b) 23.5 Gc/s, c) 34.5 Gc/s, d) 75 Gc/s (divided block).



## MICROWAVE MEASUREMENTS OF PLASMAS

This paper deals with microwave techniques for high-speed plasma measurements, the inherent difficulties introduced by the measurement system, and the finite dimensions of the plasma and the limitations of microwave focussing devices. Detailed quantitative measurements of plane wave interaction with isotropic and anisotropic plasmas are illustrated.

**Dr. M. P. BACHYNSKI, Dr. F. J. F. OSBORNE, Dr. A. I. CARSWELL, B. W. GIBBS, and C. RICHARD**

*Research Laboratories  
RCA Victor Co., Ltd., Montreal, Canada*

**T**HE electron densities found in many plasmas of interest correspond to plasma frequencies in the meter and centimeter wavelength range. Since the electrical properties of a plasma vary measurably in this range of frequencies, probing by low-strength radio signals is a useful technique for determining the characteristics of a plasma. The accurate determination of plasma properties by this method depends upon the availability of microwave techniques with appropriate time and space resolution, a detailed knowledge of the influence of the experimental configuration and microwave system on the measurements and upon the development of theory that adequately describes the physical situation.

*Final manuscript received August 2, 1965.*

A considerable program in making quantitative measurements of plasma using free-space microwave techniques has been carried out by the RCA Victor Research Laboratories in Montreal, Canada. This paper describes microwave measuring systems which have been developed, measurement considerations and techniques required for meaningful experimental results, and measurements of a helium afterglow plasma employing the aforementioned systems and techniques.

### MULTIPLE PROBE SYSTEM

In plasma diagnostics using microwaves, the information on the plasma is carried as phase and amplitude changes of a wave sensing the plasma by either reflection or transmission. In the measur-

ing system developed at the RCA Victor Research Laboratories,<sup>1,2</sup> the wave information is modified to the form of changes in amplitude and position of a standing wave. The standing wave is then measured electronically and the original wave data extracted and presented.

The sampling wave carrying the plasma information generates a standing wave by travelling through a microwave section in the opposite direction to a reference wave. This "standing wave" is, of course, changing rapidly in amplitude and position and therefore high speed measurements are required.

It is particularly convenient to make use of four probes spaced at one-eighth guide wavelength intervals to sample the standing wave. With the consecutive

probe outputs being  $V_1, V_2, V_3,$  and  $V_4,$  it is easy to show that:

$$\begin{aligned} V_1 - V_3 &= kV_r V_p \cos \phi \\ V_2 - V_4 &= kV_r V_p \sin \phi \end{aligned}$$

where  $V_r$  and  $V_p$  are the amplitude of reference and sampling waves respectively,  $\phi$  is a plasma induced phase shift, and  $k$  is a proportionality factor allowing for the sampled signal level and amplification.

These voltage differences represent the cartesian components of a vector with polar coordinates  $\rho$ , the reflection coefficient of the plasma (or  $T$ , the transmission coefficient of the plasma) and  $\phi$ , i.e. the Smith chart parameters in the reflection case. The transmission display is similarly direct and of the same form.

The fabrication of special probe sections is a disadvantage of this technique, but is not overly difficult. Such sections have relatively narrow bandwidth ( $\approx 5\%$ ) and are designed for specific frequencies. Typical microwave sections for systems operating at frequencies of 9.2, 23.5, 34.5, and 75 Gc/s are shown in Fig. 1.

**DR. FRELEIGH J. F. OSBORNE** was educated at the Royal Canadian Naval College (1946-48); obtained his B.Sc. at McGill University in 1950 and was awarded his M.Sc. at Laval University in 1951 for a thesis on Application of the Secondary Electron Emission Multiplier to a Mass Spectrometer. In 1954 he received a D.Sc. from Laval University for a thesis on Secondary Electron Emission of Beryllium Copper. He joined the Research Department of Canadian Marconi Company in 1954 as a Senior Physicist, working primarily in the fields of component reliability, systems and instrumentation. In 1956 he was made a supervisor and as such directed a variety of projects. He transferred to the Electronic Tube Plant where he developed an S-Band Electron Beam Parametric Amplifier. In January 1961 he joined the Research Laboratories of RCA Victor as a Senior Member of Scientific Staff. He has since been particularly active in the area of plasma measurements and techniques, leading and contributing to programmes on plasma diagnostics, plasma microwave structures, laboratory simulation of geophysical phenomena, and laboratory studies of the interactions between a satellite and its plasma environment. In 1965 he became Director of the Microwave and Plasma Physics Laboratory. He was active in the Royal Canadian Navy (Reserve) from 1946-1956, is a member of the Canadian Association of Physicists, the American Physical Society, the American Geophysical Union, Commission IV of the Canadian National Committee of the International Scientific Radio Union (URSI), and is listed in American Men of Science.

**DR. MORREL P. BACHYNSKI** graduated in 1952 from the University of Saskatchewan with the degree of B.Eng. in Engineering Physics. He was awarded the Professional Engineers of Saskatchewan prize for the highest scholastic standing amongst the graduating class. In the following year he obtained his M.Sc. degree in physics at the University

The technique for data display is to amplitude-modulate the microwave source at a convenient frequency which determines the duration of the measurement sampling signal and the sampling repetition rate although not the displayed sampling period. Systems in this laboratory have operated at modulation frequencies from 5 kc/s to 5 Mc/s, or a sample duration from 0.1 ms to 0.1  $\mu$ s, the latter approaching the limit of components readily available. The detected signals  $V_1, V_3$  are treated as a pair, one detector of the pair being of reversed polarity. The outputs are combined directly at the input of a high-gain AC amplifier, resulting in the required subtraction, and fed to one axis of an X-Y oscilloscope. Signals  $V_2, V_4$  are handled in exactly the same manner and fed to the other axis of the oscilloscope.

The resulting display is a line centered on the origin of a polar diagram and with correct adjustment, of length proportional to the amplitude of the wave traversing the plasma (or reflected from it), and at an angle  $\phi$ , the phase between the reference and the "plasma wave." To

clarify the display and also provide time markers, a pulse of duration about 1/10 of the measurement period is introduced at a time such as to brighten only the tip of the displayed vector, the remainder of the display being biased to visual extinction. A typical display of a decaying plasma is shown in Fig. 2.

#### MULTIPLE PROBE MICROWAVE POLARIMETER

In the presence of magnetic field, a plasma becomes doubly refracting and can simultaneously support two electromagnetic wave modes. The polarization or locus of the electric vector then becomes an important parameter in determining the interaction of an electromagnetic wave with a plasma. The polarization of an electromagnetic wave can be specified by the amplitude of two orthogonal components of the electric vector together with the phase difference between them. The measurement of these parameters of an electro-magnetic wave can be performed by the use of a turnstile transition.<sup>3</sup> The turnstile consists of two cross arms of rectangular wave-

of Saskatchewan in the field of radar investigations of the aurora. He then joined the Eaton Electronics Research Laboratory, McGill University, where he was awarded a Ph.D. degree in 1955 with a thesis on aberrations in microwave lenses. After obtaining his Ph.D. degree, Dr. Bachynski remained at the Eaton Laboratory carrying out research on the imaging properties of non-uniformly illuminated microwave lenses. In October 1955, he joined the newly created Research Laboratories of RCA Victor Company, Ltd., became Director of the Microwave and Plasma Physics Laboratories in 1958 and Director of Research in 1965. Since this time he has conducted research on electromagnetic wave propagation, microwave and plasma physics. Dr. Bachynski is a senior member of the Institute of Electrical and Electronics Engineers, a member of the professional group on Antennas and Propagation, a member of the American Physical Society, the American Geophysical Union and the Canadian Association of Physicists, and an Associate Fellow of the Canadian Aeronautics and Space Institute. He is Chairman of Commission VI of the Canadian National Committee of the International Scientific Radio Union (URSI), a member of the AIAA Technical Committee on Plasma Dynamics and a member of the National Research Council of Canada Associate Committees on Radio Science and Plasma and Gas Dynamics, is listed in American Men of Science and has been associated with McGill University teaching classes in antennas, electromagnetic theory and plasma physics. In 1963 he was awarded the David Sarnoff Award for Outstanding Individual Achievement in Engineering.

**DR. ALLAN I. CARSWELL** graduated with honors in 1956 from the University of Toronto with a B.A.Sc. in Engineering Physics. In the same year he entered the graduate school of the University of Toronto to study molecular physics. In 1960 he received his Ph.D. In 1960-61, Dr. Carswell studied

at the Institute of Theoretical Physics of the University of Amsterdam on a Canadian National Research Council Fellowship. Dr. Carswell joined RCA Victor Co. Ltd. Research Laboratories on his return to Canada in 1961, and since that time has studied the interaction of electromagnetic waves with plasma systems—including microwave scattering from supersonic plasma flow fluids, and studies of the properties of ionized gas flow systems. Recently, Dr. Carswell has also worked on gaseous lasers. He is a member of the Canadian Association of Physicists, the American Institute of Physics, and the Canadian Aeronautics and Space Institute.

**BRIAN W. GIBBS** graduated from Glebe Collegiate Institute, Ottawa in 1950. He joined the technical staff of the Pure Physics Division of the National Research Council in 1953 after studying for two years at Queen's University, Kingston. During the next seven years Mr. Gibbs was involved in the design and construction of microwave spectrometers extending into the millimeter region. In 1960 he joined the RCA Victor Research Laboratories where he has been primarily engaged in experimental studies of microwave antennas in ionized media.

**CLAUDE RICHARD** received a B.A.Sc. degree (Eng. Physics) from Laval University in 1959. In the fall of the same year he joined the Imperial College of University of London as an Athlone Fellow, where he received in 1961 a Diploma of Imperial College (D.I.C.) and a M.Sc. (Eng.) degree for his research in the field of electron applied physics. On his return from England he joined the RCA Victor Research Laboratories in Montreal where he is attached to the Microwave Research Group. He has participated on a project on the generation of negative ions in a gas discharge and is now engaged in spacial resolution studies for supersonic plasma diagnostics.

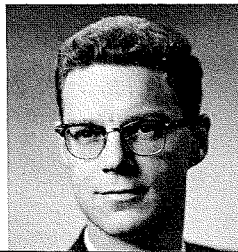
Dr. Freleigh J. F. Osborne



Dr. Morrel P. Bachynski



Dr. Allan I. Carswell



Brian W. Gibbs



Claude Richard



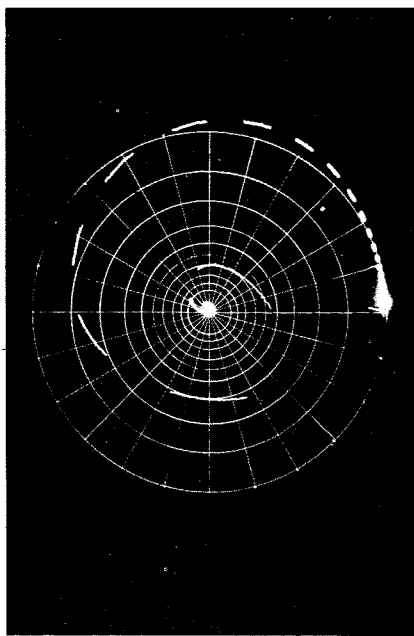


Fig. 2—Typical multiple-probe display of phase and amplitude data for a decaying plasma using oscilloscope blanking timing marks.

guide coupled together through a round guide section. By use of the turnstile, a wave of unknown polarization may be separated into two space quadrature components of the form:

$$\begin{aligned} A \cos(\omega t + \phi_1) \\ B \cos(\omega t + \phi_2) \end{aligned}$$

Hence, using the turnstile as a receiving section, the polarization of any incoming wave can be resolved. Similarly, by controlling the phases of the signals fed into adjacent rectangular sections of the turnstile, a wave of any desired polarization can be generated in the circular section and subsequently radiated.

By using the turnstile transition in a microwave receiving section, it is possible to combine each of the space quadrature components with a reference signal so as to produce standing waves which are introduced into separate multiple probe units. The multiple probe system then produces separate polar displays of each quadrature component ( $A, \phi_1$  and  $B, \phi_2$ ) together with timing markers. In this manner a simultaneous time history of both of the components can be measured and recorded.

It is possible to combine the displays from the two multiple-probe units in such a way that each probe unit shows a single point denoting the amplitude and phase angle of the field component for a given sampling period. The phase angle between the two points shows the phase difference between the quadrature components, and the radius vector shows the amplitude of the components. In some instances, an ambiguity arises as to the direction of rotation of circularly or elliptically polarized components. These can be resolved through the deliberate introduction of an additional phase shift (usually of  $90^\circ$  or  $180^\circ$ ) into one of the reference lines. The multiple probe polarimeter is capable of the same time

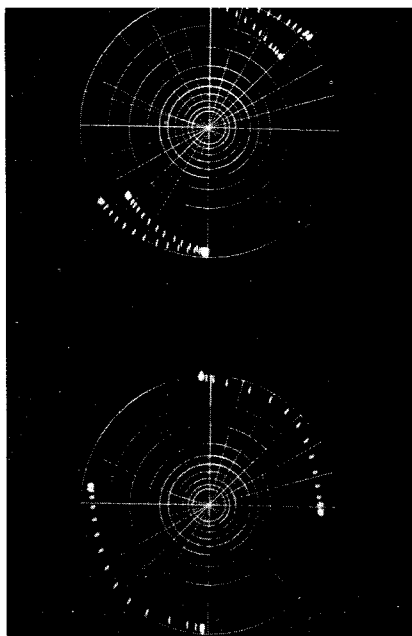


Fig. 3—Typical multiple probe polarimeter display. (Phase change of a linearly polarized wave.)

response as the normal multiple probe unit, retains the other advantages of dynamic range and scale expansion, and hence is particularly suitable for the probing of transient plasmas with microwaves.

A typical measurement using the multiple probe polarimeter is shown in Fig. 3.

#### MEASUREMENT CONSIDERATIONS AND TECHNIQUES

The determination of the properties of a plasma from measurements of the phase change and attenuation introduced by the plasma to an incident electromagnetic wave that has either been transmitted through or reflected from the plasma is well known. The accuracy of such measurements is however limited by: 1) the inability to precisely prescribe the properties of a finite plasma, and 2) the inherent characteristics of the measurement system.

Fig. 5—Field intensity distribution in the focal region of a microwave lens illuminated with an open waveguide antenna. Frequency: 34.5 Gc/s; lens diam.: 27 cm; image distance 27 cm.

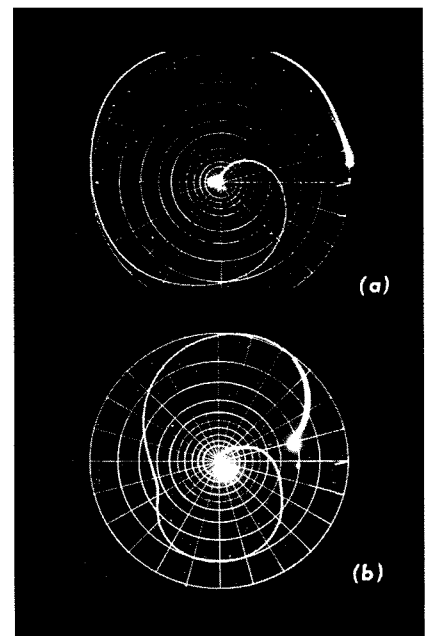
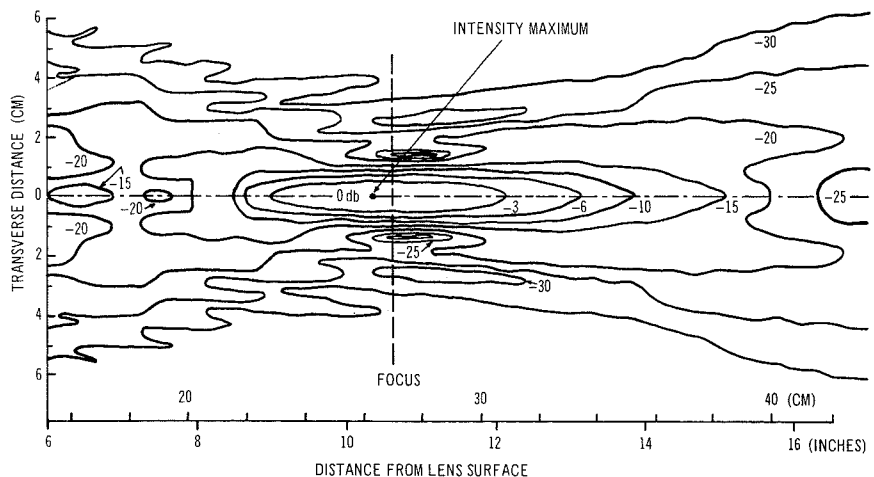
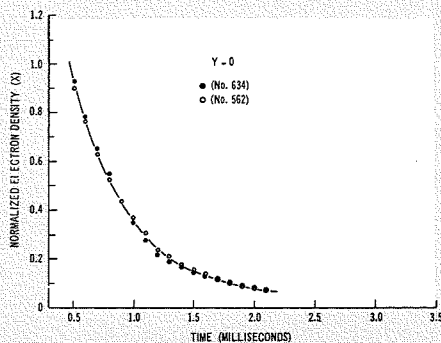


Fig. 4—Experimental measurement of the propagation of a plane electromagnetic wave through a slab of isotropic plasma for: a) plasma generated in a container which is "matched" to the incident wave; and b) plasma generated in a container which is "mismatched" to the incident wave. (Amplitude is proportional to radius vector, phase change to polar angle.)

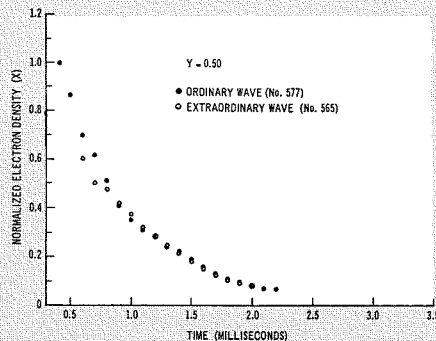
In practice the plasma is finite in extent; it may be contained by material walls, the boundaries of the plasma may not be well-defined, and the plasma may be nonuniform in both space and time. The result is refraction, reflection, absorption, and diffraction phenomena that are not easy to define and interpret, but the understanding of which is essential before accurate quantitative determination of plasma properties is possible.

The factors that need to be taken into account include:

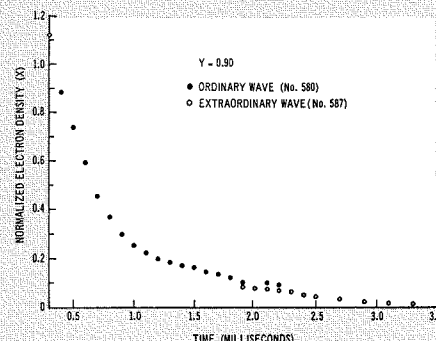
- 1) *Boundaries*—The boundaries of the plasma and the boundaries of the plasma container give rise to reflections at each interface. Hence multiple interference of various signals can occur resulting in a complex depen-



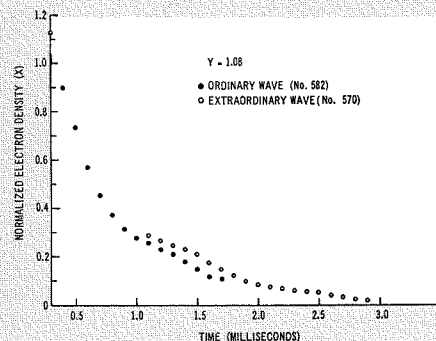
6a)  $\gamma = \omega_b/\omega = 0$



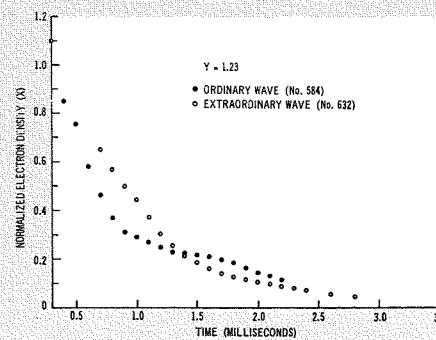
6b)  $\gamma = 0.50$



6c)  $\gamma = 0.90$



6d)  $\gamma = 1.08$



6e)  $\gamma = 1.23$

Fig. 6—Variation of electron density with time. Fig. 6a, no magnetic field; in Figs. 6b-6e, values of  $\gamma$  are as determined by the right-hand and left-hand circularly polarized wave modes.

dence of the transmission and reflection coefficient of the plasma.

- 2) *Refractive defocussing*—due to refraction at each boundary between plasma and a second medium. This generally results in the beam of energy incident on the plasma being spread out or being defocussed by the plasma. The net result is that the energy density measured by the microwave receiving system has been decreased not only by the energy absorbed by the plasma, but also by the amount it has been spread out. Hence in order to obtain a measure of the energy density absorbed by the plasma (and hence an indication of collision frequency) the refractive defocussing must be known.
- 3) *Plasma uniformity*—The interaction of a nonuniform plasma with a radio signal is in general very complex. The interaction can differ by orders of magnitude compared to that of a uniform plasma.
- 4) *Plasma kinetics*—in order to be able to make detailed quantitative comparison between theory and experiment, the thermal properties (electron and ion temperatures, thermalization, etc.) must be known.
- 5) *Plane waves*—nearly all theoretical treatments of electromagnetic wave interaction assumes plane waves. If this is not the case in a given experiment then allowance must be made for this factor.

In order to be able to make a detailed quantitative interpretation of the microwave measurements of the properties of plasmas it is also essential to have a detailed knowledge of the possible influence of the measurement system. These are determined by the experimental arrangement and include the curvature of the phase front of the incident field, the finite size and directivity of the source and receiver, the possible location of the plasma in the near field of the source, the plasma container, and the receiver. These include:

- 1) *Stray scattering*—All energy emerging from the transmitting antenna and reaching the receiver after reflection from objects surrounding the plasma container must be reduced or eliminated by placing a metal screen around the plasma container and by surrounding the antennas and the plasma container with microwave absorbing material. In this way, any energy not directed toward the plasma container is prevented from reaching the receiving antenna. Otherwise large irregular fluctuations occur in the received signal. The use of a metal screen around the plasma container gives rise to a stronger diffraction effect because of the sharp discontinuity in the refractive index at the periphery of the container. This is not really a disadvantage since even without the metal screen a certain amount of diffraction takes place which, when mixed with the stray scattering, cannot in general be treated theoretically. The theory of diffraction by an aperture in a metal screen is well known for the case of a circular aperture.
- 2) *Diffraction effects*—In most laboratory arrangements, the plasma is located in the "near field" of a diffracting aperture. The major diffraction effect is

due to the plasma container, and gives rise to the oscillatory structure of the field along the axis of the experimental system, with the result that at distances near the plasma container rapid variations in signal intensity can occur for small displacement in position (or small changes in plasma properties). It is thus essential that the receiver in any experiment designed to measure the properties of plasmas be located sufficiently far from the plasma to be in the "far" diffraction field.

- 3) *Source directivity*—The directivity of the source illuminating the plasma has a profound influence on the field in the transmitted region. An arrangement with the transmitter and/or receiver near the plasma container is very sensitive to large variations in signal intensity (due to multiple reflections). Plane wave systems are preferable wherever possible. One should note that the degree of stray scattering also depends on the directivity of the transmitting and receiving antennas. If no diffraction screen is possible because of the experimental arrangement, then directive sources can be used to reduce the stray scattering.
- 4) *Plasma container*—The plasma container itself, if large enough, (i.e. diffraction effects negligible) does not influence appreciably the microwave measurements other than by the mismatch it can introduce to the incident signal. An example of this is shown in Fig. 4. Care must be exercised in order to "match" the plasma container to the incident radiation.
- 5) *Multiple reflections*—Multiple reflections can occur between any of the source, receiver and plasma container walls. These can give rise to a multiplicity of interfering signals and have lead to false interpretation of the plasma measurements. Thus the multiple reflections must be either reduced or minimized before meaningful measurements can be made.

The difficulties discussed under the first three points cited above can be alleviated to some extent by the use of focussed microwave beams to reduce the cross-section of the RF beam in the region of the plasma and the container. This reduction in cross-section may be desirable either: 1) to "tailor" the microwave beam so that stray wall effects are minimized, or 2) to measure the properties of spatially varying plasmas with improved "resolution".

The usefulness of focussed microwave systems for these purposes has been examined in detail in the laboratory<sup>4</sup> and it has been found that in general, the improvement in spatial resolution is accompanied by additional complicating factors which do not allow accurate, quantitative measurements to be made in most cases. The central reason for this is that in any application of focussed beams for plasma diagnostics, the resultant change in the microwave signal caused by the plasma represents some average of the interaction of the beam with the plasma over the entire volume of the plasma irradiated by the signal.

The boundaries of the electromagnetic wave field in the focal region are not "sharp" and the variations of amplitude and phase exhibit a rather complex behaviour. (See Fig. 5 for a sample display of the field intensity distribution in the focal region of a lens system). As a result, the averaging process carried out by the microwave signal in the plasma is very difficult to assess accurately—especially if the plasma exhibits its own spatial variations. Hence it has been found that great care must be exercised in the use of focussed beams if meaningful results are to be obtained.

### MICROWAVE MEASUREMENTS OF PLASMAS

A detailed quantitative experimental and theoretical investigation of the propagation of the applied static magnetic field isotropic helium plasma along the direction of electromagnetic waves in an anisotropic medium has been conducted.<sup>5</sup> The experimental arrangement was designed to conform as closely as possible with the requirements of theory—appropriate range of parameters, uniform, well defined, thermalized plasma, plane waves, matched plasma container, minimum diffraction effects, various wave modes.

The variation of electron density with time in the absence of a magnetic field is shown in Fig. 6a. Two sets of results corresponding to measurements made several months apart on different plasma containers of similar design are shown. The spread of the points gives an indication of the reproducibility of the phase measurements.

Fig. 6b shows the variation of electron density with time for  $Y = \omega_p/\omega = 0.50$  as determined by both the left-hand and right-hand circularly polarized waves. Since the two wave modes behave quite differently in the plasma, this result can be interpreted as a comparison of two independent measurements of the same

plasma. The agreement between the electron densities obtained by each of the waves is excellent except at the higher electron densities where boundary effects (which have not been included in the analysis of the experimental data) become important.

At  $Y = 0.90$  and  $1.08$  (Figs. 6c and 6d) the right-hand circularly polarized (extraordinary wave) is severely attenuated at high electron densities and hence cannot be used to determine electron densities. At low electron densities however, this wave can give measurements of electron density particularly in regions where the effect on the left-hand circularly polarized (ordinary) waves are so small that quantitative determinations are subject to large errors. The two wave modes thus can be used to complement each other in measurements of electron density.

At high values of magnetic field ( $Y = 1.23$ ) shown in Fig. 6e both waves can be used to determine electron densities over extended ranges. Boundary effects become of importance and the determined values oscillate about a smooth mean value. Taking these effects into consideration the agreement between the values obtained by each wave mode are in good accord.

Attenuation measurements of the left-hand circularly polarized (ordinary) wave mode are shown in Fig. 7a. The vertical lines representing the experimental measurements indicate the range over which all experimentally determined values fell. This thus indicates the worst possible spread of the experimental determinations. The attenuation of the left-hand mode is relatively small and shows good agreement with theory over all ranges of magnetic field.

The attenuation of the right-hand circularly polarized wave is much more severe as shown in Fig. 7b. Again the results are plotted in a way to indicate the worst possible spread of the experimental measurements.

In summary, a carefully designed experiment has been conducted in which the propagation of circularly polarized plane waves through a plasma along the direction of a static magnetic field has been quantitatively investigated. Determinations of electron densities from independent measurements using the left-hand and right-hand circularly polarized wave modes show excellent agreement with each other and with theory over all ranges of magnetic fields. Attenuation measurements also agree well with theory.

### CONCLUSIONS

Microwave measuring systems, measurement techniques and microwave measurements of anisotropic plasmas as developed and performed in the RCA Victor Research Laboratories have been described. Using the above techniques and systems determination of electron densities and collision frequencies from the microwave data show excellent agreement between various modes in a plasma and with theory over all ranges of parameters in the experiment.

### BIBLIOGRAPHY

All the following authors are with RCA Victor Research Laboratories, Montreal, Canada.

1. F. J. F. Osborne, *Can. J. Phys.* 40 1620-1625 (1962)
2. F. J. F. Osborne, *Proc. 3rd Symposium in Engineering Aspects of M.H.D.*, N. W. Mather, G. W. Sutton, editors, Gordon and Breach Science Publishers N.Y.p (1963)
3. M. P. Bachynski, F. J. F. Osborne, *Gas Discharges and the Electrical Supply Industry*, J. S. Forrest, P. R. Howard, D. J. Littler, editors p553-564, Butterworths London (1962)
- 4a. A. I. Carswell, C. Richard *Focussed Microwave Systems for Plasma Diagnostics*, RCA Victor Report 7-801-32 (Dec. 1964), and *Bull. Amer. Phys. Soc.* 10 218 (1965)
- 4b. A. I. Carswell, C. Richard *Resolving Power of Focussing Systems With Coherent Illumination*, RCA Victor Report 7-801-36 (April 1965)
5. M. P. Bachynski, B. W. Gibbs—*Electromagnetic Wave Propagation in Anisotropic Plasmas Along the Direction of a Static Magnetic Field* AFRL Report No. 65-84, Dec. (1964)

Fig. 7a—Variation of attenuation of the left-hand circularly polarized wave with time for different values of magnetic field.

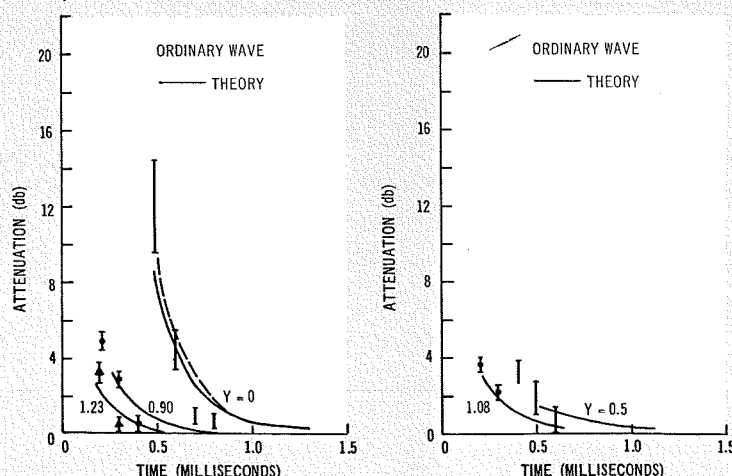
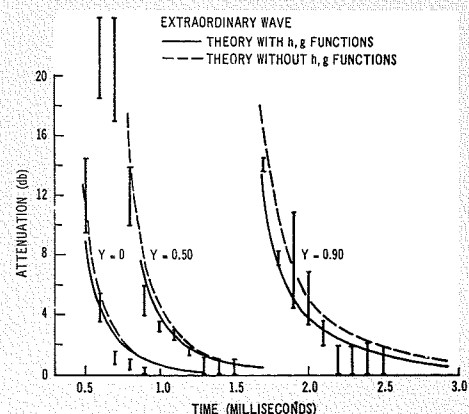


Fig. 7b—Variation of attenuation of the right-hand circularly polarized wave with time for different values of magnetic field.



# APPLICATIONS OF THE TRANSPORT COEFFICIENTS IN A PLASMA

Since the original calculations by Shkarofsky (1961) of the transport coefficients in a plasma for any degree of ionization, many predictions have been verified and new applications found. Many diverse subjects are discussed briefly in this review paper, with an extensive Bibliography to more detailed literature included. The subjects covered include: 1) electrical conductivity in shock heated argon; 2) the accepted use of the generalized Appleton-Hartree equation for the refractive index in ionospheric work; 3) verification of the prediction that the electron temperature is higher than the ion temperature above the D-layer ionosphere; 4) damping of waves near the electron cyclotron frequency; 5) the diffusion of plasma across a sufficiently low magnetic field; 6) the electrical and heat conductivity coefficients in the limit of zero current; and 7) temperature determination from electrical conductivity measurements. Other applications given in this paper are: 1) method of calculation of transport coefficients for an arbitrary variation of the electron-neutral collision frequency, not necessarily a power law; 2) relaxation times for an anisotropic temperature; 3) damping of plasma oscillations; and 4) equilibrium electron temperature in ohmic heating. Also mentioned are recent work in the fields of: 1) application to resistive, sheer, etc. instabilities; 2) plasma wave corrections to the transport coefficients; and 3) hydrothermodynamic waves.

**Dr. I. P. SHKAROFSKY**

*Research Laboratories*

*RCA Victor Co., Ltd., Montreal, Canada*

**P**LASMA transport analysis is a subject matter which is being stimulated by verification of original ideas and by new applications of the analysis.

*What are transport coefficients?* As an example, the resistance  $R$  or resistivity  $\rho$  in Ohm's law ( $V = IR$  or  $E = J\rho$ ) is a transport coefficient. Experimentally, it can be measured if sheath effects are unimportant. Theoretically, one wants a method to derive an expression for  $\rho$  in a uniform plasma. The relation is of the form:

$$\rho = m\nu/ne^2$$

where  $\nu$  is a phenomenological collision frequency between the mobile electron species (mass  $m$ , density  $n$ , charge  $e$ ) and the other particles. Several other familiar coefficients and their relations to collision frequency are:

$$1) \text{ Diffusion coefficient: } J = -eD\nabla n, \quad D = \kappa T/m\nu$$

*Final manuscript received August 18, 1965.*

$$2) \text{ Thermoelectric coefficient: } J = -\tau\nabla T, \quad \tau = nek/m\nu$$

$$3) \text{ Heat conductivity: } q = \kappa\nabla T, \quad \kappa = 5n\kappa^2 T/m\nu$$

In general, one can write for the current density flow  $J$  and heat flow  $q$  due to electric field  $E$ , density gradients  $\nabla n$  and temperature gradients  $\nabla T$ , omitting ion motion for simplicity, as follows:

$$J = \sigma E - eD\nabla n - \tau\nabla T, \\ q = \mu E - eQ\nabla n - \kappa\nabla T.$$

where  $\sigma = \rho^{-1}$ ,  $D$ ,  $\tau$ ,  $\mu$ ,  $Q$  and  $\kappa$  are transport coefficients.

In the presence of a magnetic field, all the above coefficients become tensors. Usually they can be written as a  $3 \times 3$  matrix in which the 11 and 22 elements are equal, the 12 and 21 elements have opposite sign and the only other non-zero element is the 33 one. Phenomenologically, the above relations can be generalized to include  $\omega_b = eB/m$ , the

cyclotron angular frequency. For example:

$$\rho_{11} \mp j\rho_{12} = \frac{m(\nu \pm j\omega_b)}{ne^2}$$

$$\rho_{33} = \frac{m\nu}{ne^2}$$

In the presence of a radio wave of frequency  $\omega$  propagating in the plasma, one writes:

$$\rho_{11} \mp j\rho_{12} = \frac{m[\nu + j(\omega \pm \omega_b)]}{ne^2}$$

$$\rho_{33} = \frac{m(\nu + j\omega)}{ne^2}$$

*However, the above equations are incorrect.* Whenever collisions are of importance, because of the wide range of electron velocities, a given electron with a particular velocity will collide at a different rate than other electrons moving at different velocities. Experimentally, one measures at a particular  $\omega$  and/or  $\omega_b$ , the overall effect of all the electrons, and this overall effect depends not only on the mechanism of the collision process but also on the angular frequency that would govern the motion of the electrons in the absence of collisions. As a result, collisions should affect the imaginary part as well as give rise to the real part and the angular frequency should also affect the real part of the transport coefficients. In other words, a correct equation should have *both* the real and imaginary parts of the coefficient dependent both on angular frequency and on some average of the collision frequency. The main object of transport theory is to find these correct dependences for the coefficients. Usually the simple equation still applies with some functions inserted to correct it.

## CORRECTION FACTORS

Let us seek corrections for example to the resistivity  $\rho$  or conductivity  $\sigma = \rho^{-1}$  coefficient with  $\omega_b = 0$ . Three different ways of writing down the corrected equation can be suggested with correction functions  $g$  and  $h$ :

$$\rho = \frac{m}{ne^2} (\langle \nu_g \rangle g + j\omega h)$$

$$\sigma = \frac{ne^2}{m} \frac{\langle \nu_g \rangle g' + j\omega h'}{\langle \nu_g \rangle^2 + \omega^2}$$

$$\sigma = \frac{ne^2}{m\langle \nu_g \rangle} (g'' + h'')$$

where  $\langle \nu_g \rangle$  indicates some average of the electron collision frequency.

*First, what would these  $g$  and  $h$  correction functions depend on?* They should depend on the variation of the electron-neutral collision frequency  $\nu_m$

with electron velocity. For a given variation of  $v_m$ , they should be a function of: 1) the ratio of averaged electron-neutral to electron-ion collision frequencies ( $\langle v_m \rangle / \langle v_{ei} \rangle$ ) which is a measure of the degree of ionization; 2) the ratio  $\omega / \langle v_g \rangle$  (or  $|\omega \pm \omega_b| / \langle v_g \rangle$  in the presence of a magnetic field) where  $\langle v_g \rangle = \langle v_m \rangle + \langle v_{ei} \rangle$ ; and 3) on the effective ion charge number  $Z$ , a measure of electron-ion to electron-electron interactions.

Now, any one of the three pairs of  $g$  and  $h$  correction functions can be used. Obviously, unique relations exist between these pairs, but actually the first representation<sup>1</sup> is the best. The third has been used extensively<sup>2,3</sup> but it is the most inadequate one for representation. This is because  $g''$  and  $h''$  approach zero and range over decades as the ratio of  $\omega / \langle v_g \rangle$  is increased. If the functions  $g'$  and  $h'$  are used, their range of variation is less but still not as small as if the first set of functions is adopted. The reason for this is that all analyses start from a resistivity type of equation, such as a force equation, which has to be inverted to yield conductivity, refractive index, etc. It is most appropriate then to insert correction factors into the original expression rather than in some final form. One can expect that these correction functions in the original resistivity expression will vary over a far lesser range than if inserted in subsequent relationships.

Further advantages of our  $g$  and  $h$  pairs are the following:

- 1) They approach limiting values monotonically for very low  $\omega / \langle v_g \rangle$  and very high  $\omega / \langle v_g \rangle$ . In particular, the  $g$  and  $h$  functions for the resistivity are defined so as to approach unity for very high angular frequencies.
- 2) The product  $\langle v_g \rangle g$  can be interpreted as an effective collision frequency and the product  $\omega h$  can be interpreted as an effective radio frequency.
- 3) Furthermore, it is simple to include both  $\omega$  and  $\omega_b$  terms together in the presence of a DC magnetic field by writing the  $\sigma$  elements as:

$$\sigma_{11} = \sigma_{22} \text{ (+ sign)}$$

or:

$$\begin{aligned} j\sigma_{12} &= -j\sigma_{21} \text{ (- sign)} \\ &= \frac{ne^2}{2m} \left[ \frac{1}{\langle v_g \rangle g_+ + j(\omega + \omega_b) h_+} \pm \frac{1}{\langle v_g \rangle g_- + j(\omega - \omega_b) h_-} \right] \end{aligned}$$

where  $g_+$ ,  $h_+$  are for argument  $|\omega - \omega_b| / \langle v_g \rangle$  and  $g_-$ ,  $h_-$  are the same functions for argument  $|\omega + \omega_b| / \langle v_g \rangle$ . This obviously cannot be accomplished with the third  $g''$ ,  $h''$  system. However, if a set of  $g$  and  $h$  functions is calculated in any of the three systems, even for the particular case of  $\omega = 0$  or  $\omega_b = 0$ , it can be applied

to arbitrary  $\omega$  and  $\omega_b$  using our representation. It is obviously advantageous to calculate the correction functions using the first representation, since far less points are required for calculation and as a result less computer time is necessary.

When the degree of ionization is sufficiently large that electron-ion collisions are important, we write  $v_g = v_m + v_{ei}$  where  $v_m(v)$  is usually derived from experimental data as some function of velocity and where:

$$\begin{aligned} v_{ei}(v) &= \frac{n_+ 4\pi}{v^3} \left( \frac{Ze^2}{4\pi\epsilon_0 m} \right)^2 \ln \Lambda, \\ \Lambda &= \frac{3}{2Ze^3} \frac{(4\pi\epsilon_0 \kappa T)^{\frac{3}{2}}}{(\pi n)^{\frac{1}{2}}} \end{aligned}$$

We define our collision frequency average over electron velocity distribution function  $f_0$  as:

$$\langle v \rangle = -\frac{4\pi}{3n} \int \frac{\partial f_0}{\partial v} v^3 v dv$$

so that:

$$\langle v_g \rangle = \langle v_m \rangle + \langle v_{ei} \rangle$$

where for a Maxwellian distribution  $f_0$ :

$$\begin{aligned} \langle v_{ei} \rangle &= \frac{4}{3} (2\pi)^{\frac{1}{2}} n_+ \\ &\times \left( \frac{Ze^2}{4\pi\epsilon_0 m} \right)^2 \left( \frac{\kappa T}{m} \right)^{\frac{1}{2}} \ln \Lambda \end{aligned}$$

and if  $v_m = cv^r$  for example, then:

$$\langle v_m \rangle = \frac{c\Gamma(r + \frac{5}{2})}{\Gamma(\frac{5}{2})} \left( \frac{2\kappa T}{m} \right)^{r/2}$$

Up to now, we argued quantitatively that correction factors are required. One can prove theoretically<sup>4</sup> the existence of these factors for any degree of ionization. Note that although electron-electron collisions were not mentioned in any of the collision frequency averages, such like-particle collisions will necessarily influence the transport coefficients if the degree of ionization is sufficiently high. Effectively, what we have done is to conceal all effects of electron-electron collisions in the  $g$  and  $h$  functions, whose calculation actually includes these effects. The reason for this is that it is very cumbersome to invent analytic relations for electron-electron collisions. In any case, since the  $g$  and  $h$  functions even for a slightly ionized gas are not simple expressions, but are rather tabulated functions or expressed graphically, they can be made to include all extraneous effects such as electron-electron collisions.

#### CALCULATION FOR ARBITRARY $v_m(v)$

The calculation<sup>4</sup> for the conductivity coefficient when the degree of ionization

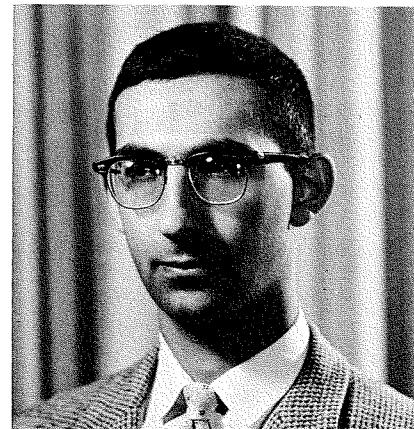
is arbitrary involves an inversion of a system of equations. For a Maxwellian distribution, we require Eqs. 57, 44, 49, 53 and 95 in Ref. 4. Eq. 95 is the generalization of Eq. 48 for the case of arbitrary variations (not necessarily a power law) of  $v_m$  with velocity. The elements of the electron-neutral interaction term thus require integration (perhaps numerical) of the averages of moments  $v^n v_m(v)$  over the distribution function. This is a new application not explicitly indicated in the original paper. It has been pointed out by the author and is being used at present by A. R. Hochstim at IDA, Washington and by C. H. Church at Westinghouse, Pittsburgh.

#### VALUES FOR THE TRANSPORT COEFFICIENTS

Let us restrict ourselves to the case when  $v_m$  varies as  $cv^l$ , a power of velocity where  $l = -3, -2, \dots, 2, 3$ . The conductivity results for any degree of ionization are tabulated and plotted in Ref. 4. If the gas is feebly ionized, the integrals can be expressed in terms of tabulated Dingle functions, from which  $g$  and  $h$  values can be derived for the conductivity. These results<sup>4</sup> are also referred to in the text by Heald and Wharton<sup>5</sup>, who plot them as shown in Fig. 1.

The other transport coefficients in the direct current and electron energy flow can similarly be presented in condensed form using respective  $g$  and  $h$  functions for each coefficient. For a strongly ionized gas, the functional parameters are  $\omega_b / \langle v_{ei} \rangle$  and  $Z$ . Plots and tables for these coefficients are given in Refs.

DR. ISSIE P. SHKAROFSKY graduated in 1952 from McGill University with a BSc degree and first class honors in physics and mathematics and obtained his MSc degree in 1953 in the fields of microwave optics and antennas. He then joined the microwave tube and noise group at the Eaton Electronics Research Laboratory and received his PhD degree in 1957 with a thesis on modulated electron beams in space-charge-wave tubes and klystrons. After graduation, he joined the RCA Victor Co., Ltd., Microwave Research Laboratory. His particular interest in plasma studies has been in the following topics: plasma transport coefficients, collisional effects in plasma, Boltzmann and Fokker-Planck theory, magnetohydrodynamics, and re-entry plasma physics. Dr. Shkarofsky is a member of the Canadian Association of Physicists, of the American Physical Society, and of the American Geophysical Union.



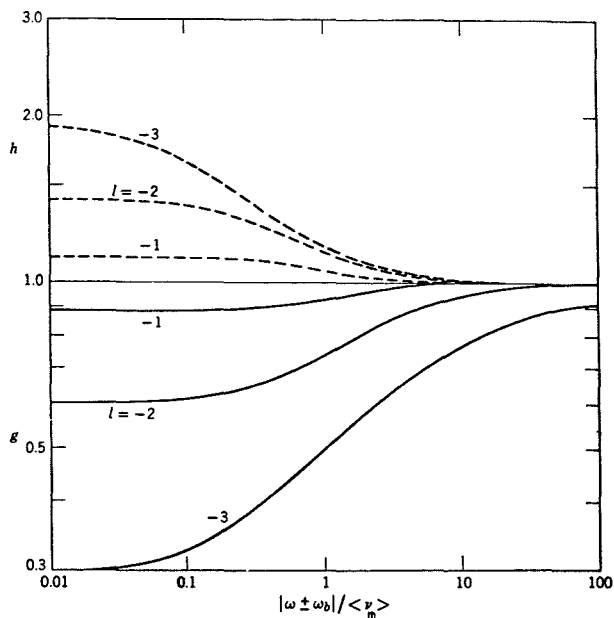


Fig. 1a—The  $g$  and  $h$  correction functions in a slightly ionized gas for electron-neutral particle collision frequencies varying as  $v^l$  with negative integral values for  $l$ . (Refs. 5 and 8).

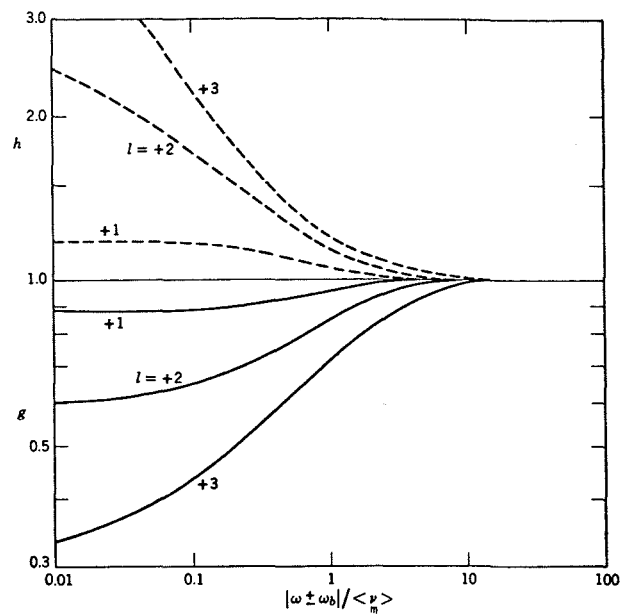


Fig. 1b—Same as Fig. 1a with positive integral values for  $l$ . (Refs. 5 and 8).

1 and 4 and abstracted in the text by Montgomery and Tidman<sup>6</sup>. In addition there are two other coefficients associated with ion motion, namely the ion heat conductivity and the tensor viscosity associated with an anisotropic pressure due to gradients in the velocity of a flowing plasma. The former is given in Ref. 1 and the latter in Refs. 1 and 7. Montgomery and Tidman<sup>6</sup> also present these coefficients. Whereas the texts in Refs. 5 and 6 only present graphs of the results, the text by Shkarofsky, Johnston, and Bachynski<sup>8</sup> gives in addition a full analysis and derivation of all the coefficients.

#### EXPERIMENTAL VERIFICATIONS (REF. 8)

##### Electrical Conductivity in Shock Heated Argon

Shock wave techniques have been used to produce highly ionized plasmas. One such method uses a driver gas in a shock tube. With argon, one can obtain a reasonable region where the gas is more or less highly ionized. Experimental conductivity results by Lau<sup>9</sup> in argon at moderate temperatures are shown in Fig. 2a. In Fig. 2b, measurements by Lin, *et al.*<sup>10</sup> at very high temperatures are also given.

The experimentally obtained values are compared with Shkarofsky's theory as outlined above, worked out for the case of Argon by Dudgeon and Michaud<sup>11</sup>, Lau<sup>9</sup>, and also by Al-Attar *et al.*<sup>12</sup>. (A similar calculation has been done for high temperature air by Shkarofsky<sup>13</sup>.) Results based on a simplified theory by Lin *et al.*<sup>10</sup> are also shown. In the Lin *et al.* theory, one adopts an effective weighted constant cross section  $n\bar{Q}_i$  for Coulomb collisions and adds it to the weighted averaged electron-neutral

particle cross section,  $n_m\bar{Q}_m$ , i.e.:

$$\sigma = \frac{ne^2}{\sqrt{m\kappa T}} \frac{1}{3} \sqrt{\frac{8}{\pi}} \frac{1}{nQ_i + n_mQ_m}$$

The above procedure is only approximate for two reasons. First, the Coulomb cross section  $nQ_i = v_{ei}/v$  varies as  $v^{-4}$  and is far from being constant with velocity; second, the dc conductivity cannot be evaluated by adding weighted cross sections as above, since the electron-electron contribution is not simple. However, as a simplified procedure, the above suffices, since it approaches proper limits for fully and

slightly ionized gases, provided the constant cross section approximation is valid for the latter. An appreciable error can however occur in the transition between these two limits, i.e. for a partially ionized gas. Indeed, Fig. 2a shows that Shkarofsky's theory provides better agreement in the transition region.

The experimental results of Lin *et al.* in Fig. 2b for a fully ionized gas are compared with transport theory which predicts that  $g = 0.5064$ , a result first worked out by Spitzer and Harm<sup>14</sup>. In this limit good agreement is also obtained with theory.

Fig. 2a—The electrical conductivity in partially ionized argon heated by shock waves. Note that  $p_1$  refers to the pressure ahead of the shock wave. The pressure, particle density and temperature behind the shock wave are all functions of the mach number (ratio of shock velocity to sound velocity). Key: dashed line, conductivity calculated by the theory<sup>10</sup> of Lin, *et al.*; solid line, conductivity calculated by Shkarofsky's method<sup>8</sup>; X's, experimental points of Lau<sup>9</sup>.

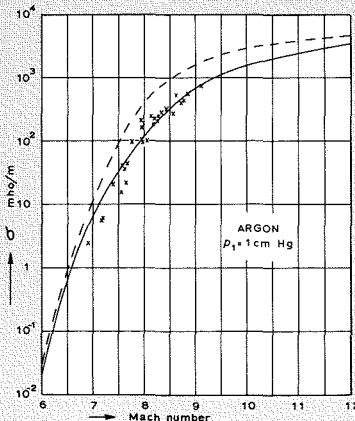
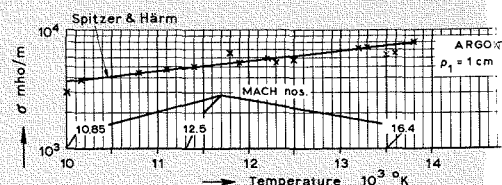


Fig. 2b—The electrical conductivity in highly ionized argon heated by shock waves. For comparison with Fig. 2a, several mach numbers are indicated. Key: solid line, conductivity calculated from Spitzer and Harm's theory (Ref. 14); X's, experimental points of Lin, *et al.* (Ref. 10).



### Generalized Appleton-Hartree Equation

Most investigations on the propagation of an electromagnetic wave in a magnetoplasma are based on the concept of constant  $\nu_m$ . The classic Appleton-Hartree equation, used for propagation in the ionosphere, has this inherent assumption. Because the electron elastic collision frequency with nitrogen molecules in the atmosphere varies as the square of electron speed, a discrepancy between classic theory and ionospheric experiments can be expected. Sen and Wyller<sup>15</sup> worked out corrections to include this speed variation of the electron-neutral particle collision frequency assuming that the gas is very slightly ionized. This is a good approximation to conditions in the *D* layer but not in the *F* layers of the ionosphere. Independently, Shkarofsky<sup>16</sup> has derived a more general theory valid for any degree of ionization. This theory essentially uses the conductivity expression in terms of *g* and *h* functions, which simplify exceedingly the analytical manipulations. It is gratifying to note that the generalized Appleton-Hartree equation for the refractive index is becoming accepted for use in ionospheric work, especially in the lower *D* layer. (See Aikin *et al*<sup>17</sup>, Crouse and Care<sup>18</sup>, Belrose and Burke<sup>19</sup>, and Kane<sup>20</sup>.) Fig. 3 shows electron densities in the *D* layer synthesized by Care<sup>18</sup> using the generalized more accurate theory and using classical theory. Large differences are evident.

### Electron Temperature Above the D-layer Ionosphere

An attempt was made to compare theoretical deductions of  $\langle \nu_e \rangle$  versus altitude using the 1959 ARDC model atmosphere with experimental data published in 1959 and 1960. Although very good agreement resulted in the *D* layer, discrepancies of factors of 2 to 4 occurred for the *E* region. (See Fig. 4, taken from Ref. 16.) To provide better agreement, Shkarofsky<sup>16</sup> postulated that the electron temperature  $T_e$  is 2 to 4 higher than the neutral (or ion  $T_i$ ) temperature given in the ARDC model. Since the plasma is neutral-dominated in the *E* region the collision frequency  $\langle \nu_m \rangle \propto T_e$  is increased likewise. Although additional evidence that  $T_e > T_i$  was available in 1959 from Langmuir probe measurements, this postulate encountered great opposition even as late as 1962 (see Bauer and Bourdeau<sup>21</sup>). After many more probe measurements by Brace and Spencer<sup>22</sup> and the conclusive backscatter measurements, especially during an eclipse, by Evans<sup>23</sup>, it is now generally accepted that  $T_e > T_i$  above the *D* layer during the day time.

### Damping of Waves Near the Electron Cyclotron Frequency

A detailed experimental and theoretical investigation of the propagation of em waves in an anisotropic plasma along the direction of the applied static magnetic field has been conducted by Bachynski and Gibbs<sup>24</sup>. The experimen-

tal arrangement was designed to conform as closely as possible with the requirements of theory—uniform, well defined, thermalized plasma, plane waves, minimum diffraction effects, etc.

Fig. 5 shows experimental data on electron density and attenuation in a slightly ionized He plasma using linearly polarization perpendicular to magnetic field. The measurements are taken as a function of time in the afterglow during which the plasma frequency  $\omega_p$  (or electron density) varies. The experimental results are compared with theory with and without the *g* and *h* correction functions. For the phase calculation, the two calculations give nearly identical results. As far as power attenuation, there is a slight difference and the experiment seems to favor the more exact theory with *g* and *h* functions. Similar measurements were done using circularly polarized waves. The velocity dependence of the collisional effects was found to be important for the right-hand wave for frequencies below  $\omega_p$ , with experiment again favoring the more exact theory.

### Diffusion of Plasma Across a Magnetic Field

Excellent results are obtained by Anisimov *et al*<sup>25</sup> on the variation of  $D_{\perp} = g \langle \nu_e \rangle / 2\kappa T / m\omega_c^2$ , the diffusion coefficient perpendicular to magnetic field and parallel to density gradient. In these experiments, the diffusion effect is separated from volume removal effects

Fig. 3—Jan., Feb., Mar. 1964 mean electron density profiles.

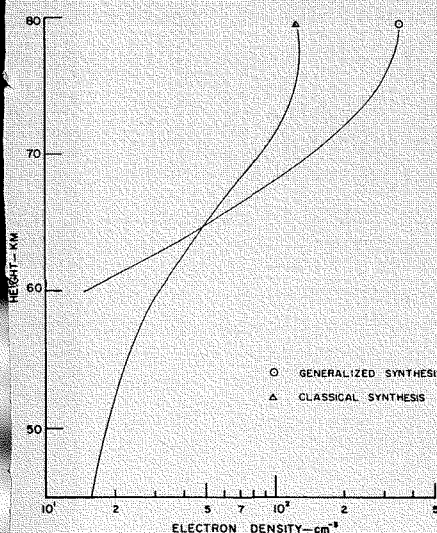


Fig. 4—Comparison (Ref. 16) of experimental data with the theoretical total collision frequency  $\langle \nu_e \rangle$  versus altitude in the ionosphere when the electron temperature is equal to the gas temperature,  $T_e = T_g$  (solid curve) and  $T_e$  is greater than  $T_g$  (dashed curve). The experimental points by various authors are indicated by vertical lines, arrows, crosses and squares.

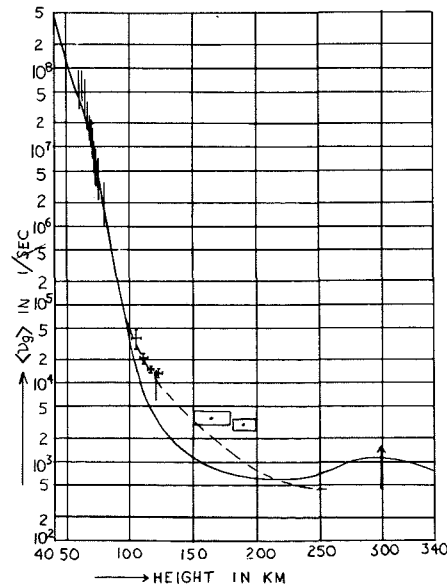
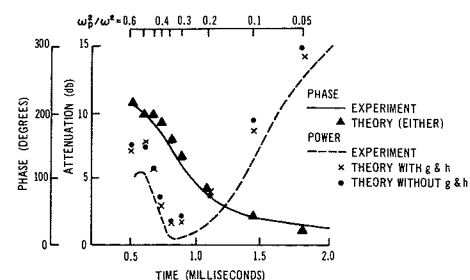


Fig. 5—Variation (Ref. 24) of phase change and intensity of a linearly polarized wave in a plasma for  $\omega_s/\omega = 0.47$ . The theory is for  $\omega_s/\omega = 0.50$ .



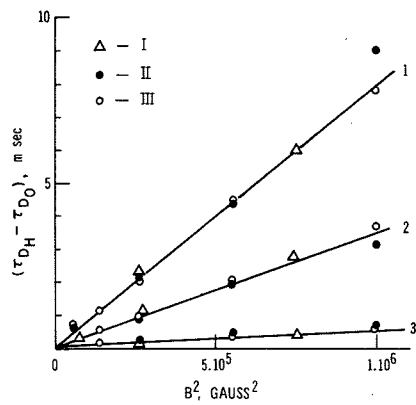


Fig. 6a—The diffusion time constant (Ref. 25) as a function of magnetic field. 1)  $n(\text{cm}^{-3}) = 3.3 \times 10^{11}$ ; 2)  $7.5 \times 10^{11}$ ; 3)  $5.2 \times 10^{12}$ . 1)  $p(\text{mm Hg}) = 2 \times 10^{-1}$ ; II)  $10^{-1}$ ; III)  $5 \times 10^{-2}$ .

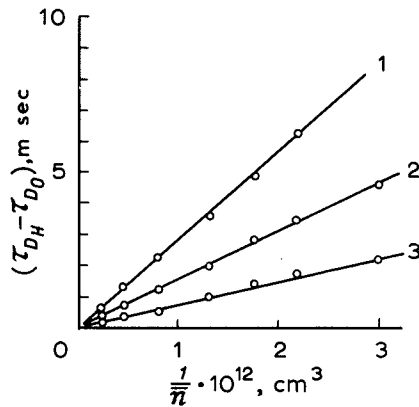


Fig. 6b—The diffusion time constant (Ref. 25) as a function of plasma density. 1)  $B(\text{gauss}) = 1,000$ ; 2) 750; 3) 500.

(the latter found to be independent of magnetic field) by subtracting the reciprocal of the time constant ( $\tau_{DH}^{-1}$ ) in the presence of a magnetic field, from that ( $\tau_{D0}^{-1}$ ) in the absence of the field. If  $\Lambda_H$  is the effective diffusion length in the presence of a magnetic field:

$$\begin{aligned} \tau_{DH} - \tau_{D0} &\approx \tau_{DH} = \frac{\Lambda_H^2}{D_{\perp}} \\ &= \frac{\Lambda_H^2 m \omega_b^2}{2 \kappa \tau \langle \nu_{ei} \rangle g} \propto \frac{B^2 T^{\frac{1}{2}}}{\bar{n}} \end{aligned}$$

since they note that  $\tau_{DH} \gg \tau_{D0}$  for their experimental conditions.

Experimentally, the magnetic field and mean electron densities are the variables. The maximum magnetic field is about 1,000 gauss, since at higher magnetic fields, anomalous diffusion occurs—not predicted by transport theory and attributed to instabilities, rapidly fluctuating electric fields or turbulence. Figs. 6a and 6b show very good agreement with experimental checks on

the linear variations with  $B^2$  and  $1/\bar{n}$  when electron-ion collisions dominate ( $\bar{n} = 5 \times 10^{11} - 10^{13} \text{ cm}^{-3}$ ).

#### Electrical and Heat Conductivities

To obtain a controlled, fully ionized plasma on which to perform direct measurements, the Princeton University group constructed a  $Q$ -machine employing alkali metals which are readily ionized up to 99% at low currents. Let  $L$  be the plasma length,  $I$  the current density,  $V$  be the voltage and  $\theta_e = \kappa T_e / e$  where  $T_e$  is the electrode plate temperature. The experimental  $V-I$  normalized characteristic of  $JL/\sigma\theta_e$  versus  $V/\theta_e$  is plotted in Fig. 7 based on the results of Rynn<sup>26</sup> in a potassium plasma. The theoretical curve with the  $\ln \Lambda$  correction includes the temperature variation of  $\ln \Lambda$  in  $\langle \nu_{ei} \rangle$  with current. The other two theoretical curves are calculated assuming  $\ln \Lambda$  has a constant value of 7, and the difference between these two curves stems from different approximations in solving the thermal energy relation for small and large currents. Agreement of theory and experiment is found up to  $V/\theta_e = 5$ . Fig. 7 illustrates that better agreement results if the actual temperature dependence of  $\ln \Lambda$  is employed, rather than the mean value. This experiment is thus sufficiently refined to indicate not only the numerical conductivity coefficient given by Spitzer and Harm<sup>14</sup> but also to some extent the variation in  $\ln \Lambda$ . The disparity at higher currents is attributed to large gradients in potential and temperature in front of the plates, and the discontinuities in the curves indicate the onset of turbulence.

Rynn<sup>26</sup> also compares values of measured electrical conductivities versus the values of Spitzer and Harm. When  $L > 10^3 l_e$  and  $l_e \gg l_D$  where  $l_e$  and  $l_D$  are average mean free path length and Debye length, experimentally determined values are 1.2 times Spitzer and Harm's value with an RMS-error of 10%. The electron thermal conductivity in the limit of zero current is also deduced in the temperature range 2,390 to 3,039°K. The average ratio of the experimental to theoretical values is 0.983 with an RMS-error of about 6½%. This is indeed excellent agreement, since the deviation falls within the theoretical accuracy of  $\pm 100/\ln \Lambda = \pm 100/7 = \pm 14\%$ .

#### Temperature Determinations

It is worthwhile pointing out that one of the standard methods of determining the electron temperature of a strongly ionized plasma is to measure its conductivity coefficient, calculate  $\langle \nu_{ei} \rangle$  and thereby deduce the temperature. In another system, finite conductivity allows diffusion of magnetic field through a

boundary separating a magnetic field-region and a plasma region. From the observed diffusion depth, one can readily calculate the conductivity and then the temperature (Ref. 27).

#### OTHER APPLICATIONS

An application pointed out previously concerned the calculation of transport coefficients for an arbitrary variation of the electron-neutral collision frequency. Other applications are briefly outlined below.

#### Relaxation Time of an Anisotropic Temperature

The same analysis that is used to give the transport coefficients can readily provide as well relaxation times (see Shkarofsky *et al.*<sup>28</sup>). In fact, the analysis on relaxation times is somewhat simpler. If one includes particle-wave interactions as well as particle-particle interactions, one finds that the relaxation of an anisotropic electron velocity distribution is a two way process whereas the ion relaxation is a three way process. For electrons, the relaxation proceeds first as a result of electron interactions with ion plasma waves and then with the combined collisional effects of electrons and ions. For ions, the relaxation proceeds as a result of ion interactions with electron plasma waves, then by ion-electron collisions and finally by ion-ion collisions. Near equilibrium, ion-electron collisions are negligible both in ion relaxation processes and in their contribution to transport coefficient (see Shkarofsky<sup>28</sup>).

#### Damping of Plasma Oscillations

Transport analysis yields effective collision frequencies which can be inserted into wave analysis to yield the damping, both of transverse waves and of longitudinal waves. For the latter, one restricts the analysis to wave lengths greater than the Debye length. The damping of electron and ion plasma waves in a fully ionized plasma is investigated by Johnston and Shkarofsky<sup>29</sup>.

#### Equilibrium Electron Temperature in Ohmic Heating

Because Coulomb interactions decrease with increasing velocity ( $\nu_{ei} \propto v^{-3}$ ), a strong electric field can give rise to time-dependent behaviour in which the electrons increase in energy. This so-called "runaway effect", if left uncontrolled, is a source of heat loss and one of the limitations of ohmic heating in controlled fusion research. If the heating process is collision dominated, one can expect a quasi-equilibrium electron temperature under the heating effects of AC or DC electric fields. Peculiar effects,

such as temperature hysteresis, nevertheless exist in certain gases when the angular frequency of the electric field differs sufficiently from the collision frequency. When rotational inelastic collisions do not occur as in monatomic gases, the radio frequency has to be greater than the collision frequency to prevent hysteresis. The opposite may be true when energy losses due to rotational collisions dominate elastic energy losses. Hysteresis in monatomic gases is also eliminated if the plasma is only slightly ionized and contains neutrals whose collision frequency (at moderate energies) does not decrease in velocity. All these results can be deduced by substituting the conductivity transport coefficient into the energy conservation equation. The analysis and all the above results are given by Shkarofsky *et al.*

#### Plasma Wave Corrections to Transport Coefficients

When the electron to ion temperature is very large, the electron transport coefficients are strongly influenced as a result of scattering by ion plasma waves with wavelengths less than the electron Debye length. These interactions are the equivalent of electron-phonon interactions in solids. The contribution of these particle-wave interactions are being studied (see Gorbunov and Silin<sup>30</sup>).

#### Hydrothermomagnetic Waves

Another field of recent study is the investigation of waves in inhomogeneous plasmas with temperature and density gradients. Using transport analysis, new classes of waves can exist in the presence of a magnetic field (see Gurevich and Gelmont<sup>31</sup>).

#### Resistive, Shear, Inertial and Universal Instabilities

Analyses on plasma instabilities originally neglected finite Larmor radius and finite resistivity effects. More recently, many new instabilities were discovered upon including these effects. Many of these analyses utilize the transport coefficients for the resistive, shear and inertial instabilities. (See for example, Refs. 32 to 37.)

#### CONCLUSION

In conclusion, we see that we are at the early stage of application of transport analysis with much more effort and practical results to be forthcoming. One can also expect further analyses of a lesser restricted nature.

#### BIBLIOGRAPHY

1. I. P. Shkarofsky, I. B. Bernstein, B. B. Robinson (RCA Victor Research Labs, Montreal and Princeton U.) "Condensed Presentation of Transport Coefficients in a Fully Ionized Plasma," *Phys. Fluids* **6**, 40-47, Jan. (1963).
2. B. B. Robinson, I. B. Bernstein "A variational Description of Transport Phenomena in

- a Plasma," *Annals of Phys. (N.Y.)* **18**, 110-169, April (1962).
3. R. Landshoff—"Transport Phenomena in a Completely Ionized Gas in the Presence of a Magnetic Field," *Phys. Rev.* **76**, 904-909, Oct. (1949).
4. I. P. Shkarofsky (RCA Victor Research Labs, Montreal) "Values of the Transport Coefficients in a Plasma for Any Degree of Ionization Based on a Maxwellian Distribution," *Can. J. Phys.* **39**, 1619-1703, Nov. (1961).
5. H. A. Heald, C. B. Wharton—"Plasma Diagnostics with Microwaves," Wiley, N.Y. (1965), pp. 69-76.
6. D. C. Montgomery, D. A. Tidman—"Plasma Kinetic Theory," McGraw Hill, N.Y. (1964). Chap. 13.
7. I. P. Shkarofsky (RCA Victor Research Labs, Montreal) "Calculation of the Pressure Tensor in a Fully Ionized Plasma," *Can. J. Phys.* **41**, 1787-1800, Nov. (1963).
8. I. P. Shkarofsky, T. W. Johnston, M. P. Bachynski (RCA Victor Research Labs, Montreal) *The Particle Kinetics of Plasmas*, Addison-Wesley, Reading, Mass. (1965), Chap. 8.
9. J. Lau—"Electric Conductivity of Inert Gases—Seed Combination in Shock Tubes," *Can. J. Phys.* **42**, 1548-1563, Aug. (1964).
10. S. C. Lin, E. L. Resler, A. Kantrowitz—"Electrical Conductivity of Highly Ionized Argon Produced by Shock Waves," *J. Appl. Phys.* **26**, 95-109, Jan. (1955).
11. E. H. Dudgeon and G. Michaud—"The Electrical Conductivity of Helium and Argon Seeded with Potassium," National Research Council, Ottawa, Report MT-52, Nov. (1963).
12. Z. Al-Attar, M. R. Barrault, M. McChesney—"Electrical Conductivity of Shock Heated Partially Ionized Argon in the Presence of a Magnetic Field," *Brit. J. Appl. Phys.* **15**, 1057-1065 (1964).
13. I. P. Shkarofsky (RCA Victor Research Labs, Montreal) "The A-C Conductivity of Air at Temperatures of 300-12,000°K in the Presence of a Static Magnetic Field," *Can. J. Phys.* **40**, 49-60, Jan. (1962).
14. L. Spitzer, R. Harm—"Transport Phenomena in a Completely Ionized Gas," *Phys. Rev.* **89**, 977-981, March (1953).
15. H. K. Sen, A. A. Wyller—"On the Generalization of the Appleton-Hartree Magnetoionic Formulas," *J. Geophys. Res.* **65**, 3931-3950, Dec. (1960).
16. I. P. Shkarofsky (RCA Victor Research Labs, Montreal) "Generalized Appleton-Hartree Equation for Any Degree of Ionization and Application to the Ionosphere," *Proc. IRE* **49**, 1857-1871, Dec. (1961); I. P. Shkarofsky, T. W. Johnston (RCA Victor Research Labs, Montreal) "Electromagnetic Waves in a Magnetized Plasma," *Bull. Am. Phys. Soc. Ser. II*, **5**, 383, June (1960).
17. A. C. Aikin, J. A. Kane, J. Troim—"Some Results of Rocket Experiments in the Quiet D-Region," *J. Geophys. Res.* **69**, 4621-4628, Nov. 1 (1964).
18. P. E. Crouse—"Methods for Obtaining Electron Density Profiles from Capacitive Ionospheric Rocket Probes," Penn. State Univ. Sc. Rep. **208**, May 15 (1964). Also: K. H. Care, Generalization of the D-Region Electron Density Synthesis Technique, Penn. State Univ. Sci. Rep. **248** (1965).
19. J. S. Belrose, M. J. Burke—"Study of the Lower Ionosphere Using Partial Reflection," *J. Geophys. Res.* **69**, 2799-2818, July 1 (1964).
20. J. A. Kane—"Re-evaluation of Ionospheric Electron Densities and Collision-Frequencies Derived from Rocket Measurements of Reflective Index and Attenuation," *J. Atm. Terr. Phys.* **23**, 338-347 (1962).
21. S. J. Bauer, R. E. Bourdeau—"Upper Atmosphere Temperatures Derived from Charged Particle Observations," *J. Atm. Sc.* **19**, 218-225, May (1962).
22. L. H. Brace, N. W. Spencer, G. R. Carignan—"Ionosphere Electron Temperature Measurements and Their Implications," *J. Geophys. Res.* **68**, 5397-5412, Oct. 1 (1963); L. H. Brace, N. W. Spencer—"First Electrostatic Probe Results from Explorer 17," *J. Geophys. Res.* **69**, 4686-4689, Nov. 1 (1964).
23. J. V. Evans—"An F Region Eclipse," *J. Geophys. Res.* **70**, 131-142, Jan. 1 (1965); "Cause of the Mid-Latitude Evening Increase in  $f_0F_2$ ," *J. Geophys. Res.* **70**, 1175-1185, Mar. 1 (1965).

24. M. P. Bachynski, B. W. Gibbs (RCA Victor Research Labs, Montreal) "Electromagnetic Wave Propagation in Anisotropic Plasmas Along the Direction of Magnetic Field: II Linear Polarization," Submitted for publication in *Phys. Fluids*.
25. A. I. Anisimov, N. I. Vinogradov, V. E. Golant, B. P. Konstantinov—"Diffusion of Charged Particles in a Dense Plasma in a Magnetic Field," *Soviet Phys.—Tech. Phys.* **7**, 884-889, April (1963).
26. N. Rynn—"Macroscopic Transport Properties of a Fully Ionized Alkali-Metal Plasma," *Phys. Fluids* **7**, 284-291, Feb. (1964).
27. F. J. F. Osborne, I. P. Shkarofsky, J. V. Gore (RCA Victor Research Labs, Montreal) "Laboratory Simulation of the Solar Wind Magnetosphere Interaction," *Can. J. Phys.* **41**, 1747-1752, Nov. (1963).
28. I. P. Shkarofsky (RCA Victor Research Labs, Montreal) "Cartesian Tensor Expansion of the Fokker-Planck Equation," *Can. J. Phys.* **41**, 1753-1775, Nov. (1963).
29. T. W. Johnston and I. P. Shkarofsky (RCA Victor Research Labs, Montreal) "Effects of Coulomb Collisions on Longitudinal Plasma Oscillations," *Can. J. Phys.* **42**, 193-199, Jan. (1964).
30. L. M. Gorbunov, V. P. Silin—"Theory of Transport Effects in a Nonisothermal Fully Ionized Plasma," *Soviet Phys.—Tech. Phys.* **9**, 305-311, Sept. (1964).
31. L. E. Gurevich, B. L. Gelmont—"On the Theory of Hydrothermomagnetic Waves in a Weakly Non-Homogeneous Plasma," *Soviet Phys.—Tech. Phys.* **9**, 1236-1241, March (1965).
32. H. P. Furth, J. Killeen, M. N. Rosenbluth, "Finite Resistivity Instabilities of a Sheet Pinch," *Phys. Fluids* **6**, 459-484, April (1963).
33. F. C. Hoh—"Instabilities Due to Resistivity Gradients in a Low Pressure Plasma," *Phys. Fluids* **7**, 956-964, July (1964).
34. B. Coppi—"Influence of Gyration Radius and Collisions on Hydromagnetic Stability," *Phys. Fluids* **7**, 1501-1516, Sept. (1964).
35. A. B. Mikhailovskii, L. I. Rudakov—"The Stability of a Spatially Inhomogeneous Plasma in a Magnetic Field," *Soviet Physics JETP* **17**, 621-625, Sept. (1963).
36. S. S. Moiseev, R. Z. Sagdeev—"Effect of Finite Electrical Conductivity on the Stability of a Plasma Confined by a Magnetic Field," *Soviet Phys.—Tech. Phys.* **9**, 196-200, Aug. (1964).
37. F. F. Chen—"Universal Overstability of a Resistive Inhomogeneous Plasma," Princeton Univ. Plasma Phys. Lab. Rep. MATT-311, Nov. (1964).

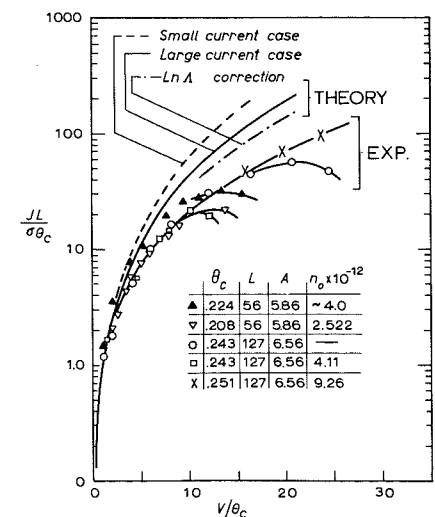


Fig. 7—Comparison (Ref. 26) of theory and experiments on  $I$  (normalized as  $J/\sigma\theta_c$ ) versus  $V$  (normalized  $V/\theta_c$ ) characteristics. In the table insert  $\theta_c = \kappa T_c/e$  is measured in eV where  $T_c$  is the plate temperature, the plasma length  $L$  in cm, the plasma cross-sectional area  $A$  in  $\text{cm}^2$  and the number density  $n_0$  in  $\text{cm}^{-3}$ .

# COMPARATIVE STUDIES OF PLASMA DIAGNOSTICS

Improvements in plasma diagnostics are of great interest because discrepancies often occur between the results of different types of plasma measurement; also, there is widespread demand for measurement methods which will supply more detailed characterization of a plasma rather than just one or two parameters. For these reasons, experiments were conducted in which Langmuir probe and microwave techniques were applied to the same plasma; these comparative studies have shown excellent agreement, and have led to better understanding of the plasmas. To obtain convenient and reproducible conditions, these plasmas were generated with high-purity rare-gas discharges and had electron densities in the range  $10^8$  to  $10^{12}$   $\text{cm}^{-3}$ . This paper summarizes the comparative density measurements and discusses the techniques, their refinements and some possible applications.

C. C. PETERSON and J. F. DIENST

*RCA Laboratories  
Princeton, New Jersey*

PLASMA phenomena have assumed a wide-ranging importance in modern technology and to RCA. The rush to apply these phenomena in such areas as microwave generation and control, radar and communications, geophysical exploration, coherent light generation, thermonuclear power generation, and many others emphasizes the pervasiveness of plasma concepts—but only hints at the diversity of measurement problems which are encountered. For example, one of the most basic plasma parameters, the carrier density, may vary in different applications over a range of  $10^{20}$  while a typical measurement set-up might be applicable over a density range of  $10^1$  to  $10^8$ . Furthermore, the density range is only one of many considerations in choosing and interpreting a plasma measurement method; additional factors including the plasma size, shape, perturbability, energy distribution, uniformity, accessibility, magnetic field, etc., may each impose new requirements in the application of general principles to a specific measurement problem.

Thus, while the concepts associated with collective plasma behavior serve to unify many different fields, the actual measurement techniques tend to become more and more specialized and corre-

spondingly difficult to compare with each other. This is one reason why the credibility and accuracy of plasma diagnostics is a frequent limitation in both practical and scientific work. In gas plasma measurements, for example, poor agreement has often been found in the results obtained by different techniques and workers<sup>1</sup>. Some of these discrepancies undoubtedly result from difficulties in reproducing plasma conditions during a sequence of measurements which are to be compared, since only a few careful studies have been made in which two or more basically different techniques have been applied simultaneously in the same plasma. However, some of these careful studies have indicated discrepancies also and thus have led to improved techniques and interpretations<sup>2,3,4</sup>.

The need for improved understanding of plasma diagnostics was also recognized by the U.S. Air Force and, with their sponsorship, the present study was undertaken at RCA Laboratories, Princeton, in which two or more techniques were applied to the same plasma<sup>5</sup>. In this work, two main experimental programs have been followed in each of which spherical Langmuir probe characteristics analyzed by the Druyvesteyn (second-derivative) method were compared with a (different) microwave density measurement. In the first case, the resonant-frequency-shift of a small shorted section of two-wire-transmission-

line immersed in the plasma was measured. In the second case, the dispersion characteristics of low-frequency surface waves on a cylindrical plasma column within a coaxial outer conductor were measured. Each of these experiments was performed in a quiescent, hot-cathode, rare-gas discharge of sufficiently high purity and appropriate geometry to permit a valid comparison of the techniques.

As will be discussed, a reasonable degree of agreement was found between the various techniques as they were used initially. With improvements in apparatus and interpretation, a higher degree of agreement and consistency was obtained and over larger ranges of density. We will summarize the comparative density measurements first, and devote the balance of the article to a discussion of the three techniques, their refinements, and some possible applications.

## MICROWAVE PROBE VERSUS LANGMUIR PROBE

Fig. 1 is a synopsis of comparative measurements obtained with the microwave probe (resonant-transmission-line-probe) and a spherical Langmuir-probe. These results were obtained in an argon plasma with electron temperatures in the range 5,000 to 15,000°K. and with the neutral gas pressure varying in the range from 0.025 torr to 0.5 torr. These conditions correspond to an electron free path,  $\lambda_e$ , which was always large compared to the transverse dimensions of the microwave probe and the radius of the Langmuir probe. However, in this range the probe dimensions were either larger than or comparable to both the ion free path,  $\lambda_i$ , and the Debye length,  $\lambda_D$ . As can be seen, the experimental points show remarkable agreement, falling nearly as close to the locus of exact agreement as the combined precision of the two measurements allows.

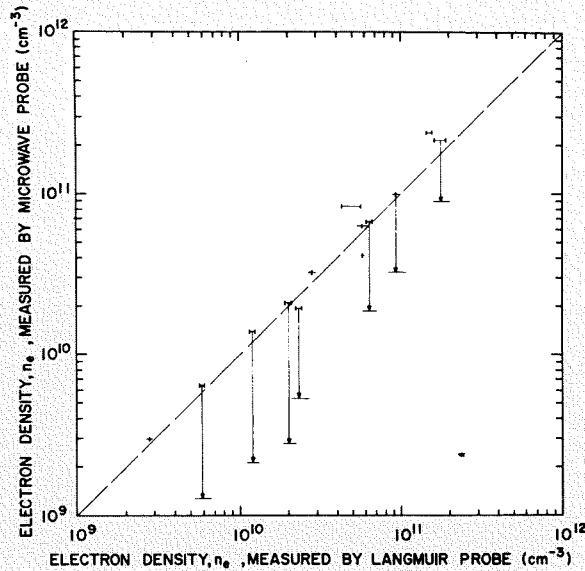
These measurements were obtained with the microwave probe biased to the potential of the surrounding plasma, which largely eliminates sheaths around the probe and allows the microwave fields to "see" the unperturbed plasma density. When the microwave probe is allowed to "float", an ion sheath forms which causes a reduction in the apparent electron density as is indicated by the arrows from some selected points in Fig. 1.

Because of the large range of parameters (density and pressure) represented in these data and the differences in the two techniques, there is a strong presumption that these measurements not only agree with each other but indicate the correct density on an absolute

*Final manuscript received September 15, 1965.*

The research reported in this paper was sponsored by the Air Force Avionics Laboratory, Research and Technology Division, Air Force Systems Command, Wright-Patterson Air Force Base, Ohio, under Contract Number AF33(657)-7814, and RCA Laboratories, Princeton, New Jersey.

Fig. 1—Correlation between plasma electron densities measured by a small spherical Langmuir-probe and a biased microwave probe in an argon discharge. The arrows indicate the density that is measured by the microwave probe when it is floating.



scale. This is important, since many techniques exist which supply an indication apparently *proportional* to the density, but with a poorly defined proportionality constant (which itself varies slowly with plasma parameters)<sup>6</sup>. In fact, the microwave probe would behave in exactly this fashion if it were not biased to plasma potential and instead were allowed to float.

Previous to the present work, Levitskii and Shashurin had also demonstrated excellent agreement between a similar microwave probe and a Langmuir-probe<sup>7</sup>. However, their studies were lim-

ited to a 3:1 density range and required adjustment of the microwave circuit as the density and frequency varied. In the present work, broad-band coupling was devised for an x-band probe to permit rapid, swept-frequency display of the probe resonance, and a pulse-biasing circuit was developed to reduce errors from thermal expansion when biasing the probe to space potential. As a result, it was possible in our work to demonstrate accurate measurements over a density range of 100:1, and this was limited in part by the range of the available test plasma.

## SURFACE WAVE DISPERSION VERSUS LANGMUIR PROBE

A comparison of density measurements by the surface wave and Langmuir-probe methods is presented in Fig. 2. These measurements were made in helium (0.1 to 0.7 torr) and xenon ( $6 \times 10^{-3}$  torr) plasmas with equivalent electron temperatures in the range 50,000 to 140,000°K. In this case  $0.1 \leq \lambda_d/r_p \leq 1$  as compared with  $0.03 \leq \lambda_d/r_p \leq 0.3$  for the Langmuir-probe data of Fig. 1; ( $r_p$  is the Langmuir-probe radius). However, the range of free path lengths,  $\lambda_e/r_p$  and  $\lambda_i/r_p$ , was similar in both cases.

According to theory, the surface wave densities  $n_e$  are to be interpreted as the average over the cross-section of the radially nonuniform plasma cylinder<sup>8</sup> while the Langmuir probe densities  $n_{ea}$  were measured on the axis of the cylinder where the density is a maximum. Theory and experiment indicate  $2 \leq (n_{ea}/n_e) \leq 3$  for these plasmas so in this case the locus of agreement is not the dashed line but the region between the two solid lines. Thus, Fig. 2 shows a very close parallel existing between the two types of measurements, and also a small but consistent discrepancy. The surface wave densities are too high relative to the Langmuir probe densities.

Except for the four points labeled *HP* or *D*, the surface wave densities in Fig. 2 have been derived from the dispersion measurements assuming the simplest possible model, a cold collisionless plasma. In two cases it was possible to make sufficiently precise phase velocity measurements to determine the electron drift velocity from the difference in phase velocity of waves propagating parallel and anti-parallel to the drift direction. These Doppler measurements

**JOSEPH F. DIENST** attended Drexel Institute of Technology from which he received the BSEE in 1955. From 1955 to 1958 he was a research associate in the Department of Electrical Engineering at Syracuse University from which he received the MEE degree in 1958. While a member of the staff at Syracuse he did research in the fields of magnetic amplifiers and tropospheric scatter propagation. In 1958 he joined the staff of Rutgers University as an Instructor in Electrical Engineering. During the years 1961 to 1963 he was also a part-time member of the research staff of RCA Laboratories where he did work in the area of microwave propagation in plasmas. He will receive the PhD degree from Rutgers University upon completion of a dissertation which he is currently writing. He became a full time member of the staff at RCA Laboratories in June, 1963, and is currently working on diagnostic

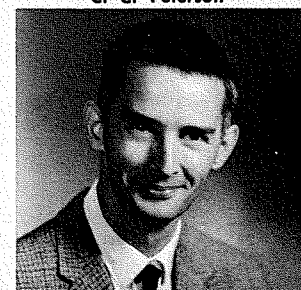
techniques in gaseous plasmas. Mr. Dienst is a member of Tau Beta Pi, Eta Kappa Nu and the IEEE.

**CHARLES C. PETERSON** attended Cornell University from which he received his Bachelor's Degree in Engineering Physics in 1951. Subsequently, he was variously a graduate student, research assistant, and research associate at that institution until 1959 when he joined RCA Laboratories. His research at Cornell included work in the fields of infrared spectroscopy of solids, electron optics, and ultra-high-vacuum electron-diffraction surface studies. He expects to receive the PhD degree for his work in the latter field this year. At RCA Laboratories he has worked on low-noise television camera tubes and diagnostic methods in gaseous plasmas. Mr. Peterson is a member of Sigma Xi and the American Physical Society.

J. F. Dienst



C. C. Peterson



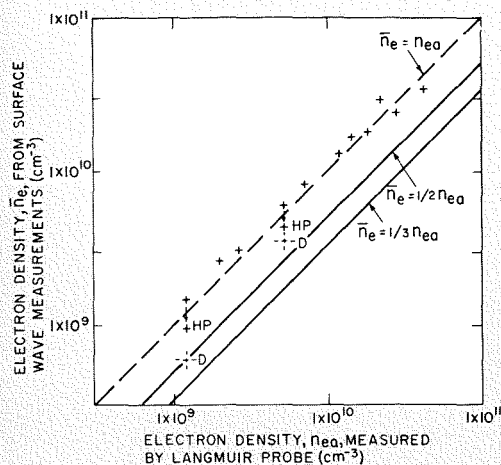


Fig. 2—Comparison of surface-wave and Langmuir-probe density measurements. Surface-wave densities were deduced from phase velocity measurements by: (1) a cold collisionless plasma model, (+); (2) a hot collisionless plasma model (+HP); (3) a Doppler shift determination (-+-D).

(which do not depend strongly on a particular plasma model) together with the discharge current and column area yielded the points labeled *D* in Fig. 2. These points are in much closer agreement with the Langmuir-probe results and indicate the inadequacy of the cold-collisionless plasma model. The discrepancy becomes somewhat larger if the effects of collisions are considered, but noticeably only at high pressures; however inclusion of an electron "pressure" term in the equation of motion for the electron fluid, the so-called hot-plasma model, improves the agreement substantially, especially at low densities. This improvement is indicated by two examples in Fig. 2, the points labeled *HP*. When both collisions and hot plasma effects are considered there is a net improvement in agreement at low densities and pressures and a net increase in the discrepancy at the higher pressures.

(For the sake of clarity we have not indicated all of these effects on the surface wave density estimates in Fig. 2.)

As will be discussed later, the hot-plasma model including collisions is believed to be most nearly accurate but requires improvement. We have only treated a radially uniform hot plasma, but there are strong reasons for believing that a radially nonuniform hot plasma model would lead to a larger correction and thus to further improvement (although it can be shown that radial nonuniformity is not important in our case if a cold plasma could be assumed). In addition, there is still the unresolved possibility that the Langmuir probe results are too low in some cases particularly at high densities. Further attempts to study this question by means of high-frequency Langmuir probe measurements have been inconclusive<sup>2b</sup>. Thus, while the comparative data of Fig. 2 indicate sufficient reliability and accuracy to justify the intelligent employment of either technique in many cases, there remains a consistent discrepancy which suggests interesting questions for further study.

#### MICROWAVE RESONANT PROBE

The microwave resonant probe technique is akin to microwave cavity techniques for measuring plasma electron densities. In both techniques, the observed shift in resonant frequency of some structure, resonating at frequencies well above the characteristic electron plasma frequency  $\omega_p$ , is related to the plasma electron density through  $\omega_p$ . In addition, both techniques can, at least theoretically, yield information on plasma loss mechanisms through a degradation of the resonator quality factor  $Q$ , concomitant with the introduction of plasma into the resonating system.

The resonant probe method has several outstanding advantages. First, rapid measurements are possible if the probe is excited by a swept-frequency source. Second, since the probe is immersed in the plasma, the only spatial requirement is that the plasma volume be larger than

the volume occupied by the probe. Third, compared to other microwave measurements, the spatial resolution of this method is better since the rf fields on the probe are confined mainly to the region between the probe wires, and it is here that the plasma has the most profound effect on the probe resonance. The main disadvantage of the resonant probe lies in the fact, as with all probe techniques, that it is immersed in the plasma and may constitute a serious perturbation.

The resonant probe that was used in the comparative measurements is shown in Fig. 3. It consists simply of a two-wire transmission line short-circuited at both ends and coupled to a small coaxial driving line through a short piece of similar line. This geometry couples the probe tightly to the coaxial line and strong absorptive resonances are observed when the length (distance between short-circuits) of the probe =  $m(\lambda_p/2)$  where  $\lambda_p$  is the wavelength of the fields along the probe and  $m$  is an integer we call the *resonance order*.

The fields on the probe are essentially *TEM* and in the low-loss limit the wavelength is determined by the shunt capacitance per unit length  $C$  through the well known distributed constant transmission-line relation  $\lambda_p = 2\pi/(\omega\sqrt{LC})$ . Obviously the resonant frequencies will depend upon the medium in which the probe is immersed, since  $C$  is proportional to the dielectric constant of this medium. In our case, the plasma is adequately described by a scalar permittivity:

$$\epsilon_p = \epsilon_0 \left( 1 - \frac{\omega_p^2}{\omega^2} \right) - j \epsilon_0 \left( \frac{\nu_c}{\omega} \right) \left( \frac{\omega_p}{\omega} \right)^2$$

for  $\nu_c \ll \omega$ , where  $\nu_c$  is a collision parameter introduced to account for any plasma loss mechanisms that may be operative. For  $\omega > \omega_p$  the plasma behaves as though it were a dielectric for which the real part of the dielectric constant  $\kappa_p$  is less than unity. Consequently, the resonant frequency of the probe is shifted to higher frequencies when the plasma is present.

The expression which relates the resonant frequency without plasma,  $\omega_0$ , to the resonant frequency with plasma,  $\omega_{op}$ , is simply  $\omega_{op}^2 = \omega_0^2 + \omega_p^2$ , and for diagnostic work this equation can be solved for the electron density  $n_0$  (in  $cm^{-3}$ ) in terms of the resonant frequencies:

$$n_0 = \frac{m_e \epsilon_0}{e^2} (\omega_{op}^2 - \omega_0^2) = 1.242 \times 10^8 (f_{op}^2 - f_0^2) \quad (1)$$

Fig. 4 illustrates the microwave probe resonance with and without plasma and was made using a conventional micro-

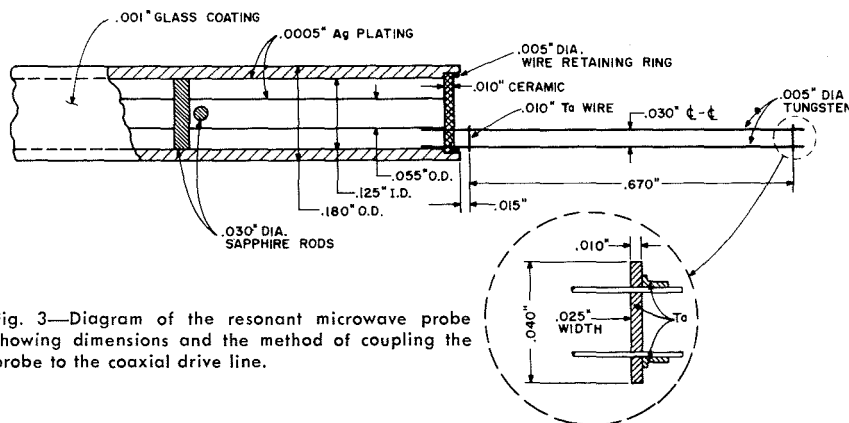


Fig. 3—Diagram of the resonant microwave probe showing dimensions and the method of coupling the probe to the coaxial drive line.

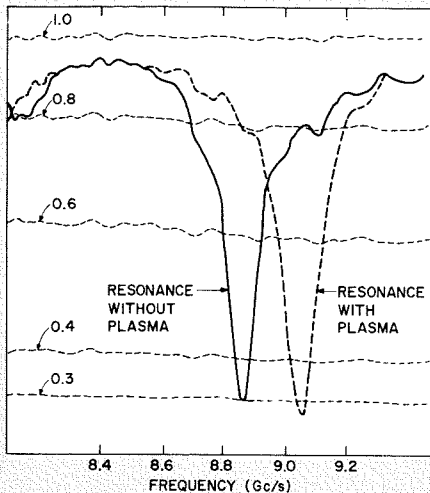


Fig. 4—Example of the microwave probe response with and without a plasma as traced directly from an X-Y recorder plot.

wave reflectometer circuit. The probe was driven by a swept-frequency oscillator through a broadband ridged waveguide to coaxial line transition. At driving frequencies far enough removed from the resonant frequency, the probe looks like a short-circuit termination at the end of the coaxial line, and the reflected wave amplitude is nearly equal to the amplitude of the incident wave ( $|\Gamma| \rightarrow 1$ ). With a good match between probe and driving line at resonance, a substantial portion of the power incident on the probe from the oscillator is absorbed and the reflected wave amplitude is small compared to the incident wave ( $|\Gamma| \rightarrow 0$ ). The power absorbed by the probe is dissipated in the dielectric and line losses.

Observed  $Q$  changes should provide a means of determining an effective collision frequency  $\nu_c$ . In our measurements, however, the probe  $Q$  was primarily determined by conductor losses and was relatively insensitive to changes in  $\nu_c$  for  $\nu_c < 10^8$ . Any  $Q$  variations attributable to  $\nu_c$  (plasma losses) were almost completely masked. Nevertheless, this technique still holds the promise of allowing a measurement of  $\nu_c$  and should be explored.

Many factors, such as tolerable spatial resolution,  $Q$ , density range, fabrication, etc., have to be considered and compromised in selecting probe dimensions and the dimensions shown in Fig. 3 were selected on the basis of such considerations. This particular probe was designed to operate with the  $m = 1$  order resonance at x-band. It was possible to resolve minimum shifts of 1 Mc/s. This, together with a 25% usable circuit bandwidth, permitted density measurements

in the range  $2.4 \times 10^8 \leq n_e \leq 5.8 \times 10^{11} \text{ cm}^{-3}$ .

Clearly, orders  $m > 1$  can be used to increase the measurable density range for a given probe. If, for example, a probe is designed to operate with the  $m = 2$  resonance (one-wavelength-long probe), it should be possible to adjust the operating frequency range and probe length so that the  $m = 1$  resonance just moves into the operating frequency band as the  $m = 2$  resonance moves out. However, if the density variation is not continuous there may be an ambiguity regarding which order is observed. Furthermore, it can be shown that optimum low-density response will be achieved for  $m = 1$ .

With the range of plasma densities and temperatures encountered in the experimental work it was found that if the microwave probe is left "floating" with respect to the plasma, ion sheaths of appreciable (compared to the interwire spacing) size form around the probe wires. Most of the RF fields on the microwave probe are concentrated in the space between the wires, and it is largely the effect of the plasma in this space which gives rise to a resonant frequency shift. Ion sheaths are regions purged of plasma electrons and, since the ions do not respond readily to the RF fields at these frequencies, the presence of such sheaths causes the probe to underestimate the density. In fact, if the probe is driven sufficiently negative with respect to the plasma, the sheaths overlap and the probe does not "see" any plasma at all—the resonant frequency shift vanishes entirely.

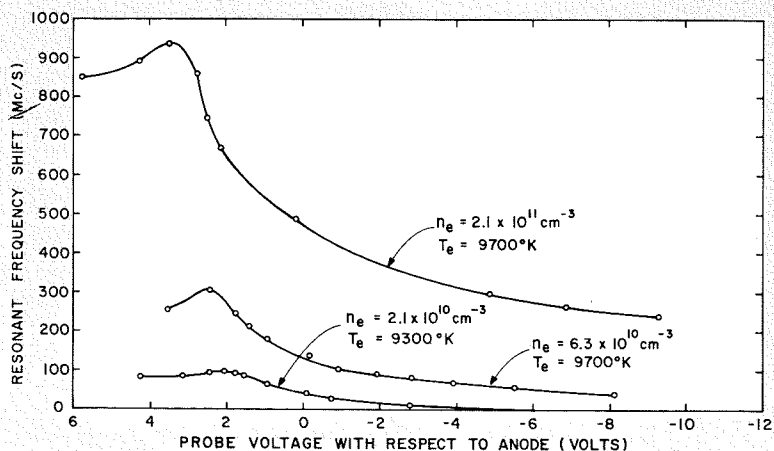
In order to eliminate the sheaths it was necessary to bias the microwave probe to plasma potential; however in doing so, the temperature of the probe

is raised and the probe expands. This, also, causes the probe to read too low. A pulsed-biasing scheme was developed in which the probe was maintained at floating or a large negative potential with respect to the plasma except during a time  $\tau$  when the sweep measurement of the resonant frequency was made. The resonance was detected by merely observing the amplitude of the wave reflected from the probe. The probe bias during the pulse time  $\tau$  was continuously adjustable and  $\tau$  was made small compared to the thermal time constant of the probe but long compared with any characteristic sheath formation times.

Fig. 5 shows the resonant frequency shift of the probe as a function of probe potential with respect to a reference electrode in the plasma. These measurements were made with the pulsed-bias technique, and the densities and temperatures noted on the curves are those obtained from Langmuir probe measurements. Notice the maximum shift which occurs in each case; this peak, or maximum shift, takes place when the probe is at plasma potential.

The vertical arrows in Fig. 1 show, for some selected points, what density the microwave probe would indicate if it were left floating. As can be seen the discrepancy between the biased- and floating-probe densities approaches an order of magnitude at low densities although it becomes smaller at high densities. Fig. 6 shows a correlation between sheath thickness and the discrepancy between the floating microwave- and Langmuir-probe densities and bears out the contention that the discrepancy is mainly due to the sheaths. The sheath sizes in Fig. 6 were computed using the planar sheath theory of Bohm<sup>9</sup> with temperatures and densities obtained from the Langmuir-probe.

Fig. 5—Resonant frequency shift of the microwave probe as a function of probe bias (pulsed) voltage. Note the peaks which occur when the probe is near space potential.



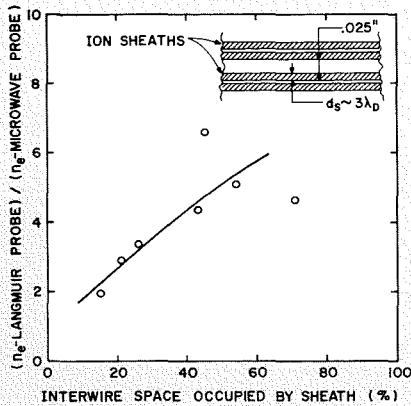


Fig. 6—Ion sheaths around the microwave probe tend to make the probe read too low (see Fig. 1).

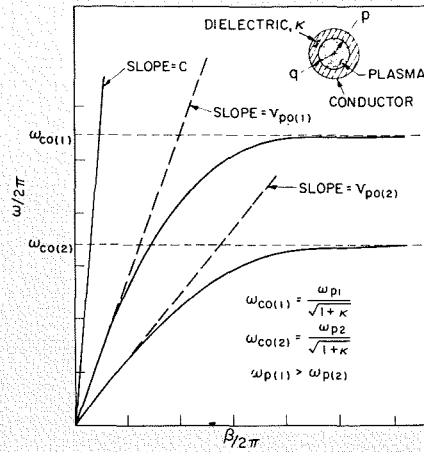


Fig. 7—Dispersion curves of the azimuthally-symmetric TM slow-wave mode on a plasma column for two different values of  $\omega_p$ .

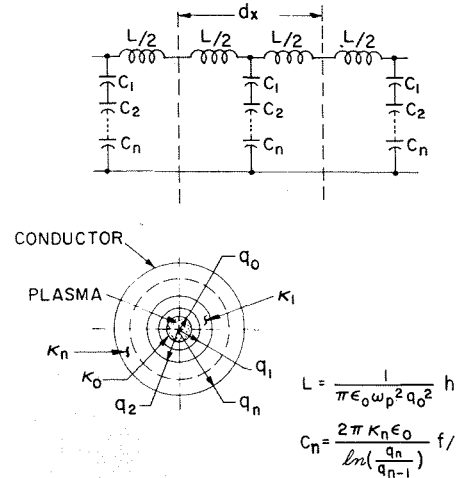


Fig. 8—Transmission-line equivalent circuit for a plasma column surrounded by dielectric shells and a metal cylinder.

### SURFACE WAVE MEASUREMENTS

This diagnostic technique uses the propagation characteristics ( $\omega$  vs.  $\beta$ ) of an axially-propagating wave on a cylindrical plasma column as a means of determining the density of the column. Here  $\beta = 2\pi/\lambda_p$  where  $\lambda_p$  is the wavelength of waves of radian frequency  $\omega$ .

At sufficiently low frequencies,  $\omega \ll \omega_p$ , a plasma column coaxial with a metal cylinder can support a class of waves which have a phase-velocity  $v_p$  less than the velocity of light. The dispersion curve for the lowest order circularly symmetric mode is shown in Fig. 7 for two different uniform plasma densities. Propagation is possible from zero frequency up to some cutoff frequency  $\omega_{co}$ . The low-frequency regime is non-dispersive and it can easily be shown assuming a cold collisionless plasma that the limiting low-frequency phase velocity is given by:

$$v_{po} = \text{Limit} \left. \frac{\omega^2}{\beta^2} \right|_{\omega \rightarrow 0} = \omega_p^2 p^2 \left[ \frac{\ln\left(\frac{q}{p}\right)}{2\kappa} \right] \quad (2)$$

Clearly, either a knowledge of  $\omega_{co}$  or  $v_{po}$  is sufficient to determine  $\omega_p$  and the corresponding plasma electron density in this case. However the low-frequency measurement was emphasized in the present work because  $\omega_p^2$  in Eq. 2 may be replaced in the case of a radially non-uniform plasma by a simple average  $\omega_p^2$  (proportional to the average density

across the column), while the  $\omega_p$  in the expression for  $\omega_{co}$  (see Fig. 7) is dependent on some unknown average of the density near the column edge<sup>8</sup>. Furthermore, an accurate determination of  $\omega_{co}$  is difficult because the attenuation is high in this region (group velocity  $[d\omega/d\beta] \rightarrow 0$ ).

If the dielectric surrounding the plasma column is not homogeneous as shown in Fig. 7 but is composed of a series of cylindrical shells with differing dielectric constant then Eq. 2 becomes

$$v_{po}^2 = \text{Limit} \left. \frac{\omega^2}{\beta^2} \right|_{\omega \rightarrow 0} = \omega_p^2 q_0^2 \left[ \frac{\ln\left(\frac{q_1}{q_0}\right)}{2\kappa_1} + \frac{\ln\left(\frac{q_2}{q_1}\right)}{2\kappa_2} + \dots + \frac{\ln\left(\frac{qn}{qn-1}\right)}{2\kappa_n} \right] \quad (3)$$

where  $p = q_0 < q_1 < q_2 < \dots$  and  $\kappa_n$  is the dielectric constant of the medium in region  $q_{n-1} < r < q_n$ .

If the attenuation constant  $\alpha$  is not small compared to the phase constant  $\beta$ , it is necessary to modify Eq. 3 in order to allow for the effect of collisions. One can easily show that the density measurement is still possible but that  $\omega^2/(\beta^2 - \alpha^2)$  should be substituted in Eq. 3 for  $\omega^2/\beta^2$ . In this case by measuring both  $\omega$  vs  $\beta$  and  $\omega$  vs  $\alpha$ , one can also obtain the effective collision frequency

$\nu_c$ . In the present work close agreement of measured and expected values of  $\nu_c$  has been noted in helium plasmas.

The form of Eqs. 2 and 3 suggests an equivalent transmission line representation, Fig. 8, with phase velocity  $v_p$  given by  $v_p^2 = 1/LC$ . Using the cold plasma permittivity  $\epsilon_p = \epsilon_0 [1 - (\omega_p^2/\omega^2)]$  it can readily be shown that for  $\omega \ll \omega_p$  a plasma column of radius  $q_0$  behaves for axial fields as though it had an equivalent inductance per unit length given by:

$$L = \frac{1}{\epsilon_0 \omega_p^2 \pi q_0^2} \quad (4)$$

Consideration of the electric field patterns as  $\lambda_p/q_0$  becomes large suggests that it is physically correct to identify  $L$  with the axial inductance of the equivalent transmission line and to treat the dielectric shells as a series combination of cylindrical capacitors as in Fig. 8. Thus, for  $q_0 = p$ :

$$\frac{1}{C} = \frac{1}{2\pi \epsilon_0} \sum_{j=1}^n \frac{\ln\left(\frac{q_j}{q_{j-1}}\right)}{\kappa_j} \quad (5)$$

Notice that  $C$  depends only on quantities external to the plasma and  $L$  depends only on the plasma density and size. This is true for the cold plasma model so long as no region of the plasma becomes under dense, i.e., providing  $\omega_p \gg \omega$  everywhere, and is in part responsible for the desirable averaging properties predicted by this model.

The improved accuracy resulting from using a (uniform) hot plasma model

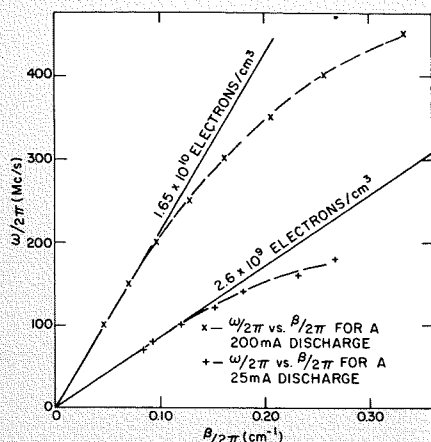


Fig. 9—Experimental dispersion curves for two helium discharges showing average densities calculated using the low-frequency phase velocities.

was mentioned earlier in discussing comparative density measurements. In this case the expression for  $1/C$ , Eq. 5, is modified by the plasma as if there were an additional dielectric shell of thickness  $\sim \lambda_d$  inside the plasma radius  $q_0$ . However, the expression for  $L$ , Eq. 4, remains unchanged. As also stated earlier, it is believed that when a nonuniform hot plasma is considered, the surface-wave-vs-Langmuir-probe correlation will become even closer. This should come about because the thickness of the additional capacitive layer inside the plasma should be determined by a larger  $\lambda_d$  depending on the density in the vicinity of the column edge.

Fig. 9 shows typical dispersion curves obtained for two 0.15-torr helium plasmas in a 2-cm-diameter discharge column. The indicated densities were calculated by means of Eq. 3 from the slopes in the non-dispersive region.

Experimentally, dispersion characteristics were measured by the method indicated in Fig. 10. Here, microwave power from the signal generator is directed to split-ring couplers at either end of the slotted line which is also of split construction to permit assembly around the discharge column. A probe travelling along the slot samples the surface wave fields within the slotted line and this signal superimposed on a large signal fed directly from the signal generator through the reference arm exhibits periodic maxima and minima with spacing  $\lambda_g$  (Fig. 11, curve *b*). If no signal is fed through the reference arm, Fig. 11 curve *a* is obtained. The

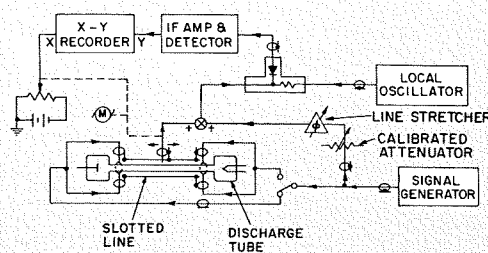


Fig. 10—Block diagram of the circuit used to measure the propagation constants ( $\alpha$  and  $\beta$ ) by the calibrated-reference-signal method.

periodicity of  $\lambda_g/2$  in this case is due to a weak reflected wave and is used to determine  $\lambda_g$  when the attenuation is not large and the reflected wave stronger. More precise measurements of  $\beta$  and  $\alpha$  are also possible by adjusting the reference arm phase shifter and attenuator for a null output at various positions of the travelling probe as indicated by curves *c* and *d* of Fig. 11.

#### LANGMUIR PROBES

A Langmuir probe is simply a small current-collecting electrode immersed in a plasma. The current-voltage ( $I_p-V_p$ ) characteristic of the probe is interpreted to yield plasma parameters, usually  $n_e$  and an average electron "temperature"  $T_e$ . Here  $I_p$  is the current flowing from probe to plasma and returning via a usually larger reference electrode connected to an external circuit, and  $V_p$  is the voltage applied between probe and reference electrode. A great variety of probe forms and specialized probe analyses have been developed in the forty-odd years since Langmuir and co-workers established the basic method<sup>10</sup>. Of these many possibilities, we have chosen to concentrate on the spherical Langmuir-probe method and to employ a second derivative (SD) analysis. Here we will describe the basic features of this method and discuss some of the interpretational ideas developed in the present work, but will omit, for the sake of brevity, any report on our studies by high-frequency methods of probe phenomena near plasma-potential and of high-frequency probe diagnostics<sup>5b</sup>.

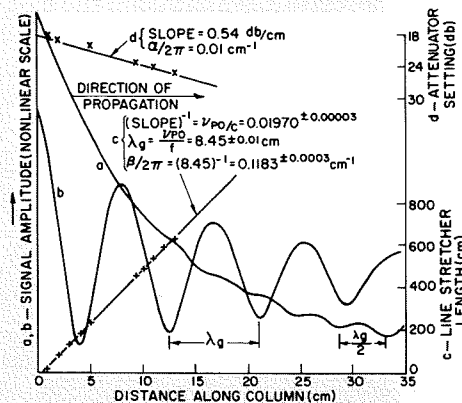


Fig. 11—A typical measurement of the propagation constants ( $\alpha$  and  $\beta$ ) of a slow-wave in a 9.6-mA Xenon discharge at 70 Mc/s. This measurement was made using the calibrated-reference-signal method: (a) amplitude of the slow-wave along the column (note the residual standing-wave pattern on the right), (b) amplitude of the sum of the slow-wave and the reference signals along the column, (c) phase-shift equivalent air-length of the slow-wave along the column, and (d) amplitude (equivalent attenuation) of slow-wave along the column.

The SD method has two important advantages which recommend it for applications where detailed accurate results are important: 1) The actual electron energy distribution is determined without prior assumption of the form of the distribution, instead of a single parameter such as  $T_e$ . 2) Densities can be measured with smaller probes and therefore with less plasma perturbation than is possible with those other Langmuir probe methods which also sample the whole of the electron energy distribution.

We illustrate the last point first. Fig. 12 indicates one of the more common methods of Langmuir probe analysis. Plasma potential  $V_s$  and the corresponding probe current  $I_{ps}$  are estimated by a linear extrapolation of the  $\log(I_p - V_p)$

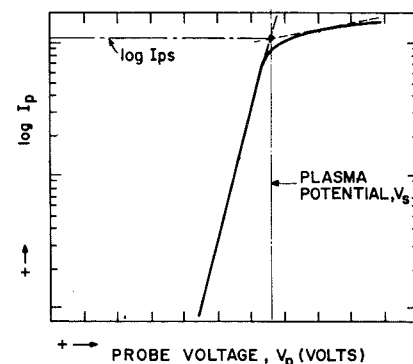


Fig. 12—Typical  $\log I_p$  vs.  $V_p$  characteristics of a Langmuir-probe showing the "customary" procedure of extrapolating the electron retarding and saturation regions to obtain the saturation current and space potential.

characteristic from the electron retarding and electron accelerating regions.

The slope  $d(\ln I_p)/dV_p = kT_e/e$  of the electron retarding region ( $V_p < V_s$ ) determines a value for  $T_e$  and thus a mean random electron velocity  $\bar{v}_e = [8kT_e/\pi m_e]^{1/2}$  where  $k$  is Boltzmann's constant and  $m_e$  is the electron mass. Then,  $n_e$  is given by:

$$n_e = \frac{4 I_{ps}}{e \bar{v}_e A_p} \quad (6)$$

where  $e$  is the electronic charge and  $A_p$  is the probe area.

The method of Fig. 12 fails unless  $(\lambda_d/V_p) \ll 1$ , since a pronounced electron saturation is required to find  $V_s$  and  $I_{ps}$ . Fig. 13 shows a typical set of characteristics obtained in the present work for a case in which  $(\lambda_d/V_p) \approx 0.6$ . The  $(I_p - V_p)$  characteristic (Fig. 13a) shows no recognizable saturation, but  $V_s$  and, hence  $I_{ps}$ , is given directly

by the zero in the SD characteristic ( $d^2 I_p/dV_p^2$ ) vs  $V_p$  (Fig. 13b) and by the corresponding deep minimum in the  $\log |SD|$  characteristic (Fig. 13c).

Fig. 13b and 13c were recorded automatically by measuring the second-harmonic current generation due to a small sinusoidal voltage superimposed on  $V_p^{11}$ . Besides indicating  $V_s$ , the SD characteristic is extremely useful in its own right. The SD in the electron retarding region is related to the normalized electron energy distribution function  $F(W)$  when energy  $W$  is measured in electron volts by:

$$\frac{d^2 I_p}{dV_p^2} = \frac{n_e e A_p (2e)^{1/2}}{4} \frac{F(W)}{W^{1/2}} \quad (7)$$

for  $W \geq 0$ , where  $W = V_s - V_p$ .

From an SD measurement one can thus obtain  $F(W)$  and then calculate any desired moment of  $F$ . For example, to determine density via Eq. 6, one needs  $\bar{v}_e$  which is given by  $\bar{v}_e = (2e/m_e)^{1/2} W^{1/2}$ .

It is frequently possible to recognize a measured SD corresponding to an energy distribution  $F$  of a particular analytic form. In fact, the SD is often simpler in form than the corresponding  $F$ . For example, the SD of a Maxwellian distribution is just the Boltzmann exponential,  $\exp[-e(V_s - V_p)/kT_e]$  and the SD of a Druyvesteyn distribution is an exponential in  $(V_s - V_p)^2$ ,  $\exp[-(V_s - V_p)^2/V_D^2]$  where  $V_D$  and  $T_e$  are parameters of the particular distributions. Fig. 14a shows the  $\log |SD|$  characteristic measured on the axis of an approximately Maxwellian helium positive column plasma. Note that  $\log |d^2 I/dV_p^2|$  is approximated by a straight line when plotted against  $(V_s - V_p)$ . Fig. 14b shows the result of raising the helium pressure. Here, the elastic electron-neutral collisions have become more important in moderating the electron energy than the electron-electron collisions and a Druyvesteyn distribution has been approximated as is shown by plotting  $\log |SD|$  vs  $(V_s - V_p)^2$ .

Fig. 14c shows a more complicated characteristic obtained in the same helium discharge represented by Fig. 14a. In this case, the characteristic was measured in an axially nonuniform transition region near the junction of the positive column with a much cooler plasma in the vicinity of the discharge tube cathode. One sees here a low energy distribution on which is superimposed a high energy group of electrons which have been accelerated through the double layer between the low temperature plasma and the column plasma.

## QUALITATIVE MEANING OF THE SD FUNCTION

The very simple form taken by the SD of the Maxwellian and Druyvesteyn distributions suggests that the SD function may have a readily interpretable physical meaning which will be useful even when the SD has no standard recognizable form. In fact the SD is proportional to the product of the total density and the probability of occupation of the available states in each energy range. Thus, recalling from statistical mechanics that the statistical weight of single particle translational energy states in an energy range  $dW$  is proportional to the product of the available volume in real space and the volume in momentum  $2\pi(2m_e)^{3/2} W^{1/2} dW$  corresponding to the energy interval  $W$  to  $(W + dW)$  we can write:

Fig. 13—Typical  $I_p$ ,  $d^2 I_p/dV_p^2$ , and  $\log |SD|$  vs.  $V_p$  curves for a small spherical Langmuir-probe ( $\lambda_d/r_p \approx 0.6$ ).

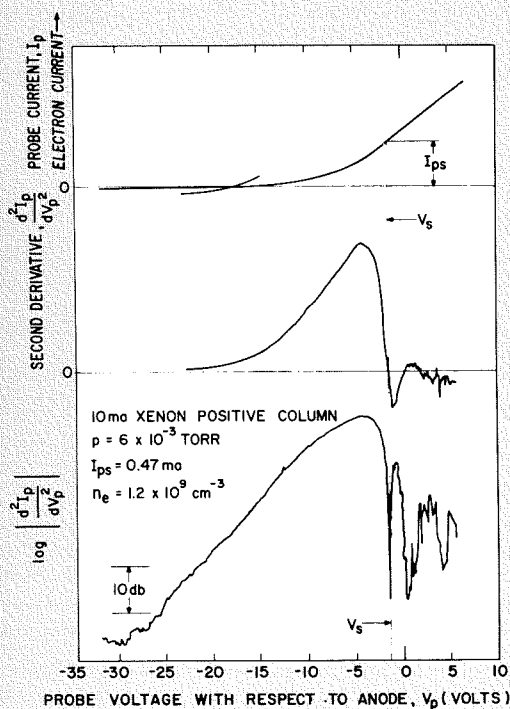
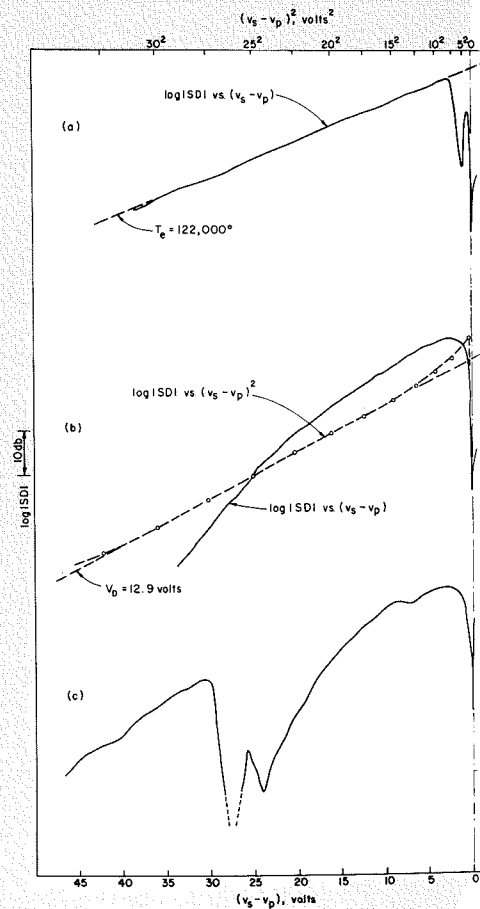


Fig. 14—Examples of SD measurements in a helium positive column (2-cm dia.). (a)  $\log |SD|$  vs.  $(V_s - V_p)$  in axially uniform region at 0.15 torr. (b)  $\log |SD|$  vs.  $(V_s - V_p)$  and  $(V_s - V_p)^2$  in axially uniform region at 0.54 torr. (c)  $\log |SD|$  vs.  $(V_s - V_p)$  in axially nonuniform region at 0.15 torr.



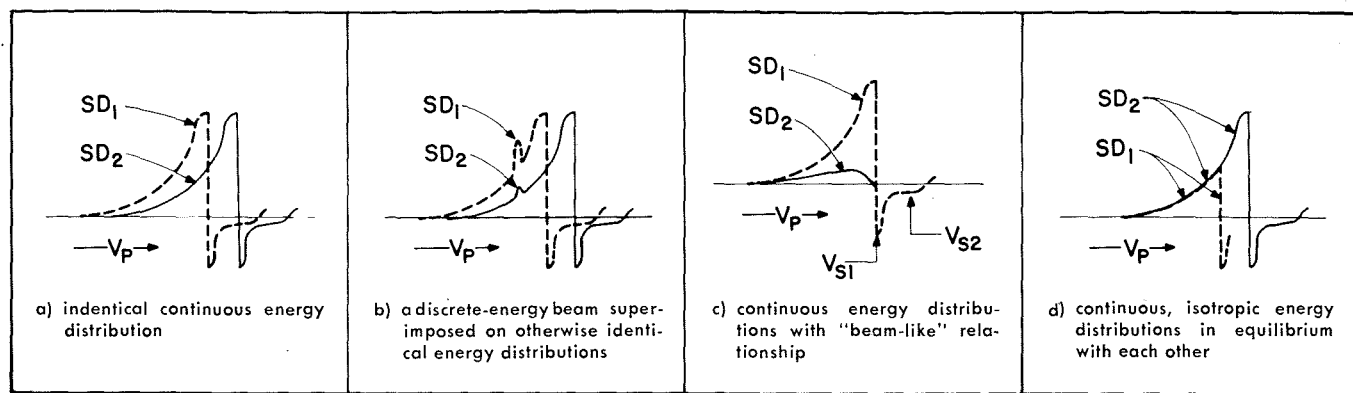


Fig. 15 — Some possible relationships between SD functions from regions of a plasma having different space potentials ( $V_{s2} > V_{s1}$ ).

$$n_e \times \frac{\text{fractional dens in } W \text{ to } (W + dW)}{\text{statistical wt of } W \text{ to } (W + dW)} \\ \propto \frac{n_e F(W) dW}{W^{1/2} dW} \propto \frac{1}{A_p} \left. \frac{d^2 I_p}{dV_p^2} \right|_{V_p = V_s - W} \quad (8)$$

Perhaps one of the more valuable by-products of the present work has been the recognition of this simple relationship (which *does not* seem to have been emphasized previously). For example, in the present work this concept proved very helpful in studying the processes responsible for various types of steady-state equilibria between different regions of the same discharge. Space prevents a detailed description of these results, but Fig. 15 presents in schematic form some of the phenomena noted in the positive column studies. Fig. 15a shows the usual effect of *axial* translation of a probe in a positive column. In this case the change in plasma potential is accompanied by both non-conservative processes (such as excitation and ionization) and direction randomizing processes (such as elastic collisions). Fig. 15d shows the typical effect of a *radial* translation with  $SD_1$  measured at larger radius than  $SD_2$ . Note that  $SD_1 = SD_2$  in the voltage range where both are electron retarding. This behavior is typical of a steady-state equilibrium between two isotropic distributions with little or no net flow between the two regions for every energy class. The condition is promoted in this case by elastic collisions, by the radially confining sheath fields, and by the symmetry existing in axial and azimuthal directions. Finally, Figs. 15b and 15c show two examples of what we call *beam-like* distributions, which occur in the absence of direction randomizing processes such as collisions. The amplitude of the SD of a beam-like distribution decreases as the beam is accelerated from region 1 to region 2 because the number of available states in

momentum space increases but the number occupied remains constant.

#### SUMMARY

Carefully-controlled, simultaneous comparative density measurements have demonstrated good agreement between two different microwave techniques and the Langmuir-probe. It was also shown that even better agreement can be obtained by refining the measurement method (pulsed-biasing of the microwave probe) or by using a more physical plasma model (hot-plasma). Each technique has its own inherent advantages which recommend it for particular applications.

The surface-wave measurement is ideal where a density and collision-frequency in a long thin plasma column are required. A gaseous laser contains a plasma of just such a geometry and the use of probes to measure density may be impossible because of their size and perturbing effect. There is no reason why the surface-wave measurement can not be properly scaled to permit application in other density ranges.

In situations where probes are permissible, the microwave probe can be quite useful since it allows very rapid measurements and can, in principle, also measure the collision frequency. By careful design the density range capability of this probe can be made very broad. In addition to application in laboratory plasmas, it can also be scaled to lower frequencies and employed for upper-atmosphere research or satellite-mounted for space measurements.

The small Langmuir-probe with second-derivative analysis provides uniquely detailed knowledge of the distribution in space and energy of plasma electrons. This type of measurement can lead to a clearer understanding of such gas discharge devices

as thermionic converters, coherent light sources, etc.

#### ACKNOWLEDGEMENTS

The authors wish to gratefully acknowledge the stimulating discussions and suggestions of many of their colleagues and, especially, the contributions of D. d'Agostini (deceased March 1963) and Dr. M. Glicksman during the early phases of the work. Thanks are also due A. E. Hahn, Jr., for his invaluable technical assistance during the long, and sometimes trying, experimental period.

#### BIBLIOGRAPHY

- Loeb, L. B., *Basic Processes of Gaseous Electronics*, University of California Press, Berkeley, Calif.; 1955, Chap. IV, Part II, "The Theory and Use of Probes."
- Anderson, J. M., "Ultimate and Secondary Electron Energies in the Negative Glow of a Cold-Cathode Discharge in Helium," *J. Appl. Phys.*, Vol. 31, p. 511; 1960.
- Levitskii, S. M. and Shashurin, I. P., "Transmission of a Signal Between Two High Frequency Probes in a Plasma," *Sov. Phys.-Tech. Phys.*, Vol. 3, p. 319; 1963.
- Crawford, F. W., "Internal Resonances of a Discharge Column," *J. Appl. Phys.*, Vol. 35, p. 1365; 1964.
- Peterson, C. C., Dienst, J. F. and d'Agostini, D. (RCA Labs, Princeton); *Simultaneous Plasma Analysis Techniques*, Tech. Rpt. AFAL-TR-65-197, Part I; 1965.
- Peterson, C. C., Dienst, J. F. and d'Agostini, D. (RCA Labs, Princeton); *Simultaneous Plasma Analysis Techniques*, Tech. Rpt. AFAL-TR-65-197, Part II; 1965.
- Harp, R. S. and Crawford, F. W., "Characteristics of the Plasma Resonance Probe," *J. Appl. Phys.*, Vol. 35, p. 3436; 1964.
- Levitskii, S. M. and Shashurin, I. P., "Resonant Microwave Probe for Measuring Charge Density in a Plasma," *Sov. Phys.-Tech. Phys.*, Vol. 6, p. 315; 1961.
- Trivelpiece, A. W., *Slow-Wave Propagation in Plasma Waveguides*, Tech. Rpt. No. 7, Calif. Inst. of Tech., Pasadena, Calif., (Available as PB151638 from Office of Tech. Serv., U.S. Dept. of Commerce); 1958; ALSO Trivelpiece, A. W. and Gould, R. W., "Space Charge Waves in Cylindrical Plasma Columns," *J. Appl. Phys.*, Vol. 30, p. 1784; 1959.
- Guthrie, A. and Wakerling, R. K. (Editors), *Characteristics of Electrical Discharges in Magnetic Fields*, p. 77, "Minimum Kinetic Energy for a Stable Sheath" by D. Bohm, McGraw-Hill Book Co., Inc., New York; 1949.
- Langmuir, I. and Mott-Smith, H., "Theory of Collectors in Gaseous Discharges," *Phys. Rev.*, Vol. 23, p. 727; 1926.
- Branner, G. R., Friar, E. M. and Medicus, G., "Automatic Plotting Device for the Second Derivative of Langmuir Probe Curves," *Rev. Sci. Instr.*, Vol. 34, p. 231; 1963.

# LASER MEASUREMENT OF ELECTRON DENSITY IN DENSE, HIGH-TEMPERATURE PLASMA

Temperatures in the range of 14,000 to 16,000 °K are attainable in the potential core region of an argon plasma jet operating in the laminar mode. Measurement of the electron concentration in such high temperature plasma by conventional probe and microwave techniques is extremely difficult. The use of laser interferometer techniques appears to be promising and in this paper electron concentration measurements obtained using a HeNe two-cavity laser interferometer are presented. Use is made of the 3.39- $\mu\text{m}$  radiation to obtain a large phase shift: the visible 6,328-angstrom radiation is used for alignment and detection. The effects of scattering of the laser radiation by the plasma jet when operated in the turbulent mode are also reviewed.

**A. BOORNARD, L. J. NICASTRO, and Dr. J. VOLLMER**

*Applied Research, DEP, Camden, N.J.*

**A. BOORNARD** received the BS in 1953 from the College of William and Mary with physics as a major and the MS in physics from Indiana University in 1955. He joined RCA and the Applied Research Section in 1957. His work experience includes gamma ray and neutron damage in semiconductors; properties of thin film superconductors; microwave generation techniques and electromagnetic wave-plasma interactions. His plasma physics work includes studies of the effects of nuclear burst induced ionization on electromagnetic wave propagation, the effects of ionized rocket engine exhausts on radar and communications, and the microwave transmission characteristics of dense high temperature plasmas. He is presently engineering leader of the Plasma Physics Group. The major activities of this group are: beam-plasma microwave generation, Cerenkov microwave generation, plasma diagnostic techniques, and the interaction of electromagnetic waves with rocket exhausts. Prior to joining RCA, Mr. Boornard served with the U.S. Army and was assigned to Frankford Arsenal in Philadelphia. His work there consisted of studies of conduction in thin metallic films, and radiation effects in metals and thin films. Mr. Boornard is a member of the American Physical Society.

**L. J. NICASTRO** received a BA in Physics from LaSalle College in 1953. In 1955-1956 he attended the University of Rochester on an Atomic Energy Commission Radiological Physics Fellowship and obtained an MA in Radiation Biology. He is presently a candidate for the PhD in Physics at Temple University. Mr. Nicastro was an instructor in Chemistry and Physics at LaSalle College, 1953-1954; a Physicist in Ballistics at the Frankford Arsenal, 1954-1955; and a Health Physicist at the Brookhaven National Laboratories during the summer of 1956. From September 1956 to March 1959, Mr. Nicastro worked in the Neutron Physics Section of the National Bureau of Standards, where his main interests were neutron spectrometry, measurements of neutron age and neutron cross-sections,

neutron detection methods, and the response of various scintillators to alpha particles. Since coming to RCA early in 1959, Mr. Nicastro has done experimental work in the areas of gaseous molecular frequency standards, laser radar, measurement of fluorescent time constants of laser materials, design and development work on a high-power, nanosecond  $\Phi$ -controlled laser, and the measurement of plasma properties using lasers. Recently, Mr. Nicastro has been involved in experimental and analytical studies in the general area of display techniques. Included in these investigations were modulation of light by means of Kerr and Faraday magneto-optic rotators, light modulation by electro-optic crystals, laser displays, and measurements of physical properties of cadmium-selenide.

**DR. JAMES VOLLMER** received a BS in General Science at Union College in 1945, an MA and PhD in Physics at Temple University in 1951 and 1956, respectively. His research activity has included plasma physics, infrared properties of materials, nuclear radiation damage to semiconductors, and studies in X-ray diffraction. After teaching for five years at Temple University, and supervising a research group for eight years at Minneapolis-Honeywell, Dr. Vollmer joined RCA in 1959. He became Leader of the Plasma Physics Group at that time. In 1963, Dr. Vollmer was promoted to Manager of Applied Physics. In this position he is responsible for research programs embracing plasmas, lasers, masers, optics, superconductivity and displays. He is a member of the American Physical Society, past President of the Philadelphia Physics Club, a Senior Member of the IEEE, a Director of the Philadelphia Science Council, a member of the Franklin Institute, and a member of the AAAS. His honors include membership in Phi Beta Kappa, Sigma Xi, and Sigma Pi Sigma. He has published many papers in professional journals, and has U.S. patents both issued and pending.

**T**HE electromagnetic properties of a plasma are completely specified if the electron density and collision frequency are known. Techniques for measuring these quantities are, therefore, of particular interest to anyone who must deal with a plasma as part of his environment. In this paper a laboratory investigation is described in which coherent radiation from a laser is used to determine the electron density in a dense, high temperature, high velocity plasma stream.

Outside the laboratory, such plasmas occur as the exhaust from rocket engines (although these are far more complex), in plasmas employed in controlled fusion research, and in magnetohydrodynamic power converters. Whereas Langmuir probes<sup>1</sup> and double probes<sup>2</sup> can be employed for measurement in stationary low temperature plasmas, they are not suitable in a flowing high temperature plasma. Such probes are subject to erosion and melting. Furthermore, they

*Final manuscript received September 13, 1965*



**A. Boornard**



**L. Nicastro**



**Dr. J. Vollmer**

produce changes in the local temperature and flow properties, which in turn alter the plasma properties. Microwave diagnostic techniques<sup>3</sup> can be used if the extent of the plasma is large compared to the wavelength and if the density is less than  $10^{13}$  electrons/cm<sup>3</sup>. Millimeter waves are useful up to  $10^{15}$  electrons/cm<sup>3</sup>. For higher electron densities, however, optical frequencies are required, for which the laser is an obvious source. (Here, optical frequencies are considered to range from far infrared to short ultraviolet.)

The laser's high degree of spatial and temporal coherence, as well as the small diameter of the beam, make it suitable as an electromagnetic probe or interferometer. In RCA Applied Research, Camden, both approaches were used to measure the electron density of plasma from an arc jet. Before discussing each approach and the results, however, a brief description of the jet is not only appropriate, but necessary.

### PLASMA ARC JET

Gaseous plasma may be produced in a variety of ways, but the most common method is by electrical discharge. In an arc jet<sup>4</sup> (Fig. 1), gas is passed through a nozzle while a large direct current is simultaneously passed from the axial cathode to the nozzle anode. The resultant plasma is highly ionized; it is at a high temperature; and it has a large flow velocity. Such jets are particularly useful because a variety of gases can be studied over wide ranges of temperature and ionization, and under distinctly different flow conditions. In contrast to other techniques for generating high-temperature plasmas, such as the shock tube, the arc jet produces an effectively steady state plasma. However, measurement of the plasma characteristics is, as noted earlier, difficult. Insertion probe techniques require complicated and expensive cooling systems; and microwave wavelengths are comparable to the dimensions of the jet, so that diffraction effects complicate the analysis.<sup>5</sup>

A further complication is that three regions of distinctly different plasma properties develop within the jet (Fig. 2). Beginning at the nozzle exit, a dense, laminar potential core exists (Region I). This region merges into a transition region (Region II) where a large decrease in temperature and increased turbulence occur. A region of fully developed turbulence (Region III) completes the jet structure. It is in Region I that measurement difficulties are most severe. The region is small, the temperature can be very high (18,000°K), and the electron density is large ( $10^{17}$  electrons/cm<sup>3</sup>). In addition, the nozzle interferes with microwave probe measurements. On the other hand, the flow is nearly laminar in this region and the gas temperature can be computed from the input power, the cable losses, the jet efficiency, and the thermal properties of the gas. All of this information is available. Thus, by assuming the gas in thermal equilibrium, then applying the Saha equation<sup>6</sup> and the ideal gas law, the electron density and temperature at the nozzle exit can be computed. Fig. 3 is a plot of these parameters for an argon plasma. Recapitulating: Region I of the arc jet is a volume of dense, high temperature plasma of known characteristics. Accordingly, it is an ideal medium for evaluating the usefulness of coherent light as a plasma diagnostic tool.

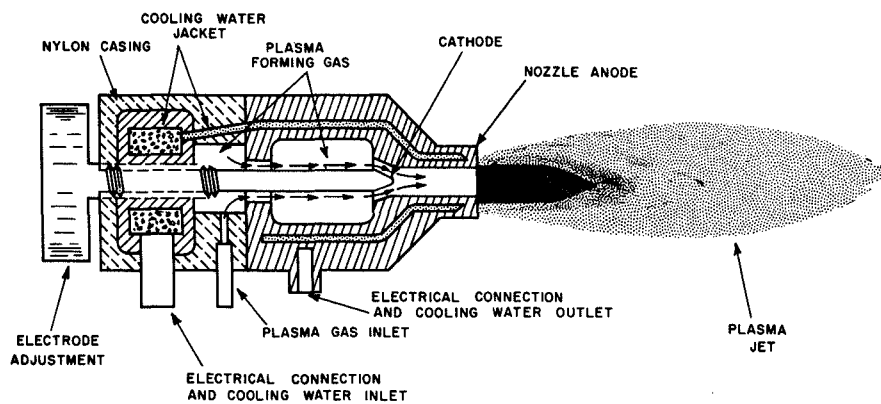


Fig. 1—Arc jet plasma generator.

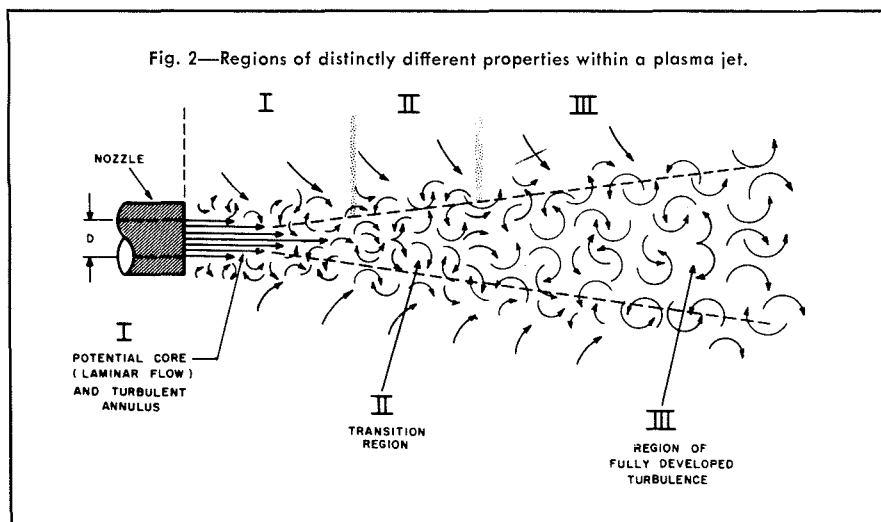


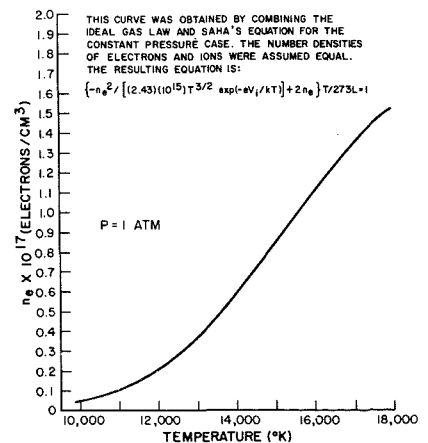
Fig. 2—Regions of distinctly different properties within a plasma jet.

### SOME FUNDAMENTAL RELATIONS

The measurement of electron density by the interaction of electromagnetic waves with a plasma rests upon a few fundamental relationships which are basic to understanding the measurement techniques.

When an electromagnetic wave propagates in a medium, the wavelength is  $\lambda_0/\eta$ , where  $\lambda_0$  is the free space wavelength and  $\eta$  is the index of refraction. In a plasma, the index of refraction is generally a complex number and is fixed

Fig. 3—Electron density vs temperature for argon.



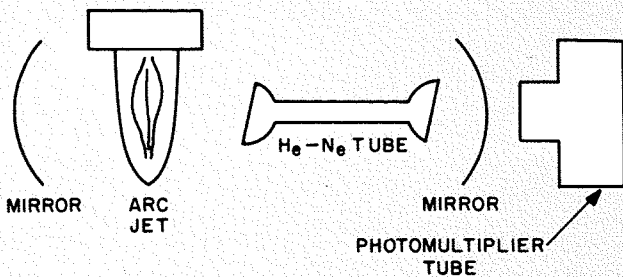
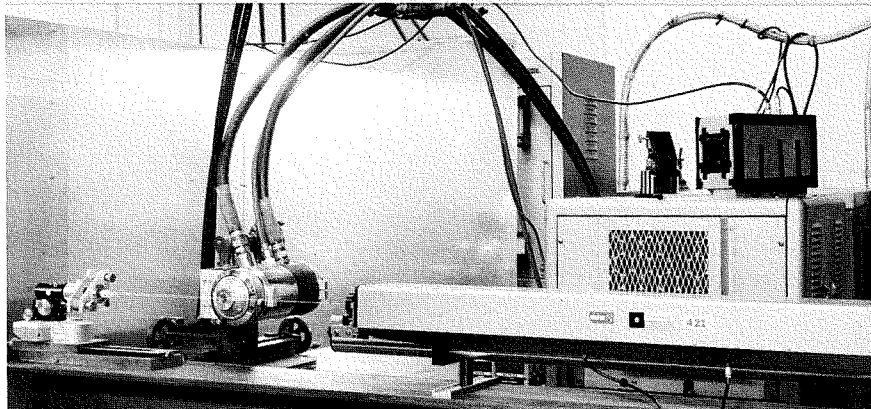


Fig. 4a—Schematic showing arc jet inside laser cavity.

Fig. 4b—Photograph of arc jet set up to intersect laser path.



not only by the electron density, but also by the collision frequency.<sup>7</sup> However, the collision frequency is almost always several orders of magnitude smaller than optical frequencies. Similarly, the plasma frequency, which is fixed by the electron density, is also small compared to optical frequencies. Under these circumstances the index of refraction of the plasma is given to a high degree of approximation by:

$$\eta \approx 1 - \left( \frac{n_e e^2 \lambda_o^2}{2\pi c^2 m_e} \right) \quad (1a)$$

where all quantities are in cgs-electrostatic units. When appropriate values of the constants are inserted, Eq. 1a becomes:

$$\eta \approx 1 - (4.48) (10^{-14}) n_e \lambda_o^2 \quad (1b)$$

In these expressions,  $n_e$  is the electron density,  $e$  is the electron charge,  $c$  is the velocity of light in free space, and  $m_e$  is the mass of the electron. Two techniques which rely upon changes of the plasma refractive index were examined to determine the electron density. One technique involves placing the plasma within a laser cavity. The second relies upon interferometric principles.

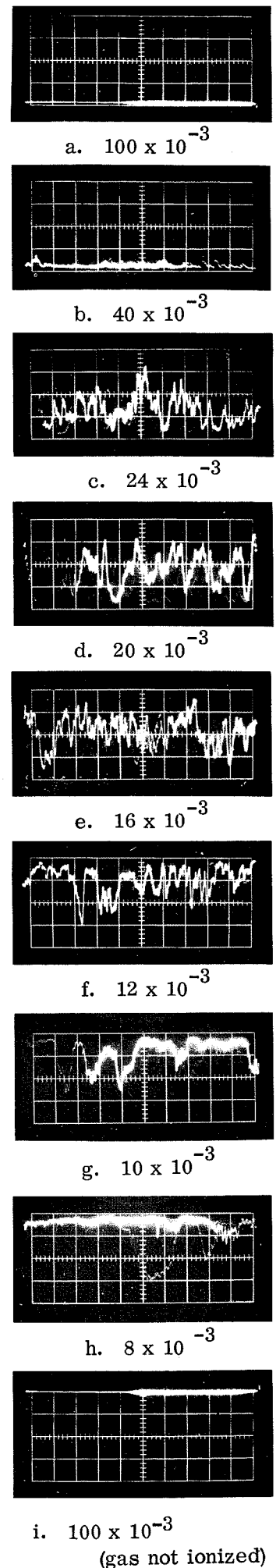
#### LASER CAVITY TECHNIQUE

The laser as a light source is basically an oscillator. It consists of an excited medium which emits radiation and a Fabry-Perot cavity.<sup>8</sup> For laser action to occur, the optical path between the mirrors constituting the cavity must be an integral number of half wavelengths. It

follows that if a medium is placed within the cavity, the optical length of the cavity is altered and the laser action will be altered. Because the effect will occur within the cavity, the gain of the laser will amplify the effect, making the device very sensitive. If Region I of the jet were to be placed as shown in Fig. 4a, and if the electron density were varied by changing the plasma temperature, the laser output would exhibit correlative variations. For given values of voltage and current in the arc, the temperature and electron density increase as the flow rate is decreased. Therefore, a regular variation in laser output would be expected as the electron density is slowly altered by changing the mass flow rate. Scope traces of the laser output, under these conditions, as detected with a photomultiplier tube, are shown in Fig. 5. Traces *a* to *h* are for decreasing flow rate.

Two effects are identifiable. One is that as the flow rate is decreased, the average laser output increases. The output is very noisy and no periodicity of average amplitude from trace to trace is present. The second is that a high frequency effect is present in traces *g* and *h*, which represent the most nearly laminar flow conditions. Consider the average effects first. The anticipated effects of electron density are washed out. It

Fig. 5—Effect of plasma variations within laser cavity. As the gas flow decreases, the gas temperature and electron density increase. Values beneath each trace are flow rates in moles/second.



appears that this results from the scattering effects of the turbulence, which exists under the high flow rate conditions. Presumably these scattering losses are so high initially that the laser fails to get above threshold (trace *a*). As the flow is reduced, the turbulence diminishes and the average laser output increases, but is still sporadic. Trace *i* shows, however, that the system lases for high velocity cold gas flow. (A trace identical to trace *i* was obtained for the no-flow condition.)

The high-frequency effect in traces *g* and *h* are attributed to fluctuations in the electron density of the plasma. However, in this configuration these fluctuations could not be evaluated. The cause of this variation in  $n_e$  is discussed and its magnitude evaluated in the next section by the use of a laser interferometer.

#### LASER INTERFEROMETER TECHNIQUE

An alternative approach to placing the plasma inside the laser cavity is to put it in one leg of a laser interferometer. Such an approach has been described by Ashby and Jephcott<sup>9</sup>, who used it to measure  $n_e$  in a plasma formed in a discharge tube. This scheme is shown in Fig. 6. The interferometer is seen to consist of two colinear cavities—a laser cavity and an external cavity. When each cavity is an even number of quarter-wavelengths long, a condition of system resonance exists and the laser output is at a maximum. If the external cavity length is then changed to an odd number of quarter wavelengths, a condition of antiresonance occurs, and the laser output becomes a minimum. A difference in cavity lengths of  $\lambda_o/2$ , corresponds to a phase difference of  $\pi$  radians for one way transmission (taking the index of refraction of air as 1). However, in the interferometer, the radiation is reflected back into the laser cavity, and consequently, a phase difference of  $\pi$  radians

occurs for a change in cavity length of  $\lambda_o/4$ .

The effective external cavity length can be altered by moving the end mirror, or by changing the refractive index of part of the medium in the external cavity. If the mirror is moved a distance  $\Delta l$  the number of cycles (fringes) observed is

$$N = \frac{\Delta l}{\lambda_o/2} \quad (2)$$

If the index of refraction of a portion of the medium in the external cavity is changed instead, the number of fringes observed is:

$$N = \frac{2}{\lambda_o} [\eta_2 - \eta_1] t \quad (3)$$

where  $t$  is the thickness of the altered medium and  $\eta_1$  and  $\eta_2$  are the initial and final indices of refraction of the medium. The configuration described here is the simplest case, since it calls for the laser cavity and the external cavity to be resonant in longitudinal modes only. If the configuration is modified to employ transverse modes, greater sensitivity is attainable<sup>10,11</sup> but these were not used in the data presented here. Eq. 3 can be recast in terms of electron density by combining it with Eq. 1b; it becomes:

$$N = (8.96) (10^{-14}) (n_{e2} - n_{e1}) t \lambda_o \quad (4)$$

It should be noted, however, that Eq. 3 is more general than Eq. 4. For example, the index of refraction will change if the number of neutral particles is changed, an effect not covered by Eq. 4. Moreover, the neutral density will usually change if the temperature changes. However, at temperatures above 10,000° K and at a pressure of one atmosphere, it is easy to show that free electron density is the overwhelming term. Eq. 4 is, therefore, appropriate for the experiments performed.

Another very important aspect of an interferometer is the wavelength depend-

ence evident in Eq. 4. Clearly, the number of fringes observed for a given change in electron density is proportional to the wavelength employed. In a He-Ne laser, two distinct ranges of wavelength can be present simultaneously—an infrared line (3.39  $\mu\text{m}$ ) and a group of lines in the visible ( $\sim 0.633 \mu\text{m}$ ). Furthermore, the infrared and visible radiation originate from the same excited atomic state. This means that if a variation is caused to occur in the infrared output of the laser, there will be an accompanying variation in the output power of the visible wavelengths. The interferometer is more sensitive if the infrared is used; the detector sensitivity is greater for the visible. This is an ideal condition. The interferometer can be set up to operate in the infrared region, i.e., the resonant and antiresonant conditions in the two cavities can be made to occur at 3.39  $\mu\text{m}$ . As these interferometric resonances occur, there will also be complementary variations in the visible, which can be easily detected.

Only one additional feature of the system requires explanation before the data can be discussed. It concerns the arc jet. As the gas flows through the electrode region, the arc is swept along the jet nozzle by the flowing gas. As a consequence of this traveling-arc behavior, the voltage across the electrodes is cyclic while the current remains constant. The result is a fluctuation in the temperature of the plasma at a rate of about 1 kc/s. If the arc is viewed through a narrow-band optical filter with a photomultiplier, the radiation from the arc is seen to vary at the same rate. Petschek, et al.,<sup>12</sup> have shown experimentally that the spectral intensity of the continuum radiation from an argon plasma may be described by:

$$I_\lambda = \frac{A n_e^2}{T^{1/2}} \quad (5a)$$

where  $A$  is constant. If the ratio of two intensities is observed, Eq. 5a can be written:

$$\frac{I_2}{I_1} = \frac{n_{e2}^2}{n_{e1}^2} \left( \frac{T_1}{T_2} \right)^{1/2} \quad (5b)$$

If  $T_2 = T_1 + \Delta T$ , then Eq. 5b can be expanded to give:

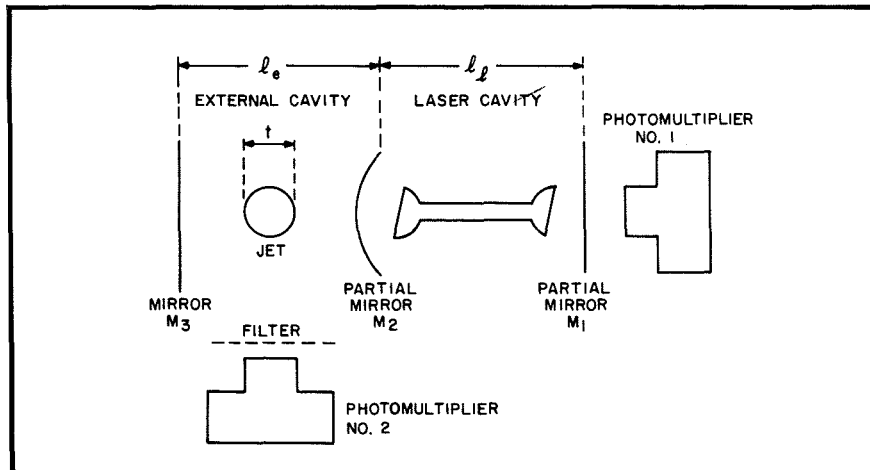
$$\frac{I_2}{I_1} \cong \left( \frac{n_{e2}}{n_{e1}} \right)^2 \left[ 1 - \frac{1}{2} \frac{\Delta T}{T_1} \right] \quad (5c)$$

If  $\Delta T/T$  is less than 5%, Eq. 5c can be further simplified to give the following result, accurate to 1%:

$$\left( \frac{I_2}{I_1} \right)^{1/2} \cong \frac{n_{e2}}{n_{e1}} \quad (5d)$$

This last equation simply recognizes that the electron density is the dominant term in Eq. 5a. Eqs. 5d and 4 show that

Fig. 6—Laser interferometer.



the absolute value of the electron density can be determined if measurements are made of the fluctuating intensity and the interferometer output.

### INTERFEROMETER EXPERIMENTS

The experiment performed can now be described. The configuration shown in Fig. 6 was employed. An additional photomultiplier tube was situated at right angles to the interferometer to view the plasma directly through a 6,328-angstrom filter. With the arc jet off and the laser on, mirror  $M_3$  was moved to increase the external cavity dimensions. The system exhibited a cyclic resonance, as expected from Eq. 2. A scope trace of this effect is shown in Fig. 7. This trace now represents a calibration curve for the interferometer. One cycle corresponds to one fringe; a swing of 9 volts represents one half of a fringe.

Next, the arc was turned on. The flow rate was  $8 \times 10^{-3}$  moles/s and laminar; the voltage was 25 volts, the current was 735 amperes, and the plasma thickness was 0.95 cm. In Fig. 8, the upper trace shows the interferometer output as the plasma electron density fluctuated. The lower trace records the fluctuating radiation from the plasma. From the interferometer output of Fig. 8, it was determined that  $N$  was less than  $1/2$ , because the interferometer output fluctuates at the same rate as the electron density and the amplitude was less than 9 volts. In addition, the largest amplitude traces of

Fig. 8, the three identified by heavy lines, are seen to occur when the minima of the interference trace coincide with the attainment of maximum electron density. The amplitude of these traces is between 4.5 and 5.5 volts, which from the calibration curve of Fig. 7 corresponds to  $N$  being between 0.34 and 0.37. Measurement of the fluctuation in amplitude of the plasma radiation is shown in Fig. 9. From this trace, it can be shown that  $I_2/I_1 = 1.25$ . Using these measured values with Eq. 4 and 5d,  $n_{e1}$  and  $n_{e2}$  can be determined.

To check the technique, the average temperature of the plasma in Region I was computed from the input power, losses, efficiency, and gas properties. Fig. 3 was used to determine an average  $n_e$ . Results from the optical technique and those computed from jet characteristics are summarized in Table I. It is clear that the agreement is well within the uncertainties of the measurement.

TABLE I—Measured and Computed Electron Concentrations in the Potential Core Region of a Laminar Argon Plasma Jet

	$n_{e1}$ electrons/ cm <sup>3</sup>	$n_{e2}$ electrons/ cm <sup>3</sup>	$n_e$ average electrons/ cm <sup>3</sup>	$T_{av}$ °K
Optical Tech- nique	$(1.0 \pm 0.1) \times 10^{17}$	$(1.2 \pm 0.1) \times 10^{17}$	$(1.1 \pm 0.1) \times 10^{17}$	—
Jet Charac- teristics	—	—	$(0.96) (10^{17})$	15,400

Fig. 7—Interferometer calibration. When mirror  $M_3$  of Fig. 6 is moved, fringes appear, as shown. Fringes obtained in this manner were used to calibrate the interferometer.

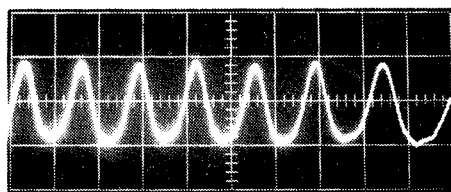


Fig. 8—Effects of variations in electron density (5V/cm). Upper trace shows interferometer output as  $n_e$  varies. Using Fig. 7, it is estimated to represent between 0.34 and 0.37 of a fringe. Lower trace is of intensity, as measured by Phototube No. 2 of Fig. 6.

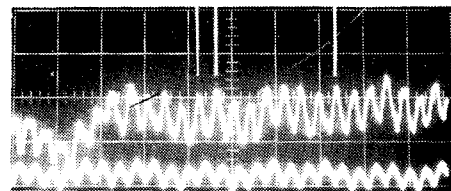
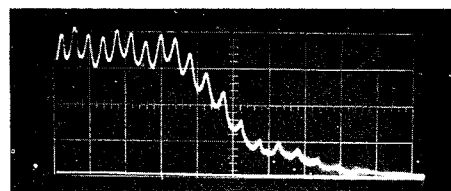


Fig. 9—Intensity measurement (2.5 V/cm): Phototube No. 2 of Fig. 6a measures the intensity of radiation from the plasma. The data shown here indicate that  $I_2/I_1 = 1.25$ . The base line is the plasma off condition.



### CONCLUSIONS

Although the results reported here are preliminary, they clearly indicate that the laser interferometer can be employed to measure electron density in dense, high-temperature, nonturbulent plasmas. However, from additional experiments it is equally clear that turbulent flow conditions prevent the use of a laser interferometer, at least when the flow is into an atmosphere which mixes to produce inhomogeneities in temperature, neutral density, and electron density.

If a perturbation in temperature is present, a simple measurement of the radiation from the plasma can be combined with the interferometer to determine  $n_e$  without a knowledge of the plasma temperature or the magnitude of the perturbation.

Interferometry in the infrared with detection in the visible is a very real advantage of the He-Ne system. Typical plasmas which might be examined using this technique are those required for studies on controlled fusion, plasmas generated to simulate the space-vehicle reentry sheath, and plasmas in high-energy shock-tube experiments. In summary, it appears that plasma diagnostics using coherent light can evolve into one more tool with which the understanding of dense, high temperature plasmas can be pursued.

### BIBLIOGRAPHY

- W. Verweij, "Probe Measurements and Determination of Electron Mobility in the Positive Column of Low-Pressure Mercury-Argon," *Phillips Research Reports*, Supplement No. 2, (1961).
- E. O. Johnson, L. Mather, "A Floating Double Probe Method for Measurements in Gas Discharges," *Phys. Rev.*, 80, No. 1, pp. 58-68 (October 1, 1950).
- M. A. Heald, *The Application of Microwave Techniques to Stellarator Research*, Project Matterhorn Report No. MATT-17 (August 26, 1959).
- G. M. Giannini, "The Plasma Jet", *Scientific American*, (August 1957).
- H. Gerdien and A. Lotz, "On a Light Source of Very High Surface Brightness", *Wissenschaftliche Veröffentlichung Lungen aus den Siemens-Werken*, 2, p. 489 (1922).
- M. P. Bachynski, K. A. Graf (RCA Victor Research Labs, Montreal); "Electromagnetic Properties of Finite Plasmas", *RCA Review XXV*, pp. 3-53, (March 1964).
- a. M. N. Saha, *Phil. Mag.*, 40, 472 (1920).
- b. M. H. Saha, *Z. Physik*, 6, 40 (1921).
- Martin Uman, *Introduction to Plasma Physics*, Ch. 7, McGraw Hill, Inc., (1964).
- A. Javan, W. R. Bennett, Jr., D. R. Herriott, "Population Inversion and Continuous Optical Maser Oscillation in a Gas Discharge Containing a He-Ne Mixture", *Phys. Rev. Letters*, 6, pp. 106-110 (1961).
- D. E. T. F. Ashby, D. F. Jephcott, "Measurement of Plasma Density Using a Gas Laser as an Infrared Interferometer", *App. Phys. Lett.*, 3, No. 1, p. 13 (July 1, 1963).
- J. B. Gerardo, J. T. Verdeyen, "The Laser Interferometer: Application to Plasma Diagnostics", *Proc. IEEE*, 52, No. 6, p. 690 (June 1964).
- A. I. Carswell, A. L. Waksberg (RCA Victor Research Labs., Montreal); "Off-Axis Feedback Modes in a 3-Mirror Laser System", *Engrg. and Res. Note*, RCA ENGINEER 1.0-2, p. 54, Aug.-Sept. 1964.
- H. E. Petschek, P. H. Rose, H. S. Glick, A. Kane, A. Kantrowitz, "Spectroscopic Studies of Highly Ionized Argon Produced by Shock Waves", *J. Appl. Phys.*, 28, No. 1, p. 83 (January 1955).

# LABORATORY SIMULATION OF REENTRY PLASMA

The technology of hypersonic flight requires detailed understanding of gas-dynamic flow-fields in which there is significant ionization—especially for the case of reentry vehicles, which interact with the atmosphere to generate very dense plasmas along their trajectories. These plasmas have very complex physical properties, and detailed quantitative measurements on the full-scale systems are very difficult. Thus, laboratory studies are done on scaled-down plasma flow-fields so that many of the variables can be controlled and measured more accurately. Studies of this type have been in progress in the RCA Victor Research Laboratories, Montreal, for a number of years, as this paper summarizes. The electromagnetic properties of such plasma flow-fields are critical in interpreting radar returns from the vehicle-plasma system and to communication with the vehicle through the plasma sheath. Both have been examined in these laboratory investigations; the results are reviewed, and the specialized facilities which have been developed are described.

**Dr. A. I. CARSWELL**

*Research Laboratories*

*RCA Victor Co. Ltd., Montreal, Canada*

**D**URING the passage of any object through the earth's atmosphere, a certain portion of the body's kinetic energy is transferred to the surrounding air. As the velocity increases, the interaction becomes more energetic and at supersonic speeds, the energy is transferred in the form of a shock wave leading to the well-known *sonic boom*. At higher velocities, (as with space vehicles reentering the atmosphere) the energy involved raises the temperature of the air in the forward region of the vehicle to temperatures sufficient to cause ionization of the constituent gases. This ionized gas (plasma) has properties vastly different from the un-ionized neutral air, and as a result, these plasma properties must be taken into account, in the design of the vehicle. This is particularly essential with respect to any communications system associated with the vehicle, since the plasma exhibits very pronounced electromagnetic properties.

In general, the interest in the reentry plasma stems from several fields including aerodynamics, and heat transfer studies. For the purposes of the present discussion however, the main emphasis will be placed on the problems of more direct interest to the communication engineer. From this point of view the problems can be divided into two general areas: 1) *radar*

*characteristics of the reentry plasma,* and 2) *reentry communications.*

## RADAR CHARACTERISTICS

The radar characteristics of the plasma are important because the ionized wake generated by the high-speed vehicle provides a significant target from which radar signals can be reflected. In order to obtain meaningful information about the vehicle for discrimination purposes, it is necessary to understand the scattering properties of the plasma wake so that the vehicle and plasma returns can be separated. (Often the wake return is 20 to 30 dB greater than the vehicle's.)

The dependence of the scattering cross-section of the wake on the vehicle and space environment is complicated

**DR. ALLAN I. CARSWELL** graduated with honors in 1956 from the University of Toronto with a B.A.Sc. in Engineering Physics. In the same year he entered the graduate school of the University of Toronto to study molecular physics. In 1960 he received his Ph.D. in 1960-61, Dr. Carswell studied at the Institute of Theoretical Physics of the University of Amsterdam on a Canadian National Research Council Fellowship. Dr. Carswell joined RCA Victor Co. Ltd. Research Laboratories on his return to Canada in 1961, and since that time has studied the interaction of electromagnetic waves with plasma systems—including microwave scattering from supersonic plasma flow fluids, and studies of the properties of ionized gas flow systems. Recently, Dr. Carswell has also worked on gaseous lasers. He is a member of the Canadian Association of Physicists, the American Institute of Physics, and the Canadian Aeronautics and Space Institute.

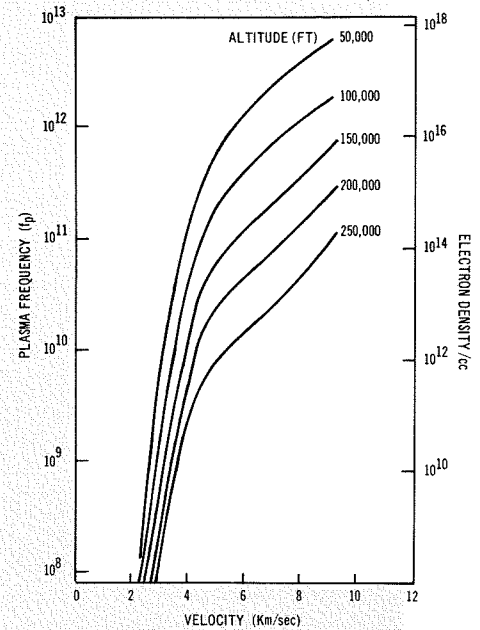
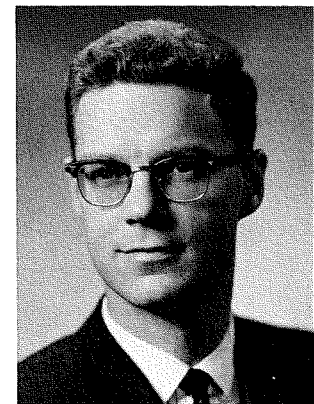


Fig. 1—Variations with velocity and altitude, of the electron density and plasma frequency at the stagnation point of a blunt body.

by the large number of parameters which are involved<sup>1</sup>. These include:

- 1) the electron density in the wake (or more accurately the plasma frequency relative to the radar frequency);
- 2) the polarization of the incident signal;
- 3) the geometry of the scattering path (aspect angle);
- 4) the dimensions of the wake (diameter and length in wavelengths;  $d/\lambda$  and  $l/\lambda$ ); and
- 5) the nature of the flow surrounding the vehicle (characterized perhaps by some Reynolds number).

Furthermore, the above parameters may vary in space and time and be complicated by additional factors such as the collisional (attenuation) effects of the wake plasma, the nonuniform electron distribution (both radially and longitudinally) in the wake, thermal non-equilibrium conditions of the plasma



*Final manuscript received August 3, 1965.*

and ablation from the vehicle itself. It thus becomes exceedingly difficult to interpret uniquely the radar scattering cross-section measurements if the scattering environment cannot be accurately specified.

Consequently, measurements made in suitable laboratory systems in which many of the parameters can be controlled can yield considerable information of value for the interpretation of free-flight radar scattering cross-section measurements<sup>2</sup>. Because of the large number of parameters involved, exact scaling of all the geometric, aerodynamic and electromagnetic properties of the full-scale system is not possible. However, the laboratory experiment can, in general, be designed to simulate some specific important aspects of the full scale problem.

### REENTRY COMMUNICATIONS

As far as the reentry communications are concerned, the problem is basically one of transmission through the complex plasma sheath surrounding the vehicle. In the simplest approximation, propagation of an electromagnetic signal in a plasma can only occur when the RF frequency is greater than the plasma frequency—the plasma frequency  $f_p$  being a convenient normalized measure of the electron density  $n$ , given approximately by:

$$f_p = 9000(n)^{1/2}$$

In Fig. 1, some sample variations of the plasma frequency and the electron density at the nose of a blunt body are presented as a function of velocity for various altitudes. From these curves it is apparent that frequencies higher

than about 1 Gc/s are required to penetrate the dense regions of a reentry plasma for communication purposes.

Apart from the use of very high frequencies, several other techniques have been suggested to aid in the penetration of the reentry plasma sheath. These include the use of magnetic fields to open up "passbands" in the plasma for certain modes of wave propagation and the seeding of chemical additives to the plasma to reduce its electron content. In both of these areas, laboratory experiments can be undertaken to assess the usefulness of the techniques over the appropriate range of conditions.

### DESIGN OF LABORATORY FACILITIES

In the design of laboratory facilities for the study of reentry plasma phenomena it is necessary to remember the basic factors involved in making meaningful measurements.

In general there are two basic requirements: 1) the availability of a theory which can adequately describe the physical situation, and 2) an experimental capability to make measurements of the quantities described by the theory. The theory and experiment are interdependent and complementary but because of the complexity of "flowing" plasma systems it is often difficult to make a direct and meaningful comparison between theory and experiment.

Usually, the theoretician is restricted in his analysis not only by the complexity of the problem but also by a lack of good quantitative experimental data which he can use as a guide.

From the experimental point of view

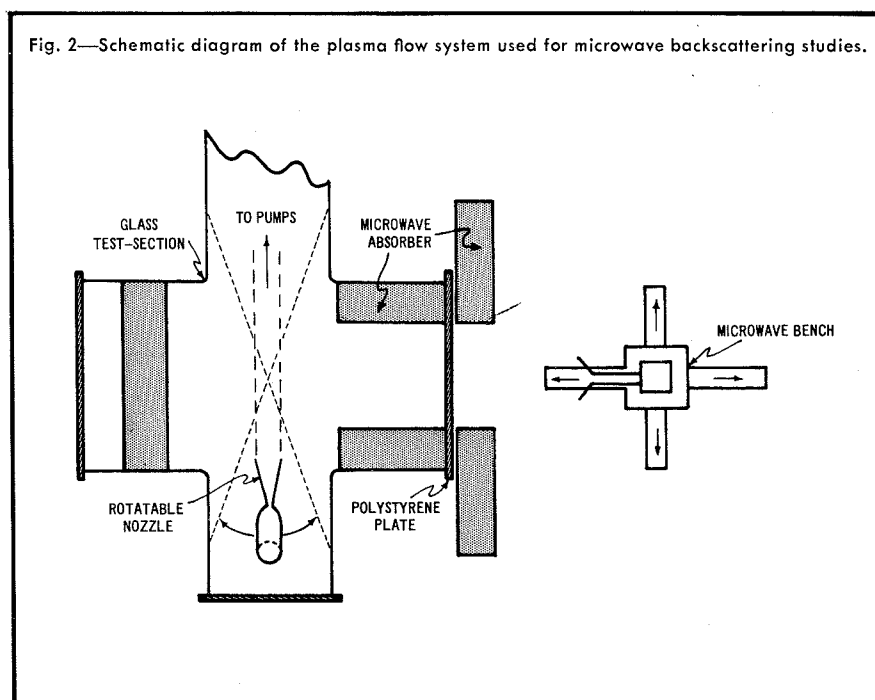
an entirely different set of difficulties arises. First, in the laboratory studies it is necessary to simulate conditions which exist in the "full-scale" reentry environment. In this case the main interest is in obtaining more information about the full-scale system from the laboratory measurements on the simulated system. This means that for any useful information to be derived, the simulation must at some stage allow a comparison of the laboratory "numbers" with the full-scale system. In the simulation of supersonic plasma flow-fields, this step is by no means trivial.

First of all, any attempt at "simulation" assumes that a detailed knowledge of the full-scale system exists and, in general this is not true. Secondly, it is not difficult to show that because of the complexity of the full-scale system (in the reentry case) it is impossible to simulate in the laboratory all of the full-scale plasma parameters exactly in a single device or experiment. Hence in a laboratory simulation, the experimentalist is forced to be satisfied with something less than an exact "scaling" of the real system.

Once the laboratory system has been established to optimize the scaling requirements, the major experimental problem lies in making meaningful measurements of the very complicated plasma flow-field structure. Although there is a rather large body of experimental work on plasma diagnostics, the art of applying these methods to obtain quantitative measurements in the various supersonic plasma flow facilities of interest is still only at a very early stage of development<sup>3</sup>. Because of this inability to relate the "measurables" in an experiment to the "plasma physics", the experimentalist is at present in the position of having to design and calibrate each diagnostic tool for each specific measurement. Under these conditions it is not surprising that discrepancies often arise between some of the measurements.

In general, there are three basic types of facility used for the laboratory simulation of the reentry environment. The first of these is the ballistic range in which projectiles are fired at velocities of up to 20,000 or 30,000 ft/s in a large evacuated tank—with the pressure being regulated to simulate a given altitude. The second type of facility is the shock tube in which gases (both ionized and neutral) are driven past a stationary model at reentry velocities and pressures. A variety of "driving" techniques are used in the shock tubes including (explosive) combustion and electromagnetic forces.

The third basic facility is the continuous flow system in which the gases are pumped continuously from a high



### BACKSCATTERING CHARACTERISTICS OF LABORATORY PLASMA FLOW FIELDS

A schematic diagram of a system<sup>2,5</sup> developed to measure the backscattering characteristics of a plasma flow field is shown in Fig. 2. Radio frequency (13.5-Mc/s) energy is used for ionizing gas passing through a small nozzle into an evacuated test section to generate a supersonic plasma jet. A microwave "radar" system is positioned to illuminate the cylindrical plasma jet which can be rotated to examine the backscattering at various angles of incidence.

Electrical (Langmuir-type) probes are used to examine the ionization distribution in the plasma. Sample results are shown in Fig. 3, for an argon jet (mach 2) at a pressure equivalent to an altitude of about 150,000 feet.

Using the concept of an effective reflecting surface<sup>3,5</sup> in the plasma (where the dielectric coefficient is zero), it is possible to estimate the effective reflecting "shape" of the plasma for various microwave frequencies.

In Fig. 3 the shape (as deduced from detailed probe studies of the flow) for  $\kappa$ -band (24 Gc/s) and x-band (9.4 Gc/s) are shown as dotted lines and in Fig. 4 sample results of actual scattering measurements from the plasma stream are given. Fig. 4a displays the amplitude variation as a function of aspect angle for a metal cylinder positioned in the tunnel in place of the plasma stream for calibration purposes, and the characteristic  $[(\sin x)/x]$  variation<sup>6</sup> is apparent. Figs. 4b and 4c show similar displays for the aspect angle variation of the scattering from the plasma jet at 9.4 and 24 Gc/s.

Referring to the effective reflecting surfaces shown in Fig. 3 it is seen that at x-band, the jet should "look" like a uniform cylinder for a length of about 15 cm, while at  $\kappa$ -band it will appear like a tapered cylinder (cone). These effects are apparent in Figs. 4b and 4c. In Fig. 4b, the scattering is symmetric with respect to the broadside position, while in Fig. 4c the pattern is quite asymmetric. Using such techniques, it is possible to measure the scattering properties of the plasma quantitatively over a range of flow conditions.

In addition to studies on essentially uniform (laminar) flow, there is also considerable interest in examining the properties of turbulent plasmas. By increasing the effective Reynolds number of the plasma jet it is possible to generate turbulent flow fields and some sample results of the microwave scattering (at normal incidence) from such systems are shown in Fig. 5.

In Fig. 5a, the difference between the scattering from a laminar and turbulent plasma stream is shown. The

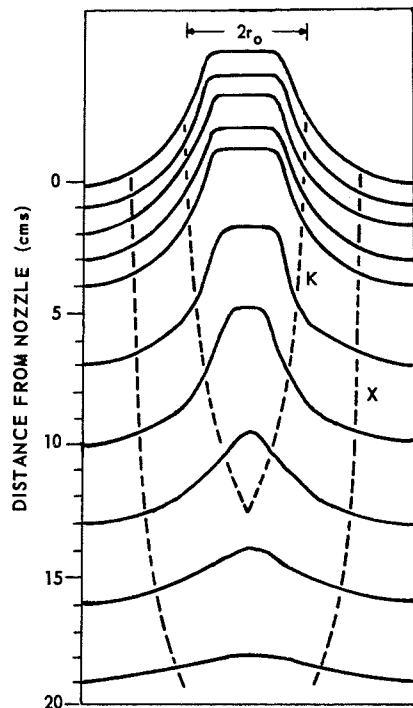


Fig. 3—"Contour map" of the electron density variation in the laboratory jet. The nozzle exit diameter is  $2r_0$  and the dotted lines represent the effective reflecting surfaces for X (9.4-Gc/s), and K-(24-Gc/s) band frequencies.

pressure region, through a nozzle into an evacuated chamber at supersonic velocities: To achieve the desired degree of ionization, the continuous flow systems incorporate an auxiliary source of ionization, usually in the form of a high power DC or RF excited arc, just upstream from the nozzle. Aside from this very intense gas heating capability, these so-called *plasma tunnels* are similar to the more conventional low-density wind tunnels.

Each of these facilities has its own special advantages and limitations for various simulation studies. These have been summarized in the literature<sup>4</sup> and will not be discussed here. However, because of the longer experimental times available in the continuous flow systems, such facilities have been used for most of the recent work at the Montreal Laboratories<sup>5,6,7</sup>.

In addition to the various flow systems for simulating the reentry environment, it is also possible to examine many of the important aspects of the plasma-electromagnetic wave interaction in nonflowing systems. Experiments of this type are also in progress in the Montreal Laboratories and some of the results will be summarized below.

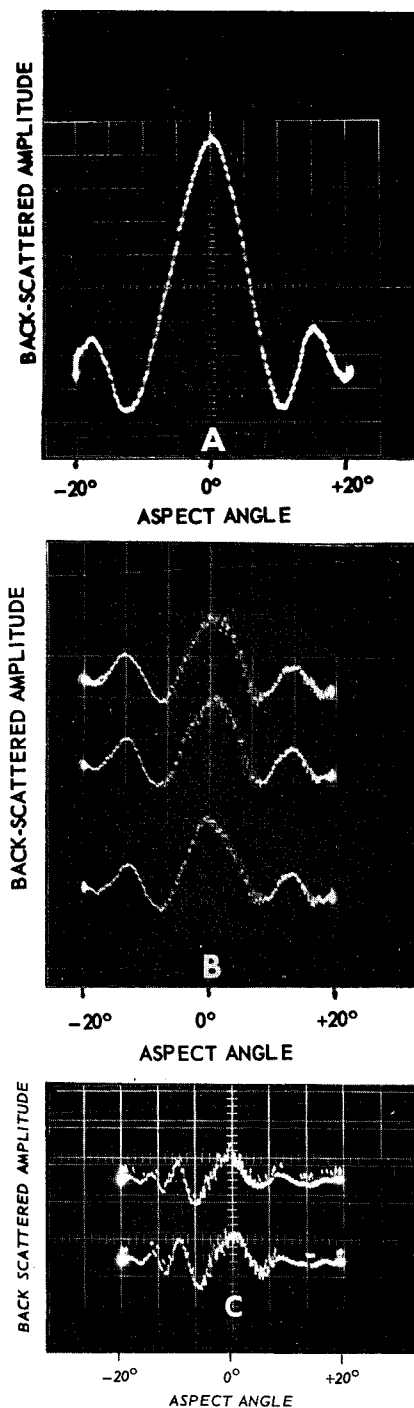


Fig. 4—Sample displays of the aspect angle variation of backscattered microwaves from: (a) metal cylinder (9.4 Gc/s), (b) laminar plasma jet (9.4 Gc/s), and (c) the same jet using 24 Gc/s.

return from the turbulent jet displays a rapidly and randomly fluctuating amplitude as shown in the photograph. An analysis of the frequency content of this signal can be made with the aid of a wave analyser and the results for two microwave frequencies (9.4 and 24 Gc/s) reflected from the same plasma jet are shown in Fig. 5b. It is seen that the spectrum has a frequency content similar to that measured for velocity fluctuations in turbulent fluid flows. Such results illustrate the possible usefulness

of microwave scattering measurements for the study of plasma turbulence.

#### STUDIES RELATED TO REENTRY COMMUNICATIONS

As already mentioned the main experimental interest in this area centers on the investigations of various possible methods for alleviating or removing the reentry communications "black-out" phenomenon. A technique which has received considerable attention in the laboratories in recent years is that involving the seeding of electronegative gases into plasma flow-fields. Such additives (e.g. the halogens) tend to replace the electrons in the plasma with heavier negative ions by the process of electron attachment with the resultant improvement in the RF transmission through the plasma (since the heavier particles do not respond appreciably to the high frequency RF field).

One such material (which exhibits a very large cross-section for electron capture) is sulfur hexafluoride ( $SF_6$ ); as a result, an extended series of measurements have been made using this seed-gas in various plasma flow systems. Sample results<sup>10,11</sup> are shown in Fig. 6 for the addition of  $SF_6$  into an argon plasma jet (about mach 2). In this figure the plasma ionization is measured by the current flowing to an electrical double-probe emersed in the jet and the rapid "quenching" of the plasma with  $SF_6$  addition is clearly seen.

The seeding problem is considerably more complex if the "air-chemistry" is taken into account (i.e. if the many energy exchange processes in the polyatomic gas constituents are included). For example, Fig. 7 shows the ionization decay in a pure nitrogen jet in a presentation similar to that of Fig. 6. With nitrogen, it is apparent that there is not a simple monotonic decay of ionization in the "afterglow" but that secondary "peaks" can occur as energy is released, by collisional processes, from various internal energy modes of the molecules (i.e. metastables, excited states, etc.). Seeding in the presence of such phenomena must be examined very carefully if meaningful measurements are to be made<sup>7</sup>.

The possible usefulness of magnetic fields to achieve communications during reentry using an appropriate magnetionic propagation mode has been discussed by several authors<sup>12,13</sup>. Recently, measurements in the Montreal Laboratories<sup>14</sup> have been made to investigate the properties of microwaves in plasmas under the influence of an external magnetic field.

In the presence of a magnetic field, it can be shown<sup>8,14</sup> that a plasma becomes doubly refracting and can

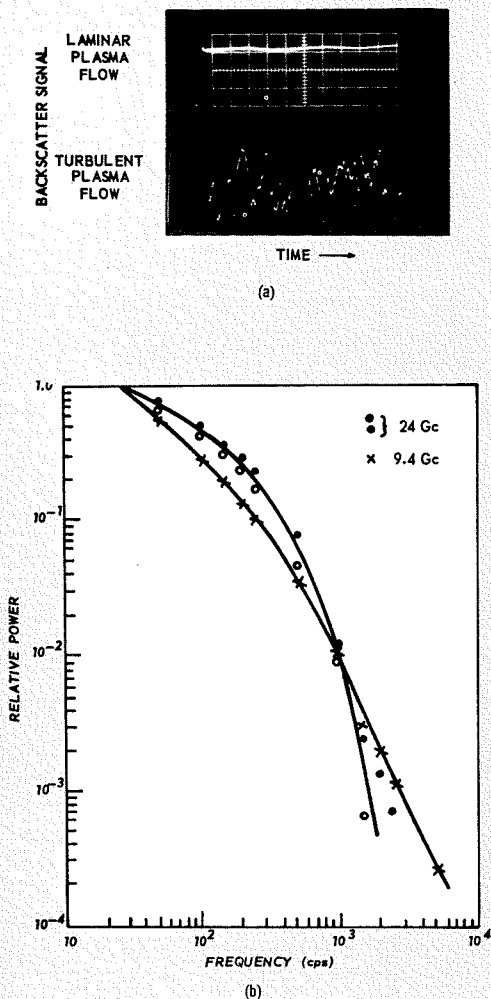


Fig. 5—(a) Sample return of X-band microwaves scattered from a plasma jet showing the difference between a laminar and turbulent flow (time scale is 1 ms/div). (b) Frequency content of the fluctuating return from a turbulent jet.

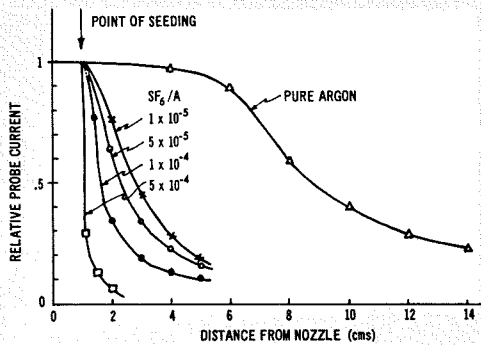


Fig. 6—Variation of the axial ion density in an argon plasma jet for various amounts of  $SF_6$  seeding.

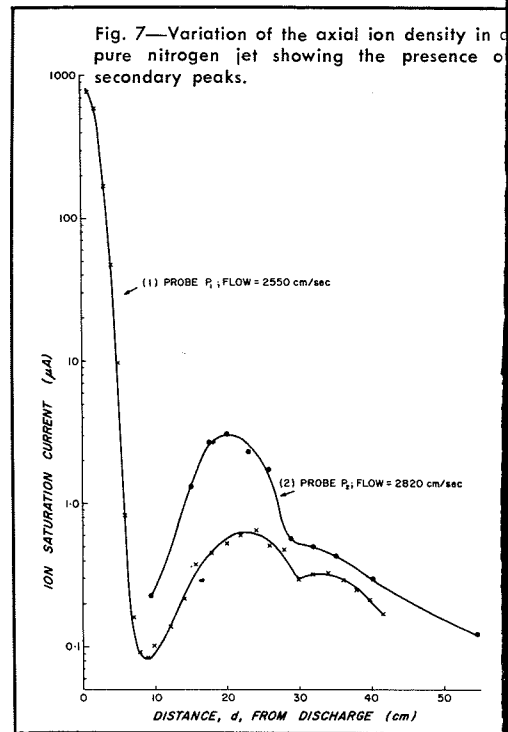


Fig. 7—Variation of the axial ion density in a pure nitrogen jet showing the presence of secondary peaks.

simultaneously support two wave modes which are called the *ordinary* and *extraordinary* waves. For the case of propagation in the direction of the magnetic field, the two basic wave modes are counter-rotating, circularly polarized waves. Examination of the propagation characteristics of these waves shows that regions of high attenuation (stop-bands) and low attenuation (pass-bands) exist for certain values of the plasma parameters and that these bands are different than those obtained in the absence of a magnetic field.

Fig. 8 shows the variation of the opaque and transparent regions of an anisotropic plasma for a range of plasma parameters for propagation along the magnetic field. The effects of collisions in the plasma on the wave propagation tend to make the band structure less distinct, i.e. there is some attenuation at all frequencies and only finite attenuation in the opaque regions. In Fig. 8,  $\omega$  is the angular wave frequency;  $\omega_p$  is the plasma frequency ( $\omega_p = 2\pi f_p$ ), and  $\omega_b$  is the electron cyclotron frequency ( $\omega_b = eB/m$ ); and  $Z$  is the normalized collision frequency ( $Z = \nu/\omega$ ). The "transparent" regions can be shown to depend upon the microwave frequency, polarization, angle of propagation with respect to the magnetic field and upon the magnitude of the electron density and magnetic field. Provided that a sufficiently strong magnetic field is applied, it is possible to make a wave of any frequency penetrate through the plasma.

Fig. 9 gives typical results for the transmission of a circularly polarized

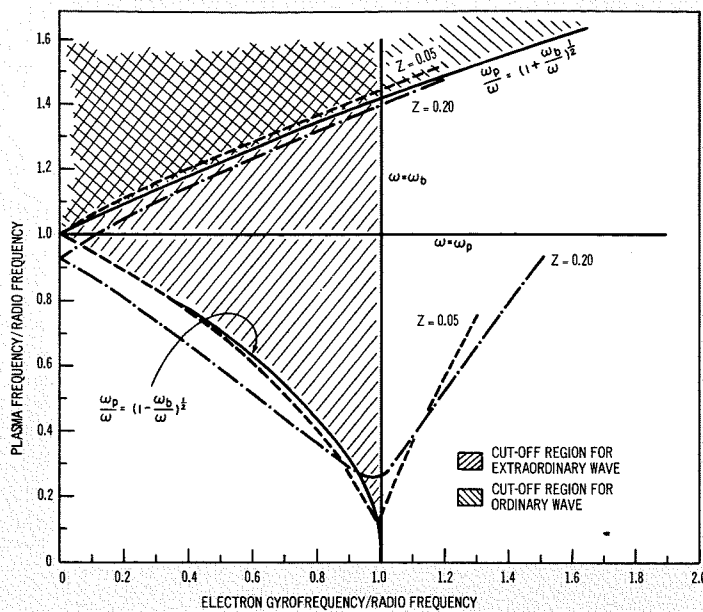


Fig. 8—Pass- and stop-bands for circularly polarized waves in a plasma propagating along the direction of an external magnetic field. "Cut-off" is defined to correspond to an attenuation of 10 dB per free-space wavelength.

wave along the director of a magnetic field through a decaying helium afterglow plasma<sup>14</sup>. For the extraordinary wave when  $\omega_b/\omega < 1$ , the plasma is more opaque than when  $\omega_b = 0$ . For  $\omega_b/\omega > 1$  however the plasma is more transparent and the direction of the phase change reverses since the index of refraction becomes greater than one. With increasing magnetic field the plasma becomes increasingly transparent to the ordinary wave as shown in Fig. 9.

For practical reentry applications, the magnitude of magnetic field required will depend upon the several parameters mentioned above. Results<sup>12,14</sup> show that in general values of several hun-

dred gauss and greater would be required so that weight, size and power supply considerations become of prime importance. However with the advent of superconducting magnets such systems for reentry applications are not unreasonable.

#### CONCLUSION

The reentry plasma environment presents many new and challenging problems in the design considerations for space-vehicle radar and communications systems. Many of the phenomena associated with the interaction of electromagnetic waves with plasma are already relatively well understood. However, to obtain the necessary quan-

titative data of practical value for system design and operation, a great deal more information is required. This can be best obtained by using controlled laboratory experimental investigations to complement the data derived from measurements made in the full scale reentry plasma.

#### BIBLIOGRAPHY

All citations except 1, 4, 8, 9, and 12 are literature authored in RCA Victor Research Laboratories, Montreal.

1. A. Gold: (RCA-MSR, Moorestown), "Radar Backscatter Characteristics During Ballistic Missile Reentry," *private communications*.
2. A. I. Carswell, M. P. Bachynski: *MIT Symp. on Radar Reflectivity Measurement*, RADC-TDR-64-25, Vol. 1, pp 382 (April 1964).
3. A. I. Carswell, M. P. Bachynski, G. G. Cloutier: "Microwave Measurements of the Electromagnetic Properties of Plasma Flow-Fields," *Proc. AIAA Fifth Biennial Gas Dynamics Symp.*, Northwestern Univ. Press (1964) pp 355.
4. J. Cordero, F. W. Diedrich, H. Hurwicz: *Aerospace Eng.* 22, 166 (1963).
5. A. I. Carswell: "Radio-Frequency-Excited Plasma Tunnel," *Rev. Sci. Instr.* 34, 1015 (1963).
- 6a. A. I. Carswell: "Two Phase Mercury Plasma Tunnel," *Rev. Sci. Instr.* 35, 1557, (1964).
- 6b. A. I. Carswell: "A Versatile Two-Phase Mercury Tunnel for Generation of Supersonic Plasma Streams," *RCA Reprint PE-194* from *RCA ENGINEER* 10-1, June-July 1964.
7. A. I. Carswell, C. Richard: *Electrochemical Properties of Seeded Plasma Flow Fields*, Semi-Annual Report to ARPA, RCA Victor Report No. 7-801-34 (Dec. 1964).
8. J. M. Kelso: *Radio Ray Propagation in the Ionosphere*, McGraw Hill (1964).
9. J. R. Mentzer: *Scattering and Diffraction of Radio Waves*, Pergamon Press (1955).
- 10a. G. G. Cloutier, A. I. Carswell: "Plasma Quenching by Electronegative Gas Seeding," *Phys. Rev. Letters* 10, 329 (1963).
- 10b. G. G. Cloutier, A. I. Carswell: "Plasma Quenching by Electronegative Gas Seeding," *Eng. and Res. Note*, *RCA ENGINEER* 9-1, June-July 1963.
11. A. I. Carswell, G. G. Cloutier: "Supersonic Plasma Streams Seeded with Electronegative Gases," *Phys. Fluids* 7, 601 (1964).
12. H. Hodara: "Use of Magnetic Fields in the Elimination of Reentry Radio Blackout," *Proc. IRE* 49, 1825 (1961).
13. M. P. Bachynski: "Electromagnetic Wave Penetration of Reentry Plasma Sheaths," *Radio Sci.*, *NBS J. Res* 69D, 147 (1965).
14. M. P. Bachynski, B. W. Gibbs, *EM Wave Propagation in Anisotropic Plasmas*, AFCL-65-84 (Dec. 1964).

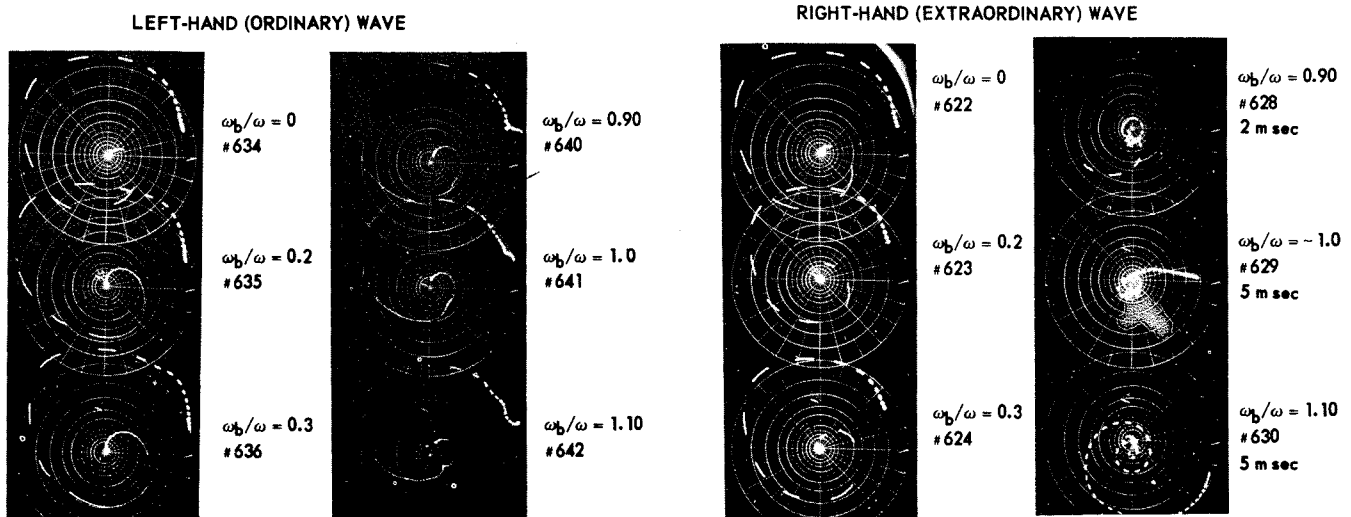


Fig. 9—Sample experimental results of the transmission of circularly polarized waves through a plasma with a magnetic field (of Fig. 8). The polar displays represent the amplitude and phase variation of the signal as a function of time in a decaying helium plasma.

# INTERACTION OF ELECTROMAGNETIC WAVES WITH IONIZED ROCKET EXHAUSTS

Three aspects of the rocket exhaust plasma which enter into the determination of electromagnetic-wave, ionized-exhaust interaction effects on communications and tracking systems are discussed. These are: 1) processes leading to the formation and loss of free electrons in the rocket-engine combustion chamber, during expansion in the thrust chamber, and within the exhaust jet; 2) spatial variation of the basic plasma parameters within the jet as governed by the gas mass density and temperature variations; 3) interaction of electromagnetic waves with the nonuniform exhaust plasma. Indications of the extent of signal attenuation to be expected in actual rocket exhausts are given.

**A. BOORNARD**

*Applied Research, DEP, Camden, N. J.*

WHEN an electromagnetic propagation path is intercepted by the ionized exhaust of a missile, severe degradation of the performance capabilities of guidance, telemetry, and tracking systems can occur. In recent years, the problem of electromagnetic interference by rocket exhausts has taken on increased significance owing to the increased size and complexity of advanced missile weapons and space systems. Most of the work dealing with electromagnetic interference caused by rocket exhausts relates to specific missile weapons systems and is classified. Accordingly, the scope of this article is limited to general considerations and to the basic phenomena pertinent to the problem of predicting the extent of the interference to be expected by the exhausts of future missiles.

The exhaust jet of a rocket engine (Fig. 1) forms an extended nonuniform plasma consisting of free electrons and ionized and neutral molecules, the latter being the combustion products of

the propellants. Within the exhaust jet, large spatial variations of the electron concentration and collision frequency exist, particularly at low altitudes and in the vicinity of internal shocks. At low altitudes, the exhaust jet is confined to a relatively small volume by the atmospheric pressure, and internal shocks occur to within a few nozzle radii downstream of the nozzle exit. As the missile ascends, the exhaust jet expands and the internal shocks become displaced farther downstream in regions where the surrounding electron concentration is relatively low. Because of the increased exhaust size propagation paths are more readily intercepted at the higher altitudes, but interference is not usually as severe because of the accompanying reduction in the plasma density.

For high-frequency waves, the electrical characteristics of the ionized exhaust are determined by the free electrons. They are set into vibration by the electric field component of the wave and undergo collisions with neutral exhaust gas molecules. The collisions re-

sult in absorption of the wave energy. By comparison, ionized molecules are much more massive and have no significant effect at high frequencies. The free electrons thus impart to the exhaust the properties of a poor conductor, or equivalently, an imperfect dielectric. Consequently, interception of electromagnetic waves by the ionized exhaust can lead to absorption, reflection, refraction and diffraction of the waves. In addition, because the properties of the ionized exhaust can fluctuate rapidly with time, amplitude and phase modulation of the intercepted waves can occur. When these effects take place, they lead in turn to signal attenuation, multipath propagation, beam distortion and other forms of interference.

The severity of the resulting interference is determined by the following:

- 1) Magnitude and spatial rate of change of the basic plasma parameters (the electron concentration,  $n_e$ , and the effective electron collision frequency for momentum transfer,  $\nu$ ).
- 2) Time rate of change of the basic plasma parameters.
- 3) Frequency of the electromagnetic wave.
- 4) Length of the propagation path through the exhaust plasma.
- 5) Physical extent of the exhaust plasma compared to the free-space wavelength.

In extreme cases, attenuation of electromagnetic waves by absorption or reflection can be large enough to result in complete loss of signal. Other manifestations of the interaction of electromagnetic waves with the ionized exhaust are inaccuracies in data telemetered from a missile and errors in range and angle determinations obtained by pulsed and cw radar systems during powered flight.

## PROPAGATION IN ROCKET EXHAUSTS

The ionized rocket exhaust forms a nonuniform plasma in which variations in electron concentration and collision frequency occur both along and normal to the direction of propagation of waves traversing the exhaust. Analysis of the effects on electromagnetic wave propagation in such plasma media is complex and some form of simplification is required. A convenient method of simplification is to treat the exhaust as being composed of a series of uniform plasma slabs, with average plasma properties assigned to each slab. The assigned properties are determined by the existing exhaust properties on either side of a particular slab (Fig. 2).

For a plane wave with harmonic time variation  $\exp(j\omega t)$ , traveling in the  $z$  direction away from the origin in a uniform medium, the solution of the wave equation for the electric field component can be written as:

$$E = E_0[\exp(j\omega t)][\exp(-\gamma z)] \quad (1)$$

*Final manuscript received August 17, 1965.*

**A. BOORNARD** received the BS in 1953 from the College of William and Mary with physics as a major and the MS in physics from Indiana University in 1955. He joined RCA and the Applied Research Section in 1957. His work experience includes gamma ray and neutron damage in semiconductors; properties of thin film superconductors; microwave generation techniques and electromagnetic wave-plasma interactions. His plasma physics work includes studies of the effects of nuclear burst induced ionization on electromagnetic wave propagation, the effects of ionized rocket engine exhausts on radar and communications, and the microwave transmission characteristics of dense high temperature plasmas. He is presently engineering leader of the Plasma Physics Group. The major activities of this group are: beam-plasma microwave generation, Cerenkov microwave generation, plasma diagnostic techniques, and the interaction of electromagnetic

waves with rocket exhausts. Prior to joining RCA, Mr. Boornard served with the U.S. Army and was assigned to Frankford Arsenal in Philadelphia. His work there consisted of studies of conduction in thin metallic films, and radiation effects in metals and thin films. Mr. Boornard is a member of the American Physical Society.



The complex propagation coefficient  $\gamma$  is equal to  $(\alpha + j\beta)$ , where  $\alpha$  and  $\beta$  are the attenuation and phase coefficients, respectively. It is related to the effective dielectric coefficient of the medium  $K$ , by

$$\gamma = jk_o K^{1/2} \quad (2)$$

where  $k_o$ , the free space propagation constant, is equal to  $\omega/c = 2\pi/\lambda_o$ .

If the medium is a plasma,  $K$  is complex and is given by<sup>1</sup>:

$$K = K_r - jK_i$$

$$= \left[ 1 - \left( \frac{\omega_p}{\omega} \right)^2 \frac{1}{1 + \left( \frac{\nu}{\omega} \right)^2} \right] - j \left[ \left( \frac{\omega_p}{\omega} \right)^2 \frac{\frac{\nu}{\omega}}{1 + \left( \frac{\nu}{\omega} \right)^2} \right] \quad (3)$$

The attenuation and phase coefficients expressed in terms of  $K$  are:

$$\frac{\alpha}{k_o} = \left( \frac{|K| - K_r}{2} \right)^{1/2} \text{ nepers} \quad (4)$$

$$\frac{\beta}{k_o} = \left( \frac{|K| + K_r}{2} \right)^{1/2} \text{ radians} \quad (5)$$

where  $|K| = (K_r^2 + K_i^2)^{1/2}$ . In the above expressions,  $\omega_p$ , the angular plasma frequency, is:

$$\omega_p^2 = \frac{n_e e^2}{m_e \epsilon_o} \quad (6)$$

where  $e$  = electron charge,  $m_e$  = electron mass, and  $\epsilon_o$  = permittivity of free space. The plasma frequency  $f_p = \omega_p/2\pi = 8.974 \times 10^3 \sqrt{n_e}$  in c/s when  $n_e$  is in  $\text{cm}^{-3}$ . The power attenuation per unit length is

$$a/z = 8.686 \alpha \quad (\text{dB/meter}) \quad (7)$$

and the phase shift per unit length is

$$\Delta\phi/z = k_o - \beta \quad (\text{radians/meter}) \quad (8)$$

The manner in which attenuation varies with plasma frequency and collision frequency is shown in Fig. 3. Here the attenuation per unit length normalized with respect to plasma frequency  $(a/z)/f_p$  is shown as a function of the normalized wave frequency  $f/f_p$ , and the normalized collision frequency,  $\nu/f_p$ . It is evident that for  $(f/f_p) \ll 1$  ( $10^{-4}$  to  $10^{-2}$ ), the attenuation always increases with decreasing collision frequency. Over this range the attenuation also decreases with decreasing wave frequency. In the range  $10^{-1} < (f/f_p) < 1$ , the attenuation attains its maximum value; again, it decreases with increasing collision frequency. However, for  $(f/f_p) > 1$  the  $(\nu/f_p)$  curves cross over and the highest attenuation generally occurs at intermediate values of  $(\nu/f_p)$ , approximately between 10 and 100. In this region the attenuation always de-

creases with increasing wave frequency. It is noted that for a plasma in which  $(\nu/f_p) \gg 1$ , the attenuation does not vary with frequency over a broad frequency range. Plasmas in which  $(\nu/f_p) \gg 1$  are encountered in many types of rocket exhausts, particularly in liquid propellant exhausts and in the exhaust jet close to the nozzle exit.

The dependence of the power reflection coefficient on plasma parameters is best illustrated by considering a plane wave normally incident upon a plasma free-space interface. A plot of the power reflection coefficient as a function of  $(f/f_p)$  and  $(\nu/f_p)$  for this case is shown in Fig. 4. The important points to be noted are that 1) the power reflection coefficient always decreases with increasing wave frequency and 2) it always decreases with increasing collision frequency. The latter dependence is of significance for many rocket exhausts, because it is the principal reason for their relatively low reflectivity at c-band and above.

#### SOURCE OF FREE ELECTRONS

Large concentrations of free electrons within the exhaust are the primary cause of signal interference. Without them interference would be negligible. Thus, the processes leading to their formation are an important part of the problem. The electron concentration levels attained in rocket exhausts are governed by a large number of engine variables, such as propellant type, combustion chamber temperature and pressure, and expansion ratio (ratio of exit plane area to throat area). For a given propellant the electron concentration at the nozzle exit increases with increasing combustion chamber temperature and pressure, specific impulse, and thrust while it decreases with increasing expansion ratio.

In general, the highest electron concentrations occur in the exhausts from solid propellants. There are two principal types of solid propellants: homogeneous propellants and composite propellants. The homogeneous type contains sufficient chemically bonded oxygen to sustain combustion, an example being nitrocellulose plasticized with nitroglycerin. Composite propellants use an organic fuel binder, usually a polymeric organic material such as polyurethane, and a separate oxidizer such as ammonium perchlorate; neither of which burns well alone. In addition, a metallized fuel such as aluminum (15 to 20% by weight) is added to increase the specific impulse. Typically, electron concentrations in excess of  $10^{11}$  electrons/ $\text{cm}^3$  can occur at the nozzle exit of solid propellant rockets. As a result, attenuation produced by

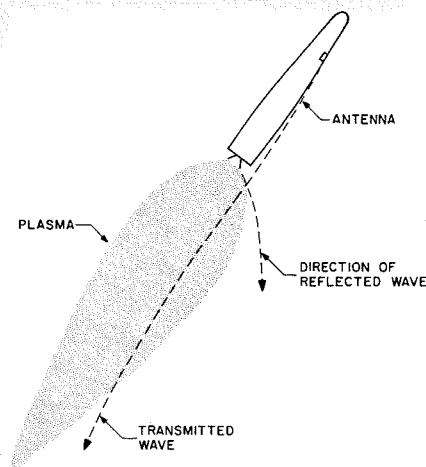


Fig. 1—Interception of an electromagnetic propagation path by a rocket exhaust. The electromagnetic wave transmitted along the indicated path from the missile-borne antenna to a remote receiving antenna is partially reflected at the exhaust plasma-air boundary and experiences further attenuation by plasma absorption within the exhaust. Refraction also occurs, so that the wave does not follow the line of sight path.

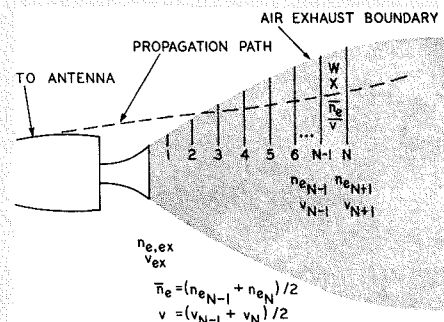


Fig. 2—Illustration of the method of dividing the nonuniform exhaust into a series of plasma slabs along the propagation path.

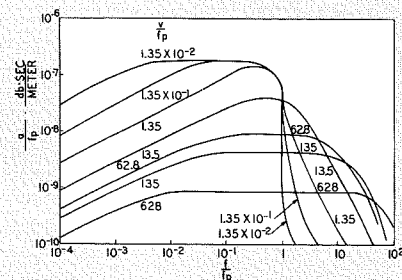


Fig. 3—Normalized plane wave attenuation as a function of the normalized wave and collision frequencies.

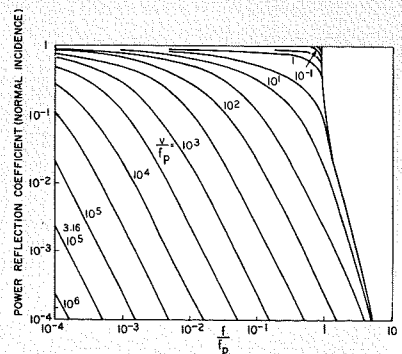


Fig. 4—Power reflection coefficient vs. normalized wave and collision frequencies.

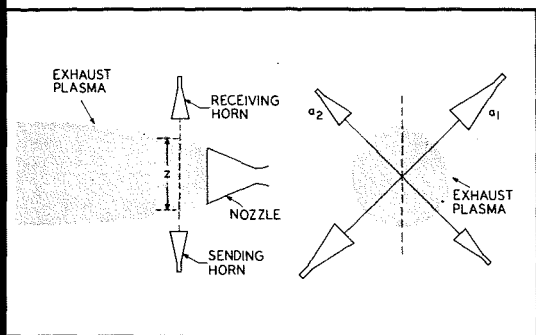


Fig. 5—Microwave probe techniques for determining the average electron concentration and collision frequency near the exit plane of a rocket exhaust.

solid propellant exhausts is usually much greater than in liquid exhausts.

Two of the most familiar and widely used liquid propellant mixtures are liquid oxygen and RP-1 (kerosene); and nitrogen tetroxide and Aerozene:50 (a 50% by weight mixture of hydrazine and unsymmetrical dimethylhydrazine). Oxygen and kerosene are used in the booster and sustainer engines of the Atlas missile and in the booster engines of the Saturn. Nitrogen tetroxide and Aerozene:50 are storable and hypergolic i.e., they ignite upon being brought into contact with each other. Accordingly, they are particularly useful in restartable and throttled engines. These characteristics make them attractive for a number of applications. Engines in which they are used include the booster and second stage of TITAN II and TITAN III-A and the trans-stage of TITAN III-A and C. Additionally, nitrogen tetroxide and Aerozene:50 will be used in the APOLLO service module and in LEM.

Typically, values of the electron concentration at the nozzle exit plane of liquid propellant rocket engines range from  $10^8$  to  $5 \times 10^{10}$  electrons/cm<sup>3</sup>, with the higher values being representative of rocket nozzles of low expansion ratio. Among the liquid propellants, a notable exception exists, namely, the combustion of liquid oxygen and liquid hydrogen for which the electron concentrations appear to be less than  $10^8$  electrons/cm<sup>3</sup>. As a result, no interference by the exhausts of rocket engines using oxygen and hydrogen is encountered at frequencies greater than the UHF band.

#### THERMAL IONIZATION

The single largest factor leading to high electron concentrations at the nozzle exit is thermal ionization in the combustion chamber of low ionization potential contaminants, such as the alkali metals potassium and sodium. The ionization potentials of potassium and sodium are 4.34 and 5.14 eV, respectively, as compared to between 12

and 15 eV for most of the other atoms and molecules found in the combustion products of the propellants. They are initially present in the form of compounds, which are easily thermally dissociated at the temperatures attained in rocket combustion chambers (3,300 to 3,600 °K). The content of alkali metals in liquid propellants is most often between 0.5 and 5 parts per million by weight, whereas in solid propellants it may range from a few to several hundred parts per million by weight of the propellant. At the temperatures and pressures (100 to 1000 lb/in<sup>2</sup> absolute) attained in the combustion chamber, fractional ionization of the alkali metals is very large. Concentrations in the range of  $10^{12}$  to  $10^{13}$  electrons/cm<sup>3</sup> and greater are attained. As a result of the high pressure within the combustion chamber, thermal equilibrium between electrons, ions, and neutral molecules exists. Thus estimates may be made of the electron concentration resulting from thermal ionization of alkali contaminants by means of the Saha equation<sup>2</sup>.

The equilibrium electron concentration  $n_e$ , for thermal ionization of a particular atomic or molecular species, is:

$$n_e = (KN)^{1/2} \left[ \left( 1 + \frac{K}{4N} \right)^{1/2} - \left( \frac{K}{4N} \right)^{1/2} \right] \quad (9)$$

where charge neutrality of the gas is assumed (i.e.,  $n_e$  equals the ion concentration  $n_i$ ) and  $N = (n_n + n_i)$  is the total number density of the given species, the neutral plus ion concentration. The Saha equilibrium constant  $K$  of the particular species is

$$K = \frac{n_e n_i}{n_n} = \left( \frac{g_e g_i}{g_n} \right) \frac{(2\pi m_e kT)^{3/2}}{h^3} \exp(-eV_i/kT) \quad (10)$$

which for alkali metal atoms may be written in a form more convenient for computation as

$$\log K = 15.384 + 3/2 \log T - 5041 V_i/T \quad (10a)$$

where  $m_e$  = electron mass,  $k$  = Boltzmann's constant,  $h$  = Planck's constant,  $T$  = temperature (°K),  $V_i$  = ionization potential; and where the  $g$ 's are

TABLE I — Electron-Molecule Cross Sections for Momentum Transfer at 2,000° K

Molecule	Cross Section (10 <sup>-15</sup> cm <sup>2</sup> )	Reference
H <sub>2</sub> O	6.4	5
CO <sub>2</sub>	1.6	6
CO	0.86	7
N <sub>2</sub>	0.84	8
NO	0.63	8
O <sub>2</sub>	0.48	8

ground state electron multiplicities, as follows:  $g_e = 2$ ,  $g_i = 1$  for alkali metal ions, and  $g_n = 2$  for alkali metal atoms.

As a representative example of the electron concentrations attainable in the combustion chamber, consider the propellant system Aerozene:50 and nitrogen tetroxide. Flame photometric analysis of a number of samples drawn from missile storage tanks<sup>3</sup> indicate the content of potassium to be one ppm in Aerozene:50 and 0.04 ppm in nitrogen tetroxide, with the content of sodium being negligible by comparison. Over the range of temperatures and pressures given above the electron concentration in the combustion chamber  $n_{e,c}$  varies from about  $2 \times 10^{12}$  to  $5 \times 10^{13}$  electrons/cm<sup>3</sup>. These values represent an upper limit to  $n_{e,c}$  since many of the electrons formed in the combustion chamber will become attached to initially neutral molecules.

As the gas expands through the rocket nozzle, its temperature and density decrease rapidly. However, the rate of recombination of electrons with ions is not fast enough to reduce the electron concentration to thermal equilibrium values during expansion. As a result, the electron concentration at the nozzle exit is much greater than would be calculated from thermal ionization at the exit temperature. Procedures for taking into account the decreasing rate of attachment during expansion have been evolved for the case in which thermal ionization of a single species and recombination of electrons with it are the dominant processes.<sup>4</sup> In general, however, the degree of ionization is governed by thermal ionization of a number of different contaminants and a multitude of competing reactions take place which tend to reduce the electron concentration. Also, thermionic emission of electrons from small particles and particle aggregates such as carbon and aluminum oxide can lead to comparable electron concentrations. Additionally, if the nozzle is ablatively cooled, thermal ionization of impurities from the ablative material can be significant. Finally, the problem of calculating the electron concentration at the nozzle exit is further complicated by the lack of accurate values of the basic reaction rates. As a result of these difficulties, no accurate means of calculating the electron concentration at the nozzle exit is available and reliance must be placed upon experimental determinations.

#### ELECTRON COLLISION FREQUENCIES

As stated previously, electron collisions result in absorption of the electromagnetic wave energy. Calculation of the electron collision frequency at the nozzle exit is not hampered by as many

**TABLE II — Electron Momentum Transfer Cross-Sections for Several Molecular Species (after Ref. 5)**

Molecule	Cross-section (CGS Units)	Temp. Range (°K)
CO	$Q = 2.08 \times 10^{-23} v^2 + 2.64 \times 10^{-16}$	$T \leq 2.5 \times 10^4$
CO <sub>2</sub>	$Qv = 4.7 \times 10^{-8}$	$T \leq 10^4$
H <sub>2</sub> O	$Qv^2 = 5.9$	$T \leq 10^4$
HCl	$Qv^2 = 1.85$	$T \leq 10^4$
NH <sub>3</sub>	$Qv^2 = 3.7$	$T \leq 10^4$
N <sub>2</sub>	$Q = 3.29 \times 10^{-23} v^2$	$288 \leq T \leq 1200$
H <sub>2</sub>	$Q = 1.45 \times 10^{-23} v^2 + 8.9 \times 10^{-16}$	$300 \leq T \leq 10^4$
H <sub>2</sub>	$Q = 8 \times 10^{-16}$	$50 \leq T \leq 5000$

\* Straight line approximation

$v$  = electron velocity

$\approx 6.22 \times 10^8 \sqrt{T} \text{ } ^\circ\text{K} \cdot \text{cm}/\text{sec}$

uncertainties as is the electron concentration. The exhausts of liquid propellant rocket engines are largely composed of the molecules H<sub>2</sub>O, N<sub>2</sub>, CO<sub>2</sub>, and CO with H<sub>2</sub>O usually being the most abundant species. The thermally dissociated products of the above molecules and their ions are also present but in much smaller concentrations. For composite solid propellants containing ammonium perchlorate, a large concentration of HCl is also present.

In rocket exhausts, collisions between electrons and ions have negligible effects as compared to collisions between electrons and neutral molecules. The effective collision frequency of electrons in the exhaust gas mixture is given by

$$\nu = \nu \sum_i N_i Q_i \quad (11)$$

where  $N_i$  is the number of molecules per unit volume of the  $i$ th species,  $Q_i$  is the velocity dependent collision cross section for the  $i$ th species and  $\nu$  is the random thermal velocity of the electrons. Electron energies in rocket exhausts are relatively low, being of the order of a few tenths of an electron volt. One electron volt corresponds to 11,605 °K. While the momentum transfer cross sections are not well known for most molecules at such low energies, they are fairly well known for H<sub>2</sub>O, CO<sub>2</sub> and CO. These are usually the most abundant molecules in rocket exhausts, and they also have the largest cross sections (see Table I). Since the exhaust gas temperature decreases continuously throughout the jet, changes in the effective collision frequency with temperature or equivalently with random thermal velocity need to be taken into account. The momentum transfer cross sections of the most important molecules are listed in Table II in terms of their velocity dependence, as given by the data of Molmud.<sup>6</sup> Typical values of the collision frequency at the nozzle exit  $\nu_{ex}$  as calculated for the exhausts of a number of rocket engines range from between about  $5 \times 10^8$  to  $5 \times 10^{11}$  per second, for high expansion ratio and low expansion ratio nozzles, respectively.

**MEASUREMENT OF EXHAUST PLASMA BY MICROWAVE ABSORPTION**

Measurement of the electron concentration and collision frequency at the nozzle exit is best accomplished by microwave probing of the exhaust during static test firings. For rockets designed for high altitude operation, testing at sea level requires the use of cut-down nozzles (to avoid the formation of shocks within the nozzle by matching the exit pressure with ambient pressure). This leads to the necessity of scaling the values of electron concentration and collision frequency obtained for the smaller expansion cut-down nozzle to the larger nozzle. Consequently, when practicable, microwave probe measurements of high altitude rocket engines are performed in a large partially evacuated chamber. Because of large-amplitude vibrations when the engine is operating and fluctuations in the exhaust jet boundary, microwave interferometers are not usually employed. Instead, use is made of the dependence of plasma absorption on wave frequency. This method relies upon the measurement of attenuation at two or more frequencies (Fig. 5).

As an illustration of the method consider the case for which  $f_{1,2} \gg \nu_p^2$  and  $f_{1,2} \nu \gg \nu_p^2$ . Reference to Table III shows that these conditions are satisfied in typical rocket exhausts for probe frequencies in the range of 40 to 70 Gc/s. For these conditions the imaginary part of the effective relative dielectric coefficient is much less than the real part and the real part is close to unity, i.e.,  $K_i \ll K_r$  and  $K_r \approx 1$ . In terms of the average angular plasma frequency and the average electron collision frequency at the exit plane,  $\omega_{p,ex}$  and  $\nu_{ex}$ , respectively, the normalized attenuation coefficient from Eq. 4 is:

$$\frac{\alpha}{k_o} \approx \frac{K_i}{2} \quad (12)$$

$$= \frac{1}{2} \left( \frac{\omega_{p,ex}^2}{\omega^2} \right) \left( \frac{\nu_{ex}}{\omega} \right) \left( 1 + \left[ \frac{\nu_{ex}}{\omega} \right]^2 \right)$$

This may be rewritten as (12a)

$$\alpha_1 \omega_1^2 + \alpha_1 \nu_{ex}^2 - \left( \frac{\nu_{ex} \omega_{p,ex}^2}{2c} \right) \approx 0$$

where  $\alpha_1$  is the power attenuation expressed in nepers/cm, measured at frequency  $f_1$ ; ( $\alpha_1 = (a_1/8.686z)$ , where  $a_1$  is the measured attenuation in dB and  $z$  is the transmission path through the exhausts in cm). Similarly, measurement of the attenuation at a second frequency  $f_2 > f_1$  leads to:

$$\alpha_2 \omega_2^2 + \alpha_2 \nu_{ex}^2 - \left( \frac{\nu_{ex} \omega_{p,ex}^2}{2c} \right) \approx 0 \quad (12b)$$

**TABLE III — Representative Values of the Plasma Parameters Attenuation Near the Nozzle and Exit of Rocket Engines**

$n_e$ ( $10^{10}$ elec- trons/cm <sup>3</sup> )	$\nu$ ( $10^{11}$ s <sup>-1</sup> )	$f_p$ (Gc/s)	$\nu/f_p$	Attenuation per Unit Length (dB/meter)	
				( $f = 5$ Gc/s)	( $f = 10$ Gc/s)
30	3	4.9	61	44.5	39.5
4	4	1.8	220	4.5	4.4
1.5	5	1.1	460	1.4	1.4
0.3	0.08	0.5	16	1.1	0.3
0.08	1.5	2.5	600	0.2	0.2

Simultaneous solution of Eqs. 12a and 12b yields for the average electron collision frequency:

$$\nu_{ex} = \left( \frac{\alpha_2 \omega_2^2 - \alpha_1 \omega_1^2}{\alpha_1 - \alpha_2} \right)^{1/2} \text{ collisions/sec} \quad (13)$$

Substitution of  $\omega_{p,ex}^2 = 3.24 \times 10^8 \pi^2 n_{e,ex}$  into Eq. 12a gives for the electron concentration at the exit plane:

$$n_{e,ex} = 1.87 \times 10^{-1} \left( \frac{\alpha_1}{\nu_{ex}} \right) (\omega_1^2 + \omega_2^2) \text{ electrons/cm}^3 \quad (14)$$

Since the exhaust jet is usually larger than the free space wavelength of the probing radiation, the microwave beam may be scanned across the exit plane to determine the transverse variation of the plasma parameters.

Having determined the average values of electron concentration and collision frequency at the nozzle exit, their variations throughout the exhaust jet can be computed. The simplest case to consider is the situation in which loss of free electrons by such processes as recombination, attachment, and diffusion is negligible, and in which formation of free electrons is also negligible. The electron formation processes include impact ionization (in the internal shocks and at the exhaust jet boundary, photo-ionization, thermal ionization and chemi-ionization. (The process by which a free electron is formed by the transfer of energy of excitation between molecules. It appears to be a significant ionization process only when the alkali impurity level is low, approximately less than 1 ppm, and when the gas temperature is relatively low, less than 1700°K.)

The latter two processes can significantly increase the number of free elec-

**TABLE IV — Dependence of Spatially Varying Electron Collision Frequency on Exit Plane and Exhaust Jet Properties**

Molecule	Functional Dependence on Thermal Velocity	$\nu/\nu_{ex} =$
H <sub>2</sub> O } HCl } NH <sub>3</sub> }	$Qv^2 = \text{constant}$	$(\rho/\rho_{ex}) \times (T_{ex}/T)^{1/2}$
CO <sub>2</sub>	$Qv = \text{constant}$	$(\rho/\rho_{ex})$
H <sub>2</sub>	$Q = \text{constant}$	$(\rho/\rho_{ex}) \times (T/T_{ex})^{1/2}$
N <sub>2</sub> } CO }	$Q/v = \text{constant}$	$(\rho/\rho_{ex}) \times (T/T_{ex})$

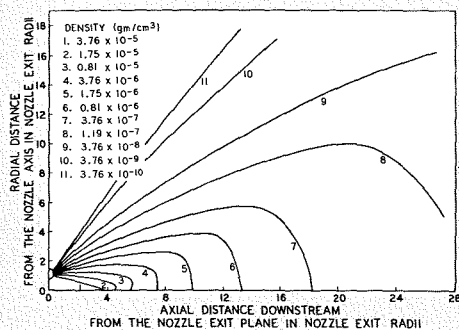


Fig. 6—Contours of constant mass density for Atlas sustainer engine exhausting into vacuum (after reference 8).

trons in the exhaust jet when afterburning of uncombusted fuel with oxygen in the atmosphere occurs. (At altitudes greater than about 200,000 feet, afterburning does not usually occur.) It is also necessary to assume that no mixing occurs between the atmosphere and the exhaust jet. Since the electron mole fraction remains constant throughout the exhaust, the simple case under consideration is commonly called the frozen flow case.

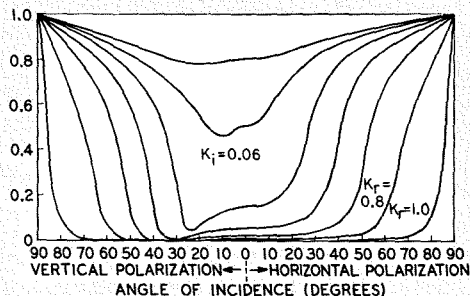
To determine the spatial variation of  $n_e$  and  $\nu$  throughout the exhaust, it is necessary to specify the axial and radial distribution of mass density and temperature within the jet. Such descriptions of the jet flow field can be calculated numerically by the method-of-characteristics solution of a compressible gas expansion<sup>8,9</sup>. A typical set of mass density contours obtained by this method for the ATLAS sustainer engine exhausting into a vacuum is shown in Fig. 6.

For the case of frozen flow, the mass density contours lead directly to corresponding contours of electron concentration since

$$n_e = \left( \frac{n_{e,ex} \rho}{\rho_{ex}} \right) \quad (15)$$

Combined with contours of constant gas temperature, the mass density contours also yield the spatial variation of collision frequency throughout the exhaust jet. The dependence of the spatially varying electron-neutral particle colli-

Fig. 7—Variation of the power reflection coefficient with angle of incidence for a uniform plasma (after reference 10).



sion frequency on  $\nu_{ex}$ ,  $T_{ex}$ , local mass density  $\rho$ , and temperature  $T$ , is given in Table IV for a number of different molecules. The average collision frequency at any point in the exhaust jet is given by Eq. 11.

Determination of the spatial variation of  $n_e$  and  $\nu$  throughout the exhaust enables estimates to be made of the attenuation of electromagnetic waves intercepted by it. First, it is necessary to determine whether attenuation by reflection at the exhaust jet-air boundary is significant for the particular propagation paths being considered. The manner in which the power reflection coefficient for a plane wave incident upon a uniform plasma varies with angle of incidence has been investigated by Bachynski, et al.<sup>10</sup>

Plots of the variation of the power reflection coefficients for horizontally and vertically polarized waves ( $R_h$  and  $R_v$ ) respectively as a function of angle of incidence are shown in Fig. 7. Curves are shown for  $K_i \ll 1$  ( $K_i = 0.06$ ), and  $K_i = 1$  and 0.8, which closely corresponds to conditions commonly attainable in liquid propellant rocket exhausts. As these plots indicate, small attenuation by reflection occurs for all but relatively large angles of incidence.

Refraction by the exhaust can be taken into account by successive application of Snell's law to each of the plasma slab sections into which the exhaust is divided. The attenuation along the propagation paths of interest may then be computed from

$$a = \sum_1^N a_N X_N \quad (16)$$

where  $X$  is the length of the propagation path through a plasma slab of width,  $w$ . The average attenuation per unit length  $a_N$  is computed from Eq. 4, with  $n_e$  and  $\nu$  of a particular slab being

$$n_e = \frac{(n_{e,N-1} + n_{e,N})}{2} \quad (17)$$

and:

$$\nu = \frac{(\nu_{N-1} + \nu_N)}{2} \quad (18)$$

While the attenuation computed in the manner outlined in this article does not take into account a number of effects, it does provide reasonable estimates of signal strength reduction, particularly for high altitude missiles and when the exhaust is large compared to the free space wavelength. Information of this type is extremely useful in determining the number and location of antennas aboard the missile and at ground stations.

## CONCLUSIONS

At present there is no accurate means of calculating the electron concentration in rocket exhausts. Such calculations

are precluded because of the extreme complexity of the large number of chemical, gas dynamic and physical processes which occur in the combustion chamber and during expansion of the combustion products through the nozzle, and within the jet. In addition, many of the basic reaction rates governing the ionization level are only known approximately. As a result, when confronted with the problem of predicting the attenuation of electromagnetic signals by a particular rocket exhaust, reliance must be placed upon experimentally determined values of the exit plane plasma parameters. These are then combined with the calculated variation of mass density and temperature within the jet to specify the spatial variation of its plasma properties. When experimentally determined exit plane values are used, reasonable estimates may be made of exhaust-induced attenuation, but only for a limited range of conditions—the most important being the absence of afterburning and the absence of large scattering at the exhaust-jet-air boundary. Considerably more knowledge concerning afterburning, scattering at the exhaust boundaries and the effects of turbulence in the ionized exhaust must be obtained before accurate characterization of rocket exhausts will be possible.

## BIBLIOGRAPHY

1. M. P. Bachynski, T. W. Johnston, and I. P. Shkarofsky (RCA Victor Res. Labs, Montreal) "Electromagnetic Properties of High Temperature Air," *Proc. IRE* 48, 347-356 (March 1960).
2. M. M. Saha and H. K. Saha, *A Treatise on Modern Physics*, Vol. 1. The Indian Press, Ltd., Allahabad and Calcutta (1934).
3. John McDonald, *Analysis for Sodium and Potassium in Titan II Propellants*, Final Report, Materials Engineering, Martin Co., Denver, Colorado (September 2, 1964).
4. D. E. Rosner, "Estimation of Electrical Conductivity at Rocket Nozzle Exit Sections," *ARS Journal* 32, 1602 (October 1962).
5. P. Molmud, *The Electrical Conductivity of Weakly Ionized Gases: Part I, Ions in Flames and Rocket Exhaust Conference*, Palm Springs, California, Space Technology Laboratories, Inc., Report No. 2586-62 (October 10-12, 1962).
6. M. P. Bachynski, I. P. Shkarofsky, and T. W. Johnston, (RCA Victor Res. Labs, Montreal) *Plasmas and the Electromagnetic Field*, to be published.
7. I. P. Shkarofsky, M. P. Bachynski, and T. W. Johnston, (RCA Victor Res. Labs, Montreal) "Collision Frequency Associated with High Temperature Air and Scattering Cross Sections of the Constituents," *Electromagnetic Effects of Re-entry*, pp. 24-26. Pergamon Press (1961).
8. S. Altshuler, M. M. Moe and P. Molmud, *The Electromagnetics of the Rocket Exhaust*, Space Technology Laboratories, Inc., Report No. GM-TR-0165-00397 (June 15, 1958).
9. R. J. Prozan, and A. R. Bowyer, *PMS Jet Wake Study Program UN-10*, Lockheed Missiles and Space Company, Report 919901 (October 9, 1961).
10. R. J. Prozan and A. R. Bowyer, *Revisions of the UN 10 Jet Wake Program*, Lockheed Missiles and Space Company, Report IDC 57-11-623 (April 20, 1962).
11. K. Graf and M. P. Bachynski, (RCA Victor Res. Labs, Montreal) *Transmission and Reflection of Electromagnetic Waves at a Plasma Boundary for Arbitrary Angles of Incidence*, RCA Victor, Research Report 7-801, 11, prepared for Electronics Research Directorate, Bedford, Mass. on AF 19(604)7291 (March 1961).

# EFFECTS ON RADAR OF PLASMA PRODUCED BY HIGH-ALTITUDE NUCLEAR DETONATION

A high-altitude nuclear detonation produces various forms of plasma which interfere with the propagation of radar waves in different ways. Such plasmas are therefore of serious significance to military system designers, since radar and/or communications system performance can be adversely affected by them. Discussed herein are characteristics of the different plasmas produced by nuclear detonations and some of their effects on radar systems (to the extent allowed by security regulations in an unclassified paper).

DR. K. SITTEL, Ldr.

*Systems Physics*

*Systems Engineering, Evaluation, and Research*

*DEP, Moorestown, N. J.*

THE concept of a plasma can be applied to natural and man-made ionization regions in the atmosphere which interact with the propagation of electromagnetic waves.

According to Langmuir's definition, a plasma is a highly ionized gas in which the negative and positive charges can be considered equal so that the overall electrical characteristic of the gas is neutral. For this discussion, this implies that the effects of space charges are not important over the wavelength of the electromagnetic waves under consideration. While the plasma concept was first used in conjunction with an electrical gas discharge, naturally produced plasma may be found erupting from the sun's surface, in the interstellar space or in our own atmosphere.

*Final manuscript received August 31, 1965.*

DR. KARL SITTEL received his PhD in Physics from the University of Frankfurt am Main, Germany in 1940. He held a staff position at the Max Planck Institute for Biophysics until 1947; he developed a complete radio sonde system including for the first time, a rocket launch capability for the German Navy. Dr. Sittel obtained a U. S. citizenship in 1953 and worked with the U. S. Navy and subsequently with the Franklin Institute of Pennsylvania, concentrating on the measurement of viscoelastic properties and sound propagation. In 1959 Dr. Sittel joined RCA where he was given the task to develop a high altitude nuclear burst effects capability. Dr. Sittel investigated the early Hard-tack nuclear-test results and applied his work to BMEWS, Space Surveillance Systems, Hard Point Defense and Urban Defense Systems. He is a member of DASA's RF-attenuation working group and directs SEER's Fishbowl Analysis program. In April 1963, he became Leader of SEER's Systems Physics group devoting much of his efforts to the

aerospace environment. Dr. Sittel has made numerous contributions to technical journals and has been granted six U. S. patents. He is listed in American Men of Science, Who's Who in the East, and in Kuerchner's Gelehrten Kalender. He is a member of the American Physics Society, Research Society of America, and the Franklin Institute.



For electrons in free space, one may define:

$$\frac{4\pi N_e e^2}{m} = \omega_p^2$$

where  $\omega_p$  has the dimensions of a frequency and is called the *circular plasma frequency*. When the wave frequency is smaller than the plasma frequency, the medium is called *overdense*; if the wave frequency is larger, it is called *underdense* in respect to the particular propagating wave. Because of the inhomogeneous character of most plasmas, the propagation of electromagnetic waves through such a plasma is a matter of considerable complexity. Fortunately, one finds in some cases that the physical situation can be considerably simplified resulting in tractable expressions for the solution of the propagation equations. The main effects encountered in the propagation of electromagnetic waves through a plasma are:

- |               |                  |
|---------------|------------------|
| 1) absorption | 4) diffraction   |
| 2) reflection | 5) scattering    |
| 3) refraction | 6) scintillation |

All these propagation effects are found in the propagation of electromagnetic waves through the normal ionosphere. This paper, however, will be concerned with the various forms of the artificial plasmas encountered subsequent to a high-altitude nuclear detonation and the specific electromagnetic wave propagation phenomena through the affected atmosphere.

Contrary to a nuclear detonation at or near the ground, the tremendous energies released from a single high-altitude nuclear detonation are almost entirely transformed into the ionization of the atmosphere. The process of depositing the tremendous energies involved are very complex. The released energy (called the *yield*) is compared with that developed by the hypothetical detonation of an equivalent amount of TNT; it is measured in *kilotons* or *megatons* of TNT (where the energy of 1 kiloton of TNT is taken as  $10^{12}$  calories).

The plasma regions of interest produced by such nuclear detonations are:

- 1) increased ionization in the D-layer
- 2) highly ionized beta-particle ionization regions
- 3) the fireball
- 4) ionized debris regions and artificial radiation belts produced by the detonation.

The remainder of this paper will discuss each of these.

## D-LAYER IONIZATION

Thermal and nuclear radiation escaping the immediate vicinity of a high-altitude nuclear detonation, or burst, will produce widespread and slowly varying ionization

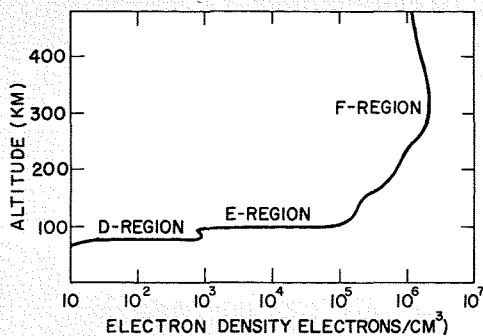


Fig. 1—Electron densities in D, E, and F regions of the ionosphere in the daytime. (Ref. 1).

Fig. 2—Radius of debris expansion and corresponding D-region electron density as function of time for a 1-megaton fission detonation in the altitude range of 40 to 70 miles. (Ref. 2).

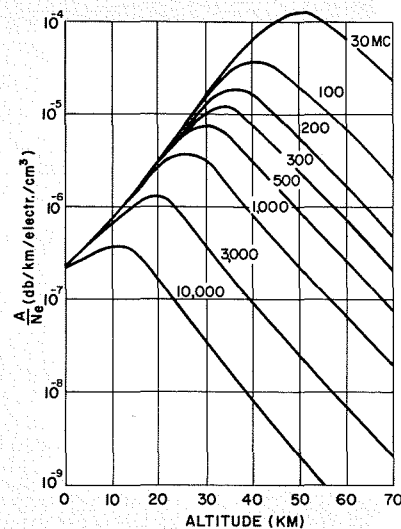
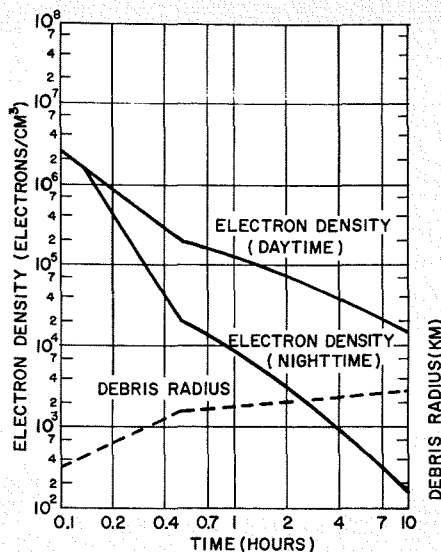


Fig. 3—Attenuation-height curves for electron neutral molecule collisions.

layers which permit simplified treatment of electromagnetic wave absorption.

Nuclear bursts above 80-km altitude show widespread ionization within the lower D-layer which produces a maximum radio-frequency attenuation roughly at the 70-km altitude level. For bursts below 100 km, the D-layer ionization is primarily produced by the initial instantaneous gamma and neutron radiation escaping the immediate burst region. This radiation comprises about 3% of the total energy yield of the burst.<sup>1</sup> The megavolt gamma photons and neutrons spread spherically around the burst point, depositing their energy in proportionality to the atmospheric density at the point of interest.

Still another instantaneous source of ionization is the thermal radiation escaping the immediate vicinity of the burst. This originates from the hot core of the nuclear reaction and comprises about 75% of the total yield.<sup>2</sup> This thermal radiation becomes important for causing widespread ionization as soon as the burst altitude approaches 100 km. Because this radiation represents the major part of the total energy yield, the resulting ionization pulse can be very high.

Contributing to the ionization and responsible for the longer-lasting ionization effects is the *delayed* ionization originating from the radioactive debris of the nuclear burst. This delayed ionization source decays with time  $t$  roughly following a  $t^{-1.2}$  law.<sup>1</sup> The delayed radiation emitted by the fission products consists of gamma ray photons and beta electrons carrying away less than 10% of their energy.<sup>2</sup>

Under daylight conditions, the ambient ionization source caused by the sun's radiation contributes to this persistent ionization source.

The time history of the resulting ionized layer depends on: 1) the *time history* of the delayed source strength

and the *magnitude* of the initial pulse ionization; and 2) the *reaction rate processes* particular to any given altitude, which tend to reduce the free electron content.

In the D layer (altitude about 65 to 80 km), the free electrons are essentially removed by attachment to neutral molecules (primarily oxygen molecules) or by recombination with ions. The density of neutral particles in the D-layer is approximately  $10^{-4}$  times the sea level density of the atmosphere, so that free electrons may exist for several minutes. This is long enough for the sun's radiation to maintain a daytime electron density of  $10^3$  electrons/cm<sup>3</sup>. The ambient electron densities under daytime conditions are shown in Fig. 1 for the D, E and F region of the atmosphere. For comparison, a 1-megaton fission-yield explosion at 70 km will raise this electron density at the explosion height instantaneously above  $10^8$  electrons/cm<sup>3</sup> as far out as 160 km from the explosion. This and all higher electron densities, however, will decrease to  $10^7$  in less than one second. The subsequent decay of the electron density will depend considerably on whether day or night conditions exist. In daytime, it will take about 1,000 seconds for the electron density to decrease to  $10^5$  electron/cm<sup>3</sup>, while during nighttime the electron density is down to  $10^4$  in less than 15 seconds.<sup>1</sup> By this time, however, the persistent gamma and beta radiation from the radioactive fission debris controls the decrease of the electron density. In Fig. 2, the D region electron density over a region roughly corresponding to the debris cloud is shown as a function of time both for day and night conditions.

The D-region ionization layer can be treated roughly as parallel layers of slowly varying electron densities. Neglecting the influence of the geomagnetic field for all frequencies much larger than the gyro frequency (1.5

Mc/s), the wave attenuation  $A$  (in dB/km) is:

$$A = 4.6 \times 10^4 N_e \left( \frac{\nu}{\omega^2 + \nu^2} \right)$$

Where  $N_e$  = electron density (cm<sup>-3</sup>),  $\nu$  = collision frequency (s<sup>-1</sup>), and  $\omega$  = angular frequency of the wave (rad/s). The collision frequency  $\nu$  is equal to the number of collisions an electron makes per second with a neutral molecule or ion. At the 70-km altitude, the collision frequency is about  $10^7$  per second. The collision frequency increases rapidly for lower altitudes. In Fig. 3, the attenuation per kilometer divided by the electron density is shown for various wave frequencies and altitudes for electron-neutral molecule collisions.

Because of the high collision frequencies in the D-layer region, the refraction of the waves is small; as long as the angular wave frequency is greater than the collision frequency, the refractive index  $n$  may be approximated by:

$$n = \left( 1 - \frac{0.8 \times N_e}{10^4 f^2} \right)^{1/2}$$

where  $N_e$  = electron density (cm<sup>-3</sup>) and  $f$  = frequency (Mc/s). This formula may be used to give a rough estimate of the refraction of a wave penetrating the D layer using Snell's law:

$$\frac{\sin \phi_1}{\sin \phi_2} = n$$

where  $\phi_1$  is the angle of incidence and  $\phi_2$  the angle of refraction. This procedure is good for the ionized D layer and for frequencies above 100 Mc/s.

In general the refraction effects calculated on the basis of a nonabsorbing medium will be larger than the true effects. The error will increase if the refractive layer is lowered in altitude. However, the error will be only of significance if large electron densities can be maintained in the lower atmosphere.

Fig. 4 shows the maximum ionization density permissible for negligible refraction for a collision frequency of  $10^7$  for various angles of incidence  $\phi_i$ .

The assumption of horizontal uniformity and slowly varying electron density with height are of course an idealization of the real state of the  $D$  layer. Actually there is a statistical distribution of the electron density as well as the other atmospheric parameters in space and time which complicates the transmission picture. However, for the  $D$  layer and distances not too close to the burst point, the simplified approach produces remarkably good results.

#### BETA TUBE

The beta electrons emitted by the fission debris spiral down the geomagnetic field lines producing some field-aligned plasma which causes scatter and scintillation.

If the nuclear burst occurred above, say, 60 km or the fission debris has risen above this altitude, the mean free path for the highly energetic beta electrons (average energy about 1 MeV) is large enough so that they can be spiraling around the geomagnetic field. In a uniform magnetic field of value  $|B|$ , the motion of an electron is described by:

$$m \cdot \frac{dv}{dt} = \frac{e}{c} (\vec{v} \times \vec{B})$$

where  $m$  = mass of the electron (gm),  $v$  = velocity vector of the electron ( $\text{cm} \cdot \text{s}^{-1}$ ),  $\vec{dv}/dt$  = first time derivative of the velocity vector ( $\text{cm} \cdot \text{s}^{-2}$ ),  $e$  = charge of the electron (ESU),  $\vec{B}$  = mag-

netic field strength vector (EMU), and  $c$  = speed of light (cm/s). The equation is written in the cgs system. The solution of this equation shows the electron motion to consist of a circular motion around the magnetic field lines with a uniform translation along the magnetic field. The circular frequency  $\omega_c$  with which the electron cycles around the field is called the *cyclotron frequency* and can be written:

$$\omega_c = 2\pi f_c = \frac{e}{cm} B$$

Or:

$$\frac{f_c}{B} = 2.799 \text{ Mc/s per gauss}$$

Assuming isotropic emission of the beta particles, half of the betas will spiral upward. The other half spiral downward toward the denser portion of the atmosphere where they will lose their kinetic energy by ionization. This downward beta stream will therefore produce a highly ionized region in the  $D$  layer which corresponds to the fission debris source. Inasmuch as the debris source is moving upward, the beta ionization region moves along horizontally as directed by the geomagnetic field. The upward portion of the betas will find only decreasing atmospheric density and preserve a good part of their kinetic energy. Consequently, the electrons follow the geomagnetic field towards a region on the opposite side of the magnetic equator called the *magnetic conjugate region*. In general, except when the debris is very high, the electrons will be absorbed in this region and cause an ionization region similar to the one near the source. The "tube" formed by the highly energetic electrons spiraling around the geomagnetic field is called the *beta tube*. The beta tube has great similarity with the phenomenon of the natural aurora and is sometimes referred to as the *auroral tube*. Where the auroral tube dips into the atmosphere, it becomes visible because of luminescence created by the interaction of the beta electrons with the atmospheric molecules. Such an artificial aurora was first observed in connection with the 1958 nuclear test of Johnston Island in the Pacific Ocean during the test detonation called SHOT TEAK, a high-altitude burst in the megaton range. Within the auroral tube, field-aligned ionization is created which will fluctuate by turbulence.

The theoretical treatment of this phenomenon is difficult. Present turbulent theory is based on stationary random processes, a requirement which is probably not fulfilled in the nuclear burst case. Furthermore, the theory has not yet been successfully developed to take account of field-aligned irregularities.

Therefore, one is forced to rely on a phenomenological approach. Booker<sup>3</sup> has used such an approach for the case of the natural aurora, assuming electron-density irregularities which have a scale length  $L$  along the geomagnetic field that is large compared to the scale length  $T$  transverse to the field. He computes the scattering cross section per unit volume ( $\sigma_c$ ) for nearly normal incidence to geomagnetic field as:

$$\sigma_c = 155 \left( \frac{1}{\lambda_p^4} \right) \left( \frac{\overline{[\Delta N_e]^2}}{N_e} \right) \left( T^2 L \exp \left[ - \frac{78.8}{\lambda^2} (T^2 + L^2 \psi^2) \right] \right)$$

where  $\lambda_p = 2\pi c/\omega_p$  = plasma wavelength,  $\psi$  = the complement of the angle between the direction of incidence and the geomagnetic field,  $(\overline{[\Delta N_e]/N_e})^2$  = the average of the square of the relative mean fluctuation of the electron density, and  $\lambda$  = radio wavelength. For unity incident power density, the Booker formula gives the backscattered power per unit solid angle, and per unit volume.

Booker's or similar approaches, may be applicable to the field-aligned ionization of a nuclear burst. The success depends on the proper selection of an autocorrelation function. Experimental cross-section analysis with respect to frequency dependence and scattering angle is used to affirm such selections.

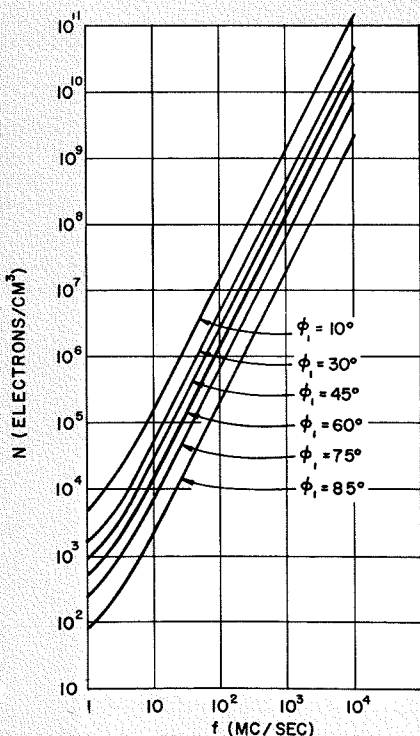
While backscattering from the beta tube is of importance when the radar line of sight is nearly perpendicular to the geomagnetic field, another phenomena called *scintillation* should become important when the line of sight is nearly parallel with the field. The scintillation phenomena is caused by the distortion of the plane wave front propagating in the direction of the cylindrical inhomogeneities. The scintillation phenomena has first been observed by the fluctuations in amplitude and phase of radio waves originating from radio star sources and propagating through the ionosphere. Again, it is Booker<sup>4</sup> who has published a scintillation theory which describes the mean square fluctuations of amplitude and angle of arrival of waves propagating through a medium of isotropic irregularities in the electron density, namely:

$$\overline{(\Delta\theta)^2} = \left( \frac{1}{4\pi^2} \right) \left( \lambda^4 r_e^2 \right) \left( \frac{[\overline{[\Delta N]^2}]}{L} \right) (\tau \sec H)$$

And:

$$\overline{\left( \frac{\Delta A}{A} \right)^2} = \left( \frac{1}{32\pi^4} \right) \left( r_e^2 \lambda^4 \sec^3 H \right) \left( \frac{h^2}{L^3} \right) \left( \frac{[\overline{[\Delta N]^2}]}{\tau} \right)$$

Fig. 4—Maximum electron density for negligible refraction  $\nu = 10^7$  (Ref. 17).



where  $(\overline{\Delta\theta})^2 =$  mean square of angle of arrival fluctuations,  $(\overline{\Delta A/A})^2 =$  mean square of relative amplitude fluctuations,  $\lambda =$  radio wavelength (cm),  $H =$  zenith angle of the radar wave penetrating the ionosphere,  $h =$  height of the scintillation layer,  $(\overline{\Delta N})^2 =$  mean square of the electron density fluctuations,  $\tau =$  layer height over which fluctuations of the electron density are of importance,  $L =$  scale length of the electron density irregularities,  $r_e = e^2/mc^2$  classical electron radius (cgs),  $e =$  electron charge (esu),  $m =$  mass of an electron (gm), and  $c =$  speed of light (cm/s).

Hewish<sup>5</sup> reports observation on the ambient ionosphere. He finds the angular scintillation proportional to the square of the wavelength in accordance with the theory. According to Rush and Colin<sup>6</sup> the relative amplitude fluctuation should become greater for propagation in the direction of the geomagnetic field lines along which the irregularities will align. Simultaneous observations of both the RMS fluctuations in angle of arrival and in amplitude should be usable to determine magnitude and time variation of large scale irregularities.

#### FIREBALL

The hot, dense ionization region forming around the burst point expands and rises as a separate highly RF-absorbing entity, and is a source of RF noise, RF reflections, and various forms of scatter.

The instantaneous energy released from a high-altitude nuclear burst produces an extremely hot inner core with a moderately hot surface temperature. From this surface, soft x-rays are emitted which are absorbed in the surrounding atmosphere.<sup>7,8</sup> By absorption and re-radiation, the energy starts to spread in what is known as an *expanding radiation front*. As a result, the affected atmosphere is completely ionized and dissociated. This portion of the atmosphere, which at altitudes below 100 km forms a well distinguishable region around the burst point, is called the *fireball*.

The fireball, an extremely hot plasma, is characterized by a distinct shape—a sharp optical discontinuity which is nearly spherical and forms after a few shakes after the burst. (A *shake* is  $10^{-8}$  seconds.) Representing a separate entity, the fireball is subject to hydrodynamic motion. Depending on the burst altitude, the fireball will expand more or less rapidly towards pressure equilibrium with the surrounding atmosphere and simultaneously rise to less dense regions. This rise may be buoyant, like an oil droplet rising in water, or ballistic under the pressure differences

created between its lower and upper boundaries. The hydrodynamic motion again depends on the height of the burst and its yield. It is buoyant for the lower regions, ballistic for higher altitudes, and a mixture between both if the fireball is created in the inbetween altitudes. In some cases, the ballistic effect may be so strong that the fireball will shoot up way above its buoyant equilibrium altitude and then fall back and settle down at a final buoyancy level.

The SHOT TREAK experiment was the detonation of a nuclear device in the megaton yield range at around 70-km altitude. Its fireball<sup>1</sup> grew within 0.3 second to a diameter of about 18 km and increased to nearly 30 km at 3.5 seconds after the burst; the fireball rose with an initial rise velocity of about 1.5 km/s and after about 60 seconds reached a height over 145 km.

The moving fireball boundary of course interferes with the surrounding atmosphere, and turbulent mixing with the cooler surrounding air alters the motion of the fireball. Pressure differences within the fireball will cause its core to rise faster than its peripheral portion, producing a toroidal shape.

The electron density within a fireball at lower altitudes will be in thermal equilibrium with the hot plasma<sup>9</sup> which rapidly cools down to temperatures below  $10,000^\circ\text{K}$ . Further cooling by adiabatic expansion, mixing, and radiation lets the electron density drop rapidly, finally reaching a slowly decreasing level where it will be maintained by that portion of the delayed radiation which is deposited within the boundary of the fireball. The degree to which the delayed beta radiation can contribute to the fireball ionization depends on the altitude of the fireball. Once the fireball reaches altitudes above 60 km, a rapidly increasing portion of the beta radiation will escape and form the beta tube. At the lower altitudes, the ionization from the fission debris forming the core of the fireball can cause a several-fold extension of the duration of a given ionization level.

The expanding and rising plasma will interfere with the geomagnetic field as long as its conductivity is high enough to freeze in the local field and to prevent any exterior field line from penetrating the plasma. The motion of the plasma can lead to considerable field distortions which may influence in turn the deposition of the field bound beta energy. After the plasma has weakened sufficiently, the field lines snap back restoring the normal field conditions.

Electromagnetic waves reaching the surface of a fireball will be reflected as long as the electron density between the

fireball and the surrounding atmosphere is large and the surface is electrically smooth. Reflections from such an overdense smooth fireball ( $\omega_p > \omega$ ) have indeed been observed. When the fireball is underdense with respect to the radar wave ( $\omega_p < \omega$ ), the wave will penetrate into the plasma and interact with the electron-density distribution within the fireball plasma. In most cases, the fireball density will be large enough so that the collisions between the electrons and the neutral molecules and ions can not be neglected. Therefore, the wave energy will be scattered and absorbed. This scattering process is known as *volume scattering*. In addition, some of the energy returning to the radar receiver will be scattered forward through small angles within the fireball region, causing fluctuations of the amplitude and phase of the returning radar signal. Kolmogoroff<sup>10</sup> developed first the statistical theory of turbulence and names like Wheelon, Booker, Batchelor, Silverman are closely connected with turbulence and scattering problems. Silverman, Wheelon and Booker attempted to describe the backscatter phenomena and to produce tangible mathematical expressions for the backscatter cross-section. Theories of backscattered signals have been summarized by Millman.<sup>11</sup> Specific applications of these concepts to scatter problems connected with the fireball of a nuclear burst have been published in the classified literature by Chesnut<sup>12</sup> from Stanford Research Institute and DeWolf<sup>13</sup> from RCA.

To a degree, the work performed to describe the backscatter obtained in the ambient atmosphere by turbulence is certainly applicable. The essential difference is that the electron densities and the inhomogeneities produced by turbulence or hydrodynamic motion within the fireball will be many orders of magnitude larger than those found in the ambient atmosphere. Furthermore, the problem is complicated by the fact that during the equalization of the various energy forms deposited within the region of the fireball, all forms of dielectric irregularities will come to bear on propagation through the fireball.

For most system considerations, the lower-altitude fireball remains an opaque obstruction for radar waves which, depending on the wave frequency, may last for significant times. The motion of the fireball does complicate the problem in many cases. Radar clutter due to main-beam or side-lobe illumination of the fireball causes additional problems not yet fully explored. Moreover, the hot plasma is a noise source which raises the noise temperature of an antenna system. Fortunately, this noise is partially reduced

by the increased attenuation in the ionized atmosphere.

#### HIGH-ALTITUDE PLASMA

A nuclear-burst-produced plasma above the essential part of the atmosphere strongly interacts with the geomagnetic field producing local and global effects.

Once a nuclear explosion takes place at altitudes essentially above 150 km, the burst energy is no longer confined by the atmosphere alone; rather, the geomagnetic field becomes the principal force acting to limit its expansion. As the x-rays are now capable of spreading their energy over thousands of miles, they are no longer responsible for forming a fireball. Instead, an analogous region is formed by the expanding debris, the kinetic energy of which produces the radial motion of expansion. Once the expanding debris plasma is slowed down by the geomagnetic field—forming a magnetic bubble by compressing the magnetic field—the field will diffuse back and interact with the debris plasma, thus causing visible striation of the debris region. During the initial phase, the energetic beta particles emitted by the debris will be trapped in the bubble which expands along the field lines producing a banana shape. Through the tips of the banana, the beta electrons (as well as some ionized debris) will start to leak out. The electrons are trapped<sup>14</sup> and are reflected back and forth between the so-called *mirror points* (about 0.1 second for each passage between two mirror points<sup>2</sup>) as long as these mirror points are well above the *D* layer.

As the geomagnetic field decreases in strength with increasing distance from the earth, the spiraling electrons experience a sideward motion which lets them drift in an easterly direction. This drift will carry the mirroring electrons around the world within a half to a few hours and produce an artificial radiation belt very much like the van Allen belt. This has first been observed<sup>15</sup> during the ARCUS experiment in 1958 and a long-lasting lower radiation belt was built up by the 1.4-megaton 400-km-altitude explosion called SHOT STARFISH.<sup>16</sup> During the latter event, some of the debris was vented from the magnetic bubble and ejected to very high altitudes where the trapping of the geomagnetic field was quite efficient. The effect of the high-altitude plasma confined within the magnetic bubble on electromagnetic wave propagation is scattering. The collision frequency can be neglected at these altitudes, but the plasma will be anisotropic because of the interaction with the geomagnetic field.

In addition, the spiraling electrons are in a state of constant acceleration and emit synchrotron radiation. In this way, the trapped electrons become a continuing noise source whose noise radiation is directional—in the direction of the electron velocity. The noise amplitude is dependent upon the angle of observation of the electron and has a maximum at the mirror points. It is generally thought that synchrotron noise will have a negligible effect on radar.

During the 1958 TEAK experiment, sudden increases in the electron density, followed by a long-lasting decrease in the *E* and *F* layer were noted by ionosonde measurements.<sup>2</sup> The starting time of this disturbance was roughly proportional to the distance from the burst point. These reductions in the ambient ionospheric electron densities can mean loss of HF propagation. The phenomenon of a spread *F* was also observed after TEAK, meaning that the height read from the ionosonde records is no longer sharply defined but seems to indicate a diffuse layer. Spread *F* may be the result of field aligned ionization causing scattering of the incident wave energy. There was also some evidence of a tilting of the ionospheric layers, which can have a detrimental effect on HF communication by causing changing multipath conditions resulting in doppler shift and fading.

#### CONCLUSIONS

There are three types of plasmas created by a high-altitude nuclear burst:

The first is a *widespread ionization*, essentially an enhancement of the natural *D* layer ionization. This plasma interferes with communication and radar frequencies ( $> 100$  Mc/s), but for radar frequencies the blackout duration is brief. The second plasma, called the *fireball*, originates from the immediate region around the burst and represents a severe modification of the natural environment. The fireball will black out radar frequencies for many minutes. In addition, the fireball plasma interferes with the geomagnetic field causing severe field distortion. Depending on the height of the fireball, appreciable radar-wave refraction may occur. In addition, the fireball will scatter the radar energy and cause additional jitter in the radar system. Plasma noise is partially alleviated by the increased atmospheric absorption.

The third type of plasma is the *field-aligned plasma*. It is produced by the fission debris betas (which tied to the geomagnetic field form the beta tube) and by the interaction of the geomagnetic field with the debris fireball at very high burst-altitudes. The beta-tube ion-

ization is of considerable intensity, causing radar-frequency blackout for several minutes, backscatter in a direction perpendicular to the field lines, and introduction of radar jitter when looking in the direction of the field lines. The very high debris fireballs and their absorption is least understood, but they too interfere with the radar waves.

Presently, the absorption and refraction caused by the quasi-uniform burst plasma such as the *D* region enhancement can be predicted fairly well. To some degree, this holds also true for the generations of these ionization regions by a burst. Further theoretical and experimental effort are needed to achieve similar prediction capability for all those phenomena based on the inhomogeneous and statistically varying characteristics of a burst-produced plasma.

The degradation of radar systems by the combination of all the phenomena discussed in this paper must be seriously considered in all future designs of military systems.

#### BIBLIOGRAPHY

1. Samuel Glasstone, *The Effects of Nuclear Weapons*, published by the U. S. Dept. of Defense and AEC, 1962.
2. "Electromagnetic Blackout Guide," *Effects of High Altitude Nuclear Bursts on Electromagnetic Waves*, Vol. 1 DASA-1229, 1961.
3. H. G. Booker, *J. Atmos. Terr. Phys.*, Vol. 8 (1956), p. 204.
4. H. G. Booker, *Proc. IRE*, Vol. 46 (1958), p. 298.
5. A. Hewish, *Proc. Roy. Soc.*, Vol. 214 (1952), p. 494.
6. S. Rush and L. Collin, *Proc. IRE*, Vol. 46 (1958), p. 356.
7. A. S. Kompaneets and E. Ya. Lantsburg, "The Heating of a Gas by Radiation," *J. Expt. Theoret. Phys.* (U.S.S.R.) 41, 1649-1654.
8. E. I. Andriankin, "Heat Wave, Radiating Energy from Front," *Zhurnal Tekhnicheskoi*, Vol. 29, No. 11, Nov. 1959, *Transl. Soviet Physics, Tech. Phys.*, Vol. 4, 1960.
- 9a. F. R. Gilmore, *Equilibrium Composition and Thermodynamic Properties of Air to 2,400°K*, Rand-RM-1543, Aug. 1955.
- 9b. F. R. Gilmore, *Additional Values for the Equilibrium Composition and Thermodynamic Properties of Air*, Rand-RM-2328, 1959.
- 10a. A. N. Kolmogoroff, *Comptn. Rend. Acad. Sci. URSS*, Vol. 30, 1941.
- 10b. P. J. Nawrocki and R. Papa, *Atmospheric Processes*, Geophysics Corp. of Am., 1961.
11. G. H. Millman, *Atmospheric and Extra Terrestrial Effects on Radio Wave Propagation* (R 61 EMH-29) HMED, General Electric Co., June 61, p. 113.
12. W. G. Chesnut, *Nucl. Radar Clutter*, Vol. 1, DASA 1556 (Secret, Restricted Data).
13. D. DeWolf, et al, *Fishbowl Data Analysis*, Final Tech. Report, Vol. 1, June 1965 (Secret, Restricted Data), DASA-1673.
14. W. N. Hess, "Man-Made Radiation Belts," *Intern-Science and Technology*, Sept. 1963.
15. "Symp. on Scientific Effects of Artificially Introduced Radiation at High Altitudes," *J. Geoph. Res.*, Vol. 64, Aug. 1959.
16. H. Maeda, et al, "On the Geomagnetic Effects of the Star Fish High Alt. Nucl. Expl.," *Journal of Geoph. Res.*, Vol. 69, 1964.
17. D. H. Archer, *Absorption and Refraction of Electromagnetic Waves in an Ionized Atmosphere*, GE-TEMPO, RM 59 TMP-11 (1959).

# GUIDED WAVES IN GASEOUS PLASMAS

The general cold longitudinally-magnetized plasma waveguide involves extremely difficult analysis, since it must consider at least two media: plasma and the gap at the wall, not to mention dielectric containers, etc. One of these is generally gyrotropic—i.e., the transverse current  $J_t$  depends on both  $E_t$  and  $B \times E_t$ . All but the simplest cases require a computer for solutions. Useful simplifying assumptions and concepts are: nongyratory media and small perturbations  $\nabla \times E \approx 0$  (large wave vector), near cutoff (small longitudinal wave vector), single medium (no gaps), very high or low frequencies, perturbation theory, and coupled modes. General features and a concrete example of the plasma waveguide problem are discussed here.

**Dr. T. W. JOHNSTON**

*Research Laboratories  
RCA Victor Co., Ltd.  
Montreal, Canada*

THE elementary waveguide is easy to understand and the derivation and discussion of the results is to be found in standard texts on the subject. But, as soon as one begins to modify the waveguide or otherwise complicate the situation the theoretical complexity of the problem increases enormously. Nonetheless, in the past it has proved invaluable to brave the complications in order to satisfy the demands of system designers.

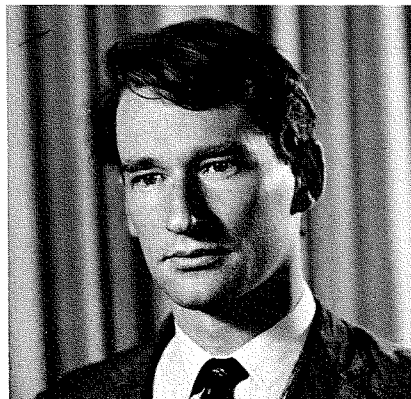
Some of the theory deals with the effect of doing things to the waveguide such as bending it, changing its shape, cutting holes or slots, or inserting posts and other obstacles. The object there was to bend, join, attenuate, change phase, launch, and detect the waves in the guide. These are all more or less permanent or slowly (mechanically) changing guide configurations involving passive isotropic elements.

In addition to these, there are passive microwave circuit elements which are not isotropic (for example, isolators) or which change rapidly with time (transmit-receive switches) and of course the active elements, the microwave tubes. The tubes and the transmit-receive switches, while they do really involve electron or plasma theory, are beyond the scope of this discussion, since they are coupled to the waveguide rather than being a part of it.

Objects like isolators require the study of the way waves propagate in wave-

guides containing media (in this case ferrite). In the endeavor to realize the potentialities of these materials, the theory for waveguides containing interesting media is developed as far as possible. The media considered are ferrite-like<sup>1</sup> (anisotropic permeability) or of the plasma variety<sup>2,3,4</sup> (possibly anisotropic permittivity). Interest in the plasma also stems from the possibility of coupling to charge streams, either of free electrons or of those in solid materials.

DR. TUDOR W. JOHNSTON graduated in 1953 with a BEng degree in Engineering Physics from McGill University. He then entered Trinity College, Cambridge, where he received his PhD degree in 1958 with a thesis on the dynamics of magnetically-focussed electron beams and phenomena related to the presence of ions in such beams. At the RCA Victor Laboratories, Dr. Johnston has carried out theoretical investigations on many aspects of plasma physics. Dr. Johnston is a member of the Canadian Association of Physicists and the American Physical Society.



A fuller review of these topics is given elsewhere.<sup>5</sup>

Another point of interest in the plasma waveguide studies is that they can provide useful results to check some aspects of general plasma theory for some plasmas where the infinite slab model (as used by Bachynski, et. al. of RCA Victor Research Laboratories, Montreal, in other current papers<sup>18</sup>) cannot be employed.

While the general features and one concrete example of the plasma waveguide problem are discussed here, two other current papers also deal with this topic, for a particular slow wave type of plasmaguide structure (Zelby<sup>19</sup> of RCA Applied Research, Camden) and for a solid-state plasma waveguide (Hirota and Toda<sup>20</sup> of Laboratories RCA, Tokyo).

## WAVEGUIDE THEORY

The basic features of a waveguide (this includes all concentric cylinder structures) are as follows:

- 1) There is an axial direction of propagation  $k_z$  and the system is taken to be uniform along this axis.
- 2) The wavelike behaviour perpendicular to this axis comes from solving the transverse wave equation ( $\nabla_t^2 + k_t^2$ ) for some variable in the system of coordinates for which the boundary conditions can be properly formulated. The media are taken to be uniform in each region with definite boundaries. A review of the exact theory up to 1961 is given in an RCA Victor Research Laboratories, Montreal, report.<sup>6</sup>

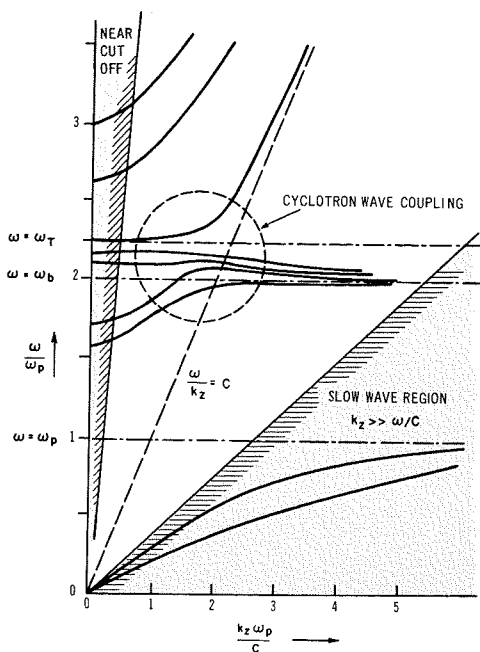


Fig. 1—Brillouin (frequency vs wavenumber) diagram for a magnetoplasma guide (from Camus et Le Mezec<sup>9</sup>).

The transverse systems most commonly discussed are either planar or circular, but others could be used. Other variable combinations may be concocted but the simplest to use are the axial components of electric  $E$  and magnetic  $H$  field. In nongyrotory mediums, the component values of effective displacement current  $D$  and magnetic induction  $B$  depend on the same components of electric  $E$  and magnetic field. For a nongyrotory medium, the modes in a given medium can be separated into *transverse electric*,  $TE$ , (where  $E_z = 0, H_z \neq 0$ ) or *transverse magnetic*,  $TM$ , (where  $H_z = 0, E_z \neq 0$ ) modes. If more than one such medium is involved, this is not true in general for the overall waveguide modes, unless there happens to be no component of either  $E$  or  $H$  in the direction of the inhomogeneity. (As an example for angle-independent modes, we can have pure  $TE$  or  $TM$  modes for concentric circular cylinders, but angular variation induces both longitudinal  $E$  and  $H$ .)

For gyrotory media, two linear combinations of  $E_z$  and  $H_z$  must be used. The ratios of the coefficients are determined by the roots of an auxiliary quadratic equation. This complicates the matter considerably.<sup>1-4,6</sup>

All this makes the analysis of the general waveguide modes very difficult.

#### PLASMA WAVEGUIDE

In spite of the difficulties mentioned above, considerable work has been done

for the longitudinally magnetized cold plasma completely filling a circular cylinder waveguide, and the general behaviour is fairly well understood.<sup>8-10</sup> A typical result is given in Fig. 1 in the form of a frequency-vs.-wave-number plot for a given plasma guide. Areas for simplified calculations are also indicated there.

The problem still remains of calculating the result for the case at hand; often: 1) the plasma cannot be considered to fill the guide, 2) there may be plasma container effects, 3) transverse variations in plasma density may be important, and 4) a host of other complications may be present. The exact cold plasma analysis may become much too clumsy for practical use, and simplifications are desperately needed.

#### SIMPLIFICATIONS

The first kind of simplification comes from considering extreme conditions under which useful approximations can be obtained by ignoring some phenomenon. Two parameters spring to mind: *extreme frequencies* and *extreme lengths*, or *wave numbers*.

A very useful simplification is the *perturbation analysis* where one considers the effect of a small change in the waveguide system from some single known state and the resultant first order correction<sup>11</sup>.

Another useful approximation technique is that of *coupled modes*.<sup>12,13</sup>

#### PERTURBATIONS

In perturbation analysis,<sup>11</sup> one examines the effect of a small change in the system from a known state. Because one is only considering small changes quite complicated perturbations may be considered—far more complicated than is feasible with a full analysis.

The change in wave number for a waveguide or frequency with a cavity is obtained by calculating the relative change in the energy of the system. If the change is a small change over a reasonable volume (for example, a low-density plasma) the perturbation assumption is that the fields are unchanged. If the change in the medium is large, but the overall effect is small because the volume involved is small (for example, the thin glass bottle containing a plasma), then the cross-section must be small. Hence, one can assume *quasistatic* formulas for calculating the changed field in the perturbing medium—that is, assuming the time derivative terms in Maxwell's equations can be neglected for the perturbation.

Four typical plasma applications are:

- 1) *Low-density plasma*—Large volume slightly perturbed from vacuum mode.

- 2) *Small Plasma or gap*—small volume possibly sharply different from plasma-filled waveguide mode.
- 3) *Thin Plasma container*—small volume different from the full or partially-full plasma waveguide mode.
- 4) *Slight gyro effect*—first-order mode splitting for angularly-dependent modes with a magnetic field.

#### LIMITING CASES

In the basic mode, without the effects of containers etc., the result may be simple to calculate in limiting cases.

The *high frequency* case is generally the approach of the wave plasma velocity to the velocity of light and gives little information except that this state is reached. It will correspond to the plasma perturbation result.

The *cut-off condition* (zero axial wave number—that is, infinite axial wavelength) is identified by the cut-off frequency, obtained by setting the axial wavenumber equal to zero in the dispersion equation. It is frequently easy to see how the wavenumber behaves near the cut-off frequency.

*Resonance* is the condition when the axial wavenumber  $k_z$  approaches infinity.

*Quasistatic approximation.* Simple equations can be obtained for large  $k_z$  (that is,  $k_z \gg \omega/c$ ) because the quasistatic condition ( $\nabla \times E = 0$ ; that is,  $-\nabla \phi = E$  also equivalent to  $c \rightarrow \infty$ ) will apply for the whole waveguide. This makes things much easier. (There is an equivalent magnetostatic simplification as well.) We have the normal slow-wave analysis, much used for microwave tubes involving distributed wave beam interaction and in plasma guides as well.<sup>4,14,15</sup> If the *transverse* dimensions of the waveguide are much smaller than the free-space wavelength, then the quasistatic analysis may be justified for all axial wave-numbers—since  $(k_z^2 + k_r^2)$  must be much larger than the square of the reciprocal of the free-space wavelength,  $k_0^2 \phi = \omega^2/c^2 = (2\pi/\lambda_0)^2$ .

#### COUPLED MODES

In coupled mode theory<sup>12,13</sup>, one considers a collection of simple modes for modified systems and then consider simultaneous solution for the interaction of coupling between these modes in the actual system under the assumption that the mode coupling is weak. If the problem is a suitable one and the modifications well chosen, very few modes need be considered. A classic case is the travelling wave tube; one mode is the electron-beam electrostatic wave and the other is the slow wave of the propagation structure. The interaction gives the gain of the structure wave.

Another advantage of mode-coupling

analysis is that it frequently gives more physical insight (from the choice and recognition of mode characteristics) than the exact calculation which usually emerges at the end of an abstract dispersion equation.

#### PLASMA GUIDE EXAMPLE

A simple example of some of the features described above is the investigation of the effect of a plasma column on the  $TE_{11}$  mode (9.2 Gc/s) of a circular cylinder waveguide. This investigation was carried out in 1963, in the Microwave and Plasma Physics Laboratories of the RCA Victor Research Laboratories, Montreal; T. W. Johnston was responsible for the theoretical work<sup>4,16</sup> and J. V. Gore and F. J. F. Osborne ran the experiment<sup>6,17</sup>.

#### Experiment

The heart of the system, waveguide and plasma bottles, is shown in Fig. 2, and the general apparatus in Fig. 3.

In the experiment, the interest was in the effects of a varying plasma density at a constant frequency. The theoretically convenient way to present the data was to plot  $k_z^2$  (or its normalized cousin  $k_z^2/k_0^2 = \lambda_0^2/\lambda_g^2$ ) against electron density or some quantity hopefully proportional to it, such as discharge current.

The guide wavelength ( $\lambda_0$ ) was measured with the bottle in place but with no plasma. The phase shift due to the plasma was measured by a four-probe microwave system, and recorded as a function of plasma current. As a consistency check, the same bottle under the same discharge conditions was used in two waveguides of different size, 2.36 cm and 2.89 cm inside diameters. The plasma diameter was about 1.6 cm. From this data, the plots of Fig. 4 were obtained.

#### Theory

The smaller waveguide was only moderately full of plasma, the larger guide rather less, so the plasma filled guide analysis did not seem a good place to start. The full analysis for a partially filled guide was used; the results are shown in Fig. 5, with the full computed points given by circles. The dashed lines give the low-density plasma *perturbation* approximation and the double-dashed lines the simple result if the waveguide were filled with plasma. One can define a filling factor which is the ratio of the slope of the perturbation line to the slope of the full guide result. On this basis, the plasma filling factor or effectiveness compared with a full guide were, for the small guide 0.670, for the large guide 0.545.

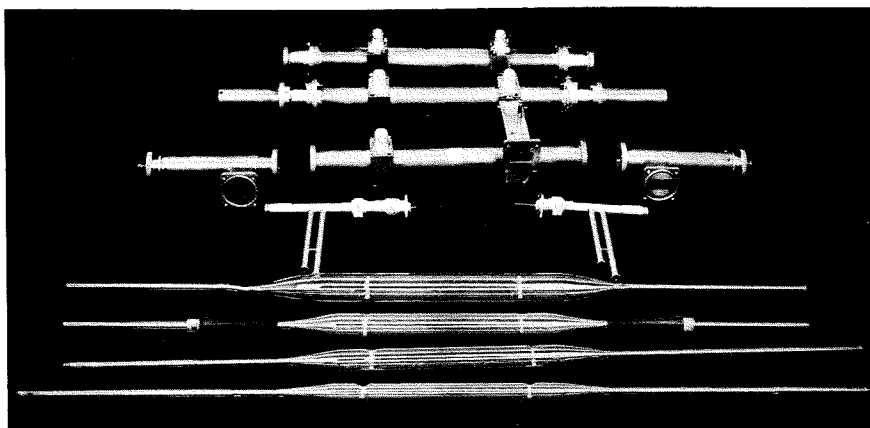


Fig. 2—Round waveguides of different size. The second guide and second bottle from the top show the system as used for the final results. The coaxial waveguide probes come through the side of the waveguide into the dimples in the plasma tubes.

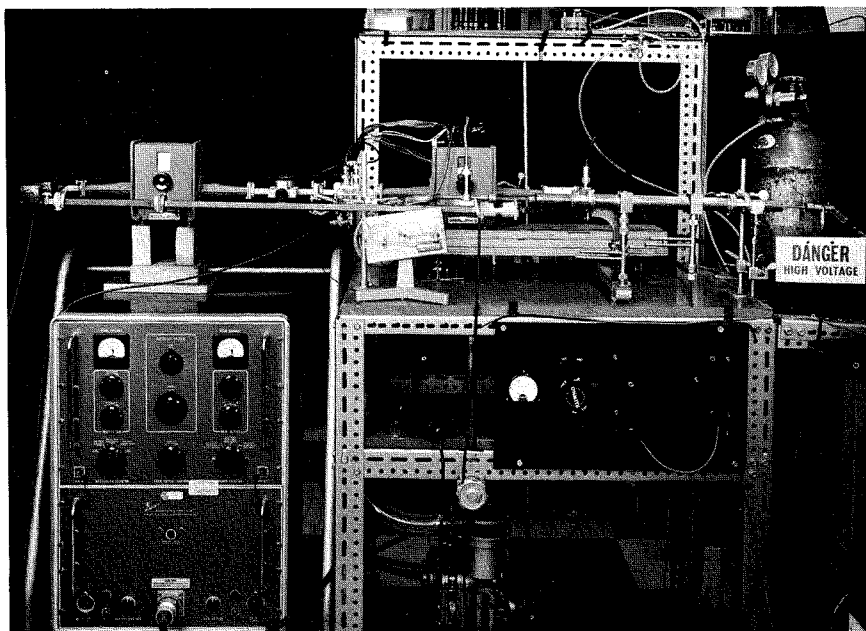


Fig. 3—General system (large guide in place; note transition). The four-probe measuring unit is just behind the manometer, the cold-cathode discharge connections are at the clips beyond each end of the round waveguide section, the coupling probes enter from the bottom. The four probe display and electronic equipment is not shown.

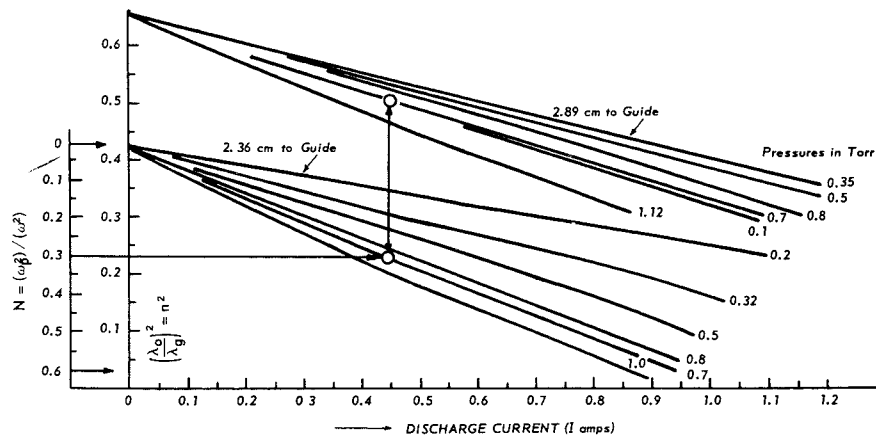


Fig. 4—Plots of  $(\lambda_0/\lambda_g)^2$  vs discharge current. From small-guide theory (Fig. 5) the value of  $\omega_p^2/\omega^2 = N$  is obtained. The circles show the corresponding results for different guides at the same pressure and discharge current, i.e. the same plasma.

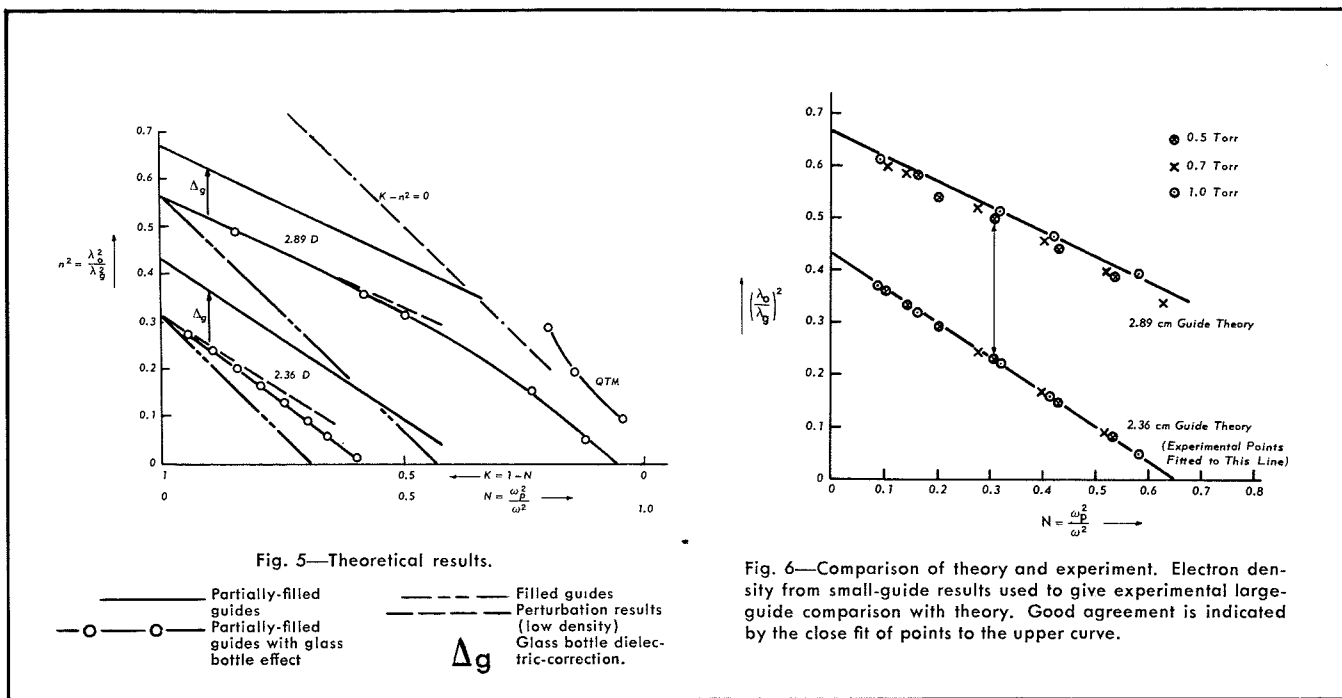


Fig. 5—Theoretical results.

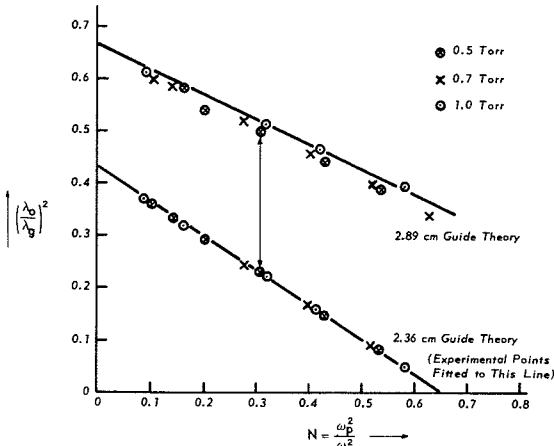


Fig. 6—Comparison of theory and experiment. Electron density from small-guide results used to give experimental large-guide comparison with theory. Good agreement is indicated by the close fit of points to the upper curve.

Now the considerable effect of the bottle containing the plasma must be accounted for. For no plasma, it is simple to remove the bottle, measure the guide wavelength, and compare it with the guide wavelength with the bottle; but this does not indicate the bottle effects with the plasma on. The procedure is to calculate the bottle effect by using *perturbation* theory for a small volume, but strong dielectric, for zero plasma. Next, one sees how it fits the observations. The fit happened to be quite good. The perturbation was then calculated for some reasonable plasma densities; it proved to change very little for the different densities, because the mode structure changed little. The dielectric perturbation correction could now be applied as a simple additive constant, as shown by the solid line without circles, for the densities of interest in Fig. 5. Thus, the perturbation analysis gave the correct plasma bottle correction.

The theoretical variation of  $\lambda_0^2/\lambda_g^2$  against electron density is thus very nearly linear over a considerable range. Perturbation theory and full theory do not diverge wildly so long as the energy distribution of the wave changes little.

#### Comparison: Theory vs. Experiment

The experimental results lie on straight lines for each pressure (Fig. 4) so that for each pressure and each guide separately the experimental curves could be fitted by using the appropriate (unknown) conversion factor from discharge current to electron density. The small-guide results were so fitted, thus fixing the electron density value for each

corresponding large guide result. The large-guide experimental and theoretical results matched extremely well (Fig. 6), demonstrating the consistency of the two results.

This excellent fit is strong evidence for the correctness of the theoretical treatment used here, and plasma waveguide theory in general.

#### REMARKS

Note that both exact theory for a special case and both kinds of perturbation theory were used in judicious combination.

Mode coupling was not used, but might be used for other waves such as the *QTM* wave of Fig. 5.

Although they are not discussed in this paper, the magnetic fields also produced interesting mode-splitting effects.

#### BIBLIOGRAPHY

- H. Suhl, L. R. Walker "Topics in Guide Wave Propagation Through Gyromagnetic Media" Part 1, *Bell Syst. Tech. J.* 33 579-659 (1954).
- W. C. Hahn "Small Signal Theory of Velocity-Modulated Electron Beams" *General Electric Rev.* 42 258-270 (1939).
- A. A. Th. M. Van Trier "Guided Electromagnetic Waves in Anisotropic Media" *Appl. Sci. Res. B* 3 305-371 (1953).
- Proc. Symp. on Electronic Waveguides*, Brooklyn Polytechnic Press (1958).
- F. J. F. Osborne, T. W. Johnston, J. V. Gore, M. B. Bachynski (RCA Vic. Res. Labs., Montreal) *Characteristics of Isotropic Plasma-Loaded Waveguides ASD-TDR-62-946* RCA Victor Res. Rep. 7-801-20.
- T. W. Johnston (RCA Vic. Res. Labs., Montreal) *Theory of Electromagnetic Wave Propagation in Plasma Loaded Structures ASD-TDR-62-945* (RCA Victor Res. Rep. 7-801-19).
- R. B. Adler "Waves on Inhomogeneous Cylindrical Structures" *Proc. IRE* 40 339-348 (1952).
- V. Bevc, T. E. Everhart "Fast Wave Propagation in Plasma-Filled Waveguides" *J. Electronics and Control* 13 185-212 (1962).
- M. Camus, J. Le Mezec "Propagation des Ondes dans un guide rempli de plasma en presence d'un champ magnetique" in *Electromagnetic Theory and Antennas, Proc. 1962 Copenhagen Symp.* pp. 323-347 Pergamon (1963).
- R. Likuski *Free and Driven Modes in Anisotropic Plasma Guides and Resonators AL-TDR-64-157* (Elec. Eng. Res. Lab. Univ. Illinois) (1964).
- R. F. Harrington *Time-Harmonic Electromagnetic Fields* McGraw Hill (1961).
- W. H. Louisell *Coupled Mode and Parametric Electronics* Wiley (1960).
- B. A. Auld, J. C. Eidson "Coupling of Electromagnetic and Quasi-Static Modes in Plasma Loaded Waveguides" *J. Appl. Phys.* 34 478-481 (1963).
- A. W. Trivelpiece, R. W. Gould "Space Charge Waves in Cylindrical Plasma Columns" *J. Appl. Phys.* 30 1734-1793 (1959).
- R. M. Bevenssee *Electromagnetic Slow Wave System* John Wiley, New York (1964).
- T. W. Johnston (RCA Vic. Res. Labs., Montreal) "Two-Region Non-Gyrotory Waveguides" (submitted to *IEEE Trans. on Microwave Theory and Techniques*) 1965.
- T. W. Johnston, J. V. Gore, F. J. F. Osborne (RCA Vic. Res. Labs., Montreal) "Isotropic Plasma Effect on the TE<sub>11</sub> Mode of a Round Waveguide" (submitted to *J. Appl. Phys.*) 1965; also RCA Victor Research Report 7-801-370.
- M. P. Bachynski, F. J. F. Osborne, A. I. Carswell, B. W. Gibbs, C. Richard (RCA Vic. Res. Labs., Montreal) "Microwave Measurements of Plasmas," *RCA ENGINEER*, this issue.
- M. P. Bachynski (RCA Vic. Res. Labs., Montreal) "An Introduction to Plasma Phenomena," *RCA ENGINEER*, this issue.
- L. W. Zelby (RCA Applied Res., Camden) "Plasma-Coated Surface As A Waveguide," *RCA ENGINEER*, this issue.
- R. Hirota, M. Toda (Labs., RCA, Tokyo) "Propagation in Solid State Plasma Waveguides—Non-Reciprocal Devices," *RCA ENGINEER*, this issue.

# PLASMA-COATED SURFACE AS A WAVEGUIDE

Waveguiding characteristics of a surface impedance externally coated with a layer of plasma are determined for a general system with primary propagation along the  $z$ -axis, and then reduced to specific cases where the surface impedance represents that of a corrugated surface, a comb structure, a dielectric, and a dielectric-coated conductor. Since plasma coatings occur around a space vehicle during reentry, they might be turned into a communications aid, instead of a problem, if the coating is utilized as a guiding structure.

Dr. L. W. ZELBY

Applied Research, DEP, Camden, N. J.

A LARGE class of problems dealing with electromagnetic waves can be analyzed in very simple terms using impedance concepts<sup>1</sup>. This is particularly true of problems involving the waveguiding characteristics of cylindrical structures. Since in any cylindrical structure the physical characteristics are preserved, under a given set of boundary conditions, no loss of generality occurs by considering the simplest case—a plane slab.

## PLANE-SLAB ANALYSIS

When a plane wave is incident on a plane slab at some arbitrary angle of incidence,  $\theta_0$ , as shown in Fig. 1, the component of the wave parallel to the surface will continue to propagate along the surface. The component normal to the surface will be partly reflected and partly transmitted. In order that the surface become a guide, it is necessary that the reflected component of the wave vanish, so that only the incident wave and the axial component of the reflected wave remain. The requirement that the field reflection coefficient  $R$  vanish is expressed by<sup>2</sup>:

$$R = \frac{Z_s - Z_n}{Z_s + Z_n} = 0 \quad (1)$$

where  $Z_s$  is the impedance presented to the normal component of the wave at the surface of the slab, and  $Z_n$  is the normal component of the wave impedance. In the case of a simple plane surface (a slab of infinite thickness) the condition  $R = 0$  occurs for parallel polarization ( $\vec{E}$  field in the plane of incidence) at Brewster's angle. In the case of a slab of finite thickness, the condition  $R = 0$ , can be satisfied by a

set of discrete surface wave modes.

If the surface in question represents one side of a slab, with the other side covered by another surface impedance, the slab transforms the impedance  $Z$  at  $z = 0$  to the impedance  $Z_s$  at  $z = d$ , where  $d$  is the thickness of the slab (see Fig. 1). Using the impedance formula<sup>3</sup>:

$$Z_s = Z_p \frac{Z + iZ_p \tan(k_p d)}{Z_p + iZ \tan(k_p d)} \quad (2)$$

where  $Z_p$  is the wave impedance of the slab and  $k_p$  is the propagation constant in the slab in the  $z$  direction. For parallel and perpendicular polarizations:

$$Z_{||} = \sqrt{\frac{\mu_0}{\epsilon_0}} \frac{\cos \theta_p}{n} \quad (3a)$$

$$Z_{\perp} = \sqrt{\frac{\mu_0}{\epsilon_0}} \frac{\sec \theta_p}{n} \quad (3b)$$

In these equations,  $n$  is the refractive index of the slab, and  $\mu_0$  and  $\epsilon_0$  are the permeability and permittivity of free space, respectively.

A plasma slab may be treated in the same manner as any other dielectric once its dielectric coefficient is specified. For the case of a cold collisionless plasma (lossless), the relative dielectric coefficient  $\epsilon_p$  can vary from minus infinity to one; i.e.:

$$-\infty < \epsilon_p = \left(1 - \frac{\omega_p^2}{\omega^2}\right) = n^2 \leq 1 \quad (4)$$

where  $\omega$  is the wave angular frequency and  $\omega_p$  is the plasma frequency. Introduction of losses would not drastically change the qualitative characteristics of the system. Whereas on lossless structures the axial propagation constant must be either pure real or pure

imaginary<sup>4</sup>, introduction of losses makes the propagation constant complex.

## GUIDED WAVES

The characteristics of guided waves supported by a lossless plasma slab can now be examined. Consider one side of the slab to be bounded by free space while the other side is covered by a material having arbitrary impedance (Fig. 1). For simplicity, the system will be assumed invariant in the  $y$  direction. Fig. 2 shows the relations between the wave propagation constants in the  $x$  and  $z$  directions, as well as their relations to the angles of incidence  $\theta_0$  and refraction  $\theta_p$ . It should be noted that real angles of incidence or refraction indicate homogeneous waves, whereas complex angles indicate inhomogeneous waves<sup>5</sup>; i.e., waves for which planes of constant phase and constant amplitude are not parallel to each other. Surface waves belong to the latter class of waves since they propagate *along* a surface and decay *transversely* to it. The planes of constant phase are perpendicular to the surface, and the planes of constant amplitude are parallel to the surface.

The character of the waves is dictated by the nature of the propagation constant. A real propagation constant indicates that the wave propagates along the structure, while an imaginary propagation constant indicates exponential decay. It can be seen from Fig. 2 that the propagation constants satisfy the following relations

$$k_x^2 + k^2 = k_0^2 \quad (5)$$

$$k_x^2 + k_p^2 = n^2 k_0^2 \quad (6)$$

Simultaneous solution of the above equations in conjunction with the requirement  $R = 0$  yields the allowed values for the propagation constant  $k_x$ .

When the dielectric coefficient of the plasma is negative ( $\omega < \omega_p$ ), there are no solutions with real  $k_x$  (for real frequencies) unless  $k$  and  $k_p$  are pure imaginary<sup>5</sup>. This implies waves decaying exponentially above and below the boundary  $z = d$ , but propagating in the  $x$  direction. An additional restriction is that  $|k_p| > |k|$  for real phase velocities and frequencies. In this case,  $Z_p$  is pure imaginary, and from Eq. 2 the impedance  $Z_s$  given by:

$$Z_s = i |Z_p| \frac{Z + i |Z_p| \tanh(|k_p| d)}{i |Z_p| + Z \tanh(|k_p| d)} \quad (7)$$

The normal component of the wave impedance,  $Z_n$ , for  $z \geq d$  is imaginary, which means that for  $R = 0$  the impedance  $Z$  must be either purely reactive (pure imaginary), zero, or infinity.

The latter two cases have been analyzed<sup>5</sup>, showing that for parallel polarization, and  $Z = 0$ , the system will support surface waves when:

$$n^2 < -\tanh(|k_p|d) \quad (8)$$

This is the only condition under which Eqs. 1, 5, and 6 can be satisfied simultaneously. On the other hand, when  $Z \rightarrow \infty$ , the system will not support surface waves.

Another interesting case arises when  $Z$  is purely reactive, an impedance which can be obtained, for example, by placing another dielectric slab at  $z \leq 0$ , or a corrugated surface or comb structure at  $z = 0$  (see Fig. 3). In each of the three instances, the impedance  $Z$  can be made either inductive or capacitive, depending on the thickness of the dielectric slab or the depth of the slots,  $l$ . If the slab is replaced with plasma or the slots are filled with plasma of  $n^2 < 0$ ,  $Z$  would still be reactive. However, it would be always either inductive or capacitive, regardless of the magnitude of  $l$  (depth of slots), and it would not be periodic as above.

It should be pointed out that simply picking  $k_p d = \pi/2$  (see Eq. 2) will not yield a reactive surface impedance regardless of whether  $Z$  is reactive or resistive, since then  $Z_s = Z_p^2/Z$ .

When the dielectric coefficient of the plasma is positive, i.e.  $\omega > \omega_p$ , for real frequencies and real phase velocities it is still required that  $|k_p| > |k|$  with  $k, k_p$  imaginary. In this case, however,

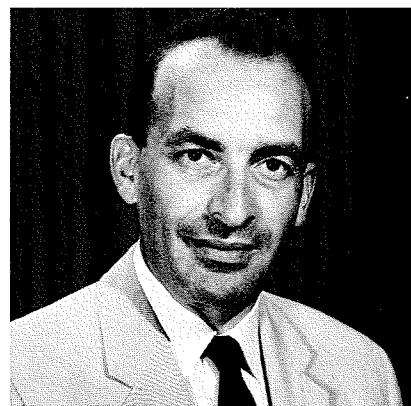
Eqs. 1, 2, 5, and 6 have no consistent solution and the plasma slab will not support surface waves<sup>5</sup>.

If it is allowed that  $k$  be real, and  $k_p$  imaginary, with  $1 > n^2 \geq 0$ , Eq. 7 still applies except that the wave for  $z \geq d$  is *not* a surface wave regardless of the value of  $Z$ . In this case, the plasma layer behaves, essentially, as a waveguide *below* cutoff, even though the index of refraction is real. The index of refraction is, however, less than one, which means that for the situation described here there is a *homogeneous* wave for  $z \geq d$ , but an *inhomogeneous* wave for  $0 \leq z < d$ ; the reflection coefficient does not vanish; and there is no restriction on frequency except that  $\omega_p < \omega < \infty$ .

### CONCLUSIONS

A plasma slab differs very little from a dielectric slab when  $\omega < \omega_p$  (dielectric coefficient negative). In such cases, the plasma layer is capable of supporting surface waves if it is terminated by a reactive impedance, or short circuit. When the dielectric coefficient of the plasma slab is positive, the layer acts as a waveguide below cutoff, and does not provide a guiding surface. In either case, however, a plasma slab can act as an impedance transformer, with a constant phase shift under some circumstances.

The transition of the analysis presented to any other cylindrical structure merely requires a substitution of functions characteristic of the geometry.



DR. L. W. ZELBY graduated from the Moore School of Electrical Engineering, University of Pennsylvania, with a BSEE in 1956 and obtained an MSEE in 1957 at the California Institute of Technology. Subsequently, he returned to the University of Pennsylvania, where he received his PhD in electrical engineering in February 1961. Dr. Zelby joined RCA in 1960 and participated in the early studies of Cerenkov interaction in the microwave region. In 1961 he returned to the University of Pennsylvania and joined the faculty of the Moore School, where he is now an Associate Professor. He continues his work at RCA in the capacity of consultant, primarily to the Cerenkov study in which he has actively participated to the present time. Dr. Zelby's major fields of endeavor have been electromagnetic propagation, electrodynamics of moving media, surface waves and plasma physics.

This substitution results in a change in the numerical values of the propagation constants only, with no resultant change in their character.

Plasma-coated structures have potential for application as high-frequency waveguides, although their use has been rather restricted by problems associated with containment of the plasma coating. (Plasma-filled closed components are readily available, on the other hand). Now it appears that these problems might be overcome by applying high electric-field intensities to cause breakdown in the vicinity of conventional guiding systems, creating a plasma coating with desirable characteristics. Such plasma-coated structures may also be used as diagnostic tools.<sup>6</sup>

A coating of this nature occurs on space vehicles during reentry. Unfortunately, this coating now causes problems in communicating with the vehicle. By utilizing the coating as a guiding structure, along the lines indicated in this paper, this problem source might become an aid rather than a hindrance.

### BIBLIOGRAPHY

1. S. A. Shelkunoff, *Electromagnetic Waves*, D. Van Nostrand Co., Inc., Princeton, N.J.; 1943.
2. H. M. Barlow and A. L. Cullen, "Surface Waves," *Proc. IEE*, vol. 100, pt III, pp. 329-341; November 1953.
3. S. Ramo and J. Whinnery, *Fields and Waves in Modern Radio*, J. Wiley and Sons, Inc. New York, N.Y., 2nd ed., p. 291; 1953.
4. R. B. Adler, "Waves on Inhomogeneous Cylindrical Structures," *Proc. IRE*, vol. 40, pp. 339-348; March, 1952.
5. L. W. Zelby (RCA Applied Research, Camden), "Surface Waves Along a Plasma-Air Boundary," *Proc. IEEE*, vol. 51, No. 12, p. 1774; December, 1963.
6. P. N. Robson and R. D. Stewart, "Surface-Wave Probe for Measuring Electron Densities in a Gaseous Plasma," *Electronic Ltrs.*, vol. 1, No. 1, pp. 13-14; March, 1965.

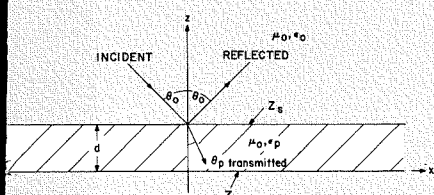


Fig. 1—Plane electromagnetic wave incident upon a uniform semi-infinite plasma slab bounded by free space and material of arbitrary impedance,  $Z$ .

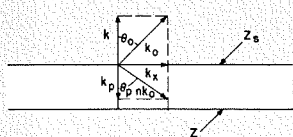
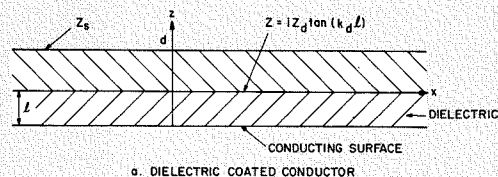
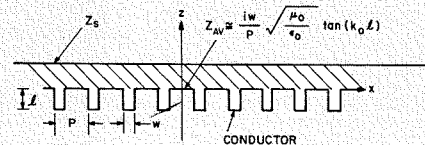


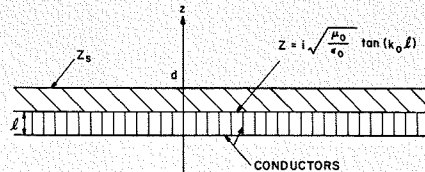
Fig. 2—Propagation constants associated with the bounded plasma slab.



a. DIELECTRIC COATED CONDUCTOR



b. CORRUGATED CONDUCTOR



c. COMB STRUCTURE

Fig. 3—Plasma slab bounded by a reactive surface impedance; a) dielectric coated conductor, b) corrugated conductor, and c) comb structure.

# RESONANCES IN THE IONOSPHERE

## MAGNETOPLASMA

ALOUETTE, the swept-frequency topside-ionosphere sounding satellite, detected ringing, evident as "spikes," on ionograms at certain frequencies. The RCA Victor Research Laboratories in Montreal have been closely involved in the subsequent study of these phenomena, which involve some extremely advanced and complex plasma theory, and which may be very valuable in developing more exotic diagnostic methods for space plasmas. These ringing phenomena proved to be the local plasma frequency, the transverse resonance frequency, and harmonics (up to the fifteenth) of the cyclotron frequency. Collisions being negligible, the classical Vlasov electron plasma dispersion equation is applicable, from which these particular ringing frequencies are easy to infer; but the complicating effects of orientation, antenna size, time behavior, etc., require and are now undergoing advanced theoretical analysis. The ALOUETTE low-frequency noise receiver also detected characteristic frequency phenomena involving ions associated with the electron-ion hybrid frequency and the zero-gyration electron-ion frequency. This paper summarizes this work and includes a Bibliography of the pertinent literature in the field.

**Dr. T. W. JOHNSTON and Dr. I. P. SHKAROFSKY**

*Research Laboratories  
RCA Victor Co., Ltd.  
Montreal, Canada*

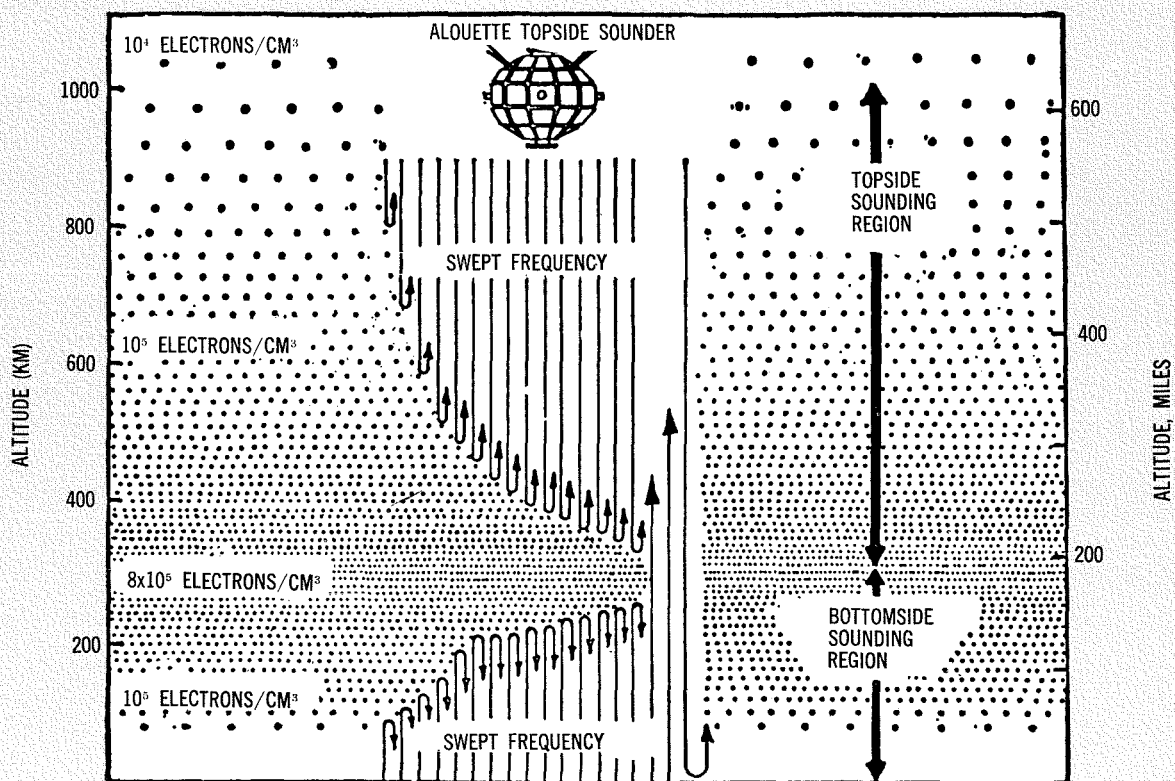


Fig. 1—Ionosphere sounders probe deeper as the frequency is increased (from Thomas<sup>1</sup>.)

A LONG-CHERISHED dream of ionospheric specialists was fulfilled when satellite-borne equipment began exploring the ionosphere from the other side with radio-sounding equipment. The era of the topside sounders had arrived. An unexpected, but fascinating and enlightening bonus has been the observation of various local plasma resonances\* excited by the sounding transmitter and detected by the echo receiver.

The RCA Victor Research Laboratories in Montreal have been closely involved in the study of these resonances, which involve some extremely advanced parts of plasma theory and which may be very valuable in the exploration of exospheric plasmas. This paper summarizes that work and includes a bibliography of pertinent literature.

The general features of the ALOUETTE swept-frequency "topside sounder" satellite, launched September 29, 1962, have been well summarized by Thomas<sup>1</sup>. ALOUETTE 1 operates like a ground-based sounder, sending out a short (100- $\mu$ s) radio pulse, listening for echoes and sweeping the frequency from 0.5 to 11.5 Mc/s to obtain a frequency-sounding profile called an *ionogram*—i.e., echo delay vs. frequency. (Incidentally, it was a team headed by J. M. Stewart of RCA Victor Research Laboratories, Montreal, which was responsible for the crash development of the wideband telemetry transmitter, which is described in the literature.<sup>30</sup>)

Another topside-sounding satellite<sup>2</sup> (known variously as TOPSI, EXPLORER XX, IONOSPHERE EXPLORER IE-1, S-48) operates at six successive fixed frequencies (in sounding order 7.22, 5.47, 3.72, 2.85, 2.0, 1.5 Mc/s) with 105 ms for a complete cycle; it was launched on August 25, 1964. Ground-based ionograms only give results for the ionosphere below the maximum electron density region, but the topside-sounder satellites give results for the upper side, impossible to obtain the ground (Figs. 1, 2). The detailed description of the ALOUETTE satellite operation is available in the published literature<sup>3</sup>.

#### IONOSPHERE RINGING

The lower-frequency portion of a typical ALOUETTE ionogram is given in Fig. 3. In addition to the ionogram itself and the frequency markers, there are a number of features at the top, often known as *spikes*, that look like icicles. They represent an immediately-observed signal that decays very slowly in time and only occur when the sounder transmitter fre-

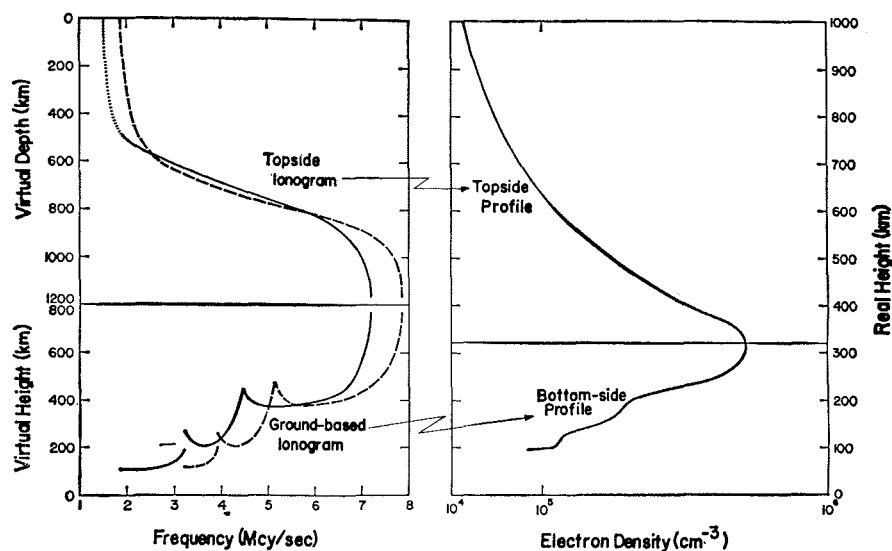


Fig. 2—Combination of top and bottom side ionograms to give complete ionosphere electron density results (from Thomas<sup>1</sup>.)

quency reaches certain critical values. These prove to be dependent on the value of magnetic field and electron density at the satellite. The ionosphere near the ALOUETTE rings at these frequencies. The fixed-frequency sounder shows similar phenomena when the ringing and sounder frequencies coincide.

The regularly-spaced series of ALOUETTE spikes were easily identified<sup>4</sup> as harmonics of the electron cyclotron frequency  $\omega_b = eB/m$ , where  $e/m$  is the electron charge-to-mass ratio and  $B$  is the magnetic field. Up to 19 cyclotron harmonics have been seen. Two other spikes, after some initial confusion, proved to be<sup>5</sup> the local plasma frequency

$\omega_p = \sqrt{ne^2/m\epsilon_0}$ , and the local transverse frequency  $\omega_T = (\omega_b^2 + \omega_p^2)^{1/2}$ . There is usually also a spike at  $2\omega_T$ , provided  $\omega_T < 2\omega_b^{5-7}$ . All these frequencies are significant in plasma theory.

To give some idea of the basic data, actual receiver records for two typical cyclotron harmonic spikes are shown in Fig. 4.

In general, a scan line showing the longest persistence can be picked out, giving a typical frequency accuracy of 15 kc/s in the range 1 to 10 Mc/s. Improvements on this figure might present a very attractive method of magnetic field measurement, avoiding the possible errors due to satellite residual magnetic

DR. ISSIE P. SHKAROFSKY graduated in 1952 from McGill University with a BSc degree and first class honors in physics and mathematics and obtained his MSc degree in 1953 in the fields of microwave optics and antennas. He then joined the microwave tube and noise group at the Eaton Electronics Research Laboratory and received his PhD degree in 1957 with a thesis on modulated electron beams in space-charge-wave tubes and klystrons. After graduation, he joined the RCA Victor Co., Ltd., Microwave Research Laboratory. His particular interest in plasma studies has been in the following topics: plasma transport coefficients, collisional effects in plasma, Boltzmann and Fokker-Planck theory, magnetohydrodynamics, and re-entry plasma physics. Dr. Shkarofsky is a member of the Canadian

Association of Physicists, of the American Physical Society, and of the American Geophysical Union.

DR. TUDOR W. JOHNSTON graduated in 1953 with a B Eng degree in Engineering Physics from McGill University. He then entered Trinity College, Cambridge, where he received his PhD degree in 1958 with a thesis on the dynamics of magnetically-focussed electron beams and phenomena related to the presence of ions in such beams. At the RCA Victor Laboratories, Dr. Johnston has carried out theoretical investigations on many aspects of plasma physics. Dr. Johnston is a member of the Canadian Association of Physicists and the American Physical Society.



Final manuscript received August 2, 1965  
\*The work on cyclotron harmonic resonances is being supported by NASA (Goddard, Fields and Plasma branch) under contract NASw-937.

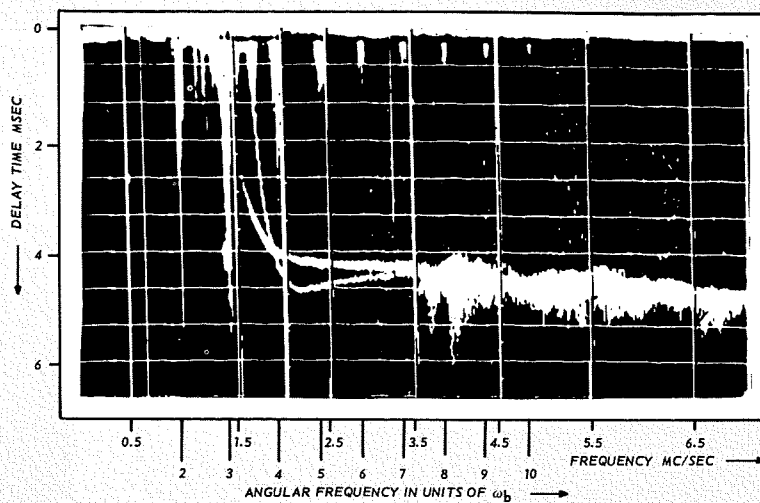


Fig. 3—Alouette ionogram taken above Quito, Ecuador, on October 7, 1962 at 13:46:58 U.T.

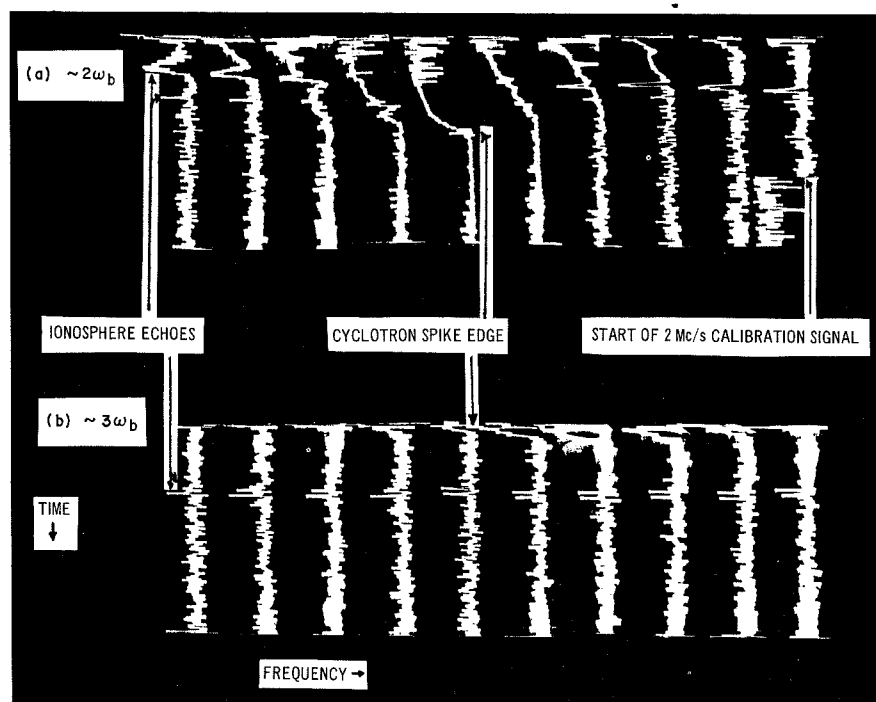


Fig. 4—Montage of A-scan lines—the raw Alouette data. These are from an Ottawa Alouette recording day 276 16:48:51 U.T. in the vicinity of (a)  $2\omega_b$ , and (b)  $3\omega_b$ . The line period is 67 ms and the transmitter/receiver center frequency shifts at a rate of roughly 15 kc/s per line.

field. The other ( $\omega_p$ ,  $\omega_r$ ) resonances related to electron density are excellent for plasma density diagnostics.

#### PLASMA THEORY

Since the ringing frequencies appear naturally in plasma theory, one can hope that the details of the excitation (such as the strength, manner of decay, effect of the various parameters) might also be derived from plasma theory. The general idea of how to do this is understood, but useful and realistic calculations are extremely formidable.

Plasma theorists are very fond of talking of small perturbations in an infinite uniform plasma permeated by a uniform magnetic field, and particularly one in

which collisions can be neglected. The plasma equation in the absence of collisional interactions is called the *Vlasov equation*, and the appropriate plasma might well be called a *Vlasov plasma*. Since 1946 when Landau<sup>8</sup> began the attack, many theorists<sup>9,10</sup> have worked on the problem of the perturbations in a spatially uniform Vlasov plasma with or without a uniform magnetic field with little, if any, experimental verification until this decade. The ionosphere in the vicinity of the ALOUETTE is an excellent Vlasov plasma, and the inhomogeneity scale is large compared with the free-space wavelengths of interest. The prospects of a first-class numerical time-decay test of the relevant long-wave-

length theory are good. Verifications of this sort would be impractical in the laboratory because of the large unbounded plasma required.

#### SATELLITE AND WAVE PACKET VELOCITIES

The ringing frequencies observed in the topside sounder data correspond to frequencies and wave numbers near which the group velocity (i.e. velocity of transport of energy or modulation, also the wave packet velocity) is much less than the electron thermal velocity. This is generally agreed upon.<sup>11-17</sup>

The concept which our Laboratory has postulated<sup>17</sup> is that the observed ringing frequencies correspond to the frequencies at which disturbances, excited by the sounder pulse and travelling at the group velocity, can travel with the satellite rather than propagating away from it. The wave packet thus rides along, keeping company with ALOUETTE, which travels much more slowly than the average electron.

The slow time decay is due to the gradual spread and decay of the wave packet. The observed resonant frequencies are just those for which the group velocity equals the satellite velocity.

For the cyclotron harmonic resonances, at least, and probably for the other resonances as well, any shift from the simple values are not observable in ALOUETTE data, so the doppler shift must be small. The wave phase velocity (wavelength/frequency) must then be reasonably large—very much greater than the satellite velocity and almost certainly much greater than the electron thermal velocity. In other words, the wavelengths are much greater than the electron orbit radius or the Debye length or the distance travelled by an electron during a wave cycle—all of the order of 10 cm. (This also makes the mathematics much easier than it would be at the worst.) The wave packets should be much larger than the wavelengths involved (believed to be of the order of 100 m).

#### WAVES OF INTEREST

The detailed work undertaken by the authors<sup>17</sup> suggests that the key points can be thought of as couplings between the so-called *electrostatic waves* and the well-known *Appleton-Hartree waves*; this is sketched in Fig. 5, a typical Brillouin diagram of angular frequency ( $\omega = 2\pi f$ , when  $f$  is the frequency) against wave number ( $k = 2\pi/\lambda$ , where  $\lambda$  is the wavelength). The slope of a dispersion ( $\omega$ -vs- $k$ ) curve in this diagram is the group velocity. The slope of the line from the origin is the phase velocity. For each coupling, there are

two possibilities of matching the satellite group velocity: 1) very close to the Appleton-Hartree regions as indicated in Fig. 5, and 2) where the phase velocity is high but the group velocity low, as required.

The method for doing the calculation was applied in our Laboratory by Nuttall, (for  $\omega_p$  and  $\omega_T$ ) who adopted the technique from fundamental particle dispersion theory<sup>15</sup>. The technique was also discovered independently by Bers<sup>18</sup> and Briggs<sup>19</sup>, with reference to beam-plasma instabilities. (The method is founded in an interesting but esoteric feature of complex dispersion equations and Fourier-Laplace transform inversion theory and will not be discussed here.)

The way has been cleared<sup>17</sup> for a final assault on the cyclotron harmonic resonance problem, in many ways the most tricky, and this assault is in progress. If it is possible within the scope of our program, there may be further developments in the consideration of the effect of satellite velocity on the plasma density resonances ( $\omega_p$  and  $\omega_T$ ).

Details of cyclotron harmonic *initial* excitation cannot be carried beyond the semi-qualitative discussion given elsewhere.<sup>20</sup>

#### ION EFFECTS AT LOW FREQUENCIES

All the phenomena discussed above are related to the electron effects. The ALOUETTE also carries a VLF receiver<sup>3,21</sup> (400 c/s to 10 kc/s) intended for the study of the well-known electron whistler waves<sup>22</sup>, but ion effects can also be seen.

Under favorable conditions, a proton gyrofrequency effect has been observed<sup>23</sup>. In addition, the effects of heavier ions (whose gyrofrequencies are below the receiver band) can be inferred through the electron-ion hybrid extraordinary wave resonance<sup>24-26</sup>. Ion-ion crossover and hybrid frequencies are also significant<sup>27-28</sup>. At the crossover frequencies, the plasma is still anisotropic, but not gyratory, and the characteristic waves are linearly polarized. (We cannot do justice to the ion effects here and refer the reader to the literature cited.)

Future generations of topside sounders<sup>29</sup> will have their lower frequency limits drastically reduced, both for sounding and passive reception and one can hope for a wealth of data on ion-ion effects.

#### SUMMARY

Resonant effects observed by the topside-sounding satellites have been (and are being) investigated, both for their interest as basic plasma phenomena and for their possible use in more exotic diag-

nostic methods for space plasmas. The basic concepts are understood, the frequencies are fairly well accounted for, and the mathematical groundwork is laid. Definite predictions and numerical results should soon be emerging from the theory.

Ion effects are also of interest, particularly the effects of the various ion species.

#### ACKNOWLEDGEMENTS

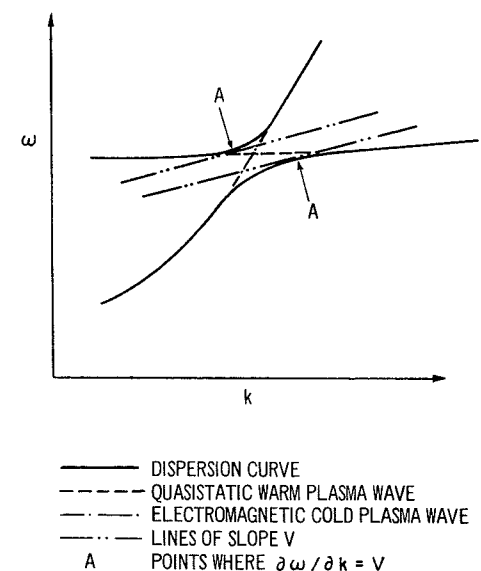
Beside the NASA-Goddard support mentioned at the beginning of the article, we would like to thank Dr. R. E. Barrington of the Canadian Defense Research Telecommunications Establishment, Ottawa, for his assistance in gaining access to ALOUETTE data for these and many other ionograms.

#### BIBLIOGRAPHY

1. J. O. Thomas "Canadian Satellite: The Topside Sounder ALOUETTE" *Science* 139, 229-232, Jan. 18 (1963)
2. W. Calvert, R. W. Knecht, T. E. Van Zandt "Ionosphere EXPLORER I Satellite: First Observations from the Fixed Frequency Topside Sounder" *Science*, 146, 391-395, Oct. 16 (1964)
3. C. A. Franklin, R. J. Bibby, R. F. Sturrock, D. F. Page "Electronic and System Design of the Canadian Ionospheric Satellite" 1963 *IEEE International Convention Record*, Vol. 11 Part 5, pp 64-72 (1963)
4. G. E. K. Lockwood "Plasma and Cyclotron Spike Phenomena Observed in Topside Ionograms" *Can. J. Phys.* 41, 190-194 (1963)
5. W. Calvert, G. B. Goe "Plasma Resonances in the Upper Ionosphere" *J. Geophys. Res.* 68, 6113-6120 (1963)
6. Unpublished correspondence between W. Calvert, J. A. Fejer and J. Nuttall (1964) on a suggestion by T. W. Johnston (RCA Vic. Res. Labs, Montreal).
7. G. Wallis "On the Harmonics of the Gyro Frequency Observed on Topside Ionograms" *J. Geophys. Res.* 70, 1113-1117 (1965)
8. L. Landau "On the Vibrations of the Electronic Plasma" *J. Phys. (USSR)* 10, 25-34, 1946 (trans. from *Zh. Exp. Teor. Fiz. USSR*, 16, 574 (1946))
9. A. G. Sitenko, K. N. Stepanov "On the Oscillations of an Electron Plasma in a Magnetic Field" *Soviet Phys. JETP*, 4, 512-520 (1957), trans. from *Zh. Exp. Teor. Fiz.* 31, 642-651 (1956)
10. I. B. Bernstein "Waves in a Plasma in a Magnetic Field" *Phys. Rev.* 109, 10-21 (1958)
11. P. A. Sturrock "Spectral Characteristics of Type II Solar Radio Bursts" *Nature*, 192, 58 (1961)
12. J. A. Fejer, W. Calvert "Resonance Effects of Electrostatic Oscillations in the Ionosphere" *J. Geophys. Res.* 69, 5049-5062 (1964)
13. P. A. Sturrock "Dipole Resonances in a Homogeneous Plasma in a Magnetic Field" *Phys. Fluids* 8, 88-95 (1965)
14. J. Nuttall (RCA Vic. Res. Labs, Montreal) "Theory of Collective Spikes Observed by the ALOUETTE Topside Sounder" *J. Geophys. Res.* 70, 1119-1126 (1965)
15. J. Nuttall (RCA Vic. Res. Labs, Montreal) "Singularities of the Green's Function for a Collisionless Magnetoplasma" *Phys. Fluids* 8, 286-296 (1965)
16. J. P. Dougherty, J. J. Monaghan "Theory of Resonances Observed in Ionograms Taken by Soundings above the Ionosphere" submitted to *Proc. Roy. Soc.* (1965)
17. I. P. Shkarofsky, T. W. Johnston (RCA Vic. Res. Labs, Montreal); *Satellite Cyclotron Harmonics* RCA Victor Res. Lab. Rep. 7-801-35 (1965). See also *Bull. Amer. Phys. Soc.* II 10 231 (paper S9), 597 (paper DE-2), 611 (paper FD3) (1965); and 1965 Plasma Physics APS Meeting, San Francisco, Calif. (paper W9); and "Cyclotron Harmonic Resonances Observed by Satellites," *Phys. Rev. Letters* 15, 51-53 (1965) (July 12) Meeting.

18. A. Bers, R. J. Briggs *Criteria for Determining Absolute Instabilities and Distinguishing Between Amplifying and Evanescent Waves* Mass. Inst. Tech. Res. Lab. Electronics Quarterly Prog. Rep. 71 122-130, Oct. 15 (1963)
19. R. J. Briggs "Electron Stream Interaction with Plasmas" *Res. Mono.* 29 Mass. Inst. Tech. Press (1964)
20. T. W. Johnston, J. Nuttall (RCA Vic. Res. Labs, Montreal); "Cyclotron Harmonic Signals Received by the ALOUETTE Topside Sounder" *J. Geophys. Res.* 69, 2305-2314 (1964)
21. R. E. Barrington, J. S. Belrose "Preliminary Results from the VLF Receiver aboard Canada's Alouette Satellite" *Nature* 198, 651-656 (1963)
22. R. A. Helliwell "Whistlers and VLF Emissions" Chap. 13 in *Research in Geophysics Vol. I* (ed. H. Odishaw) pp 319-333 Mass. Inst. Tech. Press (1964)
23. R. L. Smith, N. M. Brice, J. Katsufakis, D. A. Gurnett, S. D. Shawhan, J. S. Belrose, R. E. Barrington, "An Ion Gyrofrequency Phenomenon observed in Satellites" *Nature* 204, 274-275 (1964)
24. N. M. Brice, R. L. Smith "Recordings from the Satellite Alouette I—A Very-Low-Frequency Plasma Resonance" *Nature* 203, 926-927 (1964)
25. N. M. Brice, R. L. Smith "Lower Hybrid Resonance Emissions" *J. Geophys. Res.* 70, 71-80 (1965)
26. R. E. Barrington, J. S. Belrose, G. L. Nelms, "Ion Composition and Temperatures at 1000 km as Deduced from Simultaneous Observations of a VLF Plasma Resonance and Topside Sounding Data from the ALOUETTE I Satellite" *J. Geophys. Res.* 70, 1647-1664 (1965)
27. R. L. Smith, N. Brice "Propagation in Multi-component Plasmas" *J. Geophys. Res.* 69, 5029-5040 (1964)
28. D. A. Gurnett, S. D. Shawhan, N. M. Brice, R. L. Smith "Ion Cyclotron Whistlers" *J. Geophys. Res.* 70, 1665-1688 (1965)
29. C. D. Florida "Alouette's Successors" Paper given at the American Association for the Advancement of Science, Montreal December (1964)
30. J. C. Boag, J. Saunders, J. M. Stewart (RCA Vic. Res. Labs, Montreal); "A 2-Watt 136 Mc/s FM Crystal-controlled Transmitter" (1962) Solid State Circuits Conference, *Digest of Technical Papers*. (Published by Lewis Winner, New York.)

Fig. 5—Appleton-Hartree and electrostatic wave coupling. Group velocity equals specified velocity  $V$  at two points A, and ringing effects can be expected for a system moving at velocity  $V$ .



# LABORATORY SIMULATION OF GEOPHYSICAL PHENOMENA

This paper describes two different experiments in which complex geophysical phenomena were simulated in the laboratory. The first experiment is a scaled laboratory study of the interaction between the solar wind and the magnetosphere. The second experiment deals with the perturbations induced by a space satellite with long antennas in the surrounding environment due to the motion of the satellite in a magnetized plasma. The geophysical situation relevant to each experiment is described, as well as the laboratory arrangement and the interpretation and significance of the experimental results.

**Dr. F. J. F. OSBORNE, Dr. M. P. BACHYNSKI, J. V. GORE, and M. A. KASHA**

*Research Laboratories, RCA Victor Co., Ltd., Montreal, Canada*

**T**HE exploration of space has become more and more an investigation of plasma-magnetic-field interactions. This is due to the fact that "space" consists primarily of plasma permeated by magnetic fields, and their mutual interaction gives rise to the many geophysical phenomena observed on earth and more recently with space probes.

*Final manuscript received August 2, 1965.*

**DR. FRELEIGH J. F. OSBORNE** was educated at the Royal Canadian Naval College (1946-48); obtained his B.Sc. at McGill University in 1950 and was awarded his M.Sc. at Laval University in 1951 for a thesis on Application of the Secondary Electron Emission Multiplier to a Mass Spectrometer. In 1954 he received a D.Sc. from Laval University for a thesis on Secondary Electron Emission of Beryllium Copper. He joined the Research Department of Canadian Marconi Company in 1954 as a Senior Physicist, working primarily in the fields of component reliability, systems and instrumentation. In 1956 he was made a supervisor and as such directed a variety of projects. He transferred to the Electronic Tube Plant where he developed an S-Band Electron Beam Parametric Amplifier. In January 1961 he joined the Research Laboratories of RCA Victor as a Senior Member of Scientific Staff. He has since been particularly active in the area of plasma measurements and techniques, leading and contributing to programmes on plasma diagnostics, plasma loaded microwave structures, laboratory simulation of geophysical phenomena, and laboratory studies of the interactions between a satellite and its plasma environment. In 1965 he became Director of the Microwave and Plasma Physics Laboratory. He was active in the Royal Canadian Navy (Reserve) from 1946-1956, is a member of the Canadian Association of Physicists, the American Physical Society, the American Geophysical Union, Commission IV of the Canadian National Committee of the International Scientific Radio Union (URSI), and is listed in American Men of Science.

The use of satellites and rockets for the exploration of space is invariably expensive because of the sophistication of the instrumentation necessary and because of the cost of the rockets and launching. This technique is, however, essential because it is the only way in which most regions of space can be probed directly. It is, therefore, necessary to obtain the optimum results from

**DR. MORREL P. BACHYNSKI** graduated in 1952 from the University of Saskatchewan with the degree of B.Eng. in Engineering Physics. He was awarded the Professional Engineers of Saskatchewan prize for the highest scholastic standing amongst the graduating class. In the following year he obtained his M.Sc. degree in physics at the University of Saskatchewan in the field of radar investigations of the aurora. He then joined the Eaton Electronics Research Laboratory, McGill University, where he was awarded a Ph.D. degree in 1955 with a thesis on aberrations in microwave lenses. After obtaining his Ph.D. degree, Dr. Bachynski remained at the Eaton Laboratory carrying out research on the imaging properties of non-uniformly illuminated microwave lenses. In October 1955, he joined the newly created Research Laboratories of RCA Victor Company, Ltd., became Director of the Microwave and Plasma Physics Laboratories in 1958 and Director of Research in 1965. Since this time he has conducted research on electromagnetic wave propagation, microwave and plasma physics. Dr. Bachynski is a senior member of the Institute of Electrical and Electronics Engineers, a member of the professional group on Antennas and Propagation, a member of the American Physical Society, the American Geophysical Union and the Canadian Association of Physicists, and an Associate Fellow of the Canadian Aeronautics and Space Institute. He is Chairman of Commission VI of the Canadian National Committee of the International Scientific Radio Union (URSI), a member of the AIAA Technical Committee on Plasma Dynamics and a member of the

such a program. This can only be achieved through a proper "design of the experiment"—including the parameters to be measured and the techniques used for measurement—and through a successful interpretation of the data obtained. To achieve this, free-flight programs need to be supplemented by theoretical studies and laboratory simulation experiments. In relatively inexpensive laboratory simulation experiments, for example, control can be exercised over specific parameters and the influence of each variable ascertained. In this way, laboratory experiments can also serve an important purpose in guiding the theoretical work and in pointing to phenomena not as yet predicted. Similarly, the state of the art of many theoretical predictions is such that an experimental confirmation is desirable before applying the result to the situation in nature. Such information can be of immense value in the interpretation of full-scale experiments and can lead to the design of specific satellite and rocket experiments, as well as to the development of techniques for measurement of various natural parameters.

It is easy to show that an exact simulation of nature which satisfies all the

National Research Council of Canada Associate Committees on Radio Science and Plasma and Gas Dynamics, is listed in American Men of Science and has been associated with McGill University teaching classes in antennas, electromagnetic theory and plasma physics. In 1963 he was awarded the David Sarnoff Award for Outstanding Individual Achievement in Engineering.

**JOSEPH V. GORE** received a BA from the University of Saskatchewan in 1960. During 1960 and 1961 he conducted research on the development of a plasma betatron. In 1961 he was awarded an MA from the University of Saskatchewan. After graduation Mr. Gore was employed on the Operational Research Team, Defence Research Board, at Halifax, N.S. In the spring of 1962 he joined the Microwave Research Group of the RCA Victor Company, Ltd. Since joining the group Mr. Gore has been conducting experiments on an isotropic plasma filled waveguides and on the geophysical simulation study.

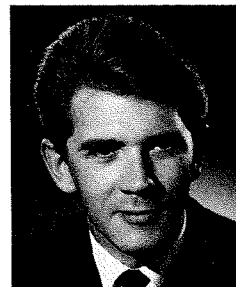
**MICHAEL A. KASHA** graduated in 1957 from London University with a BSc in Honours Physics. After a short time as a Lecturer in Maths and Physics at the Harrow Polytechnic, he joined the United Kingdom Atomic Energy Authority at Harwell, to work in the Controlled Thermonuclear Reactions Division. There he was engaged on plasma physics studies, working on the Spider experiment, an investigation of shock waves in a plasma. This work entailed the design, construction and operation, including diagnostic work, of a 30-kV 18-kJ device. In 1961 he transferred to the Culham Laboratory of the UKAEA, to work on Tarantula, a similar experiment using a 100-kV 100-kJ machine. He was concerned with the development of a 100-kV 1.4-mA, fast-acting (20-ns) switching system and various other aspects of the design and construction. He devised and developed various diagnostic devices, e.g. multicoil magnetic probes, optical interferometers, and time resolved spectrometers. Mr. Kasha joined the Research Laboratories of RCA Victor Company, Ltd. in 1964. He is an associate of the Institute of Physics in London.

Dr. F. J. F. Osborne

Dr. M. P. Bachynski

J. V. Gore

M. A. Kasha



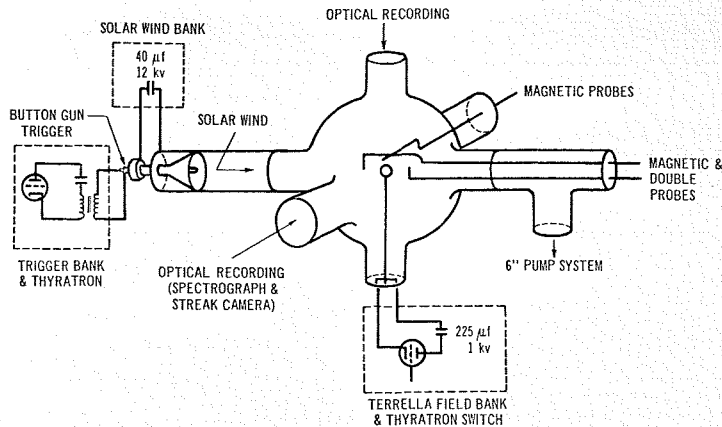


Fig. 1—Experimental configuration for geophysical simulation studies.

laws of similitude is clearly impossible. The question then arises as to whether any meaningful scaled experiments can be performed in the laboratory. The alternative to fulfilling the similitude conditions exactly is to scale the significant parameters only, and to attempt to minimize the effects of the other factors so that a particular aspect of the natural situation can be isolated and studied. The scaling considerations then involve considering the "physics" describing a particular interaction and to determine the quantities to be simulated and those to be neglected. This implies that in all probability a different set of parameters, and thus a separate scale model experiment, is required in order to study each different phenomenon of nature. Such a philosophy has been adapted in the two laboratory-simulation investigations described herein, both carried out by the RCA Victor Co., Ltd., Research Laboratories in Montreal.

These simulation experiments studied phenomena occurring in "space" which are either too complicated to study in detail theoretically, or which still require considerably more information in order to properly design the appropriate satellite instrumentation. Since appropriate scaling has been taken into account, the results should be applicable to the earth's environment.

One of the laboratory simulation experiments is concerned with the interaction between the solar wind and the magnetosphere. In particular, a study of the history of the formation and decay of the magnetosphere under the action of the solar wind has been achieved. The experimental results show: 1) the precipitation of plasma into the polar regions of the earth at late times during the solar storm; 2) the westward swing or "wag" of the tail of the magneto-

sphere during the time the solar wind acts; 3) the presence of the fluctuating electric and magnetic fields in certain regions within the magnetosphere during the time the solar wind acts; and 4) the generation of plasma structure in quasi Van Allen belts, associated with (3) above.

A second laboratory experiment simulates the perturbed region of plasma surrounding and induced by a satellite with long antennas resulting from its motion through a plasma located in a magnetic field. The experiment shows a flare or breakdown effect which occurs at high plasma densities and the general shape of the perturbed sheath region enveloping the satellite. The shape of this induced sheath can be accounted for in terms of the characteristics of a Langmuir probe and suggests that it should be possible to eliminate or greatly reduce the size of the sheath around the body of the satellite by biasing the satellite relative to its antennas.

#### SIMULATION OF SOLAR WIND MAGNETOSPHERE INTERACTION

The solar wind, or plasma, ejected from the sun streams into interplanetary space, and a portion of this wind encounters the magnetic field of the earth. Since the solar wind consists of charged particles (a fully ionized plasma) a strong interaction between the solar wind and the magnetosphere occurs. This interaction results in a distortion of the earth's magnetic field both in space and at the earth's surface (a so-called magnetic storm) and numerous other complex natural phenomena such as current systems in the earth's outer environment, aurora, etc. The complex nature of the interaction makes it extremely difficult to sort out the crucial phenomena contributing to the numer-

ous observed effects. The problem then is to try to get a better understanding of some of the phenomena involved in order to account for the observations made both by spacecraft and from the earth.

#### Method, and Some Previous Results

The experimental arrangement consists of propelling a stream of plasma with a plasma gun into the vicinity of a three-dimensional dipole magnetic field as shown in Fig. 1. Previous results<sup>1,2,3</sup> of such experiments in which the plasma has been shot at the equatorial plane of the magnetic field have shown:

- 1) a stand-off of plasma at approximately the position where the kinetic pressure of the solar wind is balanced by the magnetic pressure of the dipole magnetic field
- 2) the sweeping of the magnetic field and the formation of the front side of the magnetospheric cavity (in agreement with space measurements)<sup>4</sup>
- 3) the formation of trapped regions of plasma similar in shape and position to the natural van Allen belts
- 4) weakly trapped regions of plasma in the vicinity of the polar regions
- 5) the motion of the "dip" pole under the influence of the plasma
- 6) a westward motion of the plasma in the simulated van Allen belts
- 7) the dependence of penetration of plasma into the polar regions on the properties of the solar wind.

#### Recent Experimental Results

This paper presents new results showing the time history of the formation and decay of the magnetospheric cavity under the action of a "gust" of solar wind. This time history is illustrated in a series of photographs taken with a 1- $\mu$ s exposure at predetermined times after the launching of the plasma simulating the solar wind. Fig. 2 illustrates the plasma formation as viewed from the surface equatorial position. The views from above the polar axis are shown in Fig. 3. The measurements made at identical times should be considered simultaneously in ascertaining the time history of the interactions between the solar wind plasma and the three-dimensional dipole of the model earth or terrella.

The important features of the build-up and collapse of the magnetosphere cavity can be determined from a sequence of high-speed photographs, typical examples of which are shown in Figs. 2 and 3. The major findings are:

- 1) At 15  $\mu$ s after launching the plasma from the solar wind "gun", there is no

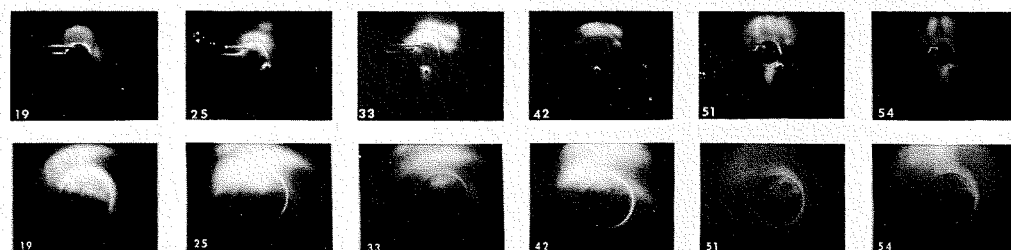


Fig. 2—View from sunrise equatorial position of solar-wind, magnetosphere interaction. Wind incident from top. Exposures, 1  $\mu$ s. Numbers refer to time in microseconds from bank firing. Primary bank energy 1.7 kJ.

Fig. 3—View from above polar axis of interactions, other conditions as in Fig. 2.

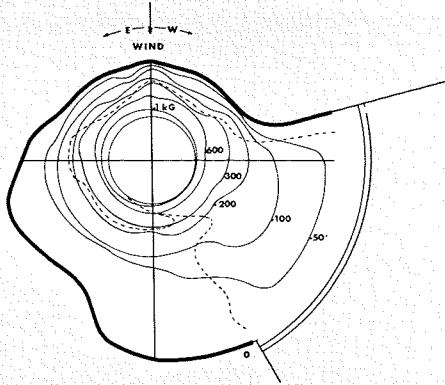


Fig. 4—Equatorial magnetic field (in gauss) at time of maximum boundary penetration. Dotted line shows contour of zero perturbation. Primary bank energy 1.7 kJ.

- visible plasma in the vicinity of the terrella. The first indication of plasma occurs at  $17 \mu\text{s}$  — a diffuse trapped region on the windward side of the terrella showing pronounced striations or periodic structure when seen from the polar axis. Some plasma at this same time penetrates into the polar regions.
- 2) This region becomes better defined (indicating a definite trapping mechanism in the dipole magnetic field), shearing into two regions (as seen from the poles), diffusing the striations and exhibiting a distinct westward motion. This plasma whose distribution resembles that of the van Allen belts in space is formed entirely by precursor radiation from the plasma gun at a time considerably in advance of the main stream of plasma which only becomes visible at  $23 \mu\text{s}$  from the time of launching.
  - 3) As it arrives, the solar-wind plasma compresses the dipole field (see the  $25\text{-}\mu\text{s}$  photograph) moving the magnetospheric boundary and the van Allen belt position nearer towards the terrella. At  $33$  to  $39 \mu\text{s}$ , equilibrium appears to have been achieved after which time the solar wind plasma decreases in pressure.
  - 4) Regions of plasma become trapped in the polar regions (in addition to the simulated van Allen belts) in the interaction times  $29$  to  $45 \mu\text{s}$ . As seen from the polar view, this plasma forms a "tail" trying to encircle the terrella (in addition to the westward motion with increasing time of the interaction).
  - 5) At about the  $45\text{-}\mu\text{s}$  time, the solar wind plasma eases its pressure. This is accompanied by a very dramatic change in the plasma trapped in the vicinity of the terrella. The plasma originally trapped in the polar regions is now absent. The plasma in the magnetospheric cavity begins to break up into a complicated structure. There is a precipitation of plasma into the polar regions in a ring structure around the dip pole (note particularly the  $51\text{-}\mu\text{s}$  polar view).
  - 6) At late times ( $>54 \mu\text{s}$ ) the "belt" structure diffuses, leaving principally the plasma trapped in the simulated van Allen belts which lasts for a long time ( $>75 \mu\text{s}$ ).

Two other features which have been measured by different techniques are equally noteworthy. The component of the magnetic field measured in the equatorial plane at the time of maximum

magnetic field compression ( $33 \mu\text{s}$ ) is shown in Fig. 4. This plot shows a magnetic field "tail" of the magnetosphere cavity swung about  $60^\circ$  westward from the wind direction in agreement with the visible plasma "tail" shown earlier. Since with very little solar wind pressure the backside of the magnetosphere must be nearly directly behind the windward direction, this implies a "wag" of the magnetospheric tail during the interaction of the earth's magnetic field in the equatorial plane is apparent from Fig. 4.

Both electrical probe and magnetic probe measurements in the plasma of the simulated van Allen belts show pronounced signal fluctuations at discrete frequencies. The frequency of these fluctuations are in the  $100\text{-kc/s}$  to  $1\text{-Mc/s}$  range—relatively low if we consider the appropriate scaling factors. These fluctuations must correspond to a magnetohydrodynamic or electrostatic disturbance and are possibly generated during the formation of the striated structure seen early in the interaction.

#### SIMULATION OF SATELLITE $V \times B$ SHEATH

Any electrically floating body immersed in a plasma will come to an equilibrium with its environment such that there is no net current to or from the body (i.e., the electronic charge on the body is constant). Because a thermalized plasma exhibits a high electron mobility relative to that of its ions, the body assumes a negative potential relative to that of its plasma environment, erecting a potential barrier or sheath to reduce its electron collection to the same amount of charge as the ion collection. This difference between the "floating potential" and the plasma potential is relatively small, of the order of a volt, and the sheath (the potential gradient region) consequently also small. If the body is a "small" satellite moving in the ionosphere, this floating sheath is modified by other effects, but the sheath or local perturbed environment which it carries is still small and generally does not significantly affect the satellite measurements.

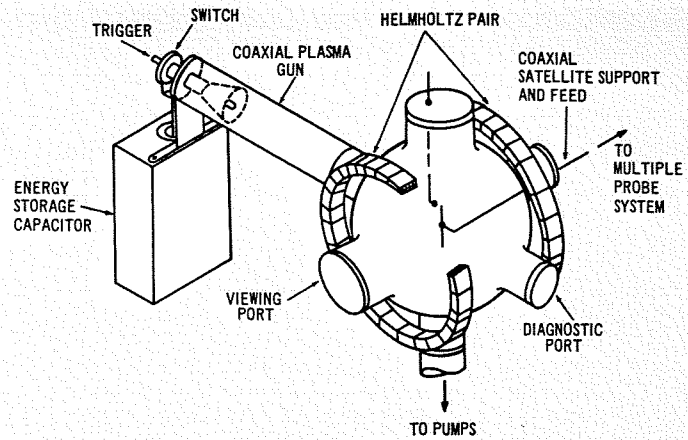


Fig. 5—Experimental configuration for flowing plasma  $V \times B$  simulation.

If however the satellite has long antennas, as is the case for topside ionospheric sounding satellites, the high velocity ( $V$ ) at which the satellite orbits and cuts the magnetic field lines of the earth ( $B$ ) can produce large potential gradients ( $V \times B$ ) along the satellite and its antennas. This potential gradient, along with the fact that the net charge collection is zero, causes a redistribution of the particle collection regions. The result is that the tip of one antenna goes to a potential collecting all the required electrons for equilibrium and also exhibits the smallest sheath radius. The potential gradient forces the remainder of the system below the floating potential where it collects only ions and exhibits large volumes of electron depletion sheaths. Measurements of the local environment by instruments on the satellite are generally made in the vicinity of the satellite body and thus often probe a region of space effectively of the satellite's making and *not* the local environment. Thus, a laboratory study has been instigated in order to ascertain the nature of this  $V \times B$  sheath, its effects on local measurements, and, if possible, suggest techniques whereby the deleterious effects can be eliminated or at least minimized.

#### Experiment Method

Examination of the laboratory requirements based upon appropriate scaling factors<sup>5</sup> shows that they can be readily achieved with present technology. However, practical considerations suggest that to investigate the sheath region around the model, it must be brought to rest in the laboratory frame of reference. Further it is desirable that the magnetic field also be stationary. Thus, whereas in space the satellite moves through an effectively stationary unipotential magnetoplasma, in the laboratory we desire that the plasma move through a stationary magnetic field containing the stationary model as shown in Fig. 5. The result is that the plasma as a conductor flows across the magnetic field lines and develops across itself a  $V \times B$  potential gradient which envelopes the unipoten-

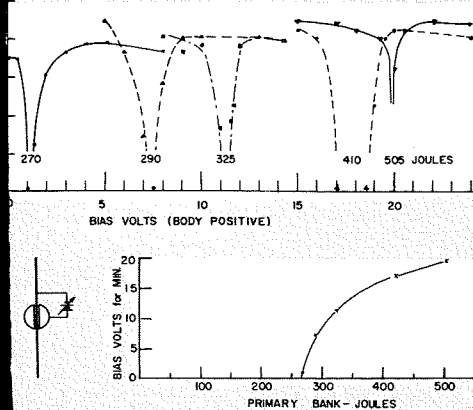


Fig. 6—"Flare" behaviour as a function of body to antenna bias.

tial model satellite. By appropriate changes in frames of reference it can be shown that the situation is analogous to that in space and when the scaling laws are obeyed is a simulation.

### Experimental Results

In the early states of this investigation, the plasma density was increased over the scaled requirement in order to make use of photographic recording. It was found that an unexpected phenomenon was present. At the tip of one antenna there appeared a luminous discharge or "flare" which reversed antenna ends as the magnetic field was reversed. It was found that this flare was associated with the antenna end furthest from the electron collection region and that its position could be modified in several ways.

As shown in Fig. 6 for a model with separate electrical connections to the body and antenna, the flare position on the antenna is a function of the bias between them (the whole system electrically floating). At a critical bias, the exact value dependent on the plasma conditions, the flare will move towards the body and disappear. With bias above the critical value, the flare reappears, then moves back to the antenna tip. Fig. 5 also shows a sharp intercept on the axis when the critical bias is plotted against primary capacitor bank energy used to generate the plasma. This capacitor bank energy is a convenient parameter to indicate the flowing plasma properties. Over the range of energy of interest, the plasma velocity is approximately constant while the plasma density increases with increasing energy. Moreover, neither shows any discontinuity which could be associated with this critical energy. The corresponding photographic records show that this flare phenomenon exhibits a distinct appearance threshold at the critical capacitor bank energy:

It also proved possible to use the modification in nature and position of the flare as a diagnostic tool for sheath investigations. If a second body such as a

small unipotential probe is introduced into the vicinity of the antenna, the flare can be used as an indication of interaction between their respective sheaths. Thus the distances at which the flare "reacts" is an approximation to the sum of the radii of the sheaths of the two bodies. The approximation results from the fact that the sensitivity of the "indicator" is not known. Fig. 7 is a record made in this manner of the  $V \times B$  sheath about a simple conducting rod. The outer solid line defines the limit at which no interaction could be observed. The singly hatched region is that of slight perturbation, whereas the interior exhibited strong reaction. The general shape is much as one might expect except for the notch towards the flare end of the antenna. This notch is a distinct and reproducible feature of these measurements and is believed to be associated with the flare itself.

It has also been shown that the flare is characterized by very high currents flowing in the antenna. It is deduced that the plasma potential gradient becomes large enough to cause a "puncture" of the sheath and that the sheath notch is a consequence of the resulting current. The current path involves the electron collection region at the flareless end and thus produces no corresponding phenomenon there.

The sheath distribution and the resulting charge collection regions can be accounted for by analogy with modified Langmuir probe characteristics. These can be modified and controlled with a potential or bias voltage.

The practical application of this technique to a satellite is not difficult if suitable potentials are available. The potential required is independent of satellite orientation and it is not necessary to continuously control the bias potential as the system is self regulating. Excessive bias merely forces the antenna more negative while the body is virtually at a fixed potential, a consequence of the small change of ion collection with bias for a system cut off to electrons. Finally the power drain on the bias supply can be readily determined for a typical satellite (e.g., ALOUETTE I). Assuming that the dominant current collection is from the satellite ramming the ions, this sheath reduction would require about 13 volts bias and a drain of 13  $\mu$ A.

### CONCLUSIONS

In simulating the interaction between the solar wind and the magnetosphere, in particular the time history of the formation and decay of the magnetosphere cavity under the action of a "gust" of solar wind has been ascertained; the important features are:

- 1) the precipitation of plasma into an annular region around the poles which occurs very late in the interaction,
- 2) the westward swing of the backside or tail of the magnetosphere during the action of the solar wind resulting in a "tail wag" of the magnetosphere during the time of the solar storm.
- 3) the presence of fluctuating electric and magnetic fields of specific frequencies within certain regions of the magnetospheric cavity.

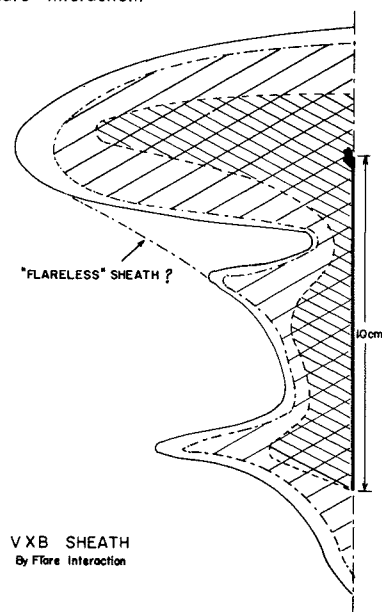
In the second program, the perturbation in the surrounding environment induced by a satellite with long antennas due to its motion in a magnetized plasma has been investigated; the results show:

- 1) a flare occurring at one end of the antenna configuration at high plasma densities,
- 2) the general shape of the sheath induced around the satellite,
- 3) that the shape of the induced sheath can be explained in terms of the modified characteristics of a Langmuir probe,
- 4) that it should be possible to eliminate or greatly reduce the size of the sheath around the satellite body by the use of a proper bias voltage between the body and the antennas.

### BIBLIOGRAPHY

- 1a. F. J. F. Osborne, I. P. Shkarofsky, and J. V. Gore (RCA Victor Research Labs., Montreal); *Can. J. Phys.* 41, 1747, 1963.
- 1b. F. J. F. Osborne, I. P. Shkarofsky, and J. V. Gore (RCA Victor Research Labs., Montreal); "Laboratory Simulation of the Interaction Between the Solar Wind and the Earth's Magnetic Field," *RCA Reprint PE-195* from the *RCA ENGINEER*, 9-5, Feb.-Mar. 1964.
2. F. J. F. Osborne, M. P. Bachynski, and J. V. Gore (RCA Victor Research Labs., Montreal); *Appl. Phys. Letters* 5, 77, 1964.
3. F. J. F. Osborne, M. P. Bachynski, and J. V. Gore (RCA Victor Research Labs., Montreal); *J. Geophys. Res.* 69, 4441, 1964.
4. L. J. Cahill and P. G. Amazeen, *J. Geophys. Res.* 68, 1835, 1963.
5. I. P. Shkarofsky (RCA Victor Research Labs., Montreal); *Simulation of Disturbances Produced by Bodies Moving Through a Plasma and of Other Geophysical Phenomena*, RCA Victor Research Report TM7-801-011. Also to be published in *Astronautica Acta*, 1965.

Fig. 7—The  $V \times B$  sheath as measured by "flare" interaction.



# INSTABILITIES IN SOLID-STATE PLASMAS

When a solid-state plasma, composed of electrons and holes, is subjected to a drifting electric field, it becomes possible to generate growing instabilities. The action in such cases is broadly analogous to traveling-wave tubes utilizing electron beams. There is much interest in such possible solid-state two-stream instabilities because of the very high frequencies that might be generated. In the most general case, with applied magnetostatic fields, these frequencies fall in the range of the hole plasma frequency or the hole cyclotron frequency. Since both of these frequencies can be brought into the millimeter and submillimeter wavelength region, there are many research laboratories actively pursuing such work, both experimentally and theoretically. This paper deals with this field in a general way, and then, several specific cases are considered in detail. Results of analysis on growing TM-modes are presented, along with the limitations dictated by the power levels needed to excite such instabilities. A more general description of the use of solid-state bulk effects, including quantum effects, for generating high-frequency radiation is also given.

**Dr. M. C. STEELE and Dr. B. VURAL**

*RCA Laboratories  
Princeton, N. J.*

**I**NSTABILITIES in a plasma can be desirable or undesirable. In gaseous plasmas, a field that has been investigated very thoroughly, we can cite examples of both situations:

*Desirable Type of Instability*—the electron beam-plasma interaction that leads to generation and amplification of high-frequency radiation.

*Undesirable Type of Instability*—the “kink” or “sausage” type of pinch instability that destroys the confinement of the plasma in a thermonuclear fusion machine.

We wish to discuss here the solid-state analogs of desirable instabilities in gaseous plasmas. It will be seen that much of the earlier work with gases can be adapted to fit the solid-state case and therefore suggest new types of potentially useful devices in the millimeter and submillimeter wave region of the spectrum.

Some of the analogies between a gaseous plasma and a solid-state plasma have already been demonstrated experimentally. An example of one of the striking analogs is the self-pinching (or constriction of current) of a plasma by the action of the self magnetic field pro-

duced by the current. This effect has recently been studied extensively in gases as a means of containing and heating the plasma in a thermonuclear fusion reactor. Several years ago, self-pinching was also demonstrated in the electron-hole plasma in solids<sup>1</sup>.

The possible solid-state two-stream instabilities are of particular interest in the study of analogies to gaseous plasmas. Since the plasma density in a solid can be more easily controlled and can attain much higher values than in a gas, these instabilities warrant further investigation. The higher plasma densities in solids lead to plasma frequencies that can easily be brought into the submillimeter wavelength region.

Another desirable feature of the mobile carrier in the solid is that their masses can be much less than the free electron mass. This property is a direct result of the background periodic potential supplied by the hot crystal. Because of this lower mass, the cyclotron frequency  $\omega_c$  can attain very high values in moderate magnetic field strengths (readily available in the laboratory).

In this paper we shall first give a broad description of the various types of streaming instabilities in solids and then

dwell, in some detail, on a particular one. Examples of specific solids, with realistic parameters, will be presented to delineate the potential advantages and limitations of such devices.

## WAVES IN SOLIDS AND THEIR INTERACTIONS

Many of the bulk effects in solids may be described in terms of waves (wave excitation and propagation). The description may be carried out either in classical or quantum mechanical language. In this paper we shall use the classical description, since it is adequate up to very high frequencies — i.e., submillimeter and far-infrared frequencies.

In general, from an energy point of view, two kinds of waves may be distinguished: 1) positive energy-carrying waves, and 2) negative energy-carrying waves. In order to excite positive energy-carrying waves, energy must be supplied from a proper source. Waves supported by transmission lines (e.g., waveguides) are positive energy-carrying waves. In solids, there are several kinds of positive energy-carrying waves. Some examples are:

- 1) *sound waves*—collective excitation of the mechanical motion of the lattice atoms.
- 2) *spin waves*—collective excitation of a system of electron spins coupled by the exchange interactions.
- 3) *electromagnetic waves*—supported by the dielectric medium.
- 4) *helicon waves*—transverse electromagnetic waves supported by free carriers in the solid in the presence of a magnetic field.
- 5) *“fast waves”*—supported by drifting free carriers.

Negative energy-carrying waves are supported by drifting free carriers.

From the examples given above it is seen that drifting carriers (in solids or vacuum) can, in general, support both positive and negative energy-carrying waves<sup>2</sup>. The reason for this is simply that an external excitation can either increase the energy of the carriers (excite positive energy-carrying waves), or decrease the energy of the carriers by extracting energy from them (excitation of negative energy-carrying waves). Therefore, a medium consisting of (or containing) mobile carriers is an extraordinary medium—on the one hand, *it is similar to circuits* (i.e., transmission lines, waveguides) because it can support positive energy-carrying modes; on the other hand, *it also can be a source of energy for amplification and oscillation*, because it can support negative energy-carrying waves.

Useful traveling-wave devices (amplifiers and oscillators) are based on the

*Final manuscript received August 6, 1965.*

interaction of a positive energy-carrying mode with a negative energy-carrying mode, assuming that these modes can couple to each other; i.e., their phase velocities must be equal and their field configurations must be similar. If the group velocities of these two interacting modes are in the same direction, interaction leads to forward wave amplification (or convective instabilities). If the group velocities are oppositely directed, interaction leads to backward wave oscillations (or nonconvective instabilities). In solids (semiconductors and semimetals) there are possibilities for both convective and nonconvective two-stream instabilities, based on the interaction of two kinds of electrons (or holes) or on the interaction of electrons and holes. In the following section we shall discuss some of these possibilities in detail.

In addition to the active interactions mentioned above, there are parametric interactions involving only positive energy-carrying modes. These interactions are due to the fact that the solid is a nonlinear medium, allowing conversion of

energy from a pump source of frequency  $\omega_p$  into a signal of frequency  $\omega_s$ , with the aid of an idler frequency  $\omega_i = \omega_p - \omega_s$ . In general, in parametric interactions, the following conditions between frequencies and wave numbers must be fulfilled:

$$\omega_p = \omega_s + \omega_i \quad (1)$$

$$k_p = k_s + k_i \quad (2)$$

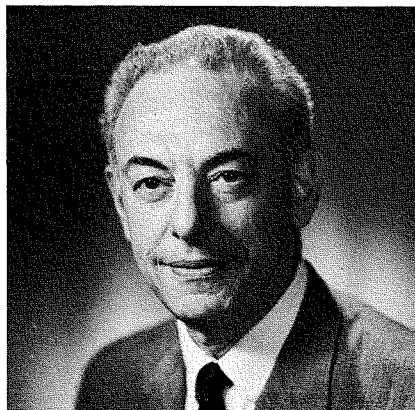
where  $\omega_{p,s,i}$  are the pump, signal and idler frequencies, respectively, and  $k_{p,s,i}$  are the pump, signal and idler wave numbers, respectively. Maser and laser actions can be interpreted as a special quantum mechanical case of parametric interactions. In these cases, the relationship between frequencies and wave numbers simply express the principles of conservation of energy and momentum:

$$\hbar\omega_p = \hbar\omega_s + \hbar\omega_i \quad (3)$$

$$\hbar k_p = \hbar k_s + \hbar k_i \quad (4)$$

We shall not discuss parametric interactions any further here. Instead, we shall return to two-stream instabilities in solids.

**DR. MARTIN C. STEELE** received his BChE (cum Laude) from Cooper Union Institute of Technology in 1940, and the MS and PhD in Physics from the University of Maryland in 1949 and 1952 respectively. He worked as an engineer for the Office, Chief of Engineers, before the war, and as a research physicist in the Naval Research Laboratory from 1947 to 1955, where he was head of the Cryomagnetic Research Group in the Solid State Division. Since 1955 he has been with RCA, as head of the Solid State Electronics Research Group and for three years (1960-63) as the first Research Director of RCA's research laboratory in Tokyo, Japan. In August, 1963 he became head of the Plasma Physics Group of the Microwave Research Laboratory at RCA Laboratories, Princeton, New Jersey. His research has covered a wide range of areas in solid state physics, including superconductivity, magnetic susceptibility, thermometry, theory of magnetic properties of metals, thermal, electric and magnetic properties of semiconductors, and the properties of plasmas in solids. He has published numerous technical papers in these fields and has refereed many articles for the Physical Review, the Journal of Applied Physics, and the Journal of the Physical Society of Japan. Dr. Steele is a Fellow of the



American Physical Society, a Member of Sigma Xi and a former Member of the Washington Academy of Science.

**DR. BAYRAM VURAL** received an Electrical Engineering degree in 1949 and the Dr. of Technical Sciences degree in 1952 from the Swiss Federal Institute of Technology, Zurich, Switzerland. From 1951 to 1953 he was associated with Brown Boveri and Company, Baden, Switzerland, working on microwave relay communication and on application of a special magnetron as communication transmitter. From 1953 to 1959 he was mainly associated with the Electronic Equipment and Tube Department of Canadian General Electric, Toronto, Canada, working mainly on microwave problems in connection with radar and communication. Dr. Vural joined RCA Laboratories as a Member of the Technical Staff in 1959. He has done theoretical work related to multivelocity flow, and high-power problems and is now engaged in electron device research, especially in two-stream instabilities in vacuum and in solids. Dr. Vural is a Senior Member of the IEEE and member of the American Physical Society. He also teaches a graduate course in Solid State electronics at Drexel Institute of Technology in Philadelphia, Pa.



## TWO-STREAM INSTABILITIES IN SOLIDS

As mentioned above, the basic two-stream instabilities are due to interaction of two kinds of drifting electrons (or holes) or to interaction of drifting electrons with holes. These three classes of mobile carrier combinations and the broad classes of materials in which they may exist are as follows:

*Class 1—Electrons and Holes*—Intrinsic semiconductors, semimetals, semiconductors with electron-hole plasmas generated by impact ionization or radiation.

*Class 2—Two different kinds of electrons*—III-V compound semiconductors such as GaAs or GaSb in which the conduction band has two minima that can be simultaneously populated.

*Class 3—Two different kinds of holes*—Semiconductors such as Ge, Si, or InSb which have light and heavy holes in the valence band.

### TM Waves

If the carrier combinations shown above are drifted in the presence of a longitudinal magnetic field, there are a number of possible growing instabilities in an electromagnetic field which has both transverse and longitudinal electric field components (TM modes). The theoretical work of Vural and Steele<sup>3</sup> on such a configuration has shown that there are four possible instabilities that can occur:

- 1) space charge-space charge interaction.
- 2) cyclotron-cyclotron interaction.
- 3) and 4) two hybrid interactions between space charge and cyclotron waves.

These instabilities occur at frequencies near the Doppler-shifted slower carrier plasma frequency  $\omega_p$ , given by (in MKS units):

$$\omega_p^2 = \frac{n e^2}{\epsilon_0 m^*} \quad (5)$$

where  $n$  = density of slow carrier,  $e$  = electronic charge,  $\epsilon_0$  = free space permittivity, and  $m^*$  = effective mass of slow carrier.

Or, they occur near the Doppler-shifted slower carrier cyclotron frequency  $\omega_c$ , given by:

$$\omega_c = \frac{e B}{m^*} \quad (6)$$

where  $B$  = applied magnetostatic field.

Since we can adjust  $\omega_p$  by appropriate doping and  $\omega_c$  by changing the value of  $B$ , these instabilities can readily be made to occur in the millimeter-wave region. In fact, in order to have such interactions, which are of the collective type, we must work at frequencies,  $\omega$ , such that  $\omega\tau > 1$ , where  $\tau$  is the scattering time pertinent to the particular situa-

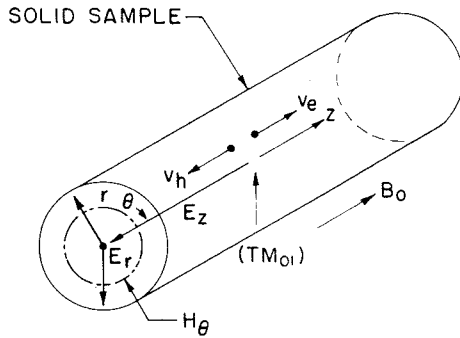


Fig. 1—Geometry and electromagnetic field configurations of an electron-hole plasma in a longitudinal magnetic field;  $r_0$  is the radius of the cylinder.

### Dispersion Relation for TM Waves

We wish to derive the dispersion relation for cylindrical geometry in which the RF is being propagated along an applied magnetic field in a  $TM_n$  mode. Fig. 1 shows the mode configuration and geometry. The following assumptions are made in deriving the dispersion relation:

- 1) The boundaries are metallic and the semiconductor or semimetal sample fills the waveguide as shown in Fig. 1.
- 2) Only first-order perturbations will be considered (small-signal assumption).
- 3) The direction of the external magnetic field and the direction of propagation coincide ( $z$  direction).
- 4) There are equal numbers of electrons and holes and the carriers

drift respectively in the positive and negative  $Z$  direction.

- 5) We assume that the phase velocity of the waves is much smaller than the velocity of light,  $v_{ph} \ll c$  (slow-wave assumption).
- 6) For electrons and holes respectively we assume constant drift velocities,  $v_e, v_h$ ; constant collision times,  $\tau_e, \tau_h$ ; and constant effective masses,  $m_e$  and  $m_h$ .
- 7) We neglect diffusion, and assume that the rate of generation and recombination of electrons and holes are the same.

From Maxwell's equations, the equation of continuity, the equations of motion and a perturbation in the form of  $\exp i(\omega t - m\theta - kz)$ , the following dispersion relation is obtained:

$$\gamma^2 = -k^2 \frac{\epsilon_l - \left\{ \frac{\omega_{pe}^2}{\left[ (\omega - kv_e) - \frac{i}{\tau_e} \right] \left[ \omega - kv_e \right]} \right\} - \left\{ \frac{\omega_{ph}^2}{\left[ (\omega + kv_h) - \frac{i}{\tau_h} \right] \left[ \omega + kv_h \right]} \right\}}{\epsilon_l - \left\{ \frac{\omega_{pe}^2 \left[ (\omega - kv_e) - \frac{i}{\tau_e} \right]}{\omega - kv_e} \right\} - \left\{ \frac{\omega_{ph}^2 \left[ (\omega + kv_h) - \frac{i}{\tau_h} \right]}{\omega + kv_h} \right\}} - \left\{ \frac{\omega_{ce}^2}{\left[ (\omega - kv_e) - \frac{i}{\tau_e} \right]^2 - \omega_{ce}^2} \right\} - \left\{ \frac{\omega_{ch}^2}{\left[ (\omega + kv_h) - \frac{i}{\tau_h} \right]^2 - \omega_{ch}^2} \right\}}$$

where:

$\gamma$  = radial propagation constant

$k$  = axial propagation constant

$\epsilon_l$  = lattice relative dielectric constant

$$\omega_{pe}^2 = \frac{ne^2}{m_e \epsilon_0}$$

$\omega_{pe}$  = plasma frequency of electrons

$v_e$  = drift velocity of electrons

$\tau_e$  = collision time for electrons

$\omega_{ce} = \frac{eB}{m_e}$  = cyclotron frequency of electrons

$$\omega_{ph}^2 = \frac{ne^2}{m_h \epsilon_0}$$

$\omega_{ph}$  = plasma frequency of holes

$v_h$  = drift velocity of holes

$\tau_h$  = collision time for holes

$\omega_{ch} = \frac{eB}{m_h}$  = cyclotron frequency of holes

tion. Since  $\tau^{-1}$ , the scattering frequency, typically ranges from 5 Gc/s to over 100 Gc/s, depending on temperature and other parameters, we are dealing here with electromagnetic waves in the millimeter and submillimeter wavelength regime. *It is precisely this region that needs new generators and amplifiers.*

For the electron-hole situation (Class 1 in the tabulation given earlier), the carriers drift in opposite directions upon applying an electric field. This results in nonconvective instabilities due to the interaction of "circuit-like" backward-wave modes, supported by the holes, and "negative energy" carrying forward-wave modes supported by the electrons.

On the other hand, for two-electron streams (Class 2) or two-hole streams (Class 3) the carriers drift in the same direction. For such cases the instabilities will be of the convective type and should therefore, in principle, lead to the possibility of traveling-wave amplifiers. The applicability of such cases to a solid depends on the existence of a two-humped electron or hole distribution which could be approximated by a two-stream model such as has been considered elsewhere<sup>3</sup>. In solids with more than one conduction (or valance) band minimum, it is theoretically possible to establish a doubled-humped electron (or hole) distribution. Clearly, much more theoretical work is needed on specific solids (such as those cited in the tabulation of Class 1, 2, 3 carriers given earlier), taking into account the effects of interband scattering, before any conclusions can be reached.

Some of the features of the  $TM$  wave instabilities are given in Figs. 1-4. Fig. 1 shows the geometry and electromagnetic field configuration of an electron-hole plasma in a longitudinal magnetic field and develops the dispersion relation for  $TM$  waves. Fig. 2 shows the dispersion diagram of drifting electron-hole plasma in a longitudinal magnetic field and interacting with  $TM$  waves (no collisions). Regions I, II, III and IV are the regions of nonconvective instabilities. Fig. 3 shows part of the calculated dispersion diagram which includes instability regions III and IV. Fig. 4 shows the rate of growth of this instability and how it is affected by collisions.

### TEM Waves

So far, we have discussed the instabilities of a drifting electron-hole plasma interacting with  $TM$  waves. There are also instabilities when a drifting electron-hole plasma interacts with transverse electromagnetic waves in the presence of a static magnetic field<sup>4</sup>. Fig. 5 shows the dispersion diagram of such a

system and the region of instability. This interaction occurs at a relatively low frequency compared to the *TM* mode discussed above. There are experimental results<sup>5</sup> with indium antimonide that appear to be related to such *TEM* wave instabilities<sup>9</sup>.

### CONCLUSIONS

We have first considered the two-stream instabilities that can exist in a solid-state plasma in the presence of an electromagnetic field which has both transverse and longitudinal electric field components and situated in a longitudinal static magnetic field. The analysis shows<sup>3</sup> that there are four regions in

which nonconvective instabilities can occur. One of these instabilities is similar to the Pine-Schrieffer case<sup>7</sup>.

The results of quantitative calculations confirm the qualitative picture which was developed in analogy to two-stream instabilities in electron beams. When collisions are taken into account, their main role is to reduce the rate of growth of the instabilities. The same situation prevails in the interaction of electron-hole plasma with transverse electromagnetic waves.

While the model examined in this paper is idealized in that it is one-dimensional and neglects the effects of diffusion and velocity distribution, it does re-

veal some interesting possibilities for achieving gain in solid-state plasmas. Because these possibilities lie in a frequency domain inaccessible to transistors, they are being examined both theoretically and experimentally.

### BIBLIOGRAPHY

1. M. Glucksman and M. C. Steele (RCA Labs., Princeton), *Phys. Rev. Lett.* **2**, 461 (1959).
2. P. A. Sturrock, *J. Appl. Phys.* **31**, 17 (1960).
3. B. Vural and M. C. Steele (RCA Labs., Princeton), *Phys. Rev.* **139**, A300 (1965).
4. J. Bok and P. Nozieres, *J. Phys. Chem. Solids* **24**, 709 (1963).
5. R. D. Larrabee and W. A. Heinbothem, Jr. (RCA Labs., Princeton), *Plasma Effects in Solids*, Dunod, Paris 1964, pp. 181-187.
6. M. C. Steele (RCA Labs., Princeton), *Plasma Effects in Solids*, Dunod, Paris 1964, pp. 189-191.
7. D. Pine and R. Schrieffer, *Phys. Rev.* **124**, 1387 (1961).

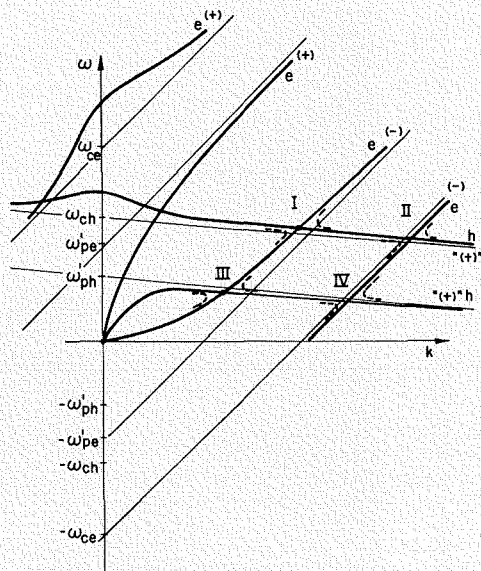


Fig. 2—Dispersion diagram of drifting electron-hole plasma in a longitudinal magnetic field and interacting with *TM*-waves (with no collisions). Regions I, II, III and IV are regions of nonconvective instabilities. The *e* and *h* refer to the modes supported by the electrons and by the holes respectively. The + and - refer to the sign of the energy carried by a given mode. The parameters  $\omega_{pe}$  and  $\omega'_{ph}$  are defined as:

$$(\omega'_{pe})^2 = \frac{\omega_{pe}^2}{\epsilon_i} \quad (\omega'_{ph})^2 = \frac{\omega_{ph}^2}{\epsilon_i}$$

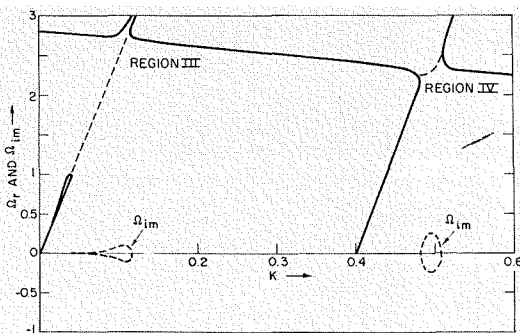


Fig. 3—Part of the dispersion diagram of a drifted electron-hole plasma calculated with parameters:

$$v_e/v_h = 25 \quad \left(\frac{\omega'_{pe}}{\omega_{ch}}\right)^2 = 0.7 \quad \frac{1}{\omega_{ch}\tau_h} = 0$$

$$\left(\frac{\omega'_{ph}}{\omega_{ch}}\right)^2 = 7 \quad \frac{\omega_{ch}}{v_h} \cdot r_0 = 0.73 \quad \frac{\tau_e}{\tau_h} = 1$$

$\Omega$  is the normalized frequency given by  $\omega/\omega_{ch}$ , and  $K$  is the normalized wave number given by  $k/(\omega_{ch}/v_h)$ .

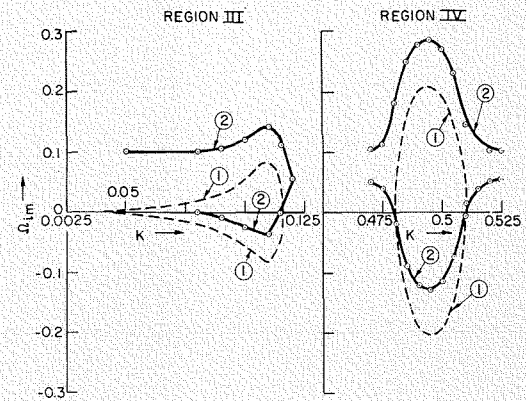


Fig. 4—Imaginary part of the normalized frequency (for Regions III and IV of Fig. 3) as function of the normalized wave number with normalized collision frequency:

$$\textcircled{1} \frac{1}{\omega_{ch}\tau_h} = 0 \quad \textcircled{2} \frac{1}{\omega_{ch}\tau_h} = 0.1$$

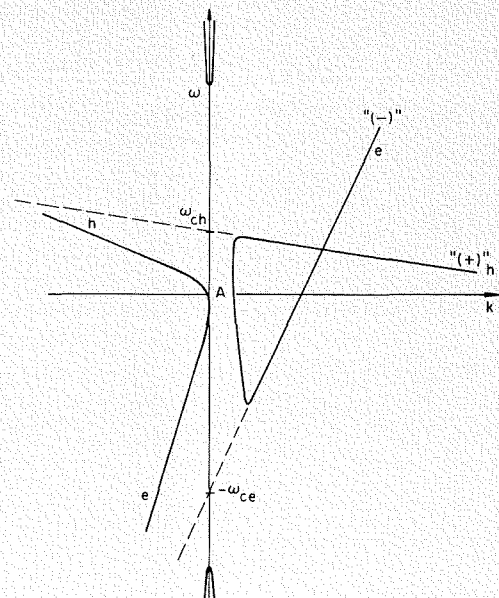


Fig. 5—Dispersion diagram for a drifting electron-hole plasma in a magnetic field and interacting with left-handed polarized transverse electromagnetic waves. Region A is the region of a nonconvective instability.

# ALFVEN WAVES IN BISMUTH PLASMA

Waves may propagate in a plasma at frequencies below the plasma or cyclotron frequency: in a magnetic field, and a plasma consisting of equal numbers of electrons and holes, these waves are Alfvén waves. Their propagation at 52 Gc/s has been studied in bismuth at 4.2°K. The two classes of waves predicted theoretically were observed, and in general their characteristics were in good agreement with calculations. It was found that the waves could be seen at weaker magnetic fields than that corresponding to the lowest cyclotron frequency of the carriers, because the proper choice of polarization can result in poor coupling to the cyclotron wave which would normally provide very strong damping for the propagation.

Dr. B. W. FAUGHNAN

Laboratories RCA Inc., Tokyo, Japan

IF a plasma is immersed in a magnetic field, a variety of electromagnetic waves may propagate, provided the conditions for moderate damping are satisfied. In a semimetal plasma such as bismuth, which has equal numbers of electrons and holes, the propagating modes are called *Alfvén waves*. The nature of these waves differ considerably from the helicon waves<sup>1</sup> which are observed in a plasma with only one mobile charge.

Alfvén waves were first postulated by H. Alfvén in 1942 to explain certain phenomena in astrophysics<sup>2</sup>. Soon after, some attempts were made to create these waves in a laboratory experiment using liquid mercury and sodium as the propagation medium. The experiments proved difficult because the wavelengths generated were comparable to the apparatus dimensions and the losses were high. Nevertheless, some aspects of the theory were verified.

More recently, it was realized that many interesting plasma phenomena occur in solids as well as gases and the semimetals have proved to be an ideal medium for the propagation of Alfvén waves. Because of the unusually high mobility of bismuth, especially at liquid helium temperatures, the damping of the waves can be quite small.

*What can be learned from a study of Alfvén waves in semimetals?* By measuring the propagation properties of Alfvén waves we can test our theoretical understanding of wave propagation in plasmas. In addition there are other important properties of plasmas which, although not essential for wave propaga-

Final manuscript received September 1, 1965.

tion, nevertheless modify the nature of the waves. For example, the low magnetic field limit for wave propagation will be determined by cyclotron resonance damping by one of the carriers. The electron and hole Fermi velocity will modify the waves particularly at low magnetic field where the Alfvén velocity is less than or equal to the Fermi velocity. From another point of view, since the Alfvén velocity depends on the effective mass of the carriers, Alfvén wave experiments can be used to study the band structure of materials, and the attenuation of the waves provide information on the relaxation time for carriers in that material.

## THEORY

The allowed modes of propagation in a solid-state plasma may be determined by solving Maxwell's equations provided the conductivity tensor of the plasma is known. It proves convenient to use the complex dielectric constant:

$$\bar{\epsilon} = \epsilon_c + \frac{\sigma}{j\omega\epsilon_0} \quad (1)$$

where  $\epsilon_c$  = lattice dielectric constant = 100 for bismuth;  $\sigma$  = plasma conductivity tensor. Then, if  $\epsilon$  is real and positive unattenuated wave propagation occurs and the phase velocity is  $V = c/\sqrt{\epsilon}$ . This is easily verified by examining Maxwell's equations.

The plasma dielectric constant for bismuth is complicated because of the anisotropic energy surfaces for electrons and holes. For simplicity we shall consider an isotropic plasma. For a linearly polarized wave propagating along the

magnetic field the plasma dielectric constant is<sup>3</sup>:

$$\epsilon = \epsilon_c - \left[ \frac{\omega_{pe}^2}{(\omega - \omega_{ce})\omega} \right] - \left[ \frac{\omega_{ph}^2}{(\omega + \omega_{ch})\omega} \right] \quad (2)$$

where  $\omega_{pe} = (n_e e^2 / m_e \epsilon_0)^{1/2}$  = plasma frequency of electrons;  $\omega_{ph} = (n_h e^2 / m_h \epsilon_0)^{1/2}$  = plasma frequency of holes;  $\omega_{ce} = eB/m_e$  = cyclotron frequency of electrons;  $\omega_{ch} = eB/m_h$  = cyclotron frequency of holes;  $n_e$  = electron concentration;  $n_h$  = hole concentration;  $m_e$  = effective mass of the electrons; and  $\epsilon_0 = 8.85 \times 10^{-12}$  in MKS units.

We make the assumption  $\omega \ll (\omega_{ce}, \omega_{ch})$  and expand  $\epsilon$  in powers of  $(\omega/\omega_{ce}, \omega/\omega_{ch})$ :

$$\epsilon = \left( \frac{\omega_{pe}^2}{\omega\omega_{ce}} - \frac{\omega_{ph}^2}{\omega\omega_{ch}} \right) + \left( \frac{\omega_{pe}^2}{\omega_{ce}^2} + \frac{\omega_{ph}^2}{\omega_{ch}^2} \right) + \dots + \text{higher order terms} \quad (3)$$

using the definitions of plasma and cyclotron frequencies, the dielectric constant can be written:

$$\epsilon = \epsilon_c + \left( \frac{e(n_e - n_h)}{\epsilon_0 \omega B} \right) + \left( \frac{n_e m_e + n_h m_h}{\epsilon_0 B^2} \right) \quad (4)$$

The lattice dielectric constant can usually be ignored except at very large magnetic fields in which case the plasma effects are suppressed and ordinary electromagnetic waves are propagated.

At moderate fields, if  $n_e \neq n_h$  the second term in Eq. 4 usually dominates over the third. This is the condition for *helicon propagation*. For an undoped

BRIAN FAUGHNAN graduated from McGill University with a BEng degree in Engineering Physics in 1955. In 1957 he received a SM degree in Electrical Engineering from M.I.T. and in 1959 PhD in Physics also from M.I.T., where he performed research on paramagnetic resonance in solids and on masers. In Sept. 1959 he joined the Technical Staff of RCA Laboratories. At RCA he worked initially on cyclotron resonance in semiconductors and after that on the study of radiation defects in silicon by means of electron spin resonance. Dr. Faughnan recently spent a year at Laboratories RCA, Inc., in Tokyo, where he studied the propagation of Alfvén waves in bismuth. Since his return to Princeton in August 1964 he has been investigating the properties of semimetal thin films.



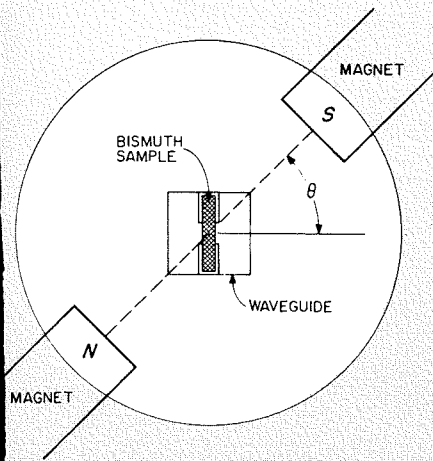


Fig. 1 — Experimental arrangement for Alfvén waveguide transmission experiments.

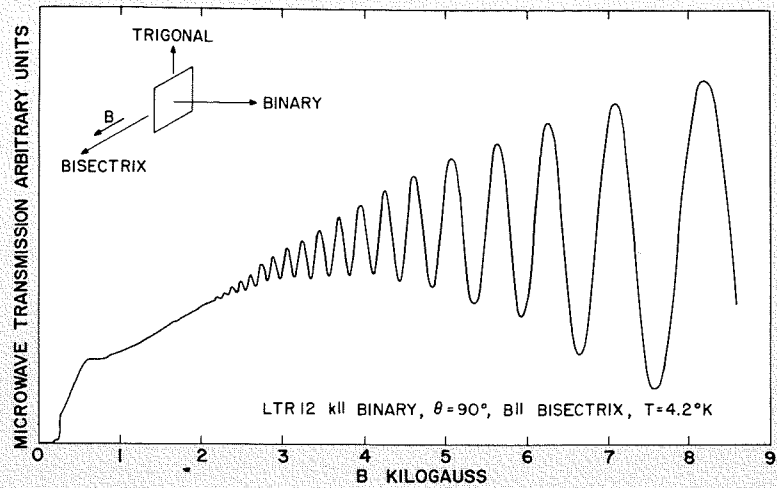


Fig. 2 — Microwave transmission in bismuth.

Fig. 3 — Plot of  $n$  vs  $1/B$  for LTR 9.

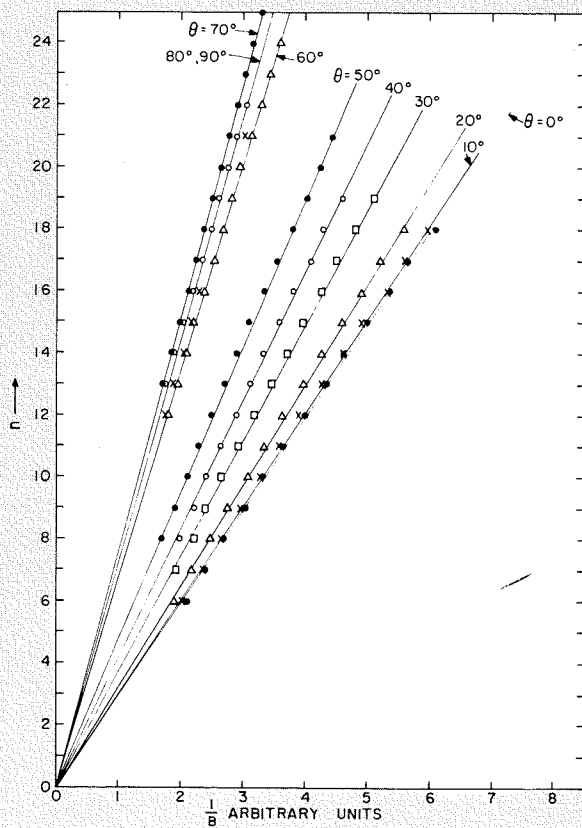
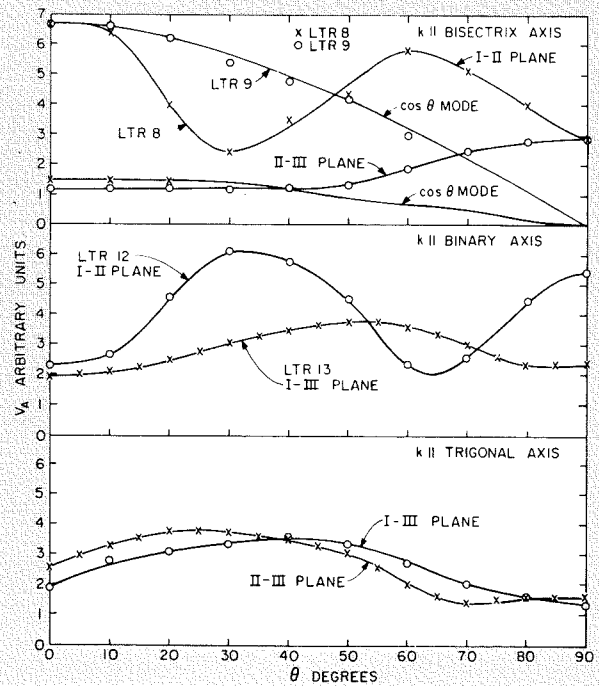


Fig. 4 — Experimental Alfvén velocity in bismuth for all principal crystal directions and for  $\theta$  between  $0^\circ$  and  $90^\circ$ . I, II, III, represent the binary, bisectrix, and trigonal directions respectively in bismuth.



semimetal,  $n_e = n_h$  and the second term vanishes. There remains:

$$\epsilon = \frac{n(m_e + m_h)}{\epsilon_0 B^2} = \frac{c^2}{V_A^2} \quad (5)$$

where:

$$V_A = \frac{B}{\sqrt{\mu_0 n(m_e + m_h)}} \quad (6)$$

= *Alfven velocity*

This is the case of *Alfven wave propagation*.

We note some differences between Alfven and helicon waves. First, the Alfven wave velocity is dispersionless, whereas the helicon velocity is proportional to the square root of the frequency.<sup>1</sup> The helicon velocity depends on the electronic charge and is independent of particle mass while the Alfven velocity depends on the mass density and is independent of charge.

There are several other differences not apparent from the simple derivation given here. For example, the helicon wave is circularly polarized and only one direction of polarization can propagate freely in the medium in any direction. The Alfven wave is linearly polarized and for most directions of propagation the plasma can support two waves independently.

The phase velocity of one of these waves has a  $\cos \theta$  dependence, where  $\theta$  is the angle between the direction of propagation and the magnetic field. If the material is anisotropic the two Alfven velocities may be different even for  $\theta = 0$ . If losses are taken into account we find that the condition for helicon propagation with small loss is  $\omega_c \tau \gg 1$  where  $\omega_c$  = cyclotron frequency and  $\tau$  = carrier collision time. For Alfven waves the condition for small damping is  $\omega \tau \gg 1$  where  $\omega$  = angular frequency of the wave. The small-damping condition on Alfven waves is the more restrictive one and it is usually necessary to perform experiments at liquid helium temperature to satisfy it.

#### A PHYSICAL INTERPRETATION OF ALFVEN WAVES

There is a simple derivation of the Alfven velocity due to Alfven<sup>4</sup> which clarifies the nature of the waves. The derivation is based on the idea that magnetic lines of force can be regarded as elastic strings. The force exerted by a magnetic field is such that the strings tend to contract and at the same time exert a lateral pressure on each other. In addition, a magnetic field inside a perfectly conducting medium will be "frozen" in the medium. Any change in the position of the magnetic field lines relative to the medium will give rise to infinite currents which would oppose the change. Thus

we can think of the system as a weighted string under tension. In analogy to the weighted string, a transverse wave motion is possible with wave velocity:

$$V = \sqrt{\frac{T}{\rho}}$$

where  $T$  = tension of the "string" and  $\rho$  = mass density.

In this case we must put:

$$T = \frac{B^2}{\mu_0} \quad \rho = n(m_e + m_h)$$

$$V_A = \frac{B}{\sqrt{\mu_0 n(m_e + m_h)}} \quad (6)$$

This is the same formula that we obtained previously using the dielectric constant approach.

#### EXPERIMENTAL STUDIES IN SOLIDS

Indirect experimental evidence for Alfven waves in solids was first observed in cyclotron resonance experiments in bismuth.<sup>5</sup> Shortly after, the direct transmission of Alfven waves through a bismuth slab was reported<sup>6</sup> and since that time a number of papers related to Alfven waves have appeared.<sup>7</sup>

Alfven wave propagation can be studied conveniently either by direct transmission of microwaves through a semimetal slab or by observing the effect of standing waves in the slab on the surface impedance of the semimetal.

An experimental arrangement for observing Alfven wave transmission is shown in Fig. 1. Microwave radiation is transmitted through the semimetal slab and then mixed with a microwave reference signal derived from the same source. As the magnetic field is varied the wave velocity inside the semimetal changes in accordance with Eq. 6. This in turn alters the phase shift of the microwaves passing through the sample. For some values of the magnetic field the reference signal and the transmitted signal will be in phase and this will produce a series of maxima. Similarly, a series of minima will result when the two signals are out of phase. The amplitude of the signal will increase with  $B$  since the losses in the sample decrease. The losses through the slab decrease with increasing  $B$  since it can be shown that the attenuation of the signal is proportional to  $\exp(-r\pi/\omega\tau)$  where  $r$  is the number of wavelengths in the sample. As  $B$  increases the number of wavelengths contained in a slab of given width decreases because the Alfven velocity is proportional to  $B$ . The  $r$ th transmission maxima is given by:

$$r = \frac{t}{\lambda_A} = \frac{tf}{v_A} \quad (7)$$

where  $t$  = sample thickness,  $\lambda_A$  = Alfven wavelength,  $f$  = microwave fre-

quency, and  $v_A$  = Alfven velocity. We can combine this with Eq. 6 for  $v_A$  to obtain:

$$r = [tf\sqrt{\mu_0 n m_e m_h}] \frac{1}{B} \quad (8)$$

An example of an Alfven wave transmission curve is shown in Fig. 2. If the transmission peaks are plotted as a function of  $1/B$  a straight line should result. This is shown in Fig. 3. The slope of the straight line is inversely proportional to the Alfven velocity and changes as the angle between the direction of propagation and the magnetic field is varied.

A complete study of propagation characteristics can be made by measuring the Alfven velocity as a function of this angle and for all principal crystal orientations. The result of such measurements is shown in Fig. 4. It is found that a reasonably good fit can be obtained between these experimental curves and theoretical predictions based on already published band parameters for bismuth.

#### SUMMARY

We have shown that Alfven waves can be readily excited in a semimetal plasma at low temperatures. The behavior of the waves in most respects is in accordance with theory and hence can be used as an experimental technique for obtaining the band parameters of a semimetal. In addition, the observed wave propagation is more complicated than the simple theory predicts in several respects and these anomalies may be used to study the behavior of solid state plasmas. For example, we find cases where a single-wave mode splits into two modes where no splitting is predicted from theory.

Although no direct application of Alfven waves has yet been found, the study of such phenomena has proved a valuable aid in elucidating the properties of semimetals. The semimetals in turn have found application as low temperature thermoelectrics and further applications such as, in thin film transistors are being actively investigated.

#### BIBLIOGRAPHY

1. S. J. Buchsbaum, "Plasma Effects in Solids" 7th International Conf. on the Physics of Semiconductors, Dunod, Paris 1964.
2. H. Alfven, *Nature* 150, 405 (1942).
3. Allis, Buchsbaum and Bers *Waves in Anisotropic Plasmas* The M.I.T. Press, Cambridge, Mass. 1963.
4. H. Alfven, *Cosmical Electrodynamics*, Clarendon Press, Oxford, England, 1950.
- 5a. J. K. Galt, W. A. Yager, F. R. Merritt, B. B. Cetlin, and A. P. Brailsford, *Phys. Rev.* 114, 1396 (1959).
- 5b. S. J. Buchsbaum and J. K. Galt, *Phys. Fluids* 4 1514 (1961).
6. G. A. Williams, *Bull. Am. Phys. Soc.* 7 409 (1962).
- 7a. J. Kirsch, *Phys. Rev.* 133 A1390 (1964).
- 7b. M. S. Khaikin, L. A. Falkovsky, V. S. Edelman and R. T. Mina, *Sov. Phys. JETP* 17, 1470 (1963).
- 7c. B. Faughnan, (RCA Labs., Princeton), *J. Phys. Soc. Japan* 20, 574 (1965).
- 7d. G. A. Williams, *Phys. Rev.* 139 A771 (1965).

# MICROWAVE EMISSION FROM SOLID-STATE PLASMAS

Microwave radiation from inductive posts of indium antimonide has been observed in a broad band spectrum extending down to at least 3 Gc/s and up to at least 44 Gc/s. This emission occurs when the indium antimonide, cooled to 77°K and placed in a DC magnetic field in excess of 3 kG, is pulsed to an average electric field ranging from 300 to 700 V/cm. The power output, integrated over the spectrum from 3 to 44 Gc/s is approximately 1 mW. It is anticipated that with more efficient coupling between the solid and output waveguide, the power level will be increased, and operation as an amplifier and a single frequency oscillator can be achieved. Low-frequency (10- to 20-Mc/s) oscillations in the sample current were also observed. In some experiments these oscillations were correlated with the microwave emission while in others no correlation could be found. Experiments were performed to determine the pertinent mechanism of the microwave emission. To date, the results of these investigations suggest that drifted solid-state plasma instabilities are involved.

**Dr. R. D. LARRABEE, W. A. HICINBOTHEN, JR., and J. J. THOMAS**

*RCA Laboratories, Princeton, N. J.*

**M**ANY of the conventional generators of energy in the millimeter and sub-millimeter wavelength range are restricted in size by the relatively short wavelengths at these high frequencies. This limitation leads to problems of construc-

*Final manuscript received May 26, 1965*

The research reported here is sponsored by Air Force Avionics Laboratory, Research and Technology Division, Air Force Systems Command, Wright Patterson Air Force Base, Ohio, under Contract AF33(615)-1608, and RCA Laboratories, Princeton, New Jersey.

tion and available output power. Consequently, these devices are relatively expensive and generally have a limited operating lifetime.

One possible solution to these problems involves the utilization of the electrical properties of solid state materials. These properties can be divided into two classes depending on whether the active portion of the device is 1) localized in some particular region of the solid or

2) distributed throughout its volume. Tunnel diodes, varactors, and crystal diodes (i.e., harmonic generators, detectors and mixers) are examples of microwave devices based on the properties of a localized junction. The maser is an example of a solid-state device employing the properties of a homogeneous crystal.

It is difficult to obtain high-frequency operation utilizing localized properties

**WALTER A. HICINBOTHEN, JR.** was employed by the Minerals and Chemicals Corporation of Menlo Park, New Jersey as a Senior Research Technician in 1955. He was awarded a Certificate of Engineering by Rutgers University in June 1964. Since 1960 he has been employed by RCA Laboratories. His present position is that of Technical Staff Associate in the Plasma Physics Group of the Microwave Research Laboratory. Mr. Hicinbothem is presently concerned with studies of plasmas in solids and interaction of microwaves with semiconductors. He is the co-author of a number of articles relating to these fields.

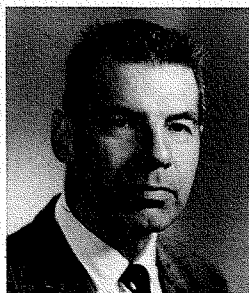
**DR. ROBERT D. LARRABEE** was awarded the BSEE at Bucknell University in June 1953 and the degree of Master of Science in Mathematics August 1953. He entered the Massachusetts Institute of Technology in September 1953 and received the degree of Science Master (without course specification) in June 1955 and the degree of Doctor of Science in Physics in June of 1957. While at MIT, he was concerned with the spectral emissivity and optical properties of tungsten (Doctoral Presentation) and the characteristics of high vacuum ionization gauges. Dr. Larrabee joined the research staff of RCA Laboratories in July 1957, and since then has spe-

cialized in semiconductor research, especially on effects related to negative mass phenomena, and more recently, on studies of plasma effects in solids including the "Oscillator," and microwave emission from indium antimonide. He is a member of Sigma Xi, Tau Beta Pi, Phi Mu Epsilon, and the IEEE.

**JOHN J. THOMAS** attended Rutgers University. During 1943-45 he was associated with the Eastern Aircraft Division of the General Motors Corporation and in 1945-46 became a member of the research laboratory of Stokes Molded

Products. Mr. Thomas joined RCA Laboratories at Princeton, New Jersey in 1946 as a member of the Microwave Research Laboratory and has been engaged in research on power tubes, plasmas, color-TV kinescopes and negative effective mass in germanium. In 1959 he was appointed a Technical Staff Associate. He is the co-author of three technical papers and holds a U.S. patent on a Microwave Modulator. He is a member of the IEEE, the IEEE Groups on Electron Devices, Microwave Theory and Techniques, and a member of the American Association for the Advancement of Science.

**W. A. Hicinbothem, Jr.**



**Dr. R. D. Larrabee**



**J. J. Thomas**



of a solid, since this also involves devices of extremely small dimensions. In addition, these devices have lead wires which produce inductive limitations at high frequencies. The tunnel diode is an example of a device in which the fundamental mechanism is sufficiently fast for submillimeter wave use, but the limitations of the geometrical size and lead inductance severely limit its high frequency capability<sup>7</sup>. The use of homogeneous solid materials not only simplifies the fabrication problems, but also is very adaptable to the distributive nature of millimeter-waveguide components. The solid-state maser has actually been operated at millimeter wavelengths<sup>2</sup>.

One can consider the electrons and holes in an intrinsic semiconductor to be a plasma, analogous to the electrons and ions in a gaseous discharge<sup>3</sup>. (Ref. 3 provides an excellent introduction to the concept of solid-state plasmas and illustrates the value of this concept in discussing experiments of wave propagation in metals and semimetals.) Such solid-state plasmas support waves and exhibit instabilities that have potential use in the generation of RF power<sup>4</sup>. Since there is a large range of plasma densities available in semiconductors and semimetals, oscillations in the vicinity of the plasma frequency can be made to fall in the millimeter and submillimeter wavelength range. These considerations have motivated theoretical studies of plasma instabilities (i.e., modes of plasma oscillation) in solids. Some of these effects have been observed in experiments with semiconductor and/or semimetal plasmas. (Reference 4 has an excellent

summary of these instabilities and their experimental observations as well as an extensive list of references to the original work.)

There are only two cases in which microwave emission has been observed from a homogeneous semiconductor. In the first case<sup>5</sup>, called the *Gunn effect*, the mechanism of emission apparently does not involve the usual plasma-like properties of semiconductors and the frequency is determined by the sample size. To date, this frequency has been limited to the lower portion of the microwave spectrum. This paper will discuss the second case<sup>6</sup>, in which microwave emission from a semiconductor plasma has been observed at frequencies as high as 44 Gc/s.

#### OBSERVATIONS OF MICROWAVE EMISSION FROM A SOLID-STATE PLASMA

All generators of microwave power can be considered as energy transducers that convert some form of applied energy to useful microwave output. For example, in the microwave maser, the energy is supplied by a local microwave oscillator and the maser converts this to an amplified version of the input microwave signal. In the present case, this energy is supplied in the form of an applied uniform DC electric field, as illustrated in Fig. 1. This electric field produces a drifting motion of the electrons and holes comprising the semiconductor plasma (i.e., causes a current to flow). This drifting motion of the carriers excites instabilities (or oscillations) in the solid-state plasma<sup>7</sup>.

While there are many semiconductor materials which could be selected for use in experiments involving field-driven plasma oscillations, it is desirable to select a material in which the carriers acquire a high drift velocity at reasonable electric fields. The III-V compound, indium antimonide, best fulfills this requirement. At the temperature of liquid nitrogen ( $-321^{\circ}\text{F}$ ) and at an electric field of  $400\text{ V/cm}$ , the electrons in indium antimonide have a drift velocity  $1/100$  of the vacuum velocity of light. Therefore, experiments were conducted to look for microwave emission from solid-state plasmas employing homogeneous, bar-shaped, single-crystal samples of indium antimonide, as shown in Fig. 1.

When electrons in indium antimonide move rapidly, they are capable of exciting electrons from the valence band to the conduction band and thus create new electron-hole pairs. This process is analogous to collision ionization in a gaseous discharge in which electron-ion pairs are generated. Such ionization establishes and maintains the semiconductor plasma of electrons and holes. Since the resulting high density of drifting carriers represents a large current, samples are usually pulsed to avoid overheating the indium antimonide.

The bar-shaped sample of Fig. 1 was mounted as a centered inductive post in a dominant mode waveguide, as illustrated in Fig. 2. The open end of this waveguide was connected to a microwave receiver that was used as a frequency selective detector of emitted microwave radiation. Provision was made for applying a uniform DC magnetic field to the

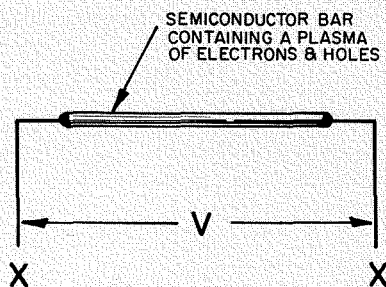
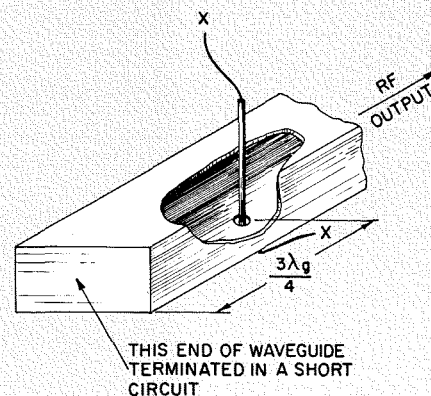


Fig. 1—A bar-shaped sample of semiconductor material with contacts and lead wires for applying an external electric field.

Fig. 2—The sample of Fig. 1 mounted as a centered inductive post in a dominant mode waveguide. The holes in the waveguide are coated with an electrically insulating epoxy resin to provide capacitive coupling between the sample and waveguide at microwave frequencies.



sample as illustrated in Fig. 3. The initial experiments were performed at 15 Gc/s (wavelength = 2 cm).

Fig. 4 shows some typical results of the pulse of current through the sample and the resulting "burst" of microwave emission as a function of time. Notice that the sample current is not constant, but has an oscillatory component riding on top of the pulse. Our experiments revealed that these current oscillations are related to, but not necessarily required for, the microwave emission.

A magnetic field in excess of about 3 kG is required in order to observe microwave emission. However, the orientation of this magnetic field relative to the direction of current flow in the sample is not critical. The microwave energy emitted from the indium antimonide sample covers a broad-band spectrum extending down to at least 3 Gc/s and up to at least 44 Gc/s (see Fig. 5). The integrated power over this frequency range is approximately 1 mW. Other characteristics of the microwave emission from indium antimonide suggest that the inductive post is generating a microwave electric field along its length and that it couples to the dominant waveguide mode by introducing a potential difference between the top and bottom surfaces of the waveguide.

It is reasonable to assume that the plasma oscillation within the semiconductor propagates with a phase velocity approximately equal to the drift velocity of the electron<sup>9</sup>. If this is so, the indium antimonide sample, used in the present experiment, would be about 100 half-wavelengths long. If some means could

be found to make the microwave electric field in alternate half-wavelength portions of the sample add instead of subtract, the microwave potential difference over the entire sample could be increased by a factor of 100. The power output integrated over the frequency range 3 to 44 Gc/s would thus be increased by a factor of 10,000. However, it is not yet clear how to couple this available energy most efficiently to a waveguide or to free space. If an efficient coupler were available one could couple the solid to a resonant cavity and possibly achieve monochromatic operation with power levels greater than one watt.

Attempts have been made to detect microwave radiation from indium antimonide at frequencies above 44 Gc/s. Simple experiments at 70 Gc/s and detailed experiments at 100 Gc/s have failed to reveal any radiation. However, the detector used in these high-frequency experiments was not sensitive enough to measure the power levels actually observed at 44 Gc/s.

#### CONCLUSIONS

Experiments<sup>6,10</sup> have shown that one can use homogeneous solid-state plasmas for the generation of microwave power, but that there are problems of coupling and of attaining monochromatic operation to be solved. The microwave emission from indium antimonide does not seem to have properties attributable to the well-known solid-state instabilities<sup>4</sup> (i.e., the oscillator, the two-stream instability, or helicons), but appears to be correlated with the properties of drifted electron-

hole plasmas currently under investigation by Steele and Vural<sup>9</sup>.

It is instructive to observe that gas plasmas can be easily operated as noise generators and also, under appropriate conditions, as monochromatic coherent oscillators and amplifiers<sup>11</sup>. There is every reason to suspect the same general behavior of solid-state plasmas. The first step toward a useful millimeter solid-state plasma generator has thus been taken.

#### ACKNOWLEDGEMENTS

The authors wish to express their appreciation to their colleagues at RCA Laboratories for many helpful discussions in the course of the above work and to M. C. Steele in particular for his advice on the design and interpretation of these experiments.

#### BIBLIOGRAPHY

1. F. Sterzer and D. E. Nelson (RCA-ECD, Pr.), *Proc. of IRE* 49, 744 (1961).
2. S. Foner, L. R. Momo, A. Mayer, *Phys. Rev. Letters* 3, 36 (1959).
3. R. Bowers (RCA Labs, Pr.), *Scientific American* 209, 46 (1963).
4. R. Bowers and M. C. Steele (RCA Labs, Pr.), *Proc. of IEEE* 52, 1105 (1964).
5. J. B. Gunn, *IBM Jour. of Research and Development* 8, 141 (1964).
6. R. D. Larrabee and W. A. Hicinbotham, Jr. (RCA Labs, Pr.), *Proceedings of International Conf. on the Physics of Semiconductors, Symposium on Plasma Effects in Solids*, Paris, France (1964), (Dunod, Paris, 1965).
7. D. Pines and J. R. Schrieffer, *Phys. Rev.* 124, 1387 (1961).
8. M. Glicksman and W. A. Hicinbotham, Jr. (RCA Labs, Pr.), *Phys. Rev.* 129, 1572 (1963).
9. M. C. Steele and B. Vural (RCA Labs, Pr.), "Instabilities in Solid-State Plasmas," *RCA ENGINEER*, this issue.
10. Kimio Suzuki, *Japanese Jour. of Applied Physics* 4, 42 (1965).
11. G. A. Swartz (RCA Labs, Pr.), "Electron Beam Plasma Amplifiers—A Future in Millimeter-Wave Amplification," *RCA ENGINEER* 10-4, 33 (Dec. 1964-Jan. 1965).

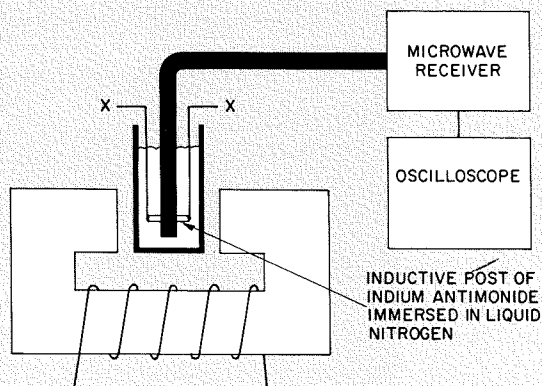


Fig. 3—Schematic diagram of the inductive post of Fig. 2, mounted in waveguide and placed in a DC magnetic field. The sample is immersed in liquid nitrogen. Microwave emission from the sample is coupled to the microwave receiver whose output is viewed on the oscilloscope.

Fig. 4—Oscillogram traces of the indium antimonide current pulse and the resulting "burst" of microwave emission. The DC magnetic field was parallel to the direction of current flow. The time scale is 0.2  $\mu$ s per major division (left to right), the temperature was 77°K and the microwave receiver was tuned to 15 Gc/s.

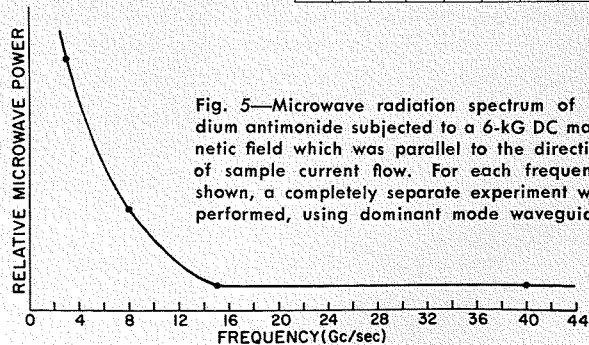
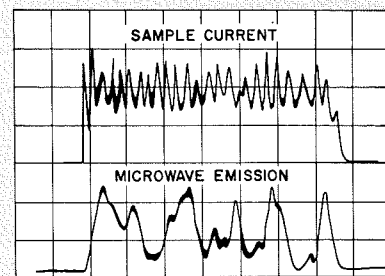


Fig. 5—Microwave radiation spectrum of indium antimonide subjected to a 6-kG DC magnetic field which was parallel to the direction of sample current flow. For each frequency shown, a completely separate experiment was performed, using dominant mode waveguide.

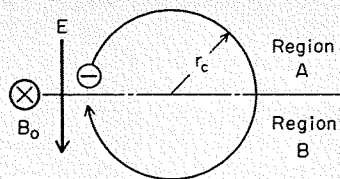


Fig. 1—Electron cyclotron motion.

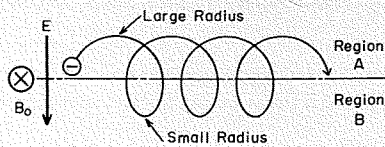


Fig. 2—Electron drifting motion.

## PROPAGATION IN SOLID-STATE-PLASMA WAVEGUIDES Nonreciprocal Devices

When a magnetic field is applied to a material containing a plasma, which had its surfaces coated with metal, the propagation properties of such solid state plasma waveguides become highly nonreciprocal. They show promise for use in miniature microwave circuits. For example, an isolator has been constructed from indium antimonide of dimensions 0.8 x 8 x 1 mm which gives 13 dB isolation at 24 Gc/s. Many other passive devices (phase shifters, couplers, circulators, switches, modulators) should be possible using these properties.

**Dr. R. HIROTA and M. TODA**  
*Laboratories RCA, Inc., Tokyo, Japan*

NONRECIPROCAL microwave circuits involving a tensor permeability were considered by Hogan<sup>1</sup> in 1952 and many examples (such as isolators, circulators, modulators, switches, and phase shifters) have been developed. A gaseous plasma waveguide<sup>2</sup> displays similar nonreciprocal properties, because of the plasma tensor permittivity in a magnetic field. The Faraday rotation and different

*Final manuscript received July 19, 1963.*

DR. RYOGO HIROTA received the BS and the MS degrees in Physics from Kyushu University in 1954 and 1956, respectively. From 1957 to 1961 he attended Northwestern University as a Fulbright exchange student and received the PhD in Physics in 1961. After a short period as a post-doctoral fellow at the Research Institute for Fundamental

losses for right-hand-polarized and oppositely-polarized waves lead to characteristics essentially similar to those of ferrites.

The *TE* surface wave<sup>3,4</sup> described here is a new type of electromagnetic wave which propagates only along one waveguide wall, determined by the propagation and external magnetic field directions. Since the theoretical upper frequency limit of the *TE* surface wave is

Physics, Kyoto University, he joined Laboratories RCA, Inc., Tokyo in 1962. His major interest is in the theories of plasma instability, transport phenomena, and propagation of waves in plasmas.

MINORU TODA received his B.Eng. degree in electrical engineering from Shizuoka University in 1960. After graduating, he joined the Department of Electronics at his Alma Mater, where he worked on millimeter wave devices. In 1962, he became a member of the technical staff of Laboratories RCA, Inc., Tokyo, where he has done research in microwave measurement, propagation and radiation in solid state plasmas. He received an RCA Achievement Award for 1963 for outstanding research in semiconductor plasma studies. He is a member of the Physical Society of Japan and the Institute of Electrical Communication Engineers of Japan.

determined by the cyclotron frequency, which is larger than 1,000 Gc/s in the experiment described below, the *TE* surface wave opens the possibility of nonreciprocal devices in the millimeter and submillimeter wavelength region.

### MOTION OF ELECTRON IN CROSSED ELECTRIC AND MAGNETIC FIELDS

In order to understand the physics of wave propagation in a plasma, let us begin with a review of electron motion in crossed electric and magnetic fields.

It is well known that an electron in an external magnetic field  $B_0$  rotates around a center with its initial velocity  $v_i$  (see Fig. 1). The cyclotron radius  $r_c$  of the rotation is determined by equating the Lorentz force acting on the electron  $ev_i B_0$  to the centrifugal force  $mv_i^2/r_c$  (in MKS units)

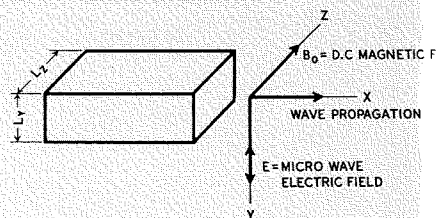
$$ev_i B_0 = \frac{mv_i^2}{r_c}$$

$$r_c = \frac{m}{eB_0} v_i \equiv \frac{v_i}{\omega_c} \quad (1)$$

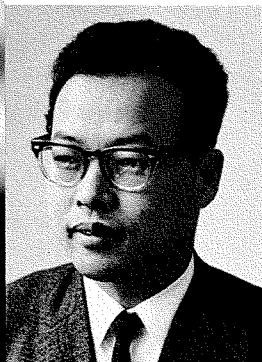
where  $m$  is the electron mass,  $e$  is the electron charge, and  $\omega_c$  is the cyclotron frequency.

Suppose that a constant electric field  $E$  with a direction perpendicular to that of  $B_0$  is applied to the electron. The electron will be decelerated or accelerated by the electric field according to whether its velocity is parallel or antiparallel to the electric field. Then (referring to Fig. 1) the velocity of the electron when it moves in the upper half circle (region *A*) becomes greater than that of the electron when it is in the lower half circle (region *B*). According to Eq. 1, the cyclotron radius of the electron in region *A* becomes greater than that of the electron in region *B*. This difference of the cyclotron radius creates a new component to the motion of the electron (see Fig. 2).

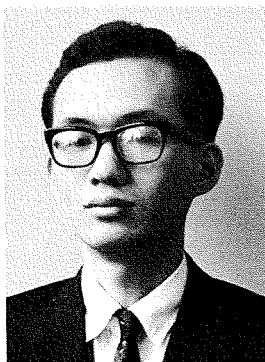
Fig. 3—Geometry for wave propagation studies.



Dr. R. Hirota



M. Toda



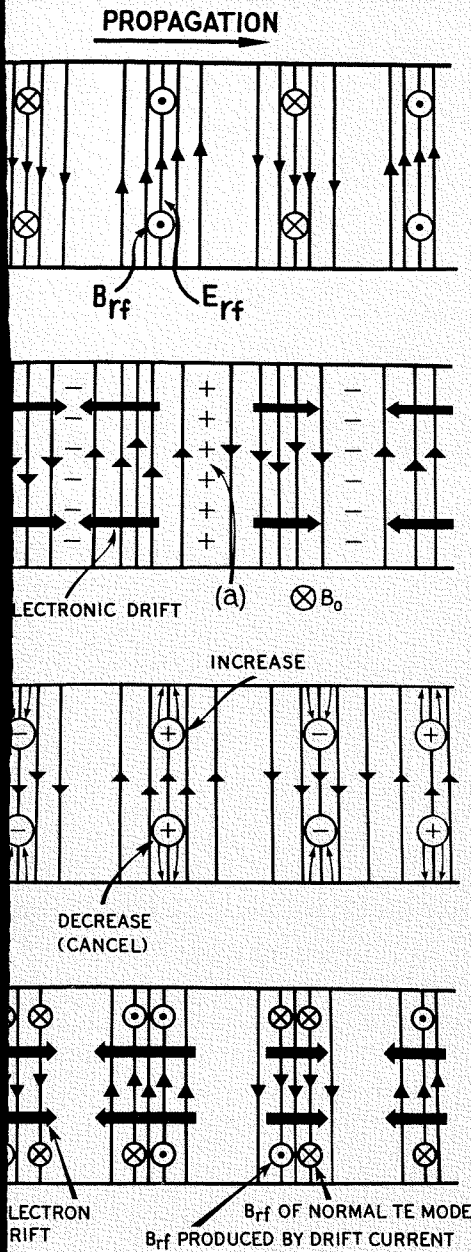


Fig. 4—Mechanism of TE surface wave formation.

From Fig. 2 it is easily understood that the direction of electron drift is perpendicular to the electric and magnetic fields. This is the so-called  $(E \times B_0)/B_0^2$  drift of the electron. Current produced by this drifting motion of electrons plays an important role in the TE surface wave propagation (to be described subsequently). Even when the electric field is varying with the angular frequency  $\omega$  the constant field approximation used above is good as long as  $\omega \ll \omega_c$ . We note that the electron cyclotron frequency  $\omega_c$  in indium antimonide (InSb) is about 1,000 Gc/s in a magnetic field of 0.5 weber/m<sup>2</sup>, because of the small effective mass of the electron. In the following, we shall re-

strict our discussion to the waves whose frequency is much less than the cyclotron frequency.

### TE SURFACE WAVE IN A TRANSVERSE MAGNETIC FIELD

In this section we shall describe a physical picture of the TE surface wave<sup>3,4</sup> which propagates along one waveguide wall determined by the direction of the propagation and the magnetic field. (See Figs. 3, 4.)

Let us start with a TE wave in the usual waveguide. The RF electric and magnetic field distributions are shown in Fig. 4i. Now we assume an electron-ion plasma and an external strong DC magnetic field in the Z-direction.

Then, as was discussed in the previous section, these electrons drift along the X-direction, which is perpendicular to the RF electric field and the DC magnetic field. This electron motion accumulates space charge in the region A (see Fig. 4ii). However, the space charge density becomes a maximum where the electric field is a maximum, because the phase of the space charge lags by  $\pi/2$  compared to that of the electric field, due to the time delay in the charge accumulation. This space charge produces an additional electric field pointed to the metal wall, which will add to the ordinary RF electric field at the upper side wall, and cancel at the lower side wall, as shown in Fig. 4iii. On the other hand, the magnetic field distribution produced by the current associated with the electron drift adds to the ordinary RF magnetic field at the upper side wall, but cancels at the lower side wall (see Fig. 4iv). Thus, the resultant magnetic field distribution is in the same form as the electric field so that all the components of the field are maximum at the metal wall and exponentially damped in the transverse direction (see Fig. 5). The damping factor  $\gamma_y$  in the Y direction is

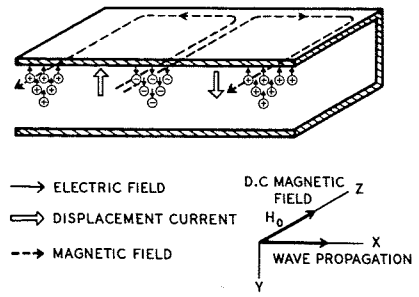


Fig. 5—Mode pattern of TE surface wave in the waveguide.

determined from the drift current  $j_x$ :

$$j_x = -\left(\frac{neE_y}{B_0}\right) = (\nabla \times H)_x$$

$$= \frac{\partial H_z}{\partial y}$$

$$= \gamma_y H_z, \text{ when } k_z = 0 \quad (2)$$

$$\gamma_y = -\left(\frac{ne}{B_0}\right)\left(\frac{E_y}{H_z}\right)$$

$$\frac{E_y}{H_z} = \sqrt{\frac{\mu_0}{\epsilon_0 \epsilon_{int} \epsilon_{ext}}} \quad (3)$$

The drift current does not directly affect the phase velocity of the wave. The dispersion relation is the same as for the ordinary TE wave:

$$\frac{\omega^2}{c^2} = k_x^2 + k_z^2 - \kappa^2 \quad (4)$$

where  $\kappa$  is the attenuation constant. We note that  $\kappa$  is a strong function of the external magnetic field so that the phase velocity changes as the magnetic field changes.

As is seen from the above discussion the TE surface wave is propagating along one surface determined by  $\vec{P} \times \vec{B}_0$ , where  $\vec{P}$  is the Poynting vector and  $\vec{B}_0$  is the external magnetic field. This property lends itself to utilization in passive

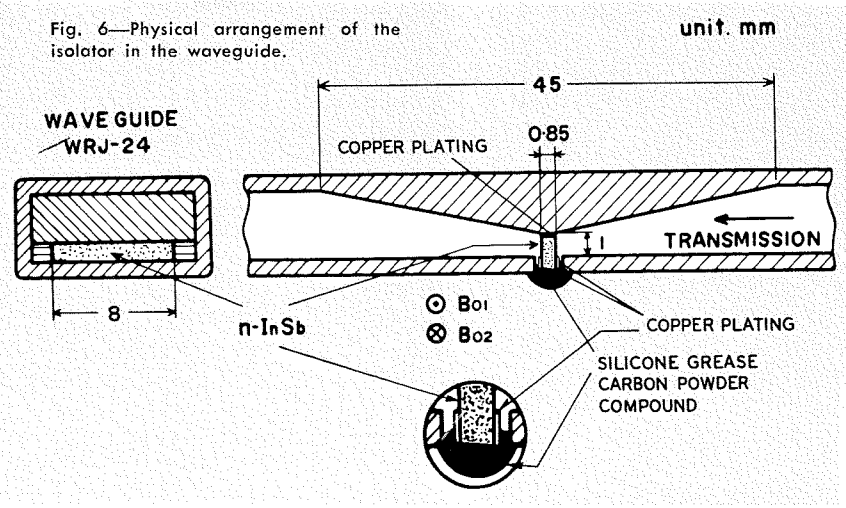


Fig. 6—Physical arrangement of the isolator in the waveguide.

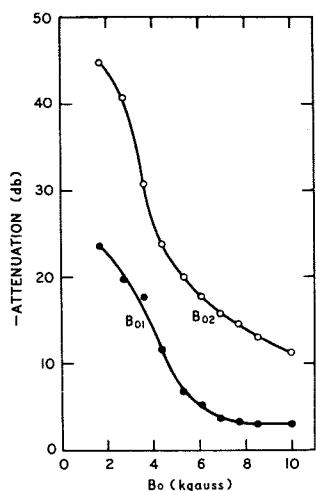


Fig. 7—Measured attenuation of microwave fields as a function of the magnetic field for forward ( $B_{01}$ ) and reversed ( $B_{02}$ ) directions of field.

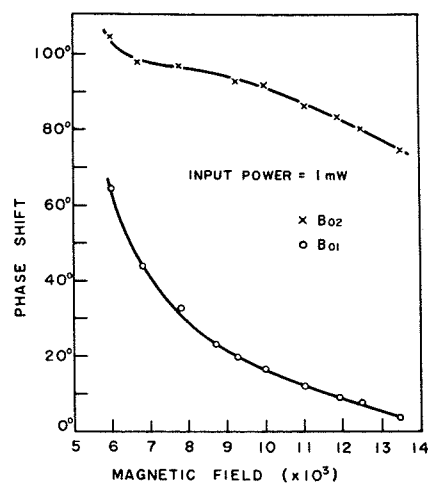


Fig. 9—Phase shift due to the change of the guide wavelength in the sample waveguide of Fig. 8, as a function of magnetic field intensity.

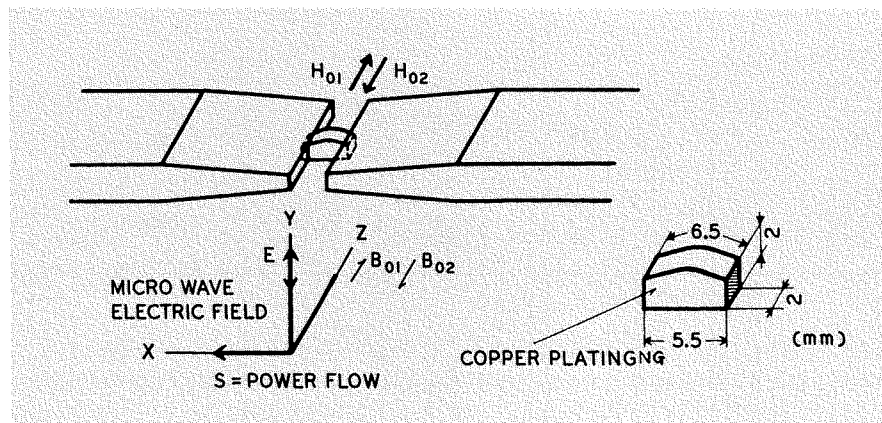


Fig. 8—Asymmetrical sample waveguide and main waveguide with dimensions.

microwave devices such as isolators, circulators, etc. It should be noted that the frequency limitation of this wave is determined by the cyclotron frequency  $\omega_c$  (shown in Eq. 1 and accompanying text) which is much higher than that of conventional devices using ferrites. In the next section we shall describe applications of this wave to an isolator and a phase shifter.

#### APPLICATIONS TO AN ISOLATOR AND A PHASE SHIFTER

##### Isolator

We have constructed an isolator<sup>5</sup> at 24 Gc/s with a forward loss of 3 dB and a backward loss of 13 dB in a magnetic field of 7 kG at 77°K.

A plate of  $n$ -InSb single crystal ( $n_0 = 8 \times 10^{18} \text{ m}^{-3}$ ) was mounted in the tapered waveguide as shown in Fig. 6. The surface of  $n$ -InSb was ground by #600 silicon carbide. The rough surface was covered with liquid polystyrene leaving bare the parts to be electroplated with copper. In order to suppress the leakage of microwave through possible small

gaps, a gold powder-silicone grease compound was used to fill the gaps. Any kind of metal powder could be used; gold powder is advantageous because it does not oxidize. The tapered waveguide was used to obtain better matching conditions and to reduce the volume of expensive  $n$ -InSb crystal. As an absorber of backward transmission, a silicone grease-carbon powder compound is used as shown in Fig. 6.

The attenuation of the transmitted microwave power, when the magnetic field direction is  $B_{01}$ , as indicated by the lower curve in Fig. 7. In this case the microwave fields are transmitted along the upper side of the crystal, where copper plating is present. The upper curve in Fig. 7 shows the attenuation for the magnetic field in the  $B_{02}$  direction, when the transmission is along the lower surface, i.e., along the vertical copper plating and the absorbing carbon powder. If the propagation direction is reversed, the microwave power should be absorbed for the magnetic field direction  $B_{01}$ , because of the symmetry of the sys-

tem. Thus, this device has the properties of an isolator.

##### Phase Shifter<sup>3</sup>

A sample with surfaces coated by copper plating but with asymmetrical dimensions was mounted as shown in Fig. 8. The phase of the signal transmitted through the sample was compared to that of a reference signal. When the magnetic field is in the  $B_{01}$  direction, the phase shift as a function of field intensity is shown by the lower curve in Fig. 9. For the field in the  $B_{02}$  direction, the phase shift is given by the upper curve.

The difference comes from the fact that the microwave is propagating along the upper side (longer path) for  $B_{02}$ , and along the lower side (shorter path) for  $B_{01}$ . The magnetic field dependence of the phase shift is explained by the dispersion relation, Eq. 4, which shows that the phase velocity is a function of the attenuation constant  $\kappa$ . The attenuation constant decreases with increasing magnetic field due to a strong magnetoresistance effect.

#### OTHER TYPES OF WAVES IN SOLID STATE PLASMA WAVEGUIDES

It is predicted<sup>6</sup> theoretically that the  $TE$  surface wave can propagate in a circular plasma waveguide in a longitudinal magnetic field and may also be used to construct an isolator and a mode coupler.

Gremillet<sup>7</sup> has constructed an isolator at frequencies up to 800 Mc/s using helicon-wave propagation in a longitudinal magnetic field. Recent theoretical investigation<sup>8</sup> shows that a wave which propagates through an inhomogeneous solid state plasma waveguide in a transverse magnetic field may also be used to construct an isolator in the VHF band operating at room temperature.

#### BIBLIOGRAPHY

- C. L. Hogan, "The Ferromagnetic Faraday Effect at Microwave Frequencies and its Applications," *Rev. Mod. Phys.*, Vol. 25, January 1953, p. 253.
- L. Goldstein, "Non-reciprocal Electromagnetic Wave Propagation in Ionized Gaseous Media," *IRE Trans. on Microwave Theory and Techniques*, Vol. MTT-6, January 1958, p. 19.
- M. Toda (Labs. RCA, Tokyo), "Propagation in a Solid State Plasma Waveguide in a Transverse Magnetic Field," *J. Phys. Soc. Japan*, Vol. 19, July 1964, p. 1126.
- R. Hirota (Labs. RCA, Tokyo), "Theory of a Solid State Plasma Waveguide in a Transverse Magnetic Field," *J. Phys. Soc. Japan*, Vol. 19, July 1964, p. 1130.
- M. Toda (Labs. RCA, Tokyo), "A New Isolator Using a Solid State Plasma Waveguide," *IEEE Trans. on Microwave Theory and Tech.*, MTT-13, January 1965.
- R. Hirota (Labs. RCA, Tokyo), "Theory of a Solid State Plasma Waveguide in a Longitudinal Magnetic Field," *J. Phys. Soc. Japan*, Vol. 19, December 1964, p. 2271.
- J. Gremillet, *Propagation des Ondes Métriques et Décamétriques dans les Semi-conducteurs en Présence d'une Induction Magnétique Continue; Effect 'Hélicon'*, Thesis, Faculty of Sciences, University of Paris, March 1964.
- R. Hirota (Labs. RCA, Tokyo), "Unidirectional Wave Propagation in an Inhomogeneous Solid State Plasma Waveguide," (submitted to *J. Phys. Soc. Japan*).

# SOLID-STATE-PLASMA DELAY LINES

When a magnetic field is applied parallel to the current in a bar of germanium at room temperature, waves of helical form (rotating inside the germanium) propagate and can in fact be amplified in the material. Since the wave propagates at about the velocity of the slower carriers, such a bar may be used as a compact delay line. Measurements have shown that the delay is relatively independent of frequency over the range of operation tested (30 to 200 kc/s). The frequencies usable depend on the dimensions, and devices of different material and different dimensions could be made to serve as delay lines covering the range from the audio up into the shortwave band.

Y. KUNIYA and Dr. M. GLICKSMAN

Laboratories RCA, Inc.

Tokyo, Japan

ONE of the prominent characteristics of electron-hole plasmas in solids is their strong coupling to electromagnetic waves, whether this involves merely propagation or also includes possible amplification. An early example of this behavior is the *oscillistor*<sup>1-3</sup>—a bar of semiconductor which was sent into large amplitude oscillation (with up to 70% of the DC power in the oscillations) by the application of a magnetic field and a current containing sufficient injected density of carriers. The behavior has been explained<sup>4</sup> in terms of an instability of the plasma to a rotating helical motion of the current, when current and

Final manuscript received July 15, 1963.

DR. MAURICE GLICKSMAN studied Engineering Physics at Queen's University, Kingston, Canada, during 1946-1949. He received his SM and PhD in Physics from the University of Chicago in 1952 and 1954, respectively. In 1949 and 1950 he worked in the Nuclear Physics section at the Atomic Energy Project, Chalk River, Canada. During 1953-1954 he served as Instructor in the Physics Department, Roosevelt University, Chicago, and in 1954 was a Research Associate in the Institute for Nuclear Studies, University of Chicago. He joined RCA Laboratories as a member of the technical staff in December 1954 and is presently in charge of a group doing plasma research in Laboratories RCA, Inc., Tokyo, Japan. In addition to earlier work in low-energy nuclear physics and the interactions of elementary particles, his interests have included the measurement of electrical and galvanomagnetic properties of semiconductors and semiconductor alloys, analysis of the problem of ballistic missile

magnetic field are parallel and sufficiently large.

This helical mode propagates with a velocity approximately equal to the ambipolar velocity

$$V_a = \frac{\mu_n \mu_p (n - p)}{\mu_n n + \mu_p p} E \quad (1)$$

where  $\mu_n$  and  $\mu_p$  are the mobilities of electrons and holes, respectively, the densities  $n$  and  $p$ . Its properties have been studied in some detail for the semiconductor germanium<sup>5</sup>. Various conditions of the semiconductor may be used: depending on the magnitude of the applied parallel magnetic field and the plasma density, the helical wave may be

defense, the properties of "hot" carriers in semiconductors, the interaction of microwaves with gaseous plasmas, and the properties of electron-hole plasmas in solids. He has received two RCA Achievement Awards for outstanding work in research. Dr. Glicksman is a member of Phi Beta Kappa, Sigma Xi and the American Physical Society.

YASUO KUNIYA graduated from the Tokyo Institute of Technology in 1955 with a B.Eng., and in 1956 with a M.Eng. He worked at the Nippon Carbon Co. from 1956 to 1957, during which time he was concerned with experimental studies of impervious graphites for high temperature reactors. The following year, he joined the Japan Atomic Energy Research Institute as a visitor, specializing in the reaction between uranium and carbon. He joined Laboratories RCA, Inc., Tokyo in 1960. He is presently engaged in the growth of thin films of compound type semiconductors.

attenuated or amplified. In a series of experiments to be described here, the velocity of these waves has been measured as a function of frequency, in the region where the mode is not attenuated strongly, to test its non-dispersive character for possible use as a delay line.

## EXPERIMENT METHODS

The specimens were cut from a 30-ohm-cm, n-type Ge ingot and etched with CP-4 (Fig. 1). The dimensions are about 1 mm x 1 mm in cross section and 25 mm in length in the [111] direction.

To change the injected carrier density,  $p^+$  and  $n^+$  contacts were attached to one end of the specimen by the alloying of (In + 1/2% Ga) and (Sn + 4% Sb), respectively.

Different injection levels were obtained by varying the resistance in series with the  $p^+$  contact<sup>5</sup>. Excitation and detection of the wave propagating along the specimen and the measurements of the electric field were accomplished using four pairs of  $n^+$  probes made of 100- $\mu$ m gold wire, doped with 0.5% Sb. (Note:  $\mu$ m, or micrometer, is the new standard term for  $10^{-6}$  meters, formerly called a micron.) The probes were attached to the specimen by a discharge welding technique. The specimen was immersed in silicone oil to maintain constant surface conditions.

The circuit used for the measurements is shown in Fig. 2. The pulse current was applied by chopping the DC current from a constant voltage power supply with a mercury relay. The pulse width was about 3 ms. Measurements of the time delay were carried out by observing the difference in time between the beginning of the driving signal at the input probes ( $a$  and  $a'$  in Fig. 2) and the beginning of the detected signal at each pair of probes ( $c$ ,  $c'$  and  $d$ ,  $d'$ ). Measurements of the amplification were carried out by observing the amplitude of the detected signal at each pair of probes. Electric fields in the range of 37 to 59 V/cm were applied to the specimen in combination with magnetic fields of intensity 0, 5,000, 6,000 and 7,000 oersteds. Injection levels were varied to investigate the effect of changing carrier density on the time delay and amplification. Signals of frequency in the range 30 to 200 kc/s were applied to the specimen through a pair of input probes ( $a$ ,  $a'$  in Fig. 2). The electric fields and corresponding carrier densities are shown in Table I. All experiments were performed at room temperature below the threshold electric and magnetic fields which cause the instability known as the *oscillistor*<sup>2,3</sup>.



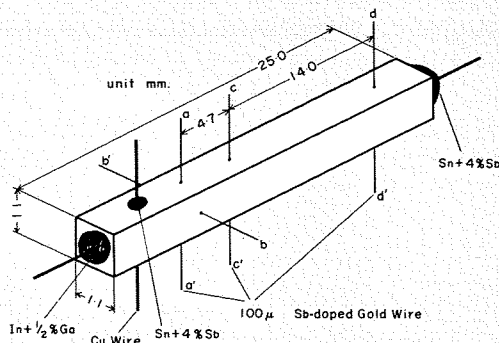


Fig. 1 — Simplified sketch of the specimen made from 30 ohm-cm n-type germanium.

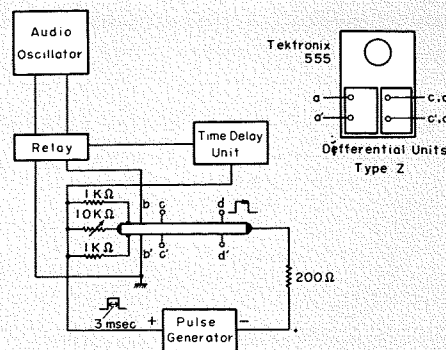


Fig. 2 — The circuit arrangement used.

### EXPERIMENT RESULTS AND DISCUSSION

The growth in amplitude with distance may be represented by the growth constant,  $k_i$ :

$$V = V_o \exp(k_i x) \quad (1)$$

where  $V_o$  and  $V$  are the amplitudes of the input and detected signals, respectively, and  $x$  is the distance between the measuring probes.

Fig. 3 shows a typical example of the dependence of the growth constant  $k_i$  on the frequency; these curves have the same qualitative dependence as those obtained by Hurwitz and McWhorter<sup>5</sup>. Fig. 4 shows waveforms of the input and detected signals, which illustrate that the detected signal is delayed from the input signal by 10.4  $\mu$ s at  $c, c'$  and 41.6  $\mu$ s at  $d, d'$ . The delay times do not depend on the frequency, but on the electric field and on the injection level.

Magnetic fields did not affect the delay time, except at large injection levels. Fig. 5 is an example of the relation between delay time and frequency for various magnetic fields. Table I summarizes electric fields, carrier densities, and average delay times.

When the signal travels from one end of the bar to the other with the group velocity  $v_g$  of the helical wave, the relation between the delay time  $t_d$  and  $v_g$  is:

$$v_g = \frac{x}{t_d} \quad (2)$$

The theory referred to earlier, which would lead to the conclusion that  $v_g = v_o$ , is based on a number of assumptions, some of which are not satisfied completely in our experiments. In par-

ticular, the theory of Hurwitz and McWhorter<sup>5</sup> assumes that the electron and hole densities are in thermal equilibrium; i.e., no injection from the end contacts. In our case this was not so, as can be seen from Table I, since  $n_o = 4.54 \times 10^{13} \text{ cm}^{-3}$  and  $p_o = 1.27 \times 10^{13} \text{ cm}^{-3}$  were the equilibrium concentrations.

If we set  $v_g = v_o$ , then:

$$v_o = A \frac{E^2}{j}$$

$$A \equiv e\mu_n\mu_p(n-p) \quad (3)$$

Here,  $j$  is the current density and  $A$  is a constant which depends only on the properties of the material.

An experimental test of this relationship can be made using the observed values of  $E, j$ , and  $t_d$ . Fig. 6 shows the measured relationship between  $A$  and the injected carrier density. Although there appears to be some dependence on the density at higher levels of injection, the curve flattens out as the injection decreases. Using the value of  $n-p$  deduced from Hall and conductivity measurements, along with the values  $\mu_n =$

$3,900 \text{ cm}^2 \cdot \text{V}^{-1} \cdot \text{s}^{-1}$  and  $\mu_p = 1,900 \text{ cm}^2 \cdot \text{V}^{-1} \cdot \text{s}^{-1}$ , we calculate that  $A = 39 \text{ C} \cdot \text{cm} \cdot \text{V}^{-2} \cdot \text{s}^{-2}$ , considerably lower than the measured values.

Thus, although the observed independence of wave velocity on magnetic field and on frequency is in agreement with theory, the absolute magnitudes of the velocity are somewhat higher than predicted. Since the theory used is a much simplified one, the exact expression being quite complex, the experimental test provides a welcome confirmation of the prediction that the delay characteristics will be independent of the magnetic field and frequency.

As can be seen from Fig. 3, the upper limit of frequency will be governed by the onset of strong attenuation. Theory predicts that amplification of the wave occurs for values of

$$E_{in} B_{in} = \left[ \frac{12}{\sqrt{2} a} \frac{kT}{e} \right] \quad (4)$$

$$\left[ \frac{(n\mu_n + p\mu_p)(n+p)}{np(\mu_n + \mu_p)^2} \right]$$

The frequency corresponding to this

TABLE II—Properties of Ge as a Function of Injection Level

Electric Field ( $E$ ) $\text{V} \cdot \text{cm}^{-1}$	Electron Density ( $n$ ) $10^{13} \text{ cm}^{-3}$	Hole Density ( $p$ ) $10^{13} \text{ cm}^{-3}$	Delay ( $t_d$ ) $\mu\text{s}$	Constant ( $A$ ) $\text{C} \cdot \text{cm} \cdot \text{V}^{-2} \cdot \text{s}^{-2}$	Injection Contacts
52.4	9.81	6.54	46.8	61.8	high
45.5	8.96	5.69	50.9	59.4	high
37.4	8.00	4.73	59.0	55.0	high
58.8	8.18	4.91	40.3	52.5	low
55.1	7.86	4.59	40.0	53.6	low
50.8	7.58	4.31	41.0	54.3	low
45.5	7.18	3.91	42.0	53.7	low
37.4	6.33	3.06	45.0	54.3	low

Fig. 3 — Growth constant as a function of frequency.

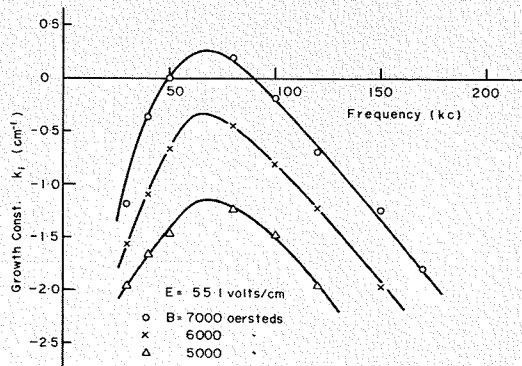
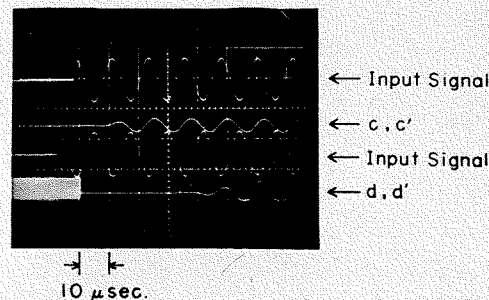


Fig. 4 — Typical examples of input and output signals. Input = 0.25 V/cm;  $c-c', d-d' = 0.1 \text{ V/cm}$ ;  $E = 45.5 \text{ V/cm}$ ;  $B = 6,000 \text{ Oe}$ ; frequency = 80 kc/s.



threshold (Eq. 4) is given approximately by:

$$f_{th} = \left( \frac{1}{\pi\sqrt{3}a} \right) \mu_a E_{th} \quad (5)$$

where the magnetic field is both low enough for  $\mu_{n,p}^2 B^2 \ll 1$ , and high enough for  $(n-p)/(n+p) \gg \mu_{n,p}^2 B^2$ ;  $a$  is the radius of the bar. All the quantities above are given in MKS units. For electric and magnetic fields higher than the threshold values, there will be a range of frequencies, above and below  $f_{th}$ , for which the waves will grow. The above equations have been verified by Hurwitz and McWhorter<sup>5</sup> for the noninjected case, with excellent agreement between theory and experiment. In the experiments reported here, there was some considerable injection, and the conditions stated above were not well satisfied. There is, however, fair agreement in thresholds, the values observed being somewhat higher than those calculated with Eq. 4.

#### DELAY LINES POSSIBLE

With the above measurements as a check, using the equations which have been verified, we can discuss the pos-

sible range of delays—in magnitude and in frequency—which are available with this new mode of wave propagation. For operation at room temperature, a material which has appreciable densities of both electrons and holes in equilibrium at room temperature is required. Germanium and other semiconductors of bandgaps smaller than or approximately equal to germanium can be used, e.g., gallium antimonide, indium arsenide, indium antimonide. Even doped semimetals may also be possible materials for use.

The frequency where there is small attenuation or gain is determined by the properties of the semiconductors, but much more directly by the size of the sample used. Table II shows this quite strongly with calculated thresholds for growth for germanium, indium arsenide, indium antimonide and bismuth, all slightly doped to provide  $n > p$ . For bars of the size used in our experiments, the frequency where growth occurs is in the kilocycle range. But when the effective radius of the sample is reduced to about 10  $\mu\text{m}$ , the frequency goes up into the FM-TV band, and if the radius is reduced a further factor of ten to around 1  $\mu\text{m}$  (films) the frequency of operation is at x-band. By simply changing the dimensions, we can produce a series of delay lines with very large delays—the delay time or wave speed only varies as the first power of the dimensions.

In Table II, the magnetic field has been assumed to be 5,000 gauss, but lower values may be used and the necessary higher electric fields calculated from the data in the table. For bismuth, although delays may be possible, the electric fields required are so large as to make it impractical to use.

#### CONCLUSIONS

The growth and time delay characteristics of the helical plasma density wave in a Ge bar have been investigated with parallel electric and magnetic fields under conditions of various injection levels. Qualitative agreement with the observations of Hurwitz and McWhorter<sup>5</sup> for the relation between growth constant and frequency were obtained. The time delay was observed to be linear with distance, of magnitude about 22  $\mu\text{s/cm}$ , and almost independent of frequency and magnetic field used in the range 30 to 200 kc/s.

It should then be possible to construct useful delay lines with low loss or some gain, covering frequencies in the audio range (effective radius 1 mm), FM-TV range (effective radius 10  $\mu\text{m}$ ) and microwave x-band (effective radius 1  $\mu\text{m}$ ). Typical parameters indicate that Ge, InAs, and InSb are likely materials.

#### ACKNOWLEDGEMENTS

The authors are grateful to K. Arikawa and K. Miyamaru for valuable technical assistance and to Dr. S. Tosima for many suggestions and discussions.

#### BIBLIOGRAPHY

1. Yu L. Ivanov and S. M. Ryvkin, "Occurrence of Current Oscillations in Specimens of Germanium Placed in an Electric Field and a Longitudinal Magnetic Field", *Sov. Phys.-Tech. Phys.* 3, 722 (1958).
2. R. D. Larrabee and M. C. Steele (RCA Labs, Princeton); "The Oscillistor—a New Type of Semiconductor Oscillator", *J. Appl. Phys.* 31, 1519 (1960).
3. R. D. Larrabee (RCA Labs, Princeton); "Conditions Existing at the Onset of Oscillistor Action", *J. Appl. Phys.* 34, 880 (1963).
4. M. Glicksman (RCA Labs, Princeton); "Instabilities of a Cylindrical Electron-Hole Plasma in a Magnetic Field", *Phys. Rev.* 124, 1655 (1961).
5. C. E. Hurwitz and A. L. McWhorter, "Growing Helical Density Waves in Semiconductor Plasmas", *Phys. Rev.* 134, A1033 (1964).

TABLE II—Possible Delay Line Materials and Designs at Room Temperature

Materials & Properties Assumed	Radius (a) $\mu\text{m}$	$E_{th} \cdot B_{th}$ $\text{V} \cdot \text{cm}^{-1} \cdot \text{G}$	Delay ( $v_g^{-1}$ ) ( $\mu\text{s/cm}$ )	Frequency ( $f_{th}$ )
<i>Germanium</i>				
$n=5 \times 10^{13} \text{ cm}^{-3}$	1,000	$8.1 \times 10^4$	190	10 kc/s
$p=3.8 \times 10^{13} \text{ cm}^{-3}$	10	$8.1 \times 10^6$	1.9	100 Mc/s
$\mu_n=3,900 \text{ cm}^2 \cdot \text{V} \cdot \text{s}$	1	$8.1 \times 10^7$	0.2	10 Gc/s
$\mu_p=1,900 \text{ cm}^2 \cdot \text{V} \cdot \text{s}$				
<i>Indium Arsenide</i>				
$n=2 \times 10^{15} \text{ cm}^{-3}$	1,000	$2.5 \times 10^4$	670	2.8 kc/s
$p=7 \times 10^{14} \text{ cm}^{-3}$	10	$2.5 \times 10^6$	6.7	28 Mc/s
$\mu_n=33,000 \text{ cm}^2 \cdot \text{V} \cdot \text{s}$				
$\mu_p=460 \text{ cm}^2 \cdot \text{V} \cdot \text{s}$				
<i>Indium Antimonide</i>				
$n=3 \times 10^{16} \text{ cm}^{-3}$	1,000	$1.1 \times 10^4$	900	2.0 kc/s
$p=1 \times 10^{16} \text{ cm}^{-3}$	10	$1.1 \times 10^6$	9	20 Mc/s
$\mu_n=78,000 \text{ cm}^2 \cdot \text{V} \cdot \text{s}$				
$\mu_p=750 \text{ cm}^2 \cdot \text{V} \cdot \text{s}$				
<i>Bismuth</i>				
$n=2 \times 10^{18} \text{ cm}^{-3}$	1,000	$1.6 \times 10^5$	—	—
$p=1 \times 10^{18} \text{ cm}^{-3}$	10	$1.6 \times 10^7$	—	—
$\mu_n=3,000 \text{ cm}^2 \cdot \text{V} \cdot \text{s}$				
$\mu_p=700 \text{ cm}^2 \cdot \text{V} \cdot \text{s}$				

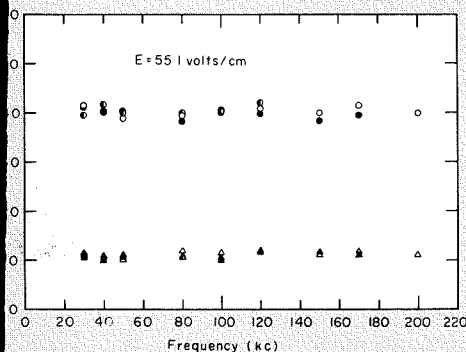


Fig. 5—Delay time as a function of frequency.

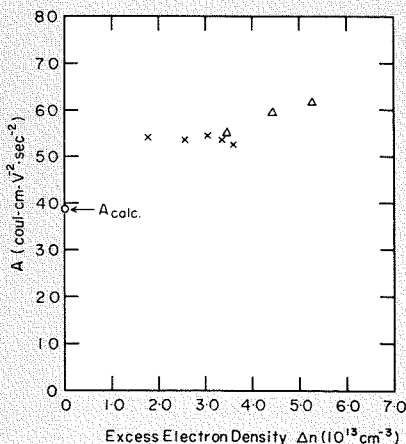


Fig. 6—Experimental and theoretical values of the constant A as a function of injection level.

# ELECTRIC PROPULSION FOR SPACECRAFT

To be practical, certain space missions require electric-propulsion engines. Deep-space-mission payload capabilities benefit from electric propulsion, since propellant weight savings relative to chemical propulsors exceed the weight penalties inflicted by extra electric-power-generation and conditioning equipment. Electric-propulsion systems are also more attractive than others, again because of reduced propellant weight, for long-term (over 1 year) orbit-corrective and attitude-control missions. In both types of missions, propulsor life expectancy is of vital importance; weight limitations are mitigated in orbit-corrective missions because of the small fractional weight of the propulsor. A laboratory-model electric-propulsion unit, developed at AED, uses electron cyclotron resonance to ionize a mercury plasma and to raise the electron temperature. Momentum is transferred to the ions in self-generated electric fields. The efficiencies, thrust levels, and life expectancies of this thruster satisfy orbit-corrective mission requirements.

**T. J. FAITH, JR. and DR. H. W. HENDEL**  
*Physical Research Group*  
*Astro-Electronics Division, DEP, Princeton, N. J.*

**E**LECTRIC propulsion<sup>1,2</sup> plants must be evaluated in relation to specific propulsive missions. The electron cyclotron resonance (ECR) plasma thruster developed at the Astro-Electronics Division can be related to such missions, and the more attractive applications identified.

## SPACE MISSIONS AND THRUSTORS

Electric propulsion missions can be divided into two representative groups:

- 1) Long duration missions reaching far into the solar system (e. g., of the MARINER type, with mission durations of approximately one year) could use electric thrusters operating continuously at high power levels (from approximately 10 to 1,000 kW) as the primary space propulsive device. The weight of the propulsion plant for such missions would be a significant fraction of the total vehicle weight.
- 2) Orbit-corrective missions of long duration (3 years), requiring 4 to 8 thruster units, could use electric thrusters operating at low power levels (50 to 500 watts). The weight of the propulsion plant for missions of this type would be a small fraction of the total vehicle weight. Station keeping for a synchronous satellite and altitude and attitude correction are typical uses for such thrusters.

Certain ambitious missions in the first category may become feasible only when the high exhaust velocities and resulting reduction of propellant weight achievable with electric propulsors are avail-

able for the mission duration required. Generally, primary electric propulsion will raise the payload fraction for such missions relative to chemical propulsion when the specific weight of the electric propulsion plant (power supply, power conditioner, and thruster) is less than 10 kilograms per kilowatt (kg/kW) of beam power. Current estimates indicate that electromagnetic-generator power-conversion systems with specific weights of 6.3 kg/kW could be developed using present technology. On the basis of advanced techniques, an overall electric propulsion plant specific weight of 1 kg/kW is predicted and should be approached to make primary electric propulsion attractive.

Thus, we see that the weight of the electric thruster itself must be less than 1 kg/kW to achieve a total specific weight in the desired range. Such a low thruster specific weight has already been realized in the NASA-Kaufmann ion engine although at present with insufficient life expectancy. Furthermore, thruster and power plant must have a high efficiency for a lighter power plant and a lower overall specific weight.

In light of this background, the following observations on the state of the art of electric thrusters for primary propulsion have been made recently<sup>3</sup>:

- 1) The NASA-Kaufmann electron bombardment ion engine (propulsive efficiency approximately 80%, thruster specific weight less than 1 kg/kW)

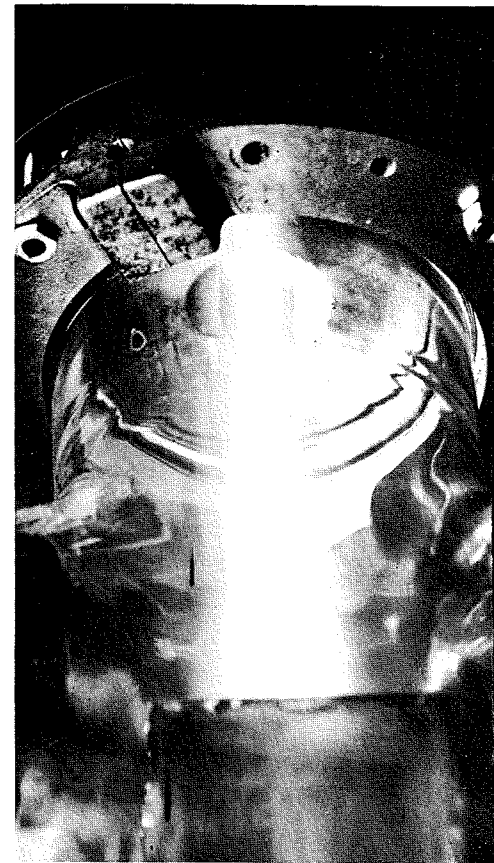


Fig. 1—Electron cyclotron resonance plasma thruster in operation.

could be used for most electric propulsion missions in its present form if the lifetime requirement can be met.

- 2) The problems of the porous-tungsten surface-ionization ion engines (EOS, Hughes),<sup>2,3</sup> unless modified by substantial improvements in technology, appear formidable enough to prevent the use of contact-ionization ion engines for primary propulsion.
- 3) There is no concrete evidence at present on which to base estimates of future performance of existing plasma thrusters relative to primary electric propulsion missions.

Power supplies compatible with ion engines discussed above and satisfying the weight restrictions have not been developed yet. In terms of mass, volume, and heat dissipation, power supply problems may turn out to be of extreme importance.

Missions using electric thrusters for primary propulsion are also remote in time (on the basis of power supply considerations, 5 to 10 years).

The first conclusion, therefore, is that development of the ECR plasma thruster toward primary propulsion missions is not advisable at this time. Ion engines could fill the thruster requirement (life expectancy?), but compatible power supplies will not be available for many years.

In contrast to primary propulsion, orbit corrective missions (as defined in

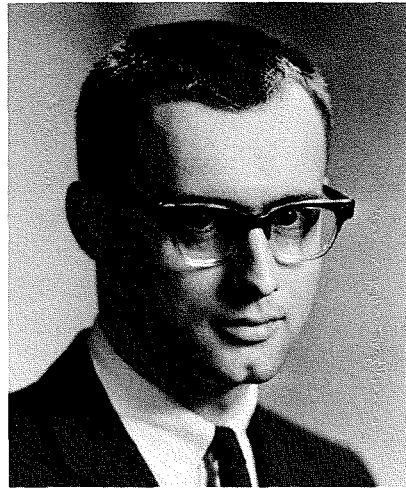


DR. HANS W. HENDEL received his BS in Physics in 1946, his MA in 1948, and his PhD (Dr. rer. nat.) in 1953, from the Technische Hochschule in Munich, Germany. During 1951, Dr. Hendel held a fellowship at M.I.T. Cambridge, and from 1953 to 1957, he developed optical systems at the Agfa Camera Works in Munich, Germany. From 1957 to 1961, as a research physicist at the USASRD, Fort Monmouth, New Jersey, he worked on plasma heating and confinement. As Leader of the Plasma Physics and Propulsion Group at RCA Astro-Electronics Division, Dr. Hendel is doing research on mechanisms applicable to space propulsion. During 1964, Dr. Hendel was in charge of Air Force sponsored work on electron cyclotron resonance plasma acceleration. Since 1963, his group has performed, among other projects, work on pumping methods for high

item (2) at the beginning of this paper) relax the weight and efficiency restrictions placed on electric propulsion plants, because of the negligible propulsion plant weight relative to satellite weight. The still longer mission duration (approximately 3 years) places an even higher premium on long life expectancy. A typical thrust for such missions is  $0.4 \times 10^{-3}$  pounds, requiring from 50 to 200 watts of primary electric power, depending on the type of electric propulsion used. Generally, up to eight thrusters connected to a single, common power and gas supply will be employed. On the basis of the low power requirement and the freedom from stringent weight limitations, presently available solar-cell panels can be used to generate the necessary power.

Such an orbit-corrective solar-electric propulsion system has been discussed recently<sup>4</sup> based on the application of so-called magnetic-expansion plasma thrusters. This thruster group, which includes the ECR thruster, converts non-directed electron energy into directed ion energy. It was determined that magnetic expansion thrusters fit orbit corrective mission requirements well, especially RF or microwave electron cyclotron resonance thrusters, because of their higher operating life expectancy.

The second conclusion, then, is that orbit corrective missions appear feasible now. The ECR thruster appears to be in a favorable position due to its long life



power gas lasers and on tuned laser spectroscopy. Dr. Faith is a member of the American Physical Society and the AIAA. He has authored 12 publications dealing with nuclear and plasma physics.

THOMAS J. FAITH, Jr., received a Bachelor of Engineering degree in 1959, and an MS in Physics in 1961, both from Stevens Institute of Technology. He was employed by the Stevens Physics Department as a Research Assistant from 1959 to 1961, where he worked in the fields of high energy physics and low temperature physics. Since June 1961, when he joined the technical staff of the Astro-Electronics Division, he has been engaged in experimental work on plasma accelerators. He is a member of the AIAA and has authored 4 publications in the field of plasma physics.

expectance, and should therefore be developed for such missions.

#### THE PLASMA THRUSTER

The ECR plasma thruster, developed at AED<sup>5-8</sup> and shown in Figs. 1 and 2, consists of three regions: 1) the *discharge region*, where the plasma is generated and heated; 2) the *region of self-generated electric field*, where plasma thermal energy is transferred into axially directed kinetic energy; and 3) the *plasma beam region*, where the fully accelerated neutral exhaust plasma emerges from the thruster.

In an earlier phase of the project, the discharge region was the interior of a rectangular s-band waveguide section. In the most recent work, a pyrex tube placed inside a cylindrical microwave cavity defined the discharge region. Microwave power was provided by a cw magnetron at 2.45 Gc/s. An axial dc magnetic field was provided by three solenoids positioned as shown in Fig. 2. Mercury vapor was supplied continuously by a heated mercury reservoir, the vapor flow rate being controlled by the reservoir temperature.

When microwave power is supplied to the discharge region, ambient electrons in the mercury vapor are heated by the microwave electric field, which supplies energy to the electrons, and the dc magnetic field, which, when set at the cyclotron resonance value (870 gauss for the applied frequency of 2.45 Gc/s), keeps

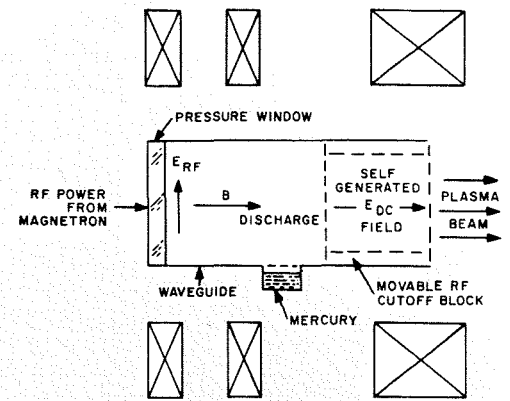


Fig. 2—Electron cyclotron resonance plasma thruster.

the electrons in phase with the electric field. The electron heating process consists of the initial electron acceleration, the acceleration mechanism being similar to that used in the cyclotron accelerator of nuclear physics, followed by thermalization through collisions. Electrons which achieve energies greater than the ionization potential (10.4 eV) can ionize ambient neutrals by inelastic collisions. The electrons liberated by the ionization process are heated, and an avalanche process is initiated, resulting finally in a steady-state plasma with equal production and loss rates. High electron temperatures are predicted by theory: the mean electron energy gain  $\bar{W}$  at cyclotron resonance between collisions in an RF field of amplitude  $E_0$  is given by:

$$\bar{W} = e^2 E_0^2 / 4m\nu^2, \quad (1)$$

where  $e$  and  $m$  are the electron charge and mass, respectively, and  $\nu$  is the electron collision frequency. When  $E_0$  is 10 V/cm, and  $\nu$  is  $5 \times 10^7$  collisions per second,  $\bar{W}$  is found to be 18 eV.

It should be noted that the electron cyclotron resonance condition is not sensitive to the charge particle density—as, for example, the plasma resonance condition is.

The applied axial magnetic field, in addition to keeping the electrons in phase with the microwave electric field, greatly reduces the radial electron diffusion rate. Electrons gyrating about magnetic field lines travel radially in steps equal to a Larmor radius  $r_L$  upon collision. When the Larmor radius is small compared to transverse vessel dimensions (as it is under this condition, since  $r_L$  is approximately 0.01 cm) the diffusion coefficient,  $D_{\perp}$ , perpendicular to the magnetic field, is given by:

$$D_{\perp} = \frac{D_{\parallel}}{1 + (\omega/\nu)^2} \quad (2)$$

where  $\omega/2\pi$  is the microwave driving frequency and  $D_{\parallel}$  is the diffusion coefficient parallel to the magnetic field

(equal to the field-free diffusion coefficient). In these experiments  $\omega/\nu$  was of the order of 1,000, so that  $D_{\perp}/D_{\parallel}$  was approximately  $10^{-6}$ .

The self-generated electric field region of the thruster is located to the right of the discharge as shown in Fig. 2. In this region the plasma ions are accelerated through an axial DC electric field generated by the energetic plasma electrons. The mechanism which sets up this field is explained as follows: The high-temperature electrons flow axially out of the discharge at a much faster rate than do the more massive low-temperature ions. However, to prevent charge buildup on the thruster, the electron and ion fluxes leaving the thruster must be equal. An electron retarding field, established at the discharge boundary, insures that this condition is satisfied by reflecting all but the high-energy electrons back into the discharge, simultaneously accelerating the ions and equalizing the electron and ion exhaust fluxes. The total potential drop<sup>9</sup> in the self-generated field can be readily calculated. An approximate relation has been derived<sup>9</sup> for the ion current density  $j_i$  at a discharge boundary:

$$j_i = \left(\frac{en}{2}\right) \left(\frac{kT_e}{M}\right)^{1/2} \quad (3)$$

where  $T_e$  is the electron temperature,  $n$  is the ion density,  $M$  is the ion mass, and  $k$  is Boltzmann's constant.

Neglecting radial flaring, ion current density in the exhaust plasma beam is assumed to be determined by Eq. 3. The electron current  $j_e$  penetrating to a point in the electric field region  $V$  volts below discharge potential (on the basis of a Maxwellian distribution), is given by:

$$j_e = \left(\frac{en}{2}\right) \left(\frac{2kT_e}{\pi m}\right)^{1/2} \left(\exp\left[\frac{-eV}{kT_e}\right]\right) \quad (4)$$

At the outer boundary of the self-generated electric field region where  $V = V_a$  (where  $V_a$  is the total ion accelerating potential), the electron and ion fluxes must be equal. Thus,  $j_i = j_e$ , and from Eqs. 3 and 4:

$$\frac{eV_a}{kT_e} = \frac{1}{2} \ln\left(\frac{2M}{\pi m}\right) \quad (5)$$

Substituting the mass value for Hg:

$$V_a \approx \frac{6kT_e}{e} \quad (6)$$

i.e., the potential difference available for

ion acceleration between the discharge region and the neutral beam is approximately six times the electron temperature in the discharge region.

The ion temperature in the discharge region is low since collisional momentum transfer from the electrons is small. In traversing the potential fall towards the beam region, ions are accelerated to an energy,  $eV_a$ , and merge with those electrons which entered the potential fall region with axial kinetic energy greater than  $eV_a$  to form the neutral plasma exhaust beam. All electrons which enter the potential fall region with axial kinetic energies less than  $eV_a$  are reflected back into the interaction region. At the boundary between discharge and self-generated electric field regions the electron current streaming toward the beam is almost three orders of magnitude higher than the ion current, as is seen from a comparison of Eqs. 3 and 4 with  $V=0$ . This high ratio of electron to ion current is necessary also for conservation of momentum.

In the direction opposite to the accelerated beam, the electron pressure reacts with the radial magnetic field component and with axial sheath (electric

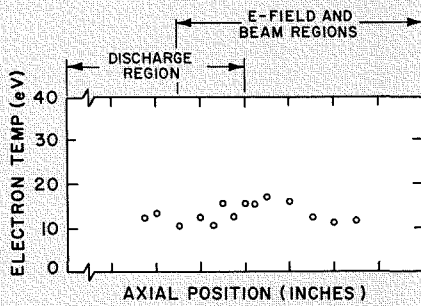


Fig. 3—Axial electron temperature distribution.

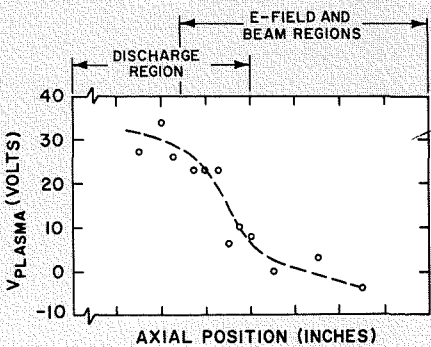


Fig. 4—Axial plasma potential distribution.

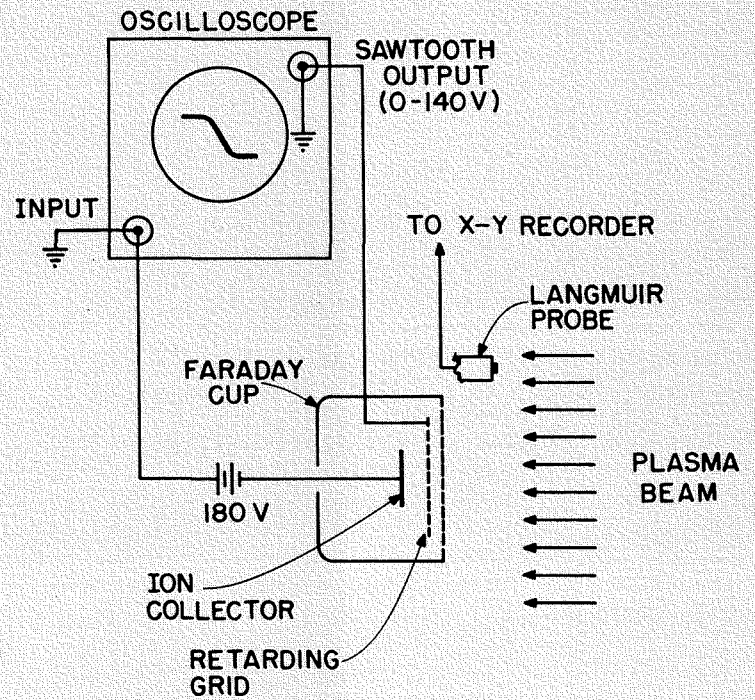


Fig. 5—Ion-energy analyzer.

fields to transfer the thrust to the rocket frame.

### EXPERIMENTAL RESULTS

The principle measurements were of plasma potential, electron temperature, and plasma density throughout the thruster; and of ion flux and kinetic energy measurements in the beam region. Propulsive efficiency was calculated from beam ion flux and energy, and measured absorbed RF power.

Electron temperature and plasma potential were measured as functions of distance along the thruster axis by a movable Langmuir probe. The resulting profiles are of particular interest since the electron temperature in the discharge and the drop in plasma potential in the electrostatic field region are theoretically related through Eq. 6. Typical electron temperature and plasma potential plots are shown in Figs. 3 and 4. The electron temperature, in general between 10 to 15 eV ( $\approx 10^5$  to  $1.5 \times 10^5$  °K), and varies only slightly along the axis. The drop in plasma potential shown in Fig. 4, while three times the discharge electron temperature, represents only about one-half

the total potential drop; it was found that the electrostatic field region extends many inches beyond the end of the waveguide (i.e., to the right of the region shown in Fig. 4).

Ion flux and kinetic energy distributions were measured in the beam region (12 inches from the end of the waveguide) by an ion energy analyzer shown schematically in Fig. 5. The analyzer consisted of a retarding grid and an ion collector housed in a Faraday cup, the plasma beam entering the cup through a gridded orifice. The ion collector was biased at minus 180 volts to repel all electrons and attract all ions passing through the retarding grid. A sawtooth voltage sweeping from ground potential to plus 140 volts was applied to the retarding grid. The current to the ion collector was displayed on the oscilloscope as a function of retarding-grid voltage. A typical oscilloscope trace is shown in Fig. 6a. The beam ion flux is obtained from the flat portion of the ion collector current trace. The ion energy distribution shown in Fig. 6b is the derivative of the oscilloscope trace plotted against  $V_g - V_{pi}$ , where  $V_g$  is the grid voltage and  $V_{pi}$  is the local plasma potential. (The required plasma potential measurement in the vicinity of the analyzer was made with a Langmuir probe positioned adjacent to the analyzer.) The energy distribution is narrow as would be expected for electrostatic acceleration through a DC potential. The center of the distribution is at a potential of 78 volts, about five times the discharge electron temperature, in reasonably good agreement with Eq. 6.

Thruster efficiency,  $\eta_t$ , defined here as the ratio of ion beam kinetic power to RF power absorbed in the discharge, was measured for a wide range of thruster configurations both at low absorbed RF powers, about 1 to 10 watt, and at higher power levels, ranging from 50 to 500 watts. The absorbed RF power was determined from the incident and reflected power measurements of a directional coupler. The beam kinetic power is the product of beam ion current and ion energy, and was calculated from ion energy analyzer data.

Efficiencies obtained at various power levels with the rectangular waveguide discharge chamber have been reported previously<sup>6,8</sup>. Here, we will compare only those results obtained at 50 watts absorbed power in the waveguide systems with the more recent results (also at about 50 watts) of experiments employing a pyrex discharge chamber inside a cylindrical microwave cavity.

Four representative accelerator configurations are shown in Fig. 7. The

order in which they appear more or less represents the chronological development of the thruster. Configurations in Figs. 7a through 7c are waveguides, and Fig. 7d is a pyrex tube. The microwave cavity is not shown in Fig. 7d. In all cases, the quartz block at the left is the upstream discharge boundary.

The main reason for the low efficiency of 2% to 4% in Fig. 7a was the presence of the cutoff block at the exit side of the discharge. This block (metal with a 1-inch-diameter hole) was employed to define the discharge boundary by reflecting microwave power incident on it. In addition, however, it acted as a mechanical obstacle, intercepting many magnetic field lines, and therefore also intercepting energetic electrons streaming along these lines, causing large losses. In Fig. 7b, the cutoff block was removed and a considerable gain in efficiency to 11% was registered. In Fig. 7c, which employed a magnetic bottle, represented an attempt to utilize the interaction between a radial magnetic field component and the azimuthal electron velocity (spiralling around the field lines) to obtain additional thrust.

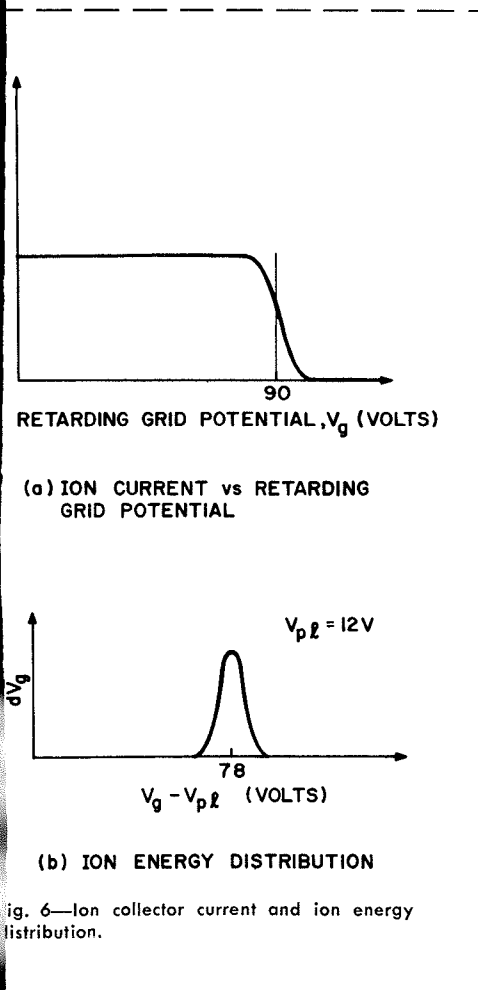


Fig. 6—Ion collector current and ion energy distribution.

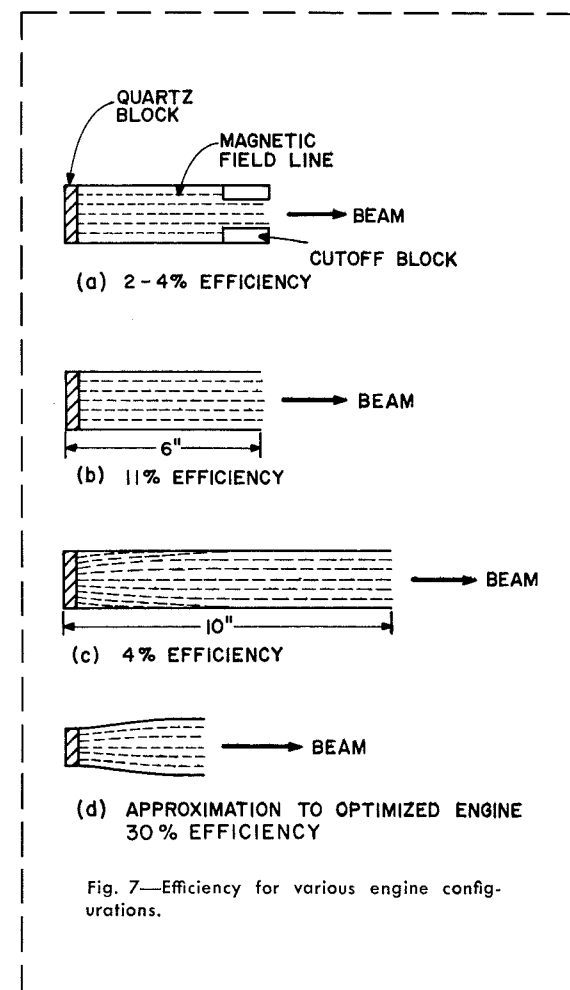


Fig. 7—Efficiency for various engine configurations.

Unfortunately, this modification necessitated (because of mechanical constraints on the existing system) lengthening the engine. The increased side-wall area which resulted contributed considerably to losses. In addition, it can be seen from Fig. 7c that some magnetic field lines near the upstream end were intercepted by the waveguide walls. This also is believed to increase losses, since, as is seen from Eq. 2, plasma flow parallel to the magnetic field B is much greater than that perpendicular to it. These losses resulted in a drop in efficiency to 4%.

On the basis of this information, an approach to an optimum configuration was visualized (Fig. 7d) as follows:

- 1) Short discharge region (ratio of emerging beam area to side wall area should be maximized),
- 2) Magnetic bottle at upstream end of discharge to enhance momentum transfer by  $\vec{V} \times \vec{B}_r$  force, and
- 3) Discharge chamber walls everywhere parallel to magnetic field lines.

Such a configuration was built in early 1965. The discharge was 2.75 inches long, the beam diameter at the discharge exit was 2 inches, and the magnetic field at the upstream discharge boundary was 1,450 gauss. Recent tests on this system have yielded very satisfactory results. An engine efficiency of 30%, a factor of almost three better than the previous high at this power, has been registered. Future improvements are expected.

Propellant utilization, defined as the ratio of fast ion flow to total (fast ion plus slow neutral) flow, has been measured in the experiments employing the pyrex discharge chamber. The total propellant mass exhausted is found by weighing the Hg charge before and after an experiment in which the duration and power level is recorded. This information together with the measured beam power determines the propellant utilization. At 50 watts of absorbed power, the propellant utilization is approximately 50%.

#### COMPARISON OF ECR WITH OTHER THRUSTORS FOR POSSIBLE MISSIONS

Boucher<sup>10</sup>, in a detailed comparison of various thruster systems, recently concluded that high-specific-impulse electric propulsion systems offer distinct weight savings over low-specific-impulse devices (cold gas jets, chemical rockets) when orbit corrective mission durations are 1 year or more.

A comparison of ECR and Kaufmann engine systems is presented in Table I for a specific mission in the orbit-corrective class: a station-keeping mission with a duration of 3 years for

**TABLE I—Thruster System Comparisons For a 3-year Station-Keeping Mission**

For a 1500-pound synchronous satellite with a total impulse requirement of 24,500 pound-seconds.

Characteristic	NASA-Kaufmann Ion Engine	ECR Thruster	
Thrust 10 <sup>-3</sup> lb	0.42	0.46	0.46
Beam Power, W	40	26.5	9
Propellant	Hg	Na	Hg
Specific Impulse (V <sub>exh</sub> /g)	4,460	2,950	1,000
Ion Energy, eV	2,000	100	100
Efficiency, %	67	25	25
Engine Power, W	60	106	36
Solar Panel Power, W	80	212	72
Propellant Utilization, %	80	80	80
<i>Thruster Component Weights:</i>			
Thrusters (8), lb	16	16	16
Propellant, lb	7	11	31
Propellant Tank, lb	4	6	15
<i>Power Supply Weights:</i>			
Solar Panel, lb	3	7	3
Power Converter, lb	10	15	10
<i>Total Thruster System Weight, lb</i>			
	40	55	75

a synchronous satellite weighing 1,500 pounds. Boucher has calculated that the total impulse required for such a mission is 24,500 pound-seconds. The principal system considerations are life expectancy and total propulsion plant weight. In each of the electrical systems considered, the propulsion system weight, including a 3-year fuel supply, is less than 1/10 the total vehicle weight as indicated in Table I. The Kaufmann engine system has a lower weight than the ECR systems; however, considering the low weight fraction, this advantage is not of greatest importance. In propulsive life expectancy, the electron cyclotron thruster appears to have the advantage. Several factors compromise the lifetime of the Kaufmann engine. First, the ion source, a dc discharge (similar to the well-known PIC discharge) requires a heated, electron-emitting cathode. The cathode is directly exposed to the discharge ions and is presently the most sensitive part of this ion engine. In addition there is the problem of accelerator grid erosion by sputtering from high energy ions, although grid erosion results have been somewhat more encouraging than the cathode results. In contrast, the ECR thruster employs an electrodeless microwave discharge which is ignited and maintained in the absence of any electron emitting filament. Furthermore, since the ion accelerating field is self-generated in the plasma by the energetic electrons, no accelerating grid structure is required. Some sputtering of the waveguide walls occurs, but this is a minor problem at low power levels since the sputtering ions have relatively low energy (0 to 100 eV, depending on plasma potential), and therefore a low sputtering yield; the problem is also lessened because the waveguide dimensional tolerances are not nearly as

stringent as, for example, accelerator grid tolerances in the ion engine. Periods of operation greater than 1,500 hours, without visible deterioration, are evidence for these conclusions.

Although considerations of weight are secondary to that of lifetime it is still imperative to minimize propulsion system weight. It is seen, from Table I, that propellant utilization (i.e., the ratio of high velocity ion flux to total flux including any thermal velocity neutral flux escaping un-ionized) must be kept high. As was previously indicated, values as high as 50% have been obtained in the laboratory, and it is felt that 80% can be approached.

#### SUMMARY

A laboratory model of an electron cyclotron resonance plasma thruster has been built and tested at AED. An efficiency of 30% has been obtained at a power level applicable to orbit corrective missions (50 watts). A propellant utilization factor of about 50% has also been achieved at this power. Systems analyses indicate that an ECR thruster using standard solar-cell panels will be competitive for a wide range of orbit-corrective missions. The long life expectancy of the electrodeless ECR thruster is a major advantage relative to other, probably shorter lived electric thrusters.

#### ACKNOWLEDGEMENT

This work was supported, in part by the AF Office of Scientific Research of the Office of Aerospace Research, under Contract No. AF49(638)-134z.

#### BIBLIOGRAPHY

1. T. T. Reboul and S. Fairweather (RCA-AED, Princeton), "Review of Electric Propulsion," *RCA ENGINEER*, Vol. 9, No. 4, Dec. 1963-Jan. 1964, p. 32.
2. G. R. Brewer, M. R. Currie, and R. C. Knechtli, "Ionic and Plasma Propulsion for Space Vehicles," *Proc. IRE*, Vol. 49, p. 1789 (1961).
3. W. R. Mickelsen and H. R. Kaufmann, *Status of Electrostatic Thrusters for Space Propulsion*. NASA Report TN D-2172, (1964).
4. G. R. Seikel, D. B. Bowditch, and S. Domitz, "Application of Magnetic Expansion Plasma Thrusters to Satellite Station Keeping and Attitude Control Missions," *AIAA preprint 64-677*, *AIAA Bulletin*, Vol. 1, 382 (1964).
5. H. W. Hendel and T. T. Reboul (RCA-AED, Princeton), "Continuous Plasma Acceleration at Electron Cyclotron Resonance," *AIAA preprint 63001*.
6. S. A. Ahmed and H. W. Hendel (RCA-AED, Princeton), "Space Charge Acceleration of Ions at Electron Cyclotron Resonance," *AIAA preprint 64-24*, *AIAA Bulletin*, Vol. 1, 12 (1964).
7. H. W. Hendel, S. A. Ahmed, and T. J. Faith (RCA-AED, Princeton), "Acceleration of an Electron Cyclotron Plasma by Self-Generated Electric Fields," *Colloquium on RF-Plasma Interactions*, Sept. 10-12, 1964, Saclay, France.
8. H. Hendel, T. Faith, and E. C. Hutter (RCA-AED, Princeton), "Plasma Acceleration by Electron Cyclotron Resonance," *RCA Review XXVI*, 200 (1965).
9. D. Bohm, E. H. S. Burhop, and H. S. W. Massey, in *Characteristics of Elec. Discharges in Magn. Fields*, ed. by A. Guthrie and R. K. Wakerling (McGraw Hill, 1949).
10. R. A. Boucher, "Electrical Propulsion for Control of Stationary Satellites," *Jl. Spacecraft and Rockets*, Vol. 1, (1964).

# PLASMA-ANODIZED LANTHANUM TITANATE DIELECTRIC THIN FILMS

R. E. WHITMORE and J. L. VOSSEN

Systems Laboratory

Communications Systems Division

DEP, New York, N.Y.

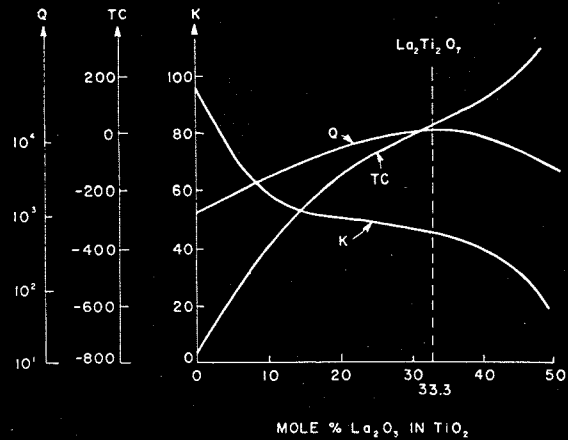


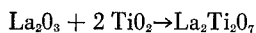
Fig. 1—Bulk dielectric properties of lanthanum titanate.

The purpose of the project described herein was to find a material and process capable of providing evaporable films of moderately high dielectric constant useful in thin film circuits.

## MATERIAL SELECTION

Of the high dielectric constant materials known, the pyrochlores, characterized by the formula  $A_2B_2O_7$  (where:  $A$  may be La, Nd, In, Y, etc., and  $B$  may be Ti, Sn, Zr, Hf, etc.) offer potentially simpler processing because this structure is rather noncritical and is readily formed.<sup>1</sup> From consideration of a number of pyrochlore systems, one ( $\text{La}_2\text{Ti}_2\text{O}_7$ ) has been selected. At the zero-temperature-coefficient point, this system has a dielectric constant of 47 and a  $Q$  in excess of 10,000. The dielectric properties are fairly insensitive to changes in composition<sup>2</sup> as shown in Fig. 1.

The metals lanthanum and titanium are first evaporated and then oxidized. The two metals have identical vapor-pressure characteristics<sup>3,4</sup> which allow excellent control of the composition. To form the titanate, a 1:1 atomic percent initial ratio is required. During oxidation, the oxides react to form the titanate:



Since lanthanum and titanium are not metallurgically soluble, there are no problems involved in the oxidation of the metals individually.<sup>5</sup>

## EVAPORATION OF THE METALS

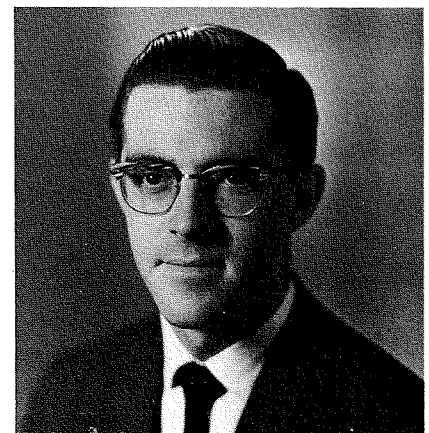
Lanthanum turnings and titanium sponge are the selected form of the evaporants. Lanthanum has a very high

Discussed is the application of plasma anodization to the pyrochlore lanthanum titanate ( $\text{La}_2\text{Ti}_2\text{O}_7$ ) and its use as a thin-film dielectric. Lanthanum and titanium are co-evaporated, followed by plasma anodization. Characteristics of the resultant thin-film dielectric represent substantial advance in the state of the art. While a disadvantage of the process is the relatively slow anodization time, this is somewhat offset because the equipment is relatively uncomplex and the process can go on unattended.

ROBERT E. WHITMORE graduated from City College of New York in 1962 with a BS in Physics. He is now doing post-graduate work for an MS in Physics at New York University. From 1958 to 1963 he was employed by the Western Union Company. Mr. Whitmore joined the Communications Systems Division in 1963 and was assigned to the thin film research laboratory. His initial contribution was the development of a multilayer evaporated permalloy film for use in majority logic circuits. He has been doing research on improved materials and evaporation techniques for thin film passive and active components with particular emphasis on high-K thin film capacitors. During the past two years he has developed the plasma anodization technique and the lanthanum titanium oxide material. Currently, Mr. Whitmore is engaged in applying integrated circuit techniques to microwave circuitry.



JOHN L. VOSSEN joined the Semiconductor and Materials Division of RCA (now Electronic Components and Devices) in 1958 after receiving a BS in Physics. While at Somerville, he worked on a variety of passive component and film deposition processes and did graduate work in Solid State Physics and Chemistry. In 1962 Mr. Vossen transferred to the Communications Systems Division in New York City where he was responsible for setting up a thin-film component research and development facility. In 1965 Mr. Vossen transferred to the RCA Laboratories in Princeton where he is currently investigating processes for the fabrication of thin-film passive components for integrated circuits. Mr. Vossen is a member of the American Physical Society, the Electrochemical Society, the American Vacuum Society, and IEEE.



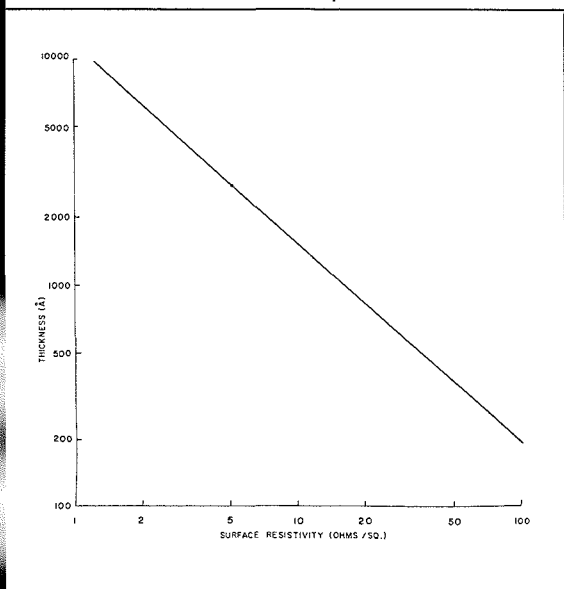
Final manuscript received May 15, 1965

oxygen affinity and readily oxidizes at ordinary temperatures with a large exotherm. This pyrophoric property of lanthanum necessitates special handling procedures. The lanthanum turnings are received packed in oil which prevents oxidation and reduces friction between the lanthanum particles. The oil is first removed from the turnings by successive washings in trichloroethylene.

The individual turnings are then pulverized and placed on a tungsten filament. The titanium sponge, requiring no preliminary treatment, is placed on the same filament in close proximity to the lanthanum. A single tungsten sheet with two dimples has proven adequate by providing a close coincidence in the evaporation rates of lanthanum and titanium. It is necessary to separate the materials in the boat because of their different melting points (La: 826°C; Ti: 1670°C). If the two materials are in contact while the filament is heated, the lanthanum melts first and the solid titanium sinks into the liquid lanthanum. As the titanium melts and outgasses, most of the material is ejected from the boat before evaporation starts.

Source temperature and film thickness are monitored, respectively by using optical pyrometry and resistivity measurements of the metal film during deposition. The sheet resistivity of La-Ti vs. film thickness is plotted in Fig. 2. (These film thickness measurements were made by W. Trigg, RCA Electronic Components and Devices, Somerville, New Jersey, using multiple beam interferometry.) Although this is not a particularly accurate method of monitoring film thickness, it serves the purpose since the La-Ti film functions not only as the

Fig. 2—Thickness of lanthanum-titanium films vs. surface resistivity.



starting point for the oxide film, but also as its own bottom electrode. Of primary concern in bottom electrodes is the resistance rather than the thickness.

#### OXIDATION BY PLASMA ANODIZATION

The two most extensively used methods of producing an oxide growth on metallic thin films are the thermal and electrochemical anodic techniques. The pyrophoric property of lanthanum originally suggested that thermal oxidation could be used advantageously to provide the oxide film. This approach was pursued with some success but was later abandoned as several problem areas involving thermal mismatch between the separate bottom electrode and the film became apparent. Conventional anodic oxidation using an aqueous electrolyte was considered as a natural alternative. While applicable in principle, this approach failed to exploit the pyrophoric property of the lanthanum, further complicated the fabrication procedure, and most importantly, no suitable electrolyte could be found. A modified form of anodic oxidation using a gaseous "electrolyte,"<sup>6,7</sup> however, was found to provide the best features of thermal and anodic oxidation and was eventually adopted.

Gaseous or plasma anodization is closely analogous to the conventional process. The gaseous "electrolyte," an oxygen ion plasma, provides a source of oxygen ions and the conducting medium for the application of an electric potential across the oxide. This technique offers several advantages not inherent in "wet" anodization. The usual temperature restrictions associated with the use of a liquid electrolyte are removed. This allows a contribution to the oxidation rate from substrate heating due to ion bombardment and the exothermic reaction of the lanthanum. Fabrication of the thin film capacitor is simplified and made more reliable as the entire process, conceptually, can be completed in a closed system in which the purity of the atmosphere is closely controlled. The oxide film thickness is a single-valued function of the forming potential, thus making control of tolerances fairly easy.

During this investigation of plasma anodized films, a separate anodization chamber was used to simplify the experimental setup and facilitate evaluation of the individual fabrication steps. The anodization was performed in a 12-inch vacuum bell jar at a pressure of 25  $\mu$ m-Hg. A schematic of the system is shown in Fig. 3. The DC gas discharge is established between two stainless steel disk electrodes and the "work area" defined by two suppressor plates.

Extraneous leakage paths have been minimized by eliminating all conductive

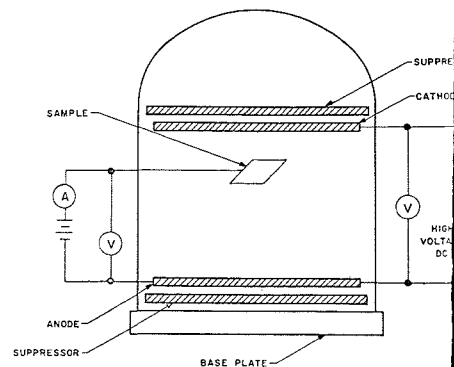


Fig. 3—Plasma anodization chamber.

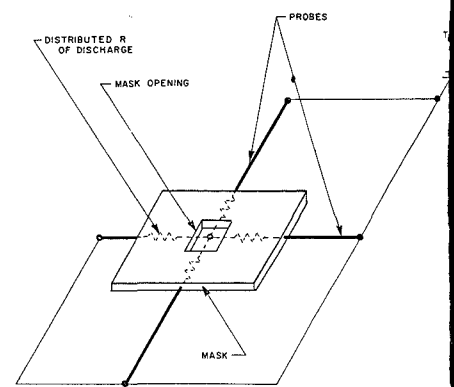


Fig. 4—Contacts to substrate via distributed resistance of the oxygen glow discharge.

materials from the work area with the exception of the metal film to be anodized. The system is operated in the "abnormal glow" discharge mode with the sample positioned in the positive column. A small DC potential is applied to the metal film to permit the formation of a thicker oxide.

The major problems in outfitting a vacuum system for plasma anodization are: 1) elimination of all metal except the sample to be anodized from the work area and 2) making electrical contact to the film being anodized.

In the present system, all supports for electrodes, suppressors and the anodization platform are porcelain standoffs. Nylon hardware is used throughout. All leads are run through glass tubing whose inside diameter is smaller than the mean free path at the anodization pressure used. The anodization platform is a lava plate machined to accept masks, substrate clamps and the contact to the film being anodized.

It is necessary to use masks of some kind while anodizing because some areas on a circuit substrate are invariably not anodizable. Even if they were, it is not desirable to anodize interconnections, resistors, etc. Therefore, one must consider the problem of how to mask. Photoresist masking is one possible method since the resist is a good insulator and effectively covers all areas not to be anodized. Photoetched metal masks must be coated with an insulator. The ideal would be a mask completely fabri-

cated of insulating material such as glass, quartz, mica, mylar, etc. Coated metal masks were used in this investigation.

Direct electrical contact to the film may be made by shimming the substrate above a coated mask with a thin piece of valve metal foil (Al, Ta, W, etc. anodizable to a field limited thickness) such that this foil makes electrical contact to all of the capacitor bottom electrodes. This foil is then connected to the power supply via a valve metal wire enclosed in glass tubing. The positioning of the foil, connection of a wire, etc. are difficult at best.

It has been found possible to connect the film to the forming supply electrically without making any direct mechanical contact. The plasma itself is a conductor of sorts ( $\rho \approx 3.5 \times 10^0$  ohm-cm, where  $\rho$  is the "average resistivity" from anode to cathode) and is capable of making the electrical contact from a probe near the film to the film through the mask opening(s). The resistance of the plasma, when used in this way, is not uniform to all parts of the system. Therefore, to achieve uniform film thickness, several probes must be introduced into the work area to obtain a uniform distribution of the forming potential on the film. This is illustrated in Fig. 4. This method of making contact will work equally well for all methods of masking. The probes are nothing more than the tips of valve metals protruding slightly from protective glass tubing. In the present system, aluminum wire is used for this purpose. The very tip anodize as it is a very sharp, and so maintains the potential in the work area. The rest of the wire anodizes eventually. The fact that the plasma is such a poor conductor means that the probes must be very close to the film being anodized; but this same effect prevents the forming potential from being virtually connected to other parts of the system (e.g. anode, cathode, suppressors and baseplate) because the resistance to these points is very high.

#### THIN FILM PROPERTIES OF PLASMA ANODIZED $\text{La}_2\text{Ti}_2\text{O}_7$

The following is a summary of the present state of the art of  $\text{La}_2\text{Ti}_2\text{O}_7$  capacitors.

In general, the material and process are found to be nearly insensitive to the type of substrate used. To date, capacitors have been prepared on: fused silica, microscope slides, Corning codes 7052 and 7059 glass, and sapphire with no apparent difference in properties. The counter-electrode used is aluminum, although Cr, Ni, Co, NiCr, and others work also.

In the plasma anodization process, the conditions generally used are: 1,200

TABLE I—Capacitance vs. DC Voltage and Polarity

V DC Volts	C(La <sup>+</sup> Ti:-) pF	C(La <sup>+</sup> Ti:+) pF
0	1604.0	1604.0
10	1608.0	1604.0
15	1610.5	1604.0
20	1616.0	1608.0

volts, 20 to 30mA at an oxygen pressure of 25  $\mu\text{m}$ . This places the discharge approximately at the point where the abnormal glow is initiated.

In the anodization system used, the sample is located approximately half way between the discharge electrodes. Except for the sample being anodized, no metal exists between these electrodes. The location of the sample in terms of discharge is in the positive column. It is very difficult to measure accurately the sheath potential on the sample, but it can be estimated from indirect evidence. In the system used at present, the sheath potential has been estimated to be between 3 and 8 volts. A figure of 5 volts is assumed under the above conditions. The sheath potential is additive with the externally applied forming potential.

The capacitance per unit area ( $C/A$  in  $\mu\text{F}/\text{in}^2$ ) is related to the forming potential (including the sheath potential) by the relation:

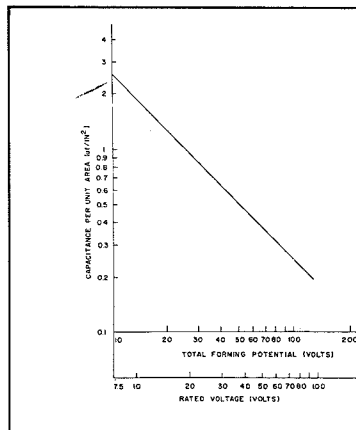
$$\frac{C}{A} = \frac{k}{V_f}$$

where  $k$  is a constant of the material which has been found to be approximately equal to 25  $\mu\text{F} \cdot \text{V} \cdot \text{in}^{-2}$  for La + Ti films.

The breakdown voltage of the capacitors is approximately equal to the total forming potential and the rated voltage has been taken as 75% of the total forming potential. Fig. 5 shows the capacitance per unit area as a function of total forming potential and rated voltage for  $\text{La}_2\text{Ti}_2\text{O}_7$ .

The room temperature insulation re-

Fig. 5—Capacitance per unit area vs. total forming potential and rated voltage ( $\text{La}_2\text{Ti}_2\text{O}_7$ ).



sistance at the rated voltage is typically 100 to 500 megohms and the capacitors are essentially nonpolar and non-voltage-sensitive, as indicated in Table I.

Frequency characteristics have been taken up to 300 kc/s. Typical response is shown in Fig. 6. These results are typical of anodic oxides.<sup>8</sup> The probable cutoff frequency is between 1 and 10 Mc/s.

The temperature coefficient of plasma anodized  $\text{La}_2\text{Ti}_2\text{O}_7$  over the range 25 to 125°C is usually slightly negative (indicating a slight excess of  $\text{TiO}_2$ ). Typical values are -50 to -100 ppm/°C.

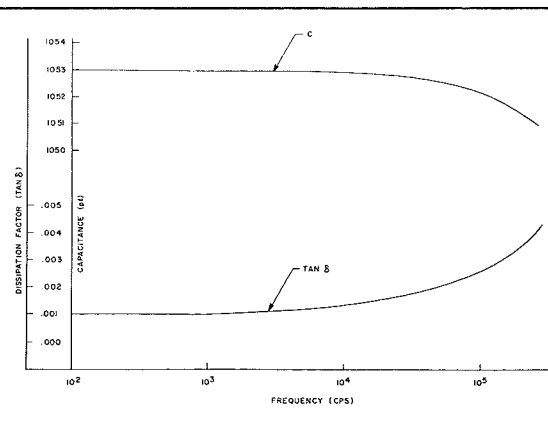
#### ADVANTAGES AND DISADVANTAGES

The advantages of plasma anodized  $\text{La}_2\text{Ti}_2\text{O}_7$  are its characteristics as outlined above. These represent a substantial improvement over the state of the art of evaporable dielectrics in nearly all respects. The only apparent disadvantage of the process is time. Since the glow discharge consists mostly of positive oxygen ions, the rate of anodization is slow. The total anodization time averages between 1 and 3 hours depending on film thickness. In one sense this is not a problem as no one must be in attendance; but equipment is still required to be in use for this cycle. Anodization facilities are not particularly large or expensive and this may partially mitigate the difficulty of the long process.

#### BIBLIOGRAPHY

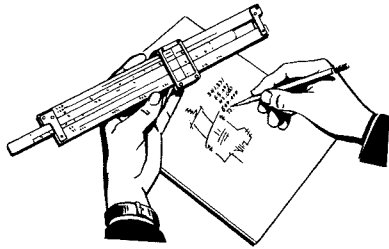
1. R. S. Roth, *J. Res. N. B. S.*, 58 (2), 75 (1957).
2. Vitro Chemical Company, Technical Bulletin, *The Use of Rare Earths and Their Allied Elements in Dielectric Ceramic Materials*.
3. R. E. Honig (RCA Labs., Princeton) *RCA Rev.*, XXIII, (4) 567, Dec. 1962.
4. C. E. Haberman & A. H. Daane, *J. Chem. Phys.*, 41, (9), 2818, November 1964.
5. M. Hansen, *Constitution of Binary Alloys*, 2nd Ed., McGraw-Hill Book Co., pp. 893, (1958).
6. J. L. Miles and P. H. Smith, *Journ. Electrochem. Soc.* 110, (12), 1240, December 1963.
7. M. C. Johnson, "The Plasma Oxidation of Metals in Forming Electronic Circuit Components," presented at 1964 Electronic Components Conference; May 5, 1964; Washington, D. C. (Subsequently published in *IEEE Trans. of Comp. Parts*, CP-11, (2), 1, June 1964.)
8. See example, L. Young, *Anodix Oxide Films*, Academic Press, (1961), pp. 157-169.

Fig. 6—Frequency characteristics of plasma anodized  $\text{La}_2\text{Ti}_2\text{O}_7$ .



# Engineering and Research NOTES

BRIEF TECHNICAL PAPERS OF CURRENT INTEREST



## General Three-Resonator Filters



R. M. KURZROK, *Systems Laboratory  
Communications Systems Division,  
DEP, New York, N. Y.*

Final manuscript received October 19, 1965

General three-resonator filters are capable of providing both bandpass and band-reject behavior. This type of filter network has been briefly considered as a generalized triple-tuned circuit.<sup>1</sup> The potential advantages of general three- and four-resonator filters have been more recently discussed by Johnson,<sup>2</sup> who considered *dissipationless* filters using *inductive couplings*. In this Note, the performance characteristics of *dissipative* general three-resonator filters using *capacitive couplings* will be presented.

Fig. 1 shows the general three-resonator filter using capacitive couplings. For the special case of no coupling between the first and third resonators,  $C_{13} = 0$ , and the filter acts as a conventional bandpass filter. The design of such a bandpass filter for a Butterworth response shape was implemented using the methods of Dishal<sup>3,4</sup> and experimental techniques. The design procedure of Cohn<sup>5</sup> is also applicable and somewhat more appropriate for filters of large percentage bandwidth. The filter resonators employed seven turns of 3/8-inch-diameter miniductor stock (i.e., air-core solenoids) which resonate at 20 Mc/s with a total capacitance of 121 pF. These inductors displayed unloaded  $Q$ 's of 245. Resonator capacitors employed fixed mica units in parallel with 1-to-75-pF Johanson trimmers. Using autotransformers for input-output couplings and capacitive interstage couplings of 17 pF (i.e.,  $C_{12} = 17$  pF), the filter response curve of Fig. 2 was obtained. Center frequency insertion loss was 0.4 dB and the relative 3-dB bandwidth was about 3.8 Mc/s. The asymmetrical response shape is primarily due to the frequency-sensitive capacitive interstage coupling elements.

The three-resonator Butterworth filter design previously described used normalized coefficients of coupling equal to 0.707 (i.e.,  $K_{12} = K_{23} = 0.707$ ). Upon letting  $C_{13} = 7$  pF, appreciable coupling between the first and third resonators is obtained. This results in a normalized coefficient of coupling  $K_{13} = (7 - 17) = 0.291$ . The response curve of this general three-resonator filter is shown in Fig. 3. It can be seen that composite bandpass and band-reject behavior is obtained. The sharpening of the low-frequency skirt is accompanied by a deterioration of selectivity on the high-frequency skirt. Peak rejection of 47 dB was obtained at a frequency of 16.9 Mc/s. Center frequency insertion loss is 0.6 dB.

For the capacity-coupled, general three-resonator filter, the frequency of peak rejection can be calculated using the following equation:

$$X = -\frac{K_{12}^2}{K_{13}} \quad (1)$$

where  $X \cong 2(f-f_0) / \Delta f_{3dB}$  = normalized frequency variable,  $f$  = frequency,  $f_0$  = filter center frequency, and  $\Delta f_{3dB}$  = filter 3-dB bandwidth.

Letting  $K_{12} = 0.707$  and  $K_{13} = 0.291$ , peak rejection is obtained when  $X = -1.71$ . Then the frequency of peak rejection will be  $20 - (1.9)(1.71) = 16.75$  Mc/s.

The insertion loss at the frequency of peak rejection  $L_f$  (in dB) is approximately equal to the sum of the two components:

$$L_f \cong P + R \quad (2)$$

$$P = 10 \log(1 + X^6) \quad (3)$$

$$R = 20 \log \left[ \frac{1}{2K_{13}d_2} \right] \quad (4)$$

where  $d_2 = Q_T / Q_{UL}$  = normalized dissipation factor of second resonator,  $Q_T = f_0 / \Delta f_{3dB}$  = total  $Q$  of filter, and  $Q_{UL}$  = unloaded  $Q$  of second resonator. Component  $P$  is the selectivity of the conventional three-resonator bandpass filter displaying a Butterworth response shape. Component  $R$  is the rejection due to the band-reject mechanism of the general filter. Letting  $X = 1.71$ ,  $K_{13} = 0.291$ , and  $d_2 = 0.02$ , then  $P = 14.1$  dB and  $R = 38.7$  dB, resulting in a composite peak rejection of 52.8 dB.

The theoretical center frequency insertion loss  $L_{cf}$  (in dB) can also be determined:

$$L_{cf} = 10 \log [A_0^2 + A^2] \quad (5)$$

$$A_0 = (d_1^2 d_2 + (K_{13}^2 d_2) + 2(K_{12}^2 d_1)) \quad (6)$$

$$A_0 = 2K_{12}^2 K_{13} \quad (7)$$

where  $d_1$  = normalized dissipation factor of first and third resonators. Letting  $d_1 = 1$ ,  $d_2 = 0.02$ ,  $K_{13} = 0.291$ , and  $K_{12} = 0.707$ , then  $A_0 = 1.022$ ,  $A = 0.291$ , and the center frequency insertion loss is 0.55 dB. If  $K_{13} = 0$ , then  $A = 0$  and the center frequency insertion loss would be 0.22 dB.

Comparing the calculated performance with measured data for the capacitively-coupled, general three-resonator filter, it can be seen that reasonable good correlation between theory and experiment has been obtained. Sharper low-frequency selectivity and peak rejection have been obtained at a price of degraded high-frequency selectivity and a modest increase in center frequency insertion loss. Only one additional circuit element has been needed. The general three-resonator filter described herein should be useful in duplexing or sideband selection application where highly asymmetrical selectivity is desirable.

**Acknowledgement:** Contract work accomplished under sponsorship of the Air Force's Rome Air Development Center, Griffiss AFB, New York.

1. N. W. Mather, "An Analysis of Triple-Tuned Coupled Circuits," *Proc. IRE*, Vol. 38, pp. 813-822, July 1950.
2. E. C. Johnson, "New Developments in Designing Bandpass Filters," *Electronic Industries*, pp. 87-90, 92, 94, Jan. 1964.
3. M. Dishal, "Design of Dissipative Band-Pass Filters Producing Desired Exact Amplitude-Frequency Characteristics," *Proc. IRE*, Vol. 37, pp. 1050-1069, Sept. 1949.
4. M. Dishal, "Alignment & Adjustment of Synchronously Tuned Multiple-Resonant-Circuit Filters," *Proc. IRE*, Vol. 39, pp. 1448-1455, Nov. 1951.
5. S. B. Cohn, "Direct-Coupled Resonator Filters," *Proc. IRE*, Vol. 45, pp. 187-196, Feb. 1957.

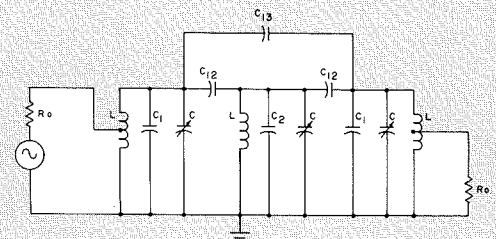


Fig. 1—General three resonator filter.

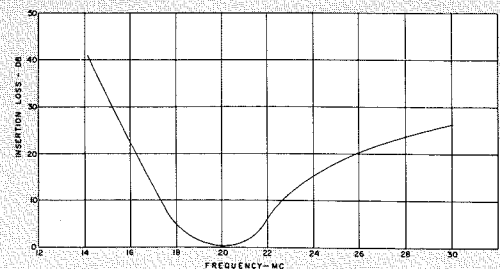


Fig. 2—Bandpass response.

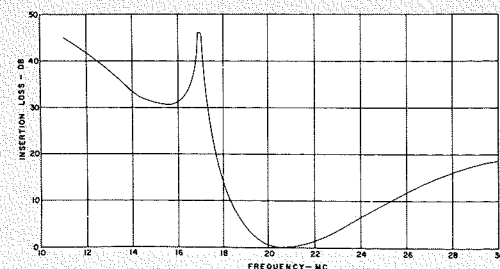


Fig. 3—Composite response.



## Asynchronously Multiplexed Channel Capacity

R. C. SOMMER, *Systems Laboratory, Communications Systems Division, DEP New York, N. Y.*

Final manuscript received July 22, 1965

With asynchronous multiplexing, it is intended that  $M$  information sources convey information to their respective destinations via a common channel without any pre-arrangement such as frequency and/or time division multiplexing. A general multiplex communication system is illustrated in Fig. 1. For  $i = 1, 2, \dots, M$ , the set of possible transmitted waveforms which  $T_{x_i}$  can produce is known only by receiver  $R_{x_i}$ . Both the transmitted signal,  $S_i$ , and received signal,  $y$ , are limited to a band  $W$ . The white gaussian noise  $n$  has an average power  $N$  and the signal  $S_i$  has an average power  $P_i$ . Since there is no pre-arrangement among the  $T_{x_i}$ , all components of the received signal  $y = S_1 + S_2 + \dots + S_M + n$  are statistically independent. For these conditions, Shannon<sup>1</sup> has shown that the rate of information transmission which is provided by  $S_j$  is:

$$R_j = H(y) - H(y - S_j)$$

i.e., the entropy of the received signal less the entropy of the interference. Since  $y - S_j$  is invariant with respect to  $S_j$ , it is possible to maximize  $R_j$  by maximizing  $H(y)$  through a suitable choice of statistics for  $S_j$ . The maximum entropy for the received signal occurs when it forms a white gaussian noise ensemble. Thus,  $S_j$  must "gaussianize"  $y$ . It is possible to maximize  $R_j$  with respect to the statistics of  $S_j$  as embodied in  $P(S_j)$  simultaneously for all  $j$  by choosing for  $S_j$  a white gaussian noise ensemble of average power  $P_j$ . For a finite value of  $M$ , however, the uniqueness of this solution has not been proven. Since the entropy rate of a white gaussian noise ensemble  $x$  of average power  $P$  is given by  $H(x) = W \log 2\pi eP$ , it follows from Eq. 1 that the information capacity which is provided by signal  $S_j$  is given by:

$$C_j = \text{Max } R_j = W \log 2\pi e \left[ \frac{M}{\sum_{i=1}^M P_i + N} \right] P(S_j) - W \log 2\pi e \left[ \frac{\sum_{i=1}^M P_i + N}{i \neq j} \right] \quad (2)$$

Define the parameters

$$\beta = \frac{\sum_{i=1}^M P_i}{N} = (\text{average total signalling power}) \div (\text{average noise power},$$

$$\text{and } \gamma_i = P_i / \sum_{j=1}^M P_j, \quad \sum_{i=1}^M \gamma_i = 1$$

where  $\gamma_i$  is the fractional signalling power which is allotted to  $S_i$ . In terms of these parameters, the total channel capacity in bits/cycle can be expressed by:

$$\frac{C}{W} = \frac{1}{W} \sum_{j=1}^M C_j = -\log_2 \left[ \frac{M}{\pi} \left( 1 - \frac{\beta \gamma_j}{\beta + 1} \right) \right] \quad (3)$$

With regard to the division of a fixed total signalling power among the  $M$  signals, it is easily shown that Eq. 3 maximizes when  $\gamma_j = 1/M$  which provides equal signalling power for each  $S_j$ . For this case, Eq. 3 reduces to:

$$\frac{C}{W} = M \log_2 \left[ \frac{M(\beta + 1)}{M(\beta + 1) - \beta} \right] \text{ bits/cycle.} \quad (4a)$$

In the limit as  $M$  approaches infinity,

$$\frac{C}{W} = \frac{\beta}{(\beta + 1) \ln 2} \doteq \frac{1.44\beta}{\beta + 1} \text{ bits/cycle.} \quad (4b)$$

The result given by Eq. 4 is plotted in Fig. 2 for  $M = 1, 2, 4$ , and infinity. Alternatively, Eq. 4a can be expressed as:

$$\frac{C}{W} = M \log_2 \left[ \frac{1 + M\alpha}{1 + (M-1)\alpha} \right] \text{ bits/cycle,} \quad (5)$$

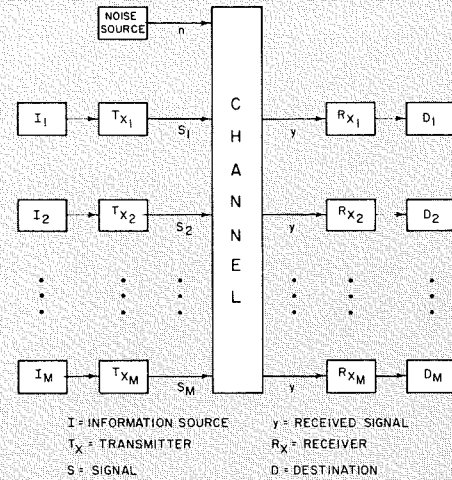
where  $\alpha = \beta/M = \text{average power per signal/average noise power}$ . The result given by Eq. 5 is plotted in Fig. 3 for  $M = 2^r$ ,  $r = 0, 1, 2, \dots, 6$ , and infinity.

Summarizing, the following result has been obtained: The capacity of an asynchronously multiplexed channel of band  $W$  perturbed by white gaussian noise of power  $N$ , when the total average signalling power is limited to  $\beta N$  and optimally divided among  $M$  signals, is given by:

$$C = WM \log_2 \left[ \frac{M(\beta + 1)}{M(\beta + 1) - \beta} \right] \text{ bits/second.}$$

With sufficiently involved encoding systems, information can be transmitted at this rate with an arbitrarily small frequency of errors. Any attempt to transmit at a higher rate must result in a finite frequency of errors.

1) C. E. Shannon and W. Weaver, *The Mathematical Theory of Communication*, University of Illinois Press, Urbana, 1949.



I = INFORMATION SOURCE      y = RECEIVED SIGNAL  
 Tx = TRANSMITTER          Rx = RECEIVER  
 S = SIGNAL                      D = DESTINATION

Fig. 1—General multiplex communication system. I = information source, Tx = transmitter, S = signal, y = received signal, Rx = receiver, and D = destination.

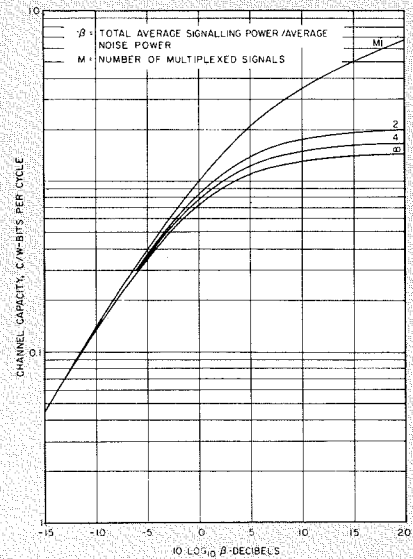


Fig. 2—From Eq. 4: Asynchronously multiplex channel capacity vs. ratio of total average signalling power to average noise power ratio. (Optimum division of signalling powers.)

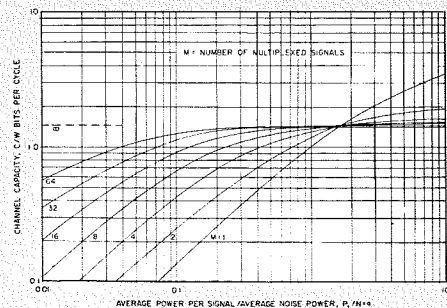
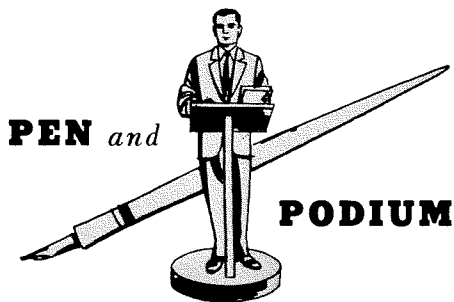


Fig. 3—From Eq. 5: same relationship as Fig. 2.



**COMPREHENSIVE SUBJECT-AUTHOR INDEX**  
to  
**RECENT RCA TECHNICAL PAPERS**

Both published papers and verbal presentations are indexed. To obtain a published paper, borrow the journal in which it appears from your library, or write or call the author for a reprint. For information on unpublished verbal presentations, write or call the author. (The author's RCA Division appears parenthetically after his name in the subject-index entry.) For additional assistance in locating RCA technical literature, contact: RCA Staff Technical Publications, Bldg. 2-8, RCA, Camden, N. J. (Ext. PC-4018).

This index is prepared from listings provided bimonthly by RCA Division Technical Publications Administrators and Editorial Representatives—who should be contacted concerning errors or omissions (see inside back cover).

Subject index categories are based upon the Thesaurus of Engineering Terms, Engineers Joint Council, N. Y., 1st Ed., May 1964.

**SUBJECT INDEX**

Titles of papers are permuted where necessary to bring significant keyword(s) to the left for easier scanning. Authors' division appears parenthetically after his name.

**ACOUSTICS**  
(theory & equipment)

**Artificial Voice**—H. F. Olson (Labs, Pr.) Audio Eng. Soc. Mtg., N.Y., Oct. 12, 1965

**Electronic Room-Acoustic Concepts**—J. E. Volkmann (Labs, Pr.) Audio Eng. Soc. Fall Convention, N.Y.C., Oct. 17, 1965

**Loudspeaker Retainer**—W. H. Moore (RCA Ltd., Ontario) TN-576, *RCA Technical Notes*, Issue No. 13, Dec. 64

**Loudspeaker System (Dual-Radial-Horn) with Congruent Cylindrical Wave Front Radiation**—J. E. Volkmann, A. J. May (Labs, Pr.) Audio Eng. Soc. Fall Convention, N.Y.C., Oct. 11-15, 1965

**Microphones, New Approach to Miniature**—R. A. Reynolds (BCD, Camden) IEEE Broadcast Group, Wash., D.C., Sept. 25, 1965; *IEEE Transactions*

**Sound Reproduction, Advances in**—H. F. Olson (Labs, Pr.) Int'l. Congress on Acoustics, Liege, Belgium, Sept. 9, 1965

**AMPLIFICATION**  
(& amplifiers)

**Audio Amplifier: Monolithic-Silicon Integrated-Circuit Type CA3007**—(Commercial Eng., ECD, Hr.) *RCA Technical Bulletin CA3007* and *RCA Application Note ICAN-5037*, Nov. 1965

**Cyclotron-Wave Amplifier, Double-Stream**—B. Vural (Labs, Pr.) Int'l. Electron Devices Mtg., Wash., D.C., Oct. 20-22, 1965

**DC Amplifier: Monolithic-Silicon Integrated-Circuit Type CA3000**—(Commercial Eng., ECD, Hr.) *RCA Technical Bulletin CA3000*, and *RCA Application Note ICAN-5030*; Nov. 1965

**Grounded-Grid Amplifiers, Series Resonant Input Circuit for**—M. V. Hoover (ECD, Lanc.) TN-642, *RCA Technical Notes*, Issue No. 15, Mar. 1965

**IF Amplifier: Monolithic-Silicon Integrated-Circuit Type CA3002**—(Commercial Eng., ECD, Hr.) *RCA Technical Bulletin CA3002* and *RCA Application Note ICAN-5036*, Nov. 1965

**Improved High-Voltage-High-Frequency Amplifier**—W. J. Hannan (DEP-AppRes, Camden) TN-637, *RCA Technical Notes*, Issue No. 15, Mar. 1965

**Negative Resistance Amplifier**—G. B. Herzog (Labs, Pr.) TN-577, *RCA Technical Notes*, Issue No. 13, Dec. 1964

**Operational Amplifier: Monolithic-Silicon Integrated-Circuit Types CA3008, CA3010**—(Commercial Eng., ECD, Hr.) *RCA Technical Bulletin CA3008-3010* and *RCA Application Note ICAN-5015*, Nov. 1965

**Receiver Requiring One Source, Front End for a**—A. S. Clorfeine (Labs, Pr.) TN-638, *RCA Technical Notes*, Mar. 1965

**RF Amplifiers: Monolithic-Silicon Integrated-Circuit Types CA3004, CA3005, CA3006**—(Commercial Eng., ECD, Hr.) *RCA Technical Bulletin CA3004* and *CA3005-3006*; and *RCA Application Note ICAN-5022*, Nov. 1965

**Tunnel Diodes in a Regenerating Mode, A New Method of Amplification Using**—A. S. Oberai (RCA Ltd., Montreal) IEEE Canadian Electronics Conf., Toronto, Oct. 4-6, 1965

**Video Amplifier: Monolithic-Silicon Integrated-Circuit Type CA3001**—(Commercial Eng., ECD, Hr.) *RCA Technical Bulletin CA3001* and *RCA Application Note ICAN-5038*, Nov. 1965

**Video Preamplifier, A Cooled Field-Effect Transistor Low-Noise**—J. O. Schroeder (ECD, Pr.) 13th Nat'l. Infrared Information Symp., Pasadena, Calif., Oct. 12-14, 1965 (Classified Session)

**ANTENNAS**

**Antenna System of Canada's First Satellite Communications Ground Station**—P. Foides (RCA Ltd., Montreal) IEEE Canadian Electronics Conf., Toronto, Oct. 4-6, 1965

**Cassegrainian Feed for Wideband Satellite Communications**—P. Foides, S. Komlos, N. K. Chitre, R. Schwerdtfeger (RCA Ltd., Montreal) *RCA Review*, Vol. XXVI, No. 3, Sept. 1965

**Positioning Mechanism (Circular Adjuster) for the Sub-Reflector of an 85-Ft Cassegrain Type Microwave Antenna**—T. Szirtes (Labs, Pr.) TN-613, *RCA Technical Notes*, Issue No. 14, Mar. 1965

**VLF-Dipole in the Ionosphere, Impedance of a Small**—D. A. deWolf (Labs, Pr.) Int'l. Scientific Radio Union (U.R.S.I.) Hanover, New Hampshire, Oct. 1965

**V-Z Panel as a Side-Mounted Antenna**—A. L. Davidson, R. N. Clark (BCD, Gibbstown) IEEE Symp., Washington, D.C., Sept. 23, 1965

**CIRCUIT ANALYSIS**  
(& theory)

**Ladder Network Synthesis by Similarity Transformation**—T. G. Marshall, Jr. (BCD, Pr.) Allerton Conf. of Circuit & System Theory, Oct. 20, 1965; *Proceedings of Allerton Conf.*

**Linear Signal Stretching in a Time-Variant System**—H. Weinstein (Labs, Pr.) *IEEE Transactions on Circuit Theory*, Vol. CT-12, No. 2, June, 1965

**Review of: "About the Algebraical Theory of the Multipositional Contacts and Its Application to the Study of Real Operating Contacts,"** (G. H. Ioanin, Hazard and Race Phenomena in Switching Circuits, Int'l. Symp. Bucharest, 1964, Circular Ltr. No. 4, Univ. Bucharest, pp 45-60)—F. H. Fowler, Jr. (DEP-CSD, Camden) Review No. 7429, *Computing Reviews*, 6-3, Mar-Apr '65

**Review of: "On the Operation of Switching Circuits with Real Operating Keys,"** (G. C. Moisil, G. H. Ioanin, Hazard and Race Phenomena in Switching Circuits, Int'l. Symp. Bucharest, 1964, Circular Ltr. No. 3, Univ. Bucharest, pp 21-44)—F. H. Fowler, Jr. (DEP-CSD, Camden) Review No. 7429, *Computing Reviews*, 6-3, Mar-Apr '65

**Review of: "The Interest of the Problem for Engineering Hazard and Race Phenomena in Switching Circuits,"** (G. C. Moisil, Int'l. Symp., Bucharest, 1964, Circular Ltr. No. 1, Univ. Bucharest, Rumania 1-21)—F. H. Fowler, Jr. (DEP-CSD, Camden) Review No. 7426, *Computing Reviews*, 6-3, Mar-Apr '65

**CIRCUITS, ELECTRONIC**  
(functional subsystems)

**Converter (Lightweight) Using Step-Width Regulator**—J. J. Klein, R. C. Kee, E. F. Dion (DEP-ASD, Burl.) East Coast Conf. on Aerospace and Navigation Electronics, Baltimore, Md., 10/27/65; *Conf. Record*

**Detector, A Combined Frequency and Phase**—E. M. Leyton (R&E, Pr.) TN-579, *RCA Technical Notes*, Issue No. 13, Dec. 1964

**Encoder-Decoder, Audio-Frequency Message**—E. Schmidt, E. Simshauser (DEP-CSD, Camden) Nat'l. Comm. Symp., Utica, N.Y., Oct. 11, 1965

**Frequency Converters, Transistor Parametric**—A. P. Anderson (RCA Ltd., Montreal) IEEE Canadian Electronics Conf., Toronto, Oct. 4-6, 1965

**Frequency Converters, Unilateralization and Widebanding of Parametric-Admittance**—J. Klapper (DEP-CSD, Camden) Nat'l. Electronic Conf., Chicago, Oct. 25-27, 1965; *Conf. Record*

**Frequency Dividers Including Insulated Gate Transistors**—J. R. Burns, R. A. Powilus (Labs, Pr.) TN-623, *RCA Technical Notes*, Issue No. 14, Mar. 1965

**Frequency Multipliers Using Hyperabrupt Varactors, High-Efficiency, High-Order, Idlerless**—S. Yuan, E. Markard (DEP-CSD, N.Y.) *RCA Review*, Vol. XXVI, No. 3, Sept. 1965

**Frequency Synthesizer (A Microelectronic Digital) for a UHF Communications Transceiver**—E. D. Menkes (DEP-CSD, Camden) J. W. Harmon (ECD, Hr.) Nat'l. Comm. Symp., Utica, N.Y., Oct. 11; *Proceedings*

**Insulated Gate Transistor Circuits**—J. Dresner, P. H. Mark (Labs, Pr.) TN-597, *RCA Technical Notes*, Issue No. 13, Dec. 1964

**Inverters, Push-Pull Saturated-Core Tunnel Diode**—R. Feryszka, P. Gardner (ECD, Som.) *RCA Review*, Vol. XXVI, No. 3, Sept. 1965

**Level-Pulse Circuit**—H. S. Miiller (Labs, Pr.) TN-599, *RCA Technical Notes*, Issue No. 13, Dec. 1964

**Limiting Circuit**—O. P. Hart, T. E. Deegan (ECD, Hr.) TN-582, *RCA Technical Notes*, Issue No. 13, Dec. 1964

**Multivibrator, Long-Delay Monostable**—J. J. Foy, Jr. (DEP-CSD, Tucson) TN-620, *RCA Technical Notes*, Issue No. 14, Mar. 1965

**Oscillator, Modulated High-Frequency Tunnel-Diode**—D. J. Carlson (H. I., Indpls.) TN-578, *RCA Technical Notes*, Issue No. 13, Dec. 1964

**Oscillator, Zener-Controlled**—D. P. Dorsey (Labs, Pr.) TN-612, *RCA Technical Notes*, Issue No. 14, Mar. 1965

**Phase Detector, Unijunction**—D. P. Dorsey (Labs, Pr.) TN-592, *RCA Technical Notes*, Issue No. 13, Dec. 1964

**Pulse Generator**—E. M. Fulcher (EDP, Palm Beach) TN-636, *RCA Technical Notes*, Issue No. 15, Mar. 1965

**Receiver Requiring One Source, Front-End for a**—A. S. Clorfeine (Labs, Pr.) TN-638, *RCA Technical Notes*, Mar. 1965

**Rectifier, High-Efficiency Low-Voltage**—J. L. Lowrance (DEP-AED, Pr.) TN-627, *RCA Technical Notes*, Issue No. 15, Mar. 1965

**Rectifier Voltage Regulator, Balanced Multiphase**—D. Rosenthal, H. E. Hawlk (DEP-CSD, N.Y.) TN-625, *RCA Technical Notes*, Issue No. 14, Mar. 1965

**Sawtooth Voltage Wave Generator**—L. Arlan (DEP-ASD, Burl.) TN-587, *RCA Technical Notes*, Dec. 1964

**Switching Network**—D. P. Dorsey (Labs, Pr.) TN-609, *RCA Technical Notes*, Issue No. 14, Mar. 1965

**Transcharger Circuit, Ferroelectric**—A. G. Samusenko (Labs, Pr.) TN-601, *RCA Technical Notes*, Issue No. 13, Dec. 1964

**Transfluxor, Increasing the Number of Control Levels in a**—A. I. Stoller (Labs, Pr.) TN-621, *RCA Technical Notes*, Issue No. 14, Mar. 1965

**Trigger Circuit, Tunnel-Diode Distable**—M. Cooperman (DEP-AppRes, Camden) TN-590, *RCA Technical Notes*, Issue No. 13, Dec. 1964

**Voltage Regulator, Overload-Responsive**—P. Anzalone (DEP-CSD, Camden) TN-616, *RCA Technical Notes*, Issue No. 14, Mar. 1965

**CIRCUITS, PACKAGED**

**Guide and Power Connector for a Printed-Circuit Card**—J. A. Vallee, R. G. Schilling (EDP, Palm Beach) TN-603, *RCA Technical Notes*, Issue No. 13, Dec. 1964

**Printed Circuit Board Testing Device**—C. A. Rosencrans (DEP-CSD, Camden) TN-594, *RCA Technical Notes*, Issue No. 13, Dec. 1964

**CIRCUITS, INTEGRATED**

**DTL Gates (Low-Power): Monolithic-Silicon Integrated-Circuit Types CD2200** (dual 4-input positive NAND), **CD2201** (quadrule 2-input positive NAND), and **CD2203** (J-K Flip-Flop with set-reset)—(Commercial Engineering, ECD, Hr.) *RCA Technical Bulletin CD2200-2201* and *CD2203*; and *RCA Application Note ICAN-5024*, Nov. 1965

**ECCL Gates (Ultra-High Speed): Monolithic-Silicon Integrated-Circuit Types CD2150** (dual 4-input positive OR-NOR); **CD2151** (dual 4-input positive OR-NOR with PHANTOM-OR capability); and **CD2152** (8-input positive OR-NOR with PHANTOM-OR capability)—(Commercial Eng., ECD, Hr.) *RCA Technical Bulletin CD2150-2151-2152* and *RCA Application Note ICAN-5025*, Nov. 1965

**ECCL Gates (High-Speed): Monolithic-Silicon Integrated-Circuit Types CD2100** (dual 4-input positive OR-NOR) and **CD2101** (quadrule 2-input positive NOR)—(Commercial Eng., ECD, Hr.) *RCA Technical Bulletin CD2100-2101*, and *RCA Application Note ICAN-5025*, Nov. 1965

**Audio Amplifier: Monolithic-Silicon Integrated-Circuit Type CA3007**—(Commercial Eng., ECD, Hr.) *RCA Technical Bulletin CA3007* and *RCA Application Note ICAN-5037*, Nov. 1965

**DC Amplifier: Monolithic-Silicon Integrated-Circuit Type CA3000**—(Commercial Eng., ECD, Hr.) *RCA Technical Bulletin CA3000*, and *RCA Application Note ICAN-5030*; Nov. 1965

**IF Amplifier: Monolithic-Silicon Integrated-Circuit Type CA3002**—(Commercial Eng., ECD, Hr.) *RCA Technical Bulletin CA3002* and *RCA Application Note ICAN-5036*, Nov. 1965

**Operational Amplifier: Monolithic-Silicon Integrated-Circuit Types CA3008, CA3010**—(Commercial Eng., ECD, Hr.) *RCA Technical Bulletins CA3008-3010 and RCA Application Note ICAN-5015*, Nov. 1965

**RF Amplifiers: Monolithic-Silicon Integrated-Circuit Types CA3004, CA3005, CA3006**—(Commercial Eng., ECD, Hr.) *RCA Technical Bulletins CA3004 and CA3005-3006*; and *RCA Application Note ICAN-5022*, Nov. 1965

**Video Amplifier: Monolithic-Silicon Integrated-Circuit Type CA3001**—(Commercial Eng., ECD, Hr.) *RCA Technical Bulletin CA3001 and RCA Application Note ICAN-5038*, Nov. 1965

**Extending Integrated Circuits**—M. Kidd, L. C. Drew (DEP-ASD, Burl.) East Coast Conf. on Aerospace and Navigation Electronics, Baltimore, Md., Oct. 27, 1965; *Conf. Record*

**Temperature-Determining Apparatus, Integrated-Circuit**—E. A. Williams (DEP-ASD, Burl.) TN-644, *RCA Technical Notes*, Issue No. 15, Mar. 1965

## COMMUNICATION, DIGITAL (equipment & techniques)

**Encoder-Decoder, Audio-Frequency Message**—E. Schmidt, E. Simshauser (DEP-CSD, Camden) Nat'l. Comm. Symp., Utica, N.Y., Oct. 11, 1965

**Frequency Synthesizer (A Microelectronic Digital) for a UHF Communications Transceiver**—E. D. Menkes (DEP-CSD, Camden) J. W. Harmon (ECD, Hr.) Nat'l. Comm. Symp., Utica, N.Y., Oct. 11; *Proceedings*

## COMMUNICATIONS SYSTEMS

**Adaptive Techniques, System**—M. Masonson (DEP-CSD, N.Y.) MIL-E-CON 9, Wash., D.C., Sept. 23, 1965; *Conf. Proceedings*

**Message Channel Monitoring**—C. J. Moore (DEP-CSD, Camden) AUTODIN Message Switching Centers, Nat'l. Comm. Symp., Oct. 11, 1965, Utica, N.Y.; *Proceedings*

**Multiple-Access Considerations for Communications Satellites**—Dr. F. Assadourian, J. Jacoby (DEP-CSD, N.Y.) MIL-E-CON 9, Wash., D.C., Sept. 24, 1965; *Conf. Proceedings*

**Submarine, Significance of the**—H. G. Munson (Labs, Pr.) Nassau Club, Princeton, N.J., Oct. 27, 1965

## COMMUNICATION THEORY (& information theory)

**Ladder Network Synthesis by Similarity Transformation**—T. G. Marshall, Jr. (BCD, Pr.) Allerton Conf. of Circuit & System Theory, Oct. 20, 1965; *Proceedings of Allerton Conf.*

## COMMUNICATION, VOICE (equipment & techniques)

**Amateur Transmitters, Synchronous Switching and Overload Protection for**—G. D. Hanchett (ECD, Som.) Int'l. Radio Hamfest and Conf., N. Laredo, Mexico, Aug. 14, 1965

**We Got Across**—F. D. Whitmore (DEP-C.E., Camden) "73", Nov. 1965

**Transceiver (2-Meter), Transistors and Nuvisitors in a**—R. M. Mendelson (ECD, Som.) Tri-Country Amateur Radio Club, N.J., Oct. 25, 1965

## COMPUTERS (systems)

**Review of: "Computer Progress in Czechoslovakia; I—Self-Correcting Computer Digital Information Processors"** (J. Oblonsky, Interscience Pub. N.Y. 1962, pp 740, \$27.00)—F. H. Fowler, Jr. (DEP-CSD, Camden) Review No. 7082, *Computing Reviews*, 6-1, Feb-Mar '65

## COMPUTER APPLICATIONS (scientific)

**Differential Equations in General Problem Solving, Applications of**—R. W. Klopfenstein (Labs, Pr.) *Association for Computer Machinery*, Vol. 8, No. 9, Sept., 1965

## COMPUTER APPLICATIONS (data processing)

**Electronic Voting System**—R. C. Stiefel (EDP, Cherry Hill) TN-605, *RCA Technical Notes*, Issue No. 13, Dec. 1964

**Review of: "Expected Critical Path Lengths in PERT Networks,"** (D. R. Fulkerson, RAND Corp., Santa Monica, Mar. 1962)—F. H. Fowler, Jr. (DEP-CSD, Camden) Review No. 7195, *Computing Reviews*, 6-3, Mar-Apr '65

## COMPUTER COMPONENTS

**Clock Distribution Scheme**—M. Cooperman (DEP-AppRes, Camden) TN-631, *RCA Technical Notes*, Issue No. 15, Mar. 1965

**Indexing Mechanism (Card or Part)**—L. F. Wolf (EDP, Palm Beach) TN-614, *RCA Technical Notes*, Issue No. 14, Mar. 1965

**Long-Sequence Generators, Technique for Driving**—R. H. Bergman (DEP-AppRes, Camden) TN-633, *RCA Technical Notes*, Issue No. 15, Mar. 1965

**(Punch-Card Reader): Assembly of Contact Strips**—E. A. Dameran, K. G. Kaufmann (EDP, Camden) TN-607, *RCA Technical Notes*, Issue No. 14, Mar. 1965

**Read-Write Switching Arrangement**—C. M. Wright (RCA Svc. Co., Wash., D.C.) TN-617, *RCA Technical Notes*, Issue No. 14, Mar. 1965

**Shift Network**—R. Gollub (EDP, Cherry Hill) TN-604, *RCA Technical Notes*, Issue No. 13, Dec. 1964

**Shift Pulse Generator**—H. R. Kaupp (DEP-AppRes, Camden) TN-591, *RCA Technical Notes*, Issue No. 13, Dec. 1964

## COMPUTER STORAGE

**Card Memory, Fixed Resistor**—J. Guarracini, M. H. Lewin, H. R. Beelitz (Labs, Pr.) *IEEE Trans. on Electronic Computers*, Vol. EC-14, No. 3, June, 1965

**Memories in Present and Future Generations of Computers**—J. A. Rajchman (Labs, Pr.) *WESCON Brochure*, Session 12, Aug. 26, 1965

**Thin-Film Scratch-Pad Memory System, An Experimental 65-Nanosecond**—G. Ammon (DEP-AppRes, Camden) *Proceedings of the Fall Joint Computer Conf.*, Oct. 21, 1965

## DISPLAYS

**(Lamps): Detailed Description Ceramic or Ceramic Metal Lamps**—R. A. Krey (ECD, Hr.) TN-610, *RCA Technical Notes*, Issue No. 14, Mar. 1965

**Transcharger Circuit, Ferroelectric**—A. G. Samusenko (Labs, Pr.) TN-601, *RCA Technical Notes*, Issue No. 13, Dec. 1964

## EDUCATION (& training)

**Problems in Junior College Science Teaching: I—Technical Preparation in Science**—H. O. Hook (Labs, Pr.) Nat'l. Science Teachers Assoc., Eastern Regional Conf., Sept. 25, 1965

## ELECTROMAGNETIC WAVES (theory; phenomena)

**Correlation Function of a Power-Law Folding Device**—G. E. Roberts, H. Kaufman (RCA Ltd., Montreal) *Int'l. Journal of Electronics*, Vol. 1, No. 5, May 1965

**Cross-Polarized Electromagnetic Backscatter from Turbulent Plasmas**—R. S. Ruffine, D. A. deWolf (Labs, Pr.) *Journal of Geophysical Research*, Vol. 70, No. 17, Sept., 1965

**Ferrite Phase Shifter, Design and Performance of a 20-kW Latching Nonreciprocal X-Band**—W. A. Schilling (ECD, Pr.) W. W. Siekanowicz (ECD, Pr.) E. Walsh (ECD, Pr.) I. Bardash (DEP-MSR, Mrstn.) J. Gordon (Labs, Pr.) Nat'l. Electronics Conf., Chicago, Ill., Oct. 23, 1965; *Conf. Record*

**Frequency Converters, Unilateralization and Widening of Parametric-Admittance**—J. Klapper (DEP-CSD, Camden) Nat'l. Electronic Conf., Chicago, Oct. 25-27, 1965; *Conf. Record*

**Line-of-Sight Propagation Through Quasi-Optical Irregularities**—D. A. deWolf (Labs, Pr.) Symp. on Electromagnetic Wave Theory, Technological Univ., Delft, Julianalaan, The Netherlands, Sept. 6-11, 1965

**Microwave Power by Parametric Frequency Multiplication in Transistors**—M. Caulton, H. Sobol (Labs, Pr.) and R. L. Ernst (DEP-CSD, Camden); Nat'l. Electronic Conf., Chicago, Oct. 25-27, 1965; *Conf. Record*

**Solid State Plasma Waveguide in a Transverse Magnetic Field, Microwave Propagation in a, Part II**—R. Hirota, K. Suzuki (Labs, Pr.) 20th Annual Mtg. of the Physical Society of Japan, Oct. 10-15, 1965

## ELECTRO-OPTICS (systems & techniques)

**Measurement of the Longitudinal Component of the Electromagnetic Field at the Focus of a Coherent Beam**—A. I. Carswell (RCA Ltd., Montreal) *Physical Review Letters*, Vol. 15, No. 16, Oct. 18, 1965

**Optical Carrier with PSK Subcarrier Modulation, Circuit for Generating an**—W. J. Hannan, H. E. Haynes (DEP-AppRes, Camden) TN-611 *RCA Technical Notes*, Issue No. 14, Mar. 1965

**Resolving Powers of Focussing Systems with Coherent Illumination**—A. I. Carswell, C. Richard (RCA Ltd., Montreal) *Applied Optics*, Vol. 4, No. 10, Oct. 1965

**Video Preamp, A Cooled Field-Effect-Transistor Low-Noise**—J. O. Schroeder (ECD, Pr.) 13th Nat'l. Infrared Information Symp., Pasadena, Calif., Oct. 12-14, 1965 (Classified Session)

**Visual Detection, Resolution and Time Factors in**—B. Hillman (DEP-ASD, Burl.) Military Operations and Research Symp., Sand Point Naval Air Station, Seattle, Wash., Oct. 26, 1965

## ENERGY CONVERSION (& power sources)

**Homopolar Generator**—A. Hom (Labs, Pr.) TN-643, *RCA Technical Notes*, Issue No. 15, Mar. 1965

**Microwave Power by Parametric Frequency Multiplication in Transistors**—M. Caulton, H. Sobol (Labs, Pr.) and R. L. Ernst (DEP-CSD, Camden) National Electronic Conf., Chicago, Oct. 25-27, 1965; *Conf. Record*

**Photovoltaics, Progress in**—P. Rappaport (Labs, Pr.) Photovoltaic Specialist Conf., Washington, D.C., Greenbelt, Md., Oct. 18-20, 1965

**(Solar Cells): A Comparison of Silicon and Gallium Arsenide Solar Cells for a Solar Mission**—J. V. Foster, J. R. Swain (NASA-AMES Res. Center) S. H. Winkler, F. R. Schwarz (DEP-AED, Pr.) 1965 Photovoltaic Specialists Conf. Goddard Space Flight Center, Washington, D.C., Oct. 20, 1965

**Solar Cells, GaAs Thin-Film**—P. Vohl, D. Perkins, S. G. Ellis (Labs, Pr.) Photovoltaic Specialist Conf., Greenbelt, Md., Oct. 18-20, 1965

**(Solar Cells): The Effect of Li on Radiation Damage in Silicon Solar Cell Devices**—J. J. Wysocki, B. Goldstein, P. Rappaport (Labs, Pr.) 1965 Photovoltaic Specialist Conf., Greenbelt, Md., Oct. 18-20, 1965

**Solar Cells, Wrap-Around-Contact**—K. S. Ling, J. M. Toole (ECD, Mountaintop) Photovoltaic Specialists Conf., Oct. 18, 1965

**Thermionic Converters, Development of a Parametric Equation to Describe the Performance of**—R. J. Buzzard, P. K. Shefsiek (ECD, Lanc.) Thermionic Conv. Specialists Conf., San Diego, Calif., Oct. 25-27, 1965

**(Thermionic Converters): Oxygen as a Controllable, Reversible, and Beneficial Additive in the Cesium Converter**—W. E. Harbaugh, R. E. Shoemaker (ECD, Lanc.) Thermionic Conversion Specialists Conf., San Diego, Calif., Oct. 25-27, 1965

**Thermionic Energy Converter, Volt-Ampere Characteristic of the**—K. C. Hernqvist (Labs, Pr.) Int'l. Conf. on Thermionic Elec. Power Generation, London, England, Sept. 20, 1965

**(Thermionics): Heat Pipe Performance**—W. B. Hall (ECD, Lanc.) Thermionic Conv. Specialists Conf., San Diego, Calif., Oct. 25-27, 1965

## ENVIRONMENTAL ENGINEERING

**Accelerometer Characteristics, Unpublished**—B. Mangolds (DEP-AED, Pr.) 35th Symp. on Shock and Vibration, New Orleans, La., Oct. 25, 1965

**Shaker Shock-Capabilities, Extending**—J. Fagen, J. McClanahan (DEP-AED, Pr.) 35th Symp. on Shock and Vibration, New Orleans, La., Oct. 28, 1965

## FILTERS, ELECTRIC

**Miss Filter, Ultra-Slope**—R. Glasgal (DEP-CSD, N.Y.) TN-580, *RCA Technical Notes*, Issue No. 13, Dec. 1964

## GEOPHYSICS

**Cyclotron Harmonic Resonances Observed by Satellites**—I. P. Shkarofsky, T. W. Johnston (RCA Ltd., Montreal) *Physical Review Letters*, Vol. 15, No. 2, July 12, 1965

**Geophysics and Astrophysics in the Laboratory**—F. J. F. Osborne, M. P. Bachynski (RCA Ltd., Montreal) *Proc. of the Sixth Biennial Gas Dynamics Symp.*, Northwestern Univ. Press, 1965

**Lunar Magnetospheric Configuration, A Possible**—F. J. F. Osborne, M. P. Bachynski (RCA Ltd., Montreal) *Journal of Geophysical Research*, Vol. 70, No. 19, Oct. 1, 1965

**Meteor Trail Decay, Recombination and**—B. B. Robinson (Labs, Pr.) *Journal of Geophysical Research*, Vol. 70, No. 15, Aug. 1965

**Raman Components of Laser Backscatter, Remote Observations Using**—J. Cooney (DEP-AED, Pr.) 2nd Int'l. Symp. on Electromagnetic Sensing of the Earth From Satellites. Amer. Geophysical Univ., Amer. Meteorological Soc. & Optical Soc. of Amer., Miami Beach, Fla., Nov. 24, 1965

## GRAPHIC ARTS

**Optical Printer System**—G. J. Waas (EDP, Camden) TN-645, *RCA Technical Notes*, Issue No. 15, Mar. 1965

## INTERFERENCE (& noise)

**Reduction of Impulse Noise by Interruption of Signal Flow Using a Field Effect Transistor**—G. F. Rogers (H.L. Indpls.) TN-640, *RCA Technical Notes*, Issue No. 15, Mar. 1965

## LABORATORY EQUIPMENT (& techniques)

**Crucible**—P. Goldstein (Labs, Pr.) TN-581, *RCA Technical Notes*, Issue No. 13, Dec. 1964

**Cutting Electro-Optical Modulator Crystals, Method and Apparatus for**—A. Sussman (Labs, Pr.) TN-595, *RCA Technical Notes*, Issue No. 13, Dec. 1964

**Diffusion Technique, A Solid-to-Solid**—J. Scott, J. Olmstead (ECD, Som.) *RCA Review*, Vol. XXVI, No. 3, Sept. 1965

**(Electron Microscope): Estimating Resolving Power by the Fresnel Fringe Method**—Dr. J. H. Reiser (BCD, Camden) Electron Microscope Soc. of America, N.Y., Aug. 25, 1965

**Electron Microscope, Future Developments of the**—Dr. J. H. Reiser (BCD, Camden) Temple Univ. for Post Graduate Class in Dermal Pathology, Sept. 28, 1965

**Electron Microscopy Image-Intensification of Low Temperature Phase Transformations in Semiconductors**—Dr. J. W. Coleman, M. D. Coutts, K. Sadashige (BCD, Camden) Electron Microscope Soc. of America, N.Y., Aug. 24-28, 1965

Geophysics and Astrophysics in the Laboratory—F. J. F. Osborne, M. P. Bachynski (RCA Ltd., Montreal) *Proc. of the Sixth Biennial Gas Dynamics Symp.*, Northwest-ern Univ. Press, 1965

Growing Cuprous Chloride Modulator Crystals, Method for—A. G. Salerno, L. J. Buszko (ECD, Som.) TN-596, *RCA Technical Notes*, Issue No. 13, Dec. 1964

Magnetometer, Simple Force—R. L. Harvy (Labs, Pr.) *The Review of Scientific Instruments*, Vol. 36, No. 8, Aug. 1965

Pure Inorganic Materials Analyses, Requirements of a General Analytical Laboratory in—S. J. Adler (Labs, Pr.) 9th Conf. on Analytical Chemistry, Gatlinburg, Tenn., Oct. 12, 1965

Pure Materials Analyses, Electrical Measurements for—L. R. Weisberg (Labs, Pr.) Conf. Analytical Chemistry, Gatlinburg, Tenn., Oct. 12, 1965

Temperature-Determining Apparatus, Integrated-Circuit—E. A. Williams (DEP-ASD, Burl.) TN-644, *RCA Technical Notes*, Issue No. 15, Mar. 1965

## LASERS

$\text{CaF}_2:\text{Im}^{2+}$  and the  $\text{CaF}_2:\text{Dy}^{2+}$  Optical Maser Systems—Z. J. Kiss (Labs, Pr.) 3rd International Conf. on Quantum Electronics, Paris

Laser Color Switching—J. M. Hammer, C. P. Wen (Labs, Pr.) Int'l. Electron Devices Mtg., Washington, D.C., Oct. 20-22, 1965

Laser Digital Devices—W. F. Kosonocky (Labs, Pr.) NATO Scientific Conf., Paris, France, Sept. 6-9, 1965

Laser Induction Pumping—H. J. Gerritsen, P. V. Goedertier (Labs, Pr.) TN-606, *RCA Technical Notes*, Issue No. 14, Mar. 1965

Raman Components of Laser Backscatter, Remote Observations Using—J. Cooney (DEP-AED, Pr.) 2nd Int'l. Symp. on Electromagnetic Sensing of the Earth From Satellites, Amer. Geophysical Univ., Amer. Meteorological Soc. & Optical Soc. of Amer., Miami Beach, Fla., Nov. 24, 1965

Solid-State Laser, A High-Efficiency High-Power—R. J. Pressley, P. V. Goedertier (Labs, Pr.) 1965 Int'l. Electron Device Conf., Washington, D.C., Oct. 20-22, 1965

## LINGUISTICS (& speech recognition)

Artificial Voice—H. F. Olson (Labs, Pr.) Audio Eng. Soc. Mtg., N.Y., Oct. 12, 1965

Speech Investigation Apparatus—H. E. Haynes, T. B. Martin (DEP-AppRes, Camden) TN-632, *RCA Technical Notes*, Issue No. 15, Mar. 1965

## LOGIC (theory)

Adaptive Techniques, System—M. Masonson (DEP-CSD, N.Y.) MILE-CON 9, Wash., D.C., Sept. 23, 1965; *Conf. Proceedings*

Propositional Calculus, An Approach to Heuristic Problem Solving and Theorem Proving in the—S. Amarel (Labs, Pr.) Conf. on Computer Science & Systems, Univ. of Western Ontario, Canada, Sept. 10-11, 1965

Review of: "A Method of Producing a Boolean Function Having an Arbitrary Prescribed Prime Implicant Table," (J. F. Gimpel, Princeton Univ., Princeton, N.J., Tech. Report No. 35, Mar. 1964, 23 ppd)—F. H. Fowler, Jr. (DEP-CSD, Camden) Review No. 7665, *Computing Reviews*, 6-3, May-June '65

Review of: "A Reduction Technique for Prime Implicant Tables," (J. F. Gimpel, Princeton Univ., Princeton, N.J., Tech. Report No. 40, Aug. 1964, 9 pp)—F. H. Fowler, Jr. (DEP-CSD, Camden) Review No. 7666, *Computing Reviews*, 6-3, May-June '65

Review of: "Implication Techniques for Boolean Functions (R. S. Gaines, Princeton Univ., Princeton, N.J., Tech. Report No. 39, Aug. 1964, 9 pp)—F. H. Fowler, Jr. (DEP-CSD, Camden) Review No. 7738, *Computing Reviews*, 6-3, May-June '65

Review of: "Principles and Application of Boolean Algebra," (S. A. Adelfo, Jr., C. F. Nolan, Hayden Pub. Co., N.Y., 1964, pp 319, \$8.00)—F. H. Fowler, Jr. (DEP-CSD, Camden) Review No. 7421, *Computing Reviews*, 6-3, Mar-Apr '65

Threshold Functions, Enumeration of Seven-Argument—R. C. Winder (Labs, Pr.) *IEEE Transactions on Electronic Computers*, Vol. EC-14, No. 3, June, 1965

## LOGIC ELEMENTS (& circuits)

Counter—E. Gloates, L. J. Busch (EDP, Camden) TN-615, *RCA Technical Notes*, Issue No. 14, Mar. 1965

Counter Circuit—A. Prieto (EDP, Palm Beach) TN-618, *RCA Technical Notes*, Issue No. 14, Mar. 1965

DTL Gates (Low-Power): Monolithic-Silicon Integrated-Circuit Types CD2200 (dual 4-input positive NAND), CD2201 (quadruple 2-input positive NAND), and CD2203 (J-K Flip-Flop with set-reset)—(Commercial Engineering, ECD, Hr.) *RCA Technical Bulletins CD2200-2201 and CD2203*; and *RCA Application Note ICAN-5024*, Nov. 1965

ECCSL Gates (Ultra-High Speed): Monolithic-Silicon Integrated-Circuit Types CD2150 (dual 4-input positive OR-NOR) CD2151 (dual 4-input positive OR-NOR with PHANTOM-OR capability); and CD2152 (8-input positive OR-NOR with PHANTOM-OR capability)—(Commercial Eng., ECD, Hr.) *RCA Technical Bulletin CD2150-2151-2152* and *RCA Application Note ICAN-5025*, Nov. 1965

ECCSL Gates (High-Speed): Monolithic-Silicon Integrated-Circuit Types CD2100 (dual 4-input positive OR-NOR), and CD2101 (quadruple 2-input positive NOR)—(Commercial Eng., ECD, Hr.) *RCA Technical Bulletin CD2100-2101*, and *RCA Application Note ICAN-5025*, Nov. 1965

High Speed Logic Circuit—M. D'Agostino (ECD, Som.) TN-622, *RCA Technical Notes*, Issue No. 14, Mar. 1965

High Speed Logic Arrangement—B. Walker (DEP-AppRes, Camden) TN-598, *RCA Technical Notes*, Issue No. 13, Dec. 1964

Laser Digital Devices—W. F. Kosonocky (Labs, Pr.) NATO Scientific Conf., Paris, France, Sept. 6-9, 1965

Latching Comparator Circuit Using Transistors—N. DiSanti, D. Hempel, D. Chase (DEP-CSD, N.Y.) TN-643, *RCA Technical Notes*, Issue No. 15, Mar. 1965

Review of: "On the Minimum Stage Realization of Switching Functions Using Logic Gates with Limited Fan-In," (G. L. Hicks, A. J. Bernstein, Princeton Univ., Princeton, N.J., Tech. Report No. 38, Aug. 1964, 12 pp)—F. H. Fowler, Jr. (DEP-CSD, Camden) Review No. 7737, *Computing Reviews*, 6-3, May-June '65

Review of: "Reducing Variable Dependency in Combinational Circuits," (A. J. Bernstein, Princeton Univ., Princeton, N.J., Tech. Report No. 37, July 1964, 9 pp)—F. H. Fowler, Jr. (DEP-CSD, Camden) Review No. 7734, *Computing Reviews*, 6-3, May-June '65

Universal Interface Circuit—R. K. W. Yee (ECD, Natick) TN-628, *RCA Technical Notes*, Issue No. 15, Mar. 1965

## MANAGEMENT

Product Assurance Interfaces in the Space Age—H. L. Wuerffel (DEP-AED, Pr.) Canadian Electronics Conf., Oct. 5, 1965, Toronto, Canada

## MATHEMATICS

Mathematics and the Physical Sciences—R. B. Marsten (DEP-AED, Pr.) Cinnaminson Jr. Sr. High School, Cinnaminson, N.J., Nov. 5, 1965

Paraboloid and a Hyperboloid of Surface of Revolutions, The Method of Total Variation of Parameters for Determination of the Best-Fit Surface and Its RMS Value of  $\alpha$ —T. Szirtes (RCA Ltd., Montreal) IEEE Canadian Electronics Conf., Toronto, Oct. 4-6, 1965

Propositional Calculus, An Approach to Heuristic Problem Solving and Theorem Proving in the—S. Amarel (Labs, Pr.) Conf. on Computer Science & Systems, Univ. of Western Ontario, Canada, Sept. 10-11, 1965

Review of: "Operations Research: Process and Strategy," (D. S. Stoller, Univ. of Calif. Press, Berkeley and Los Angeles 159 pp, \$5.00)—F. H. Fowler, Jr. (DEP-CSD, Camden) *Control Engineering*, July 1965

Review of: "Principles and Application of Boolean Algebra," (S. A. Adelfo, Jr., C. F. Nolan, Hayden Pub. Co., N.Y., 1964, pp 319, \$8.00)—F. H. Fowler, Jr. (DEP-CSD, Camden) Review No. 7421, *Computing Reviews*, 6-3, Mar-Apr '65

Review of: "The Theory and Probability," (B. V. Gnedenko, Charles Pub. Co., N.Y., 1962, pp 471, \$8.75)—F. H. Fowler, Jr. (DEP-CSD, Camden) Review No. 8028, *Computing Reviews*, 6-4, July-Aug '65

## MECHANICAL DEVICES

Bearing, Hollow Pivot-Point—R. J. Gehrung (H.I., Indpls.) TN-639, *RCA Technical Notes*, Issue No. 15, Mar. 1965

Indexing Mechanism (Card or Part)—L. B. Wolf (EDP, Palm Beach) TN-614, *RCA Technical Notes*, Issue No. 14, Mar. 1965

Positioning Mechanism (Circular Adjuster) for the Sub-Reflector of an 85-Ft Cassegrain Type Microwave Antenna—T. Szirtes (Labs, Pr.) TN-613, *RCA Technical Notes*, Issue No. 14, Mar. 1965

Thin-Walled Cylinders, Process for Making—A. O. Farrar (ECD, Hr.) TN-600, *RCA Technical Notes*, Issue No. 13, Dec. 1964

## MEDICAL ELECTRONICS

Contact Lens Tonometer—R. E. Morey (Labs, Pr.) TN-602, *RCA Technical Notes*, Issue No. 13, Dec. 1964

Telemetering Internal Biological Potentials with Passive-Tip Capsules—F. L. Hatke, L. E. Flory, V. K. Zworykin (Labs, Pr.) *Proceedings of the 5th Int'l. Conf. of Medical Electronics*, July 22, 1965

## OPTICS

Contrast-Enhancement Technique, Optical—W. A. Rose, L. P. Tabor (DEP-MSR, Mrstn.) TN-626, *RCA Technical Notes*, Issue No. 15, Mar. 1965

Infrared Polarizer—H. J. Gerritsen (Labs, Pr.) TN-608, *RCA Technical Notes*, Issue No. 14, Mar. 1965

## PLASMA PHYSICS

Amplification and Time-Delay Characteristics of the Plasma Density Wave in Germanium—Y. Kuniya (Labs, Pr.) *Japan Journal of Applied Physics*, Vol. 4, 1965

Cross-Polarized Electromagnetic Backscatter from Turbulent Plasmas—R. S. Ruffine, D. A. deWolf (Labs, Pr.) *Journal of Geophysical Research*, Vol. 70, No. 17, Sept. 1965

Microwave Radiation from Plasmas in Semiconductors and Experiments with InSb, Theory on—M. Toda (Labs, Pr.) Int'l. Conf. on Microwave Behavior of Ferrimagnetics and Plasmas, London, England, Sept. 13-17, 1965

Plasma Sheath Reduction by Electron Attachment Processes—A. I. Carswell, C. Richard (RCA Ltd., Montreal) Plasma Sheath Symp., Boston, Sept. 21-23, 1965

Plasma Surface Waves, Effects of Low-Frequency Instabilities on—L. S. Napoli, G. A. Swartz, H. T. Wexler (Labs, Pr.) *Physics of Fluids*, Vol. 8, No. 6, June, 1965

Solid State Plasma Waveguide in a Transverse Magnetic Field, Microwave Propagation in  $\alpha$ ; Part III—R. Hirota, K. Suzuki (Labs, Pr.) 20th Annual Mtg. of the Physical Society of Japan, Japan, Oct. 10-15, 1965

## PROPERTIES, ACOUSTIC

Superconducting Diode as a High-Frequency Sound Detector—B. Abeles, K. Keller, Y. Goldstein (Labs, Pr.) *Electronics Letters*, June, 1965

## PROPERTIES, ATOMIC (& molecular; crystallography)

Adsorption Phenomena in Terms of Two-Dimensional Fermi Statistics—J. D. Levine (Labs, Pr.) Int'l. Conf. on Thermionic Electrical Power Generation, London, England, Sept. 20-24, 1965

Band Structure of Bismuth Telluride, Bismuth Selenide and Their Respective Alloys—D. L. Greenaway, G. Harbecke (Labs, Pr.) Lecture-Seminar at Brown Univ., Providence, R. I., Sept. 30, 1965

Controlled Sublimation Technique and Its Utilization for the Crystal Growth of Hexamine—G. E. Gottlieb (Labs, Pr.) *Journal of the Electrochemical Society*, Vol. 112, No. 9, Sept., 1965

Cutting Electro-Optical Modulator Crystals, Method and Apparatus for—A. Sussman (Labs, Pr.) TN-595, *RCA Technical Notes*, Issue No. 13, Dec., 1964

Defect Structure in Silicon Surfaces After Thermal Oxidation—A. W. Fisher, J. A. Amick (Labs, Pr.) Electrochemical Soc. Mtg., Buffalo, N.Y.

Electron-Electron-Ion Collisional Recombination Coefficient—R. C. Stabler (Labs, Pr.) Gaseous Electronics Conf., Honeywell Research Inst., Minneapolis, Minn., Oct. 20-22, 1965

Growing Cuprous Chloride Modulator Crystals, Method for—A. G. Salerno, L. J. Buszko (ECD, Som.) TN-596, *RCA Technical Notes*, Issue No. 13, Dec. 1964

Ionic Crystals, The Observation of Intrinsic Surface States on—P. Mark, J. D. Levine (Labs, Pr.) Amer. Physical Soc. Conf., Chicago, Ill., Oct. 28-30, 1965

Ionic Crystals, Theory of Intrinsic Surface States on—P. Mark, J. D. Levine (Labs, Pr.) Amer. Physical Soc. Conf., Chicago, Ill., Oct. 28-30, 1965

Polar Impurities in Ionic Crystals, Collective Behavior of—W. Zernik (Labs, Pr.) *The Physical Review*, Vol. 139, No. 3A, Aug., 1965

Transport Phenomena of InSb in High Electric and Magnetic Fields—K. Ando (Labs, Pr.) 20th Annual Mtg. of the Physical Soc. of Japan, Japan, Oct. 10-15, 1965

Transverse Striations in Bi-Sb Alloy Single Crystals—W. M. Yim (Labs, Pr.) Metallurgical Soc. of Amer. Inst. Metallurgical Engrs., Detroit, Michigan, Oct. 17, 1965

## PROPERTIES, CHEMICAL (& preparation; analysis)

Diffusion Technique, A Solid-to-Solid—J. Scott, J. Olmstead (ECD, Som.) *RCA Review*, Vol. XXVI, No. 3, Sept. 1965

Nb<sub>3</sub>Sn Vapor-Deposition Process, Further Developments in the—H. C. Schindler, K. Strater (ECD, Hr.) AIME Metallurgical Soc. Symp. on Refractory Metals, Oct. 20, 1965

Phosphorus-Boron System, The Chemistry of the—C. C. Wang (Labs, Pr.) Amer. Chemical Society Symp., Atlantic City, N.J., Sept. 12, 1965

Pure Inorganic Materials Analyses, Requirements of a General Analytical Laboratory in—S. J. Adler (Labs, Pr.) 9th Conf. on Analytical Chemistry, Gatlinburg, Tenn., Oct. 12, 1965

Pure Materials Analyses, Electrical Measurements for—L. R. Weisberg (Labs, Pr.) Conf. Analytical Chemistry, Gatlinburg, Tenn., Oct. 12, 1965

Vacuum Evaporation of Ag<sub>2</sub>Te—R. Dabben (ECD, Pr.) 13th Nat'l. Infrared Information Symp., Pasadena, Calif., Oct. 12-14, 1965 (Classified Session)

## PROPERTIES, ELECTRONIC

Amplification and Time-Delay Characteristics of the Plasma Density Wave in Germanium—Y. Kuniya (Labs, Pr.) *Japan Journal of Applied Physics*, Vol. 4, 1965

Absorption of Transverse Microwave Phonons by Al-Pb Superconducting Diodes—B. Abeles, Y. Goldstein (Labs, Pr.) *Physics Letters*, Vol. 18, No. 1, Aug., 1965

Conducting Mechanism in Single Crystal B-Indium Sulfide In<sub>2</sub>S<sub>3</sub>—W. Rehwald, G. Harbecke (Labs, Pr.) *The Journal of Physical and Chemistry of Solids*, Vol. 26, No. 8, Aug., 1965

**Conduction of Electrons in Solids, Combined Effects of Sound and Electric Fields Upon the**—R. Klein, W. Rehwald (Labs, Pr.) Swiss Physical Society Mtg., Geneva, Switzerland, Sept., 1965

**Electron Emission from Solidifying Uranium Surfaces**—P. Sahn (Labs, Pr.) *Journal of Applied Physics*, Vol. 36, No. 8, Aug., 1965

**Electronic Interactions Between Silicon and Silicon Dioxide**—A. G. Revesz (Labs, Pr.) Int'l. Symp. on Basic Problems in Thin Film Physics, Göttingen, Germany, Sept. 6-11, 1965

**Fabrication-Parameter Effects on Structural and Electronic Properties of Thin CdS and CdSe Films**—F. V. Shallcross (Labs, Pr.) AIME Electronic Materials CMTE, Technical Conf., San Francisco, Calif., Sept. 7-9, 1965

**Glass Compositions (New) Showing Electronic Conductivity**—D. W. Roe (ECD, Lanc.) *Journal of Electrochemical Soc.*, Oct. 1965

**Langmuir Current Limit in the Presence of a Magnetic Field**—Joan Lurie (DEP-AED, Pr.) The Electron Devices Mtg., Washington, D.C., Oct. 20, 1965

**Phonons in a One-Dimensional Crystal, Decay Rate of**—J. Conway (Labs, Pr.) *Physics Letters*, Vol. 17, No. 1, June, 1965

**Polarized Absorption and Emission in an Octacoordinate Chelate of  $Eu^{3+}$** —J. Blanc, D. L. Ross (Labs, Pr.) *Journal of Chemical Physics*, Aug., 1965

**Resistance in the Mixed State of Type II Superconductors, On the Nature of**—J. Pearl (Labs, Pr.) *Physics Letters*, Vol. 17, No. 1, June, 1965

**Superconducting Properties of Ternary and Quaternary Alloys of Niobium**—R. E. Enstrom (Labs, Pr.) 4th Symp. on Refractory Metals, French Lick, Ind., Oct. 3-5, 1965

**Triplet State in Phthalocyanines, Observations of the**—W. F. Kosonocky, S. E. Harrison, R. Stander (Labs, Pr.) *The Journal of Chemical Physics*, Vol. 43, No. 3, Aug., 1965

**Seebeck Coefficient in N-Type Germanium-Silicon Alloys: Competition Region**—A. Amith (Labs, Pr.) *The Physical Review*, Vol. 139, No. 5A, Aug., 1965

**Tunneling in III-V Compound p-n Junctions**—J. Shewchun, R. M. Williams (Labs, Pr.) *Physical Review Letters*, Vol. 15, No. 4, July, 1965

## PROPERTIES, MAGNETIC

**Intrinsic Hysteresis in Type II Superconductors**—M. Cardona, J. Gittleman, B. Rosenblum (Labs, Pr.) *Physics Letters*, Vol. 17, No. 2, July, 1965

**Zeeman Spectra (High-Magnetic-Field) of  $Ni^{2+}$  and  $Co^{2+}$  in  $ZnO$** —H. A. Weakliem (Labs, Pr.) Zeeman Centennial Conf., Amsterdam, Netherlands, Sept. 6, 1965

## PROPERTIES, MECHANICAL

**Force Transmissibilities in Spacecraft Structures**—C. Osgood (DEP-AED, Pr.) 35th Symp. on Shock and Vibration, New Orleans, La., Oct. 28, 1965

## PROPERTIES, OPTICAL

**Crystal Growth and Electro-Optic Effect of Bismuth Germanate,  $Bi_4(GeO_4)_3$** —R. Nitsche (Labs, Pr.) *Journal of Applied Physics*, Vol. 36, No. 8, Aug., 1965

**Infrared Dielectric Constant and Ultraviolet Optical Properties of Solids with Diamond, Zinblend, Wurtzite, and Rocksalt Structure**—M. Cardona (Labs, Pr.) *Journal of Applied Physics*, Vol. 36, No. 7, July, 1965

**Preparation and Optical Properties of Group IV-VI Chalcogenides Having the  $Cd_2$  Structure**—R. Nitsche, D. L. Greenaway (Labs, Pr.) Colloque Int'l. Sur Derivés Semi-Metalliques, Paris, France, Sept. 1-3, 1965

**Photoconductive Detector, Sensitive Broadband**—H. S. Sommers, Jr., E. K. Gatchell (Labs, Pr.) Optical Soc. Mtg., Phila., Pa., Oct. 6-8, 1965

**Photoconductivity in  $CdGa_2S_4$** —H. Kiess (Labs, Pr.) Schweiz. Naturf. Gesellschaft, Geneva, Switzerland, Sept. 24-25, 1965

## PROPERTIES, THERMAL

**Surface Superconductivity, Thermal Conductivity for the Study of**—T. Seidel (Labs, Pr.) 5th Conf. on Thermal Conductivity, Denver, Colo., Oct. 20-22, 1965

## RADAR

**Ferrite Phase Shifter, Design and Performance of a 20-kW Latching Nonreciprocal X-Band**—W. A. Schilling (ECD, Pr.) W. W. Siekanowicz (ECD, Pr.) E. Walsh (ECD, Pr.) I. Bardash (DEP-MSR, Mrstn.) I. Gordon (Labs, Pr.) Nat'l. Electronics Conf., Chicago, Ill., Oct. 23, 1965; *Conf. Record*

**Radar Cross-Section at Long Waves**—H. Benecke (DEP-SEER, Mrstn.) *AMRAC Proceedings*, XII, Part 1, 1965

## RADIATION DETECTION (& measurement)

**Photomultipliers (New) for Pulse Counting**—H. R. Krall (ECD, Lanc.) IEEE Nuclear Science Symp., San Francisco, Calif., Oct. 18-20, 1965; *IEEE Symp. Preprint*, Oct. 1965

## RADIATION EFFECTS

**(Solar Cells): The Effect of Li on Radiation Damage in Silicon Solar Cell Devices**—J. J. Wysocki, B. Goldstein, P. Rappaport (Labs, Pr.) 1965 Photovoltaic Specialist Conf., Greenbelt, Md., Oct. 18-20, 1965

**Transistors, High-Energy Radiation Damage in Silicon**—G. Brucker, W. Dennehy, A. Holmes-Siedle (DEP-AED, Pr.) *IEEE Proceedings on Nuclear Science*, Nov. Issue, 1965

## RADIO BROADCASTING (entertainment)

**Stereo and SCA Operation, Analysis of System Characteristics of**—A. H. Bott (BCD, Meadow Lands) IEEE Broadcast Group, Washington, D.C., Sept. 24, 1965; *IEEE Transactions on BTR*

## RADIO RECEIVERS (entertainment)

**FM Tuners (3- and 4-Coil) Using N-P-N Silicon Transistors, Performance Analysis of**—R. V. Fournier, C. H. Lee, R. T. Peterson (ECD, Som.) Nat'l. Electronics Conf., Chicago, Ill., Oct. 25-27, 1965; *Conf. Record*

## RECORDING (techniques & materials)

**Sensing the Width of a Moving Tape, Apparatus for**—R. T. Ziehm, H. Morello (EDP, Camden) TN-583, *RCA Technical Notes*, Issue No. 13, Dec. 1964

**Wideband Direct Recording with High Frequency Bias**—W. B. Hendershot (Record Div., Indpls.) 11th Conf. on Magnetism & Magnetic Mat'ls., San Francisco, Calif., Nov. 16, 1965; *Conf. Record*

## RECORDING (audio equipment)

**Vertical Tracking Angle of Stereophonic Phonograph Pickups, Techniques for Measuring the**—J. G. Woodward (Labs, Pr.) *Journal of the Audio Engineering Society*, Vol. 13, No. 3, July, 1965

## RECORDING (digital equipment)

**Read-Write Switching Arrangement**—C. M. Wright (RCA Svc. Co., Wash., D.C.) TN-617, *RCA Technical Notes*, Issue No. 14, Mar. 1965

## RECORDING (image equipment)

**Electronic Splicing in RCA Tape Recorders**—M. B. Finkelstein (BCD, Camden) SMPTE Conf., Detroit, Michigan, Oct. 13, 1965

## RELIABILITY (& quality control)

**System Effectiveness, A Queuing Approach to**—R. E. Purvis, R. L. McLaughlin (RCA Svc. Co., Cherry Hill) 3rd ASQC Product Maintainability Working Seminar, Phila., Pa. Oct. 12-13, 1965

## SOLID-STATE DEVICES

**(Diodes): Surface Potential Measurements of Lithium Drifted Germanium Diodes**—D. E. Davies, P. P. Webb (RCA Ltd., Montreal) IEEE Nuclear Science Symp., San Francisco, Oct. 18-20, 1965

**Low-Input-Voltage Power Conditions, A Review of**—P. D. Gardner (ECD, Som.) IEEE Electron Devices Mtg., Washington, D.C., Oct. 21-23, 1965

**Tetrad, A Low-Power MOS**—N. Ditrick, M. Mitchell (ECD, Som.) IEEE Electron Devices Mtg., Washington, D.C., Oct. 21-23, 1965

**Transfluxor, Increasing the Number of Control Levels in a**—A. I. Stoller (Labs, Pr.) TN-621, *RCA Technical Notes*, Issue No. 14, Mar. 1965

**Transistor, Indium Antimonide Thin-Film**—V. L. Frantz (Labs, Pr.) *Proceedings IEEE*, July, 1965

**(Transistors): Analysis of a High-Power, High-Frequency Planar Transistor Structure Using the Equivalent Network Approach**—A. P. Anderson, K. Thomson (RCA Ltd., Montreal) IEEE Canadian Electronics Conf., Toronto, Oct. 4-6, 1965

**(Transistors): Detection Techniques for Non-destructive Second-Breakdown Testing**—P. Schiff, R. L. Wilson (ECD, Som.) IEEE Electron Devices Mtg., Washington, D.C., Oct. 21-23, 1965

**(Transistors): Experimental Demonstration and Theory of a Solution to Second Breakdown in Silicon Power Transistors**—D. Stolnitz (ECD, Som.) IEEE Electron Devices Mtg., Washington, D.C., Oct. 21-23, 1965

**Transistors, Gallium Arsenide MOS**—H. Becke, R. Hall, J. White (ECD, Som.) *Solid-State Electronics*, Oct. 1965

**Transistors, High-Energy Radiation Damage in Silicon**—G. Brucker, W. Dennehy, A. Holmes-Siedle (DEP-AED, Pr.) *IEEE Proceedings on Nuclear Science*, Nov. Issue 1965

**(Transistors, MOS): Noise in Metal-Oxide-Semiconductor Field-Effect Transistors**—D. R. Nicol (RCA Ltd., Montreal) IEEE Canadian Electronics Conf., Toronto, Oct. 4-6, 1965

**Transistor (VHF) with Second-Breakdown Protection, Design of a**—D. R. Carley, R. Rosenzweig (ECD, Som.) IEEE Electron Devices Mtg., Washington, D.C., Oct. 21-23, 1965

## SPACE COMMUNICATION (mass media & scientific)

**Antenna System of Canada's First Satellite Communications Ground Station**—P. Folds (RCA Ltd., Montreal) IEEE Canadian Electronics Conf., Toronto, Oct. 4-6, 1965

**Cassegrainian Feed for Wideband Satellite Communications**—P. Folds, S. Kolmos, N. K. Chitre, R. Schwerdtfeger (RCA Ltd., Montreal) *RCA Review*, Vol. XXVI, No. 3, Sept. 1965

**Multiple-Access Considerations for Communications Satellites**—J. Jacoby, Dr. F. Assadourian (DEP-CSD, N.Y.) MIL-E-CON 9, Wash., D.C., Sept. 24, 1965; *Conf. Proceedings*

**Plasma Sheath Reduction by Electron Attachment Processes**—A. I. Carswell, C. Richard (RCA Ltd., Montreal) Plasma Sheath Symp., Boston, Sept. 21-23, 1965

## SPACE ENVIRONMENT

**Space Research, Canadian Industry in**—F. G. R. Warren (RCA Ltd., Montreal) IEEE Canadian Electronics Conf., Toronto, Oct. 4-6, 1965

## SPACE NAVIGATION (& guidance; tracking)

**Review of: "A Critical Look at Vehicle Control Techniques,"** E. B. Stear, *Astronautics and Aerospace Eng.* 1, 7, Aug. '63—F. H. Fowler, Jr. (DEP-CSD, Camden) Review No. 6932, *Computing Reviews*, 6-1, Feb.-Mar. '65

## SPACECRAFT (& space missions)

**Force Transmissibilities in Spacecraft Structures**—C. Osgood (DEP-AED, Pr.) 35th Symp. on Shock and Vibration, New Orleans, La., Oct. 28, 1965

**Planning of Space Missions, Graphical Synthesis and**—S. G. Miller (DEP-SEER, Mrstn.) *Proc. 2nd Space Congress*, Cocoa Beach, Fla., Apr. 1965

**Ranger Mission**—H. J. Sheetz (DEP-AED, Pr.) Morris County Engineers Club, Morris-town, N. J., Oct. 19, 1965

**(Solar Cells): A Comparison of Silicon and Gallium Arsenide Solar Cells for a Solar Mission**—J. V. Foster, J. R. Swain (NASA-AMES Res. Center) S. H. Winkler, F. R. Schwarz (DEP-AED, Pr.) 1965 Photovoltaic Specialists Conf. Goddard Space Flight Center, Washington D.C., Oct. 20, 1965

**Spacecraft Technology**—H. Perkel (DEP-AED, Pr.) IEEE Student Branch Caldwell Labs., Columbus, Ohio, Oct. 12, 1965

## SPACECRAFT INSTRUMENTATION

**PCM Encoder for the ISIS-A Satellite**—W. A. Evans, R. G. Harrison, M. J. J. Teare (RCA Ltd., Montreal) IEEE Canadian Electronics Conf., Toronto, Oct. 4-6, 1965

**Ranger Television System**—B. P. Miller (DEP-AED, Pr.) *RCA Review*, Vol. XXVI, No. 3, Sept. 1965

**(Telemetry): A 400-MC, 5W Solid State FM/PM Modulated Transmitter for Spacecraft Telemetry**—J. Abdulezer, J. C. Boag, J. Saunders (RCA Ltd., Montreal) IEEE Canadian Electronics Conf., Toronto, Oct. 4-6, 1965

## SUPERCONDUCTIVITY (& cryoelectrics)

**Absorption of Transverse Microwave Phonons by Al-Pb Superconducting Diodes**—B. Abeles, Y. Goldstein (Labs, Pr.) *Physics Letters*, Vol. 18, No. 1, Aug., 1965

**Cryogenic Techniques, Communications Applications of**—B. B. Bossard (DEP-CSD, N.Y.) Nat'l. Science Foundation Lecture Series, Boulder, Colo., Aug. 1965

**High-Frequency Sound Detector, Superconducting Diode as a**—B. Abeles, K. Keller, Y. Goldstein (Labs, Pr.) *Electronics Letters*, June, 1965

**Intrinsic Hysteresis in Type II Superconductors**—M. Cardona, J. Gittleman, B. Rosenblum (Labs, Pr.) *Physics Letters*, Vol. 17, No. 2, July, 1965

**Resistance in the Mixed State of Type II Superconductors, On the Nature of**—J. Pearl (Labs, Pr.) *Physics Letters*, Vol. 17, No. 1, June, 1965

**Superconducting Properties of Ternary and Quaternary Alloys of Niobium**—R. E. Enstrom (Labs, Pr.) 4th Symp. on Refractory Metals, French Lick, Ind., Oct. 3-5, 1965

**Surface Superconductivity, Thermal Conductivity for the Study of**—T. Seidel (Labs, Pr.) 5th Conf. on Thermal Conductivity, Denver, Colo., Oct. 20-22, 1965

## TELEVISION BROADCASTING (entertainment)

**TV Camera Setup Without Outside Test Equipment**—A. Reisz (BCD, Camden) IEEE Broadcast Group, Washington, D.C., Sept. 25, 1965

Vidicons, Recent Advances in—S. Lasof (ECD, Lanc.) IEEE Broadcast Symp., Washington, D.C., Sept. 23-25, 1965; *IEEE Trans. on BTR*

#### TELEVISION EQUIPMENT (non-entertainment)

Ranger Television Systems—B. P. Miller (DEP-AED, Pr.) *RCA Review*, Vol. XXVI, No. 3, Sept. 1965

Storage Vidicons, Resolution, Noise, and Harmonic Analysis in—P. Parzen (DEP-AED, Pr.) Optical Soc. of America, Phila., Pa., Oct. 7, 1965

#### TELEVISION RECEIVERS (entertainment)

Color Noise Reduction—R. N. Rhodes, A. Macovski (H.I., Indpls.) TN-586, *RCA Technical Notes*, Issue No. 13, Dec. 1964

Dual Triode APC Phase Detector—R. N. Rhodes (H.I., Indpls.) TN-584, *RCA Technical Notes*, Issue No. 13, Dec. 1964

Sawtooth Voltage Wave Generator—L. Arlan (DEP-ASD, Burl.) TN-587, *RCA Technical Notes*, Dec. 1964

Single-Tube Oscillator and Reactance Tube Combination—R. N. Rhodes (H.I., Indpls.) TN-585, *RCA Technical Notes*, Issue No. 13, Dec. 1964

Television Sound Signal Recovery Circuit—L. A. Freedman (DEP-AED, Pr.) TN-593, *RCA Technical Notes*, Issue No. 13, Dec. 1964

UHF Local-Oscillator Switching-Circuit Transient Protection—P. C. Olsen (H.I., Indpls.) TN-589, *RCA Technical Notes*, Issue No. 13, Dec. 1964

Vertical Deflection Compensation—A. H. Rickling (H.I., Indpls.) TN-588, *RCA Technical Notes*, Issue No. 13, Dec. 1964

#### THIN FILMS (techniques & properties)

Comment on: "Potential Distribution and Negative Resistance in Thin Oxide Films" (by T. W. Hickmott, J.A.P., Vol. 35, p. 2679, 1964)—A. G. Revez (Labs, Pr.) *Journal of Applied Physics*, Vol. 36, No. 7, July 1965

Deposition of Silicon Upon Sapphire Substrates—P. Robinson, C. W. Mueller (Labs, Pr.) AIME Meeting of Material Science and Technology in Integrated Electronics, San Francisco, Calif., Sept. 20, 1965

Electronic Interactions Between Silicon and Silicon Dioxide—A. G. Revez (Labs, Pr.) Int'l. Symp. on Basic Problems in Thin Film Physics, Göttingen, Germany, Sept. 6-11, 1965

Fabrication-Parameter Effects on Structural and Electronic Properties of Thin CdS and CdSe Films—F. V. Shallcross (Labs, Pr.) AIME Electronic Materials CMTE, Technical Conf., San Francisco, Calif., Sept. 7-9, 1965

#### TUBES, ELECTRON (design & performance)

Photomultipliers (New) for Pulse Counting—H. R. Krall (ECD, Lanc.) IEEE Nuclear Science Symp., San Francisco, Calif., Oct. 18-20, 1965; *IEEE Symp. Preprint*, Oct. 1965

Special Tube Types—L. W. Aurick (ECD, Lanc.) *S-9 Magazine*, Sept. 1965

Storage Vidicons, Resolution, Noise, and Harmonic Analysis in—P. Parzen (DEP-AED, Pr.) Optical Soc. of America, Phila., Pa., Oct. 7, 1965

Traveling-Wave Tube (Multifunction)—A Versatile Microwave Component for Military Systems—M. Milten, H. J. Wolkstein, G. Hodowanec, R. McMurrough (ECD, Hr.) IEEE Electron Devices Mtg., Washington, D.C., Oct. 20-22, 1965

Vidicons, Recent Advances in—S. Lasof (ECD, Lanc.) IEEE Broadcast Symp., Washington, D.C., Sept. 23-25, 1965; *IEEE Trans. on BTR*

#### TUBE COMPONENTS (materials & fabrication)

Filament for Beam Tube—H. B. Law (Labs, Pr.) TN-635, *RCA Technical Notes*, Issue No. 15, Mar. 1965

Frame Grid—G. M. Rose, Jr. (ECD, Hr.) TN-634, *RCA Technical Notes*, Issue No. 15, Mar. 1965

Glass Compositions (New) Showing Electronic Conductivity—D. W. Roe (ECD, Lanc.) *Journal of Electrochemical Soc.*, Oct. 1965

(Heaters): Rectifier Tube—W. K. Batzle, W. L. Arnold (ECD, Hr.) TN-624, *RCA Technical Notes*, Issue No. 14, Mar. 1965

Target-to-Mesh Spacing Means for Image Orthicon Tubes—P. W. Kaseman, J. G. Ziedonis (ECD, Lanc.) TN-630, *RCA Technical Notes*, Issue No. 15, Mar. 1965

Target-to-Mesh Spacing System for Image Orthicon Tubes—J. G. Ziedonis, P. W. Kaseman (ECD, Lanc.) TN-629, *RCA Technical Notes*, Issue No. 15, Mar. 1965

(Thermionics): Heat Pipe Performance—W. B. Hall (ECD, Lanc.) Thermionic Conv. Specialists Conf., San Diego, Calif., Oct. 25-27, 1965

Thin-Walled Cylinders, Process for Making—A. O. Farrar (ECD, Hr.) TN-600, *RCA Technical Notes*, Issue No. 13, Dec. 1964

#### VACUUM (techniques)

Pumping System and Single-Wall Chamber for  $10^{-13}$  Torr—W. G. Henderson, J. T. Mark (ECD, Lanc.) Amer. Vacuum Society Symp., NYC, Sept. 29, Oct. 1, 1965

Spaced Bellows—M. E. Moi (Labs, Pr.) TN-619, *RCA Technical Notes*, Issue No. 14, Mar. 1965

Vacuum Evaporation of Ag<sub>2</sub>Te—R. Dalven (ECD, Pr.) 13th Nat'l. Infrared Information Symp., Pasadena, Calif., Oct. 12-14, 1965 (Classified Session)

### AUTHOR INDEX

Subject listed opposite each author's name indicates where complete citation to his paper may be found in the subject index. Where an author has more than one paper, his name is repeated for each.

#### BROADCAST AND COMMUNICATIONS PRODUCTS DIV.

Both, A. H. radio broadcasting  
Clark, R. N. antennas  
Coleman, Dr. J. W. laboratory equipment  
Coutts, M. D. laboratory equipment  
Davidson, A. L. antennas  
Finkelstein, M. B. recording (image)  
Marshall, Jr., T. G. circuit analysis  
Reisner, Dr. J. H. laboratory equipment  
Reisner, Dr. J. H. laboratory equipment  
Reisz, A. television broadcasting  
Reynolds, R. A. acoustics  
Sadashige, K. laboratory equipment

#### DEP AEROSPACE SYSTEMS DIVISION

Arlan, L. circuits, electronic  
Dion, E. F. circuits, electronic  
Drew, L. C. circuits, integrated  
Hillman, B. electro-optics  
Kee, R. C. circuits, electronic  
Kidd, M. circuits, integrated  
Klein, J. J. circuits, electronic  
Williams, E. A. circuits, integrated

#### DEP APPLIED RESEARCH

Ammon, G. computer storage  
Bergman, R. H. computer components  
Cooperman, M. circuits, electronic  
Cooperman, M. computer components  
Hannan, W. J. electro-optics  
Hannan, W. J. amplification  
Haynes, H. E. electro-optics  
Haynes, H. E. linguistics  
Kaupp, H. R. computer components  
Martin, T. B. linguistics  
Walker, B. logic elements

#### DEP ASTRO-ELECTRONICS DIV.

Brucker, G. radiation effects  
Cooney, J. geophysics  
Dennehy, W. radiation effects  
Fagen, J. environmental engineering  
Freedman, L. A. television receivers  
Holmes-Siedle, A. radiation effects  
Lorraine, J. L. circuits, electronic

Lurie, Joan properties, electrical  
Mangolds, B. environmental engineering  
Marsten, R. B. mathematics  
Miller, B. P. spacecraft instrumentation  
Osgood, C. properties, mechanical  
Parzen, P. television equipment  
Perkel, H. spacecraft  
Schwarz, F. R. energy conversion  
Sheetz, H. J. spacecraft  
Winkler, S. H. energy conversion  
Wuerffel, H. L. management  
McClanahan, J. environmental engineering

#### DEP CENTRAL ENGINEERING

Whitmore, F. D. communication, voice

#### DEP COMMUNICATIONS SYSTEMS DIV.

Anzalone, P. circuits, electronic  
Assadourian, Dr. F. communications systems  
Bossard, B. B. superconductivity  
Chase, D. logic elements  
DiSanti, N. logic elements  
Ernst, R. L. electromagnetic waves  
Fowler, Jr. F. H. logic  
Fowler, Jr. F. H. circuit analysis  
Fowler, Jr. F. H. circuit analysis  
Fowler, Jr. F. H. logic elements  
Fowler, Jr. F. H. logic elements  
Fowler, Jr. F. H. mathematics  
Fowler, Jr. F. H. logic  
Fowler, Jr. F. H. mathematics  
Fowler, Jr. F. H. circuit analysis  
Fowler, Jr. F. H. computer applications  
Fowler, Jr. F. H. computers  
Foy, Jr. J. J. circuits, electronic  
Glasgal, R. filters, electric  
Hawik, H. E. circuits, electronic  
Hempel, D. logic elements  
Jacoby, J. communications systems  
Klapper, J. circuits, electronic  
Markard, E. circuits, electronic  
Masonson, M. communications systems  
Menkes, E. D. circuits, electronic  
Moore, C. J. communications systems  
Rosencrans, C. A. circuits, packaged  
Rosenthal, D. circuits, electronic  
Schmidt, E. circuits, electronic  
Simshauser, E. circuits, electronic  
Yuan, S. circuits, electronic

#### DEP MISSILE AND SURFACE RADAR DIV.

Bardash, I. electromagnetic waves  
Rose, W. A. optics  
Tabor, L. P. optics

#### DEP SYSTEMS ENGINEERING AND EVALUATION RESEARCH

Benecke, H. radar  
Miller, S. G. spacecraft

#### ELECTRONIC COMPONENTS AND DEVICES

Arnold, W. I. tube components  
Aurick, L. W. tube, electron  
Batzle, W. K. tube components  
Becke, H. solid-state devices  
Buszko, L. J. laboratory equipment  
Buzard, R. J. energy conversion  
Carley, D. R. solid-state devices  
D'Agostino, M. logic elements  
Dalven, R. properties, chemical  
Deegan, T. E. circuits, electronic  
Ditrick, N. solid-state devices  
Farrar, A. O. mechanical devices  
Feryszka, R. circuits, electronic  
Fournier, R. V. radio receivers  
Gardner, P. circuits, electronic  
Gardner, P. D. solid-state devices  
Hall, R. solid-state devices  
Hall, W. B. energy conversion  
Hanchett, G. D. communication, voice  
Harbaugh, W. E. energy conversion  
Harmon, J. W. circuits, electronic  
Hart, O. P. circuits, electronic  
Henderson, W. G. vacuum  
Hodowanec, G. tubes, electron  
Hoover, M. V. amplification  
Kaseman, P. W. tube components  
Kaseman, P. W. tube components  
Krall, H. R. radiation detection  
Krey, R. A. displays  
Lasof, S. television broadcasting  
Lee, C. H. radio receivers  
Ling, K. S. energy conversion  
Mark, J. T. vacuum  
Mendelson, R. M. communication, voice  
McMurrough, R. tubes, electron  
Milden, M. tubes, electron  
Mitchell, M. solid-state devices  
Olmstead, J. laboratory equipment  
Peterson, R. T. radio receivers  
Roe, D. W. properties, electrical  
Rose, Jr. G. M. tube components  
Rosenzweig, R. solid-state devices  
Salerno, A. G. laboratory equipment  
Schiff, P. solid-state devices  
Schilling, W. A. electromagnetic waves  
Schindler, H. C. properties, chemical  
Schroeder, J. O. amplification  
Scott, J. laboratory equipment  
Shefsiek, P. K. energy conversion  
Shoemaker, R. E. energy conversion  
Siekawicz, W. W. electromagnetic waves  
Slonitz, D. solid-state devices  
Strater, K. properties, chemical  
Toole, J. M. energy conversion  
Walsh, E. electromagnetic waves  
White, J. solid-state devices

Wilson, R. L. solid-state devices  
Wolkstein, H. J. tubes, electron  
Yee, R. K. W. logic elements  
Ziedonis, J. G. tube components  
Ziedonis, J. G. tube components

#### ELECTRONIC DATA PROCESSING

Busch, L. J. logic elements  
Damerou, E. A. computer components  
Fulcher, E. M. circuits, electronic  
Gleates, E. logic elements  
Gollub, R. computer components  
Kaufmann, K. G. computer components  
Morello, H. recording  
Prieto, A. logic elements  
Schilling, R. G. circuits, packaged  
Stiefel, R. C. computer applications  
Wales, J. A. circuits, packaged  
Wolf, L. B. graphic arts  
Wolf, L. B. computer components  
Ziehm, R. T. recording (techniques & materials)

#### HOME INSTRUMENTS DIVISION

Carlson, D. J. circuits, electronic  
Gehring, R. J. mechanical devices  
Macovski, A. television receivers  
Olson, P. C. television receivers  
Rhodes, R. N. television receivers  
Rhodes, R. N. television receivers  
Rhodes, R. N. television receivers  
Rickling, A. H. television receivers  
Rogers, G. F. interference

#### RESEARCH AND ENGINEERING (Staff)

Leyton, E. M. circuits, electronic

#### RCA LABORATORIES

Abeles, B. properties, acoustic  
Abeles, B. properties, electrical  
Adler, S. J. laboratory equipment  
Amarel, S. logic  
Amick, J. A. properties, atomic  
Amith, A. properties, electrical  
Ando, K. properties, atomic  
Beelitz, H. R. computer storage  
Blanc, J. properties, electrical  
Burns, J. R. circuits, electronic  
Cardona, M. properties, magnetic  
Cardona, M. properties, optical  
Caulton, M. electromagnetic waves  
Clorfaine, A. S. amplification  
Conway, J. properties, electrical

deWolf, D. A. antennas  
 deWolf, D. A. electromagnetic waves  
 deWolf, D. A. electromagnetic waves  
 Dorsey, D. P. circuits, electronic  
 Dorsey, D. P. circuits, electronic  
 Dorsey, D. P. circuits, electronic  
 Dresner, J. circuits, electronic  
 Ellis, S. G. energy conversion  
 Enstrom, R. E. properties, electrical  
 Fisher, A. W. properties, atomic  
 Flory, L. E. medical electronics  
 Frantz, V. L. solid-state devices  
 Gatchell, E. K. properties, optical  
 Gerritsen, H. J. optics  
 Gerritsen, H. J. lasers  
 Gittleman, J. properties, magnetic  
 Goedertier, P. V. lasers  
 Goedertier, P. V. lasers  
 Goldstein, B. energy conversion  
 Goldstein, P. laboratory equipment  
 Goldstein, Y. properties, acoustic  
 Goldstein, Y. properties, electrical  
 Gordon, I. electromagnetic waves  
 Gottlieb, G. E. properties, atomic  
 Greenaway, D. L. properties, optical  
 Greenaway, D. L. properties, atomic  
 Guaracini, J. computer storage  
 Hammer, J. M. lasers  
 Harbeke, G. properties, electrical  
 Harbeke, G. properties, atomic  
 Harrison, S. E. properties, electrical  
 Harvey, R. L. laboratory equipment  
 Hatke, F. L. medical electronics  
 Hernqvist, K. G. energy conversion  
 Herzog, G. B. amplification  
 Hirota, R. electromagnetic waves  
 Hom, A. energy conversion  
 Hook, H. O. education  
 Keller, K. properties, acoustic  
 Kiess, H. properties, optical  
 Kiss, Z. J. lasers  
 Klein, R. properties, electrical

Klopfenstein, R. W. computer applications  
 Kosonocky, W. F. properties, electrical  
 Kosonocky, W. F. lasers  
 Kuniya, Y. plasma physics  
 Law, H. B. tube components  
 Levine, J. D. properties, atomic  
 Levine, J. D. properties, atomic  
 Levine, J. D. properties, atomic  
 Lewin, M. H. computer storage  
 Mark, P. properties, atomic  
 Mark, P. properties, atomic  
 Mark, P. H. circuits, electronic  
 May, A. J. acoustics  
 Miller, H. S. circuits, electronic  
 Moi, M. E. vacuum  
 Morey, R. E. medical electronics  
 Mueller, C. W. thin films  
 Munson, H. G. communications systems  
 Napoli, L. S. plasma physics  
 Nitsche, R. properties, optical  
 Nitsche, R. properties, optical  
 Olson, H. F. acoustics  
 Olson, H. F. acoustics  
 Pearl, J. properties, electrical  
 Perkins, D. energy conversion  
 Powlis, R. A. circuits, electronic  
 Pressley, R. J. lasers  
 Rajchman, J. A. computer storage  
 Rappaport, P. energy conversion  
 Rappaport, P. energy conversion  
 Rehwald, W. properties, electrical  
 Rehwald, W. properties, electrical  
 Revesz, A. G. properties, electrical  
 Revesz, A. G. thin films  
 Robinson, B. B. geophysics  
 Robinson, P. thin films  
 Rosenblum, B. properties, magnetic  
 Ross, D. L. properties, electrical  
 Ruffine, R. S. electromagnetic waves  
 Sahm, P. properties, electrical  
 Samusenko, A. G. circuits, electronic  
 Seidel, T. properties, thermal

Shallcross, F. V. properties, electrical  
 Shewchun, J. properties, electrical  
 Sobol, H. electromagnetic waves  
 Sommers, Jr., H. S. properties, optical  
 Stabler, R. C. properties, atomic  
 Standler, R. properties, electrical  
 Stoller, A. I. circuits, electronic  
 Susman, A. laboratory equipment  
 Suzuki, K. electromagnetic waves  
 Swartz, G. A. plasma physics  
 Szirtes, T. antennas  
 Toda, M. plasma physics  
 Vohl, P. energy conversion  
 Volkmann, J. E. acoustics  
 Volkmann, J. E. acoustics  
 Vural, B. amplification  
 Wang, C. C. properties, chemical  
 Weekliem, H. A. properties, magnetic  
 Weinstein, H. circuit analysis  
 Weisberg, L. R. laboratory equipment  
 Wen, C. P. lasers  
 Wexler, H. T. plasma physics  
 Williams, R. M. properties, electrical  
 Winder, R. C. logic  
 Woodward, J. G. recording (audio)  
 Wysocki, J. J. energy conversion  
 Yim, W. M. properties, atomic  
 Zernik, W. properties, atomic  
 Zworykin, V. K. medical electronics

Carswell, A. I. electro-optics  
 Chitre, N. K. antennas  
 Davies, D. E. solid-state devices  
 Evans, W. A. spacecraft instrumentation  
 Faldes, P. antennas  
 Faldes, P. antennas  
 Harrison, R. G. spacecraft instrumentation  
 Johnston, T. W. geophysics  
 Kaufman, H. electromagnetic waves  
 Kamlos, S. antennas  
 Moore, W. H. acoustics  
 Nicol, D. R. solid-state devices  
 Oberai, A. S. amplification  
 Osborne, F. J. F. geophysics  
 Osborne, F. J. F. geophysics  
 Richard, C. plasma physics  
 Richard, C. electro-optics  
 Roberts, G. E. electromagnetic waves  
 Saunders, J. spacecraft instrumentation  
 Schwardfeger, R. antennas  
 Shkarofsky, I. P. geophysics  
 Szirtes, T. mathematics  
 Teare, M. J. J. spacecraft instrumentation  
 Thomson, K. solid-state devices  
 Warren, F. G. R. space environment  
 Webb, P. P. solid-state devices

#### RCA SERVICE COMPANY

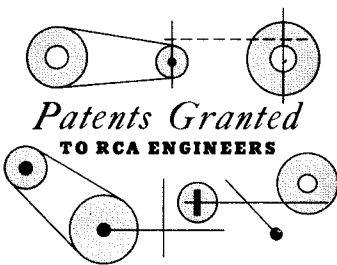
McLaughlin, R. L. reliability  
 Purvis, R. E. reliability  
 Wright, C. M. computer components

#### RECORD DIVISION

Hendershot, W. B. recording (techniques & materials)

#### RCA VICTOR CO., LTD. (Montreal)

Abdulazer, J. spacecraft instrumentation  
 Anderson, A. P. circuits, electronic  
 Anderson, A. P. solid-state devices  
 Bachynski, M. P. geophysics  
 Bachynski, M. P. geophysics  
 Boag, J. C. spacecraft instrumentation  
 Carswell, A. I. plasma physics  
 Carswell, A. I. electro-optics



### Patents Granted TO RCA ENGINEERS

AS REPORTED BY RCA DOMESTIC  
 PATENTS, PRINCETON  
 DEFENSE ELECTRONIC PRODUCTS

Logical Gating and Routing Circuit—H. Zimmerman (DEP, Camden) *U.S. Pat. 3,191,067*, June 22, 1965 (assigned to U.S. Gov't.)

Plural-Channel Pulse Generator with Feedback Controlling Duration of Output Pulses from Said Channels—R. W. Scheyhing, A. A. Gorski (DEP-MSR, Mrstn.) *U.S. Pat. 3,193,768*, July 6, 1965 (assigned to U.S. Gov't.)

Logical and Circuit Utilizing a Tunnel Diode—M. M. Kaufman (DEP-AppRes, Camden) *U.S. Pat. 3,207,924*, Sept. 21, 1965

Tunnel Diode Device—R. H. Bergman (DEP-AppRes, Camden) *U.S. Pat. 3,209,162*, Sept. 28, 1965

Negative Resistance Diode Circuit—M. Cooperman (DEP-AppRes, Camden) *U.S. Pat. 3,209,170*, Sept. 28, 1965

Monostable Circuit for Generating Pulses of Short Duration—W. G. Rumble (W.C., Van Nuys) *U.S. Pat. 3,209,173*, Sept. 28, 1965

Switching Circuits—H. D. Blaustein, J. A. Pierce (DEP-CSD, Camden) *U.S. Pat. 3,209,339*, Sept. 28, 1965

Negative Resistance Circuits—B. Rabinovici, C. A. Renton (DEP-CSD, N.Y.) *U.S. Pat. 3,210,564*, Oct. 5, 1965

Processing Apparatus Utilizing Simulated Neurons—F. L. Putzrath (DEP-CSD, Camden) *U.S. Pat. 3,211,832*, Oct. 12, 1965

Method for Preparing Cured Polymeric Etch Resist Using a Xerographic Developer Containing a Curable Polymer—S. W. Johnson (DEP, Camden) *U.S. Pat. 3,215,527*, Nov. 2, 1965

Difference Amplifier Including Delay Means and Two-State Device Such as Tunnel Diode—T. R. Mayhew (DEP-AppRes, Camden) *U.S. Pat. 3,215,854*, Nov. 2, 1965

Control Circuit for Ferroelectric Gate—H. T. Gnuse (DEP-W.C. Div., Van Nuys) *U.S. Pat. 3,215,990*, Nov. 2, 1965

#### ELECTRONIC COMPONENTS AND DEVICES

Phosphor Deposition—H. A. Stern (ECD, Lanc.) *U.S. Pat. 3,199,939*, Aug. 10, 1965, (assigned to U.S. Gov't.)

Signal Translating Circuit—F. Sterzer (ECD, Pr.) *U.S. Pat. 3,207,991*, Sept. 21, 1965

Negative Resistance Amplifier Utilizing a Directional Filter—F. Sterzer (ECD, Pr.) *U.S. Pat. 3,208,003*, Sept. 21, 1965

Method of Fabricating Electron Tubes—H. V. Knauf, Jr. (ECD, Hr.) *U.S. Pat. 3,208,137*, Sept. 28, 1965

High Voltage Electron Discharge Diode—O. H. Schade, Sr. (ECD, Hr.) *U.S. Pat. 3,209,395*, Sept. 28, 1965

Memory Matrix Assembly with Separate, Interconnecting Arm Members—L. B. Smith, A. J. Erikson (ECD, Needham, Mass.) *U.S. Pat. 3,209,336*, Sept. 28, 1965

Circuit and Structure for Photo-Amplifier Using One Large and One Small Photocell—C. P. Hadley (ECD, Lanc.) *U.S. Pat. 3,214,591*, Oct. 26, 1965

Cathode Assembly for Electron Tube—E. R. Larson (ECD, Hr.) *U.S. Pat. 3,214,626*, Oct. 26, 1965

Cathode Assembly for Electron Tube—E. R. Larson (ECD, Hr.) *U.S. Pat. 3,214,628*, Oct. 26, 1965

Ohmic Contacts to III-V Semiconductive Compound Bodies—L. D. Armstrong, E. G. Buckley (ECD, Som.) *U.S. Pat. 3,214,654*, Oct. 26, 1965

Manufacture of Electron Discharge Devices Having Cathodes—C. H. Meltzer (ECD, Hr.) *U.S. Pat. 3,214,821*, Nov. 2, 1965

Orienting Articles of Manufacture—W. T. Ackermann (ECD, Hr.) *U.S. Pat. 3,215,238*, Nov. 2, 1965

Methods and Materials for Metallizing Ceramic or Glass Bodies—R. A. Krey (ECD, Hr.) *U.S. Pat. 3,215,555*, Nov. 2, 1965

Color Display System Utilizing Biasing Means to Reduce the Effect of Mismatch—A. M. Morrell (ECD, Lanc.) *U.S. Pat. 3,215,771*, Nov. 2, 1965

Double-Ended High Frequency Electron Tube—W. J. Helwig (ECD, Hr.) *U.S. Pat. 3,215,886*, Nov. 2, 1965

#### HOME INSTRUMENTS DIVISION

Television Tuner—T. D. Smith (H.I. Indpls.) *U.S. Pat. 3,205,720*, Sept. 14, 1965

Flyback Transformers—R. E. Hurley (H. I., Indpls.) *U.S. Pat. 3,213,399*, Oct. 19, 1965

#### RCA LABORATORIES

Methods of Making a Sheet Array of Magnetic Metal Elements—G. R. Briggs (Labs, Pr.) *U.S. Pat. 3,206,342*, Sept. 14, 1965

Apparatus for Fabricating an Indexing Element for a Color Image Reproducing Device—R. D. Thompson (Labs, Pr.) *U.S. Pat. 3,206,546*, Sept. 14, 1965

Magnetic Metal Sheet Memory Array and Method of Making It—G. R. Briggs (Labs, Pr.) *U.S. Pat. 3,206,732*, Sept. 14, 1965

Memory Systems Having Flux Logic Memory Elements—G. R. Briggs (Labs, Pr.) *U.S. Pat. 3,206,733*, Sept. 14, 1965

Memory Systems Having Flux Logic Memory Elements—G. R. Briggs (Labs, Pr.) *U.S. Pat. 3,206,734*, Sept. 14, 1965

Methods of Preparing Etch Resist Using an Electrostatic Image Developer Composition Including a Resin Hardener—E. C. Giaimo, Jr. (Labs, Pr.) *U.S. Pat. 3,207,601*, Sept. 21, 1965

Logic Circuit Employing Transistors and Negative Resistance Diodes—G. B. Herzog (Labs, Pr.) *U.S. Pat. 3,207,913*, Sept. 21, 1965

Superconductor Circuits—R. W. Ahrons (Labs, Pr.) *U.S. Pat. 3,207,921*, Sept. 21, 1965

Semiconductor Devices—C. W. Mueller (Labs, Pr.) *U.S. Pat. 3,208,924*, Sept. 28, 1965

Process for Preparing Luminescent Materials—P. N. Yocum, S. M. Thomsen (Labs, Pr.) *U.S. Pat. 3,208,950*, Sept. 28, 1965

Pulse Generator Employing Minority Carrier Storage Diodes for Pulse Shaping—J. J. Amodei (Labs, Pr.) *U.S. Pat. 3,209,171*, Sept. 28, 1965

Simultaneous Identical Electrostatic Image Recording on Multiple Recording Elements—R. G. Olden (Labs, Pr.) *U.S. Pat. 3,210,185*, Oct. 5, 1965

Semiconductor Devices—S. M. Christian (Labs, Pr.) *U.S. Pat. 3,211,970*, Oct. 12, 1965

Magnetic Systems Using Multi-Aperture Cores—J. A. Rajchman, A. W. Lo (Labs, Pr.) *U.S. Pat. 3,212,067*, Oct. 12, 1965

Thermoelectric Apparatus—H. S. Sommers, Jr. (Labs, Pr.) *U.S. Pat. 3,212,272*, Oct. 19, 1965

Purification Apparatus Utilizing a Thermoelectric Heat Pump—H. S. Sommers, Jr. (Labs, Pr.) *U.S. Pat. 3,212,999*, Oct. 19, 1965

Magnetic Record Reproducing Apparatus—V. K. Zworykin, P. K. Weimer (Labs, Pr.) *U.S. Pat. 3,213,206*, Oct. 19, 1965

Electrical Heater—C. J. Young (Labs, Pr.) *U.S. Pat. 3,214,572*, Oct. 26, 1965

Transistor Exponential Circuit—C. A. Von Urff, Jr. (Labs, Pr.) *U.S. Pat. 3,214,603*, Oct. 26, 1965

Photosensitive Information Retrieval Device—V. K. Zworykin (Labs, Pr.) *U.S. Pat. 3,215,848*, Nov. 2, 1965

Binary Inverter Circuit Employing Unipolar Field Effect Transistors—M. E. Seleyk (Labs, Pr.) *U.S. Pat. 3,215,861*, Nov. 2, 1965

Pulse Translating Apparatus—C. J. Hirsch (Labs, Pr.) *U.S. Pat. 3,216,012*, Nov. 2, 1965

#### BROADCAST AND COMMUNICATIONS PRODUCTS DIVISION

Polarity Responsive Switching Circuit for Reducing Decision Ambiguity—F. M. Brook, L. A. Manaresi (BCD, Camden) *U.S. Pat. 3,210,570*, Oct. 5, 1965

Linearized Field-Effect Transistor Circuit—G. F. Rogers (BCD, Pr.) *U.S. Pat. 3,213,299*, Oct. 19, 1965

Switch for Providing a Positional Binary Number Code—J. G. Young (BCD, Camden) *U.S. Pat. 3,215,790*, Nov. 2, 1965

#### ELECTRONIC DATA PROCESSING

Rigid Information Storage Device Upon Which a Layer of Resilient Material is Disposed—E. A. Damerau, R. H. Jenkins (EDP, Camden) *U.S. Pat. 3,212,075*, Oct. 12, 1965

#### RCA VICTOR CO., LTD.

Ferroelectric Device, Ferroelectric Body and Method of Fabrication Thereof—E. Fatuzzo, G. Harbeke, W. Ruppel (RCA Ltd., Switzerland) *U.S. Pat. 3,213,027*, Oct. 19, 1965

## Meetings

JAN. 25-27, 1966: 12th Symp. on Reliability, IEEE, G-R, ASQC, et al.; Sheraton Palace Hotel, San Francisco, Calif. **Prog. Info.:** A. R. Park, Genl. Precision Inc., 1370 Encinitas Rd., San Marcos, Calif.

JAN. 26-29, 1966: American Physical Society Mtg.; New York City, **Prog. Info.:** K. K. Darrow, The American Phys. Soc., 538 W. 120th St., New York, N.Y.

JAN. 31-Feb. 2, 1966: Intl. Symp. on Information Theory, IEEE, G-IT; UCLA, Los Angeles, Calif. **Prog. Info.:** A. V. Balakrishnan, Dept. of Engrs., Univ. of Calif., Los Angeles, Calif.

FEB. 2-4, 1966: 7th Winter Conv. on Aerospace & Electronic Systems, IEEE, G-AES, L.A. District; Los Angeles, Calif. **Prog. Info.:** IEEE Office, 3600 Wilshire Blvd., Los Angeles, Calif.

FEB. 9-11, 1966: Intl. Solid State Circuits Conf., IEEE, G-CT, Univ. of Pa.; Univ. of Penna. & Sheraton Hotel, Phila., Pa. **Prog. Info.:** J. D. Meindl, U.S. Army Elec. Command, Fort Monmouth, N.J.

FEB. 24-26, 1965: Interdisciplinary Aspects of Radiative Energy Transfer Mtg., Amer. Phys. Soc.; Philadelphia, Pa. **Prog. Info.:** J. J. Welsh, Space Sciences Lab., Genl. Electric Co., Valley Forge Space Tech. Center, Box 8555, Phila., Pa.

FEB. 28-MARCH 2, 1966: American Crystallographic Association Mtg., Amer. Phys. Soc.; Austin, Texas. **Prog. Info.:** W. L. Kehl, Secretary, Gulf Res. and Dev. Co., PO Drawer 2038, Pittsburgh, Pa.

MARCH 2-4, 1966: Scintillation & Semiconductor Counter Symp., IEEE, G-NS; Shoreham Hotel Wash., D.C. **Prog. Info.:** W. A. Higinbotham, Brookhaven Natl. Labs., Upton, L.I., N.Y.

MARCH 21-25, 1966: IEEE Intl. Convention, IEEE, All Groups, TAB Comms.; Coliseum & New York Hilton Hotel, N.Y., N.Y. **Prog. Info.:** IEEE Headquarters, Box A, Lenox Hill Station, N.Y., N.Y.

MARCH 22-23, 1966: Biomagnetics Mtg., Amer. Phys. Soc.; Univ. of Illinois. **Prog. Info.:** M. F. Barnothy, Univ. of Illinois, 833 S. Wood St., Chicago, Ill.

MARCH 30-APR. 1, 1966: Engineering Aspects of Magnetohydrodynamics Mtg., Amer. Soc. of Mech. Engrs., IEEE, AIAA; Princeton University. **Prog. Info.:** R. G. Jahn, Guggenheim Labs., Forrestal Res. Center, Princeton, N.J.

MARCH 31-APR. 1, 1966: Conf. on Analysis & Synthesis of Networks, IEEE W. German Section VDE; Stuttgart, W. Germany. **Prog. Info.:** H. H. Burghoff, 6 Frankfurt S10, Stresemann Allee 21, VDE Haus, W. Germany.

APR. 12-24, 1966: Cleveland Electronics Conf., IEEE Cleveland Section, et al.; Cleveland, Ohio. **Prog. Info.:** IEEE Headquarters, Box A, Lenox Hill Station, N.Y., N.Y.

APR. 12-15, 1966: 4th Quantum Elec. Conf., IEEE, G-ED, G-MTT, et al.; Towne House, Phoenix, Ariz. **Prog. Info.:** J. P. Gordon, Bell Telephone Labs., Murray Hill, N.J.

APR. 18-19, 1966: 1st Natl. ISA Symp. on Maintenance, ISA; Wilmington, Delaware. **Prog. Info.:** H. S. Wilson, Div. Dir., Moore Products Co., 2011 Concord Pike, Wilmington, Delaware.

APR. 18-21, 1966: Spring URSI-IEEE Mtg., IEEE-URSI; Natl. Academy of Science, Wash., D.C. **Prog. Info.:** IEEE Headquarters, Box A, Lenox Hill Station, N.Y., N.Y.

APR. 20-22, 1966: 1966 INTERMAG (Intl. Conf. on Magnetics), IEEE, G-MAG, VDE, AF; Liederhalle, Stuttgart, Germany. **Prog. Info.:** Dr. E. W. Pugh, IBM Corp., 1000 Westchester Ave., White Plains, N.Y.

APR. 20-22, 1966: Southwestern IEEE Conf. & Elec. Exhib. (SWIEECCO), IEEE, Region 5; Dallas Meml. Auditorium, Dallas, Texas. **Prog. Info.:** Dr. Robert Carrel, Collins Radio Co., Dallas, Texas.

## PROFESSIONAL MEETINGS

### DATES and DEADLINES

Be sure deadlines are met—consult your Technical Publications Administrator or your Editorial Representative for the lead time necessary to obtain RCA approvals (and government approvals, if applicable). Remember, abstracts and manuscripts must be so approved BEFORE sending them to the meeting committee.

APR. 26-28, 1966: 1966 Region Six Ann. Conf., IEEE; Pioneer Intl. Hotel, Tucson, Ariz. **Prog. Info.:** Dr. L. O. Huelsman, Tech. Papers Chairman, 1966 IEEE Region Six Ann. Conf., c/o Department of EE, Univ. of Ariz., Tucson, Ariz.

APR. 26-28, 1966: Spring Joint Computer Conf., IEEE, AFIPS, ACM; Boston Civic Ctr., Boston, Mass. **Prog. Info.:** Dr. H. Anderson, Digital Equip. Corp., Maynard, Mass.

### Calls for Papers

MARCH 21-25, 1966: 1966 IEEE Intl. Convention, IEEE; N.Y. Hilton Hotel and the Coliseum. **Deadline:** Abstracts, 10/15/65; Manuscripts, 1/14/66. **FOR INFO.:** IEEE Headquarters, Box A, Lenox Hill Station, N.Y., N.Y.

APR. 20-22, 1966: 1966 Intl. Nonlinear Magnetics Conf. (INTERMAG), IEEE, G-Mag VDE; Stuttgart, Germany. **Deadline:** Abstracts, 12/7/65; Manuscripts, 4/1/66. **TO:** Dr. E.W. Pugh, IBM Corp., 1000 Westchester Ave., White Plains, N.Y.

APR. 26-28, 1966: Spring Joint Computer Conf., IEEE, AFIPS, ACM; Boston Civic Ctr., Boston, Mass. **For Deadline Info.:** IEEE Headquarters, Box A, Lenox Hill Station, N.Y., N.Y.

MAY 2-4, 1966: 1966 AIAA Communications Satellite Systems Conf., AIAA, IEEE; Wash., D.C. **Deadline:** Abstracts, 11/30/65; Manuscripts, 3/21/66. **TO:** N. Feldman, Electronics Dept., The Rand Corp., 1700 Main St., Santa Monica, Calif.

MAY 4-6, 1966: 1966 Electronic Components Conf., EIA, IEEE; Marriott Twin Bridges Motor Hotel, Wash., D.C. **Deadline:** Abstract, 10/8/65; Manuscripts, 1/30/66. **TO:** R. A. Gerhold, Chairman, Tech. Prog. Committee, U.S. Army Electronics Command, (AMSEL-KL-1), Fort Monmouth, N.J.

MAY 10-12, 1966: 15th Natl. Telemetry Conf., IEEE, AIAA-ISA; Prudential Center, Boston, Mass. **Deadline:** Abstracts, 1/15/66. **TO:** J. Kelley, Program Chairman, NASA-Electronics Res. Center, 575 Technology Sq., Cambridge, Mass.

MAY 11-13, 1966: 12th Natl. ISA Analysis Instrumentation Symp., ISA; The Shamrock Hilton, Houston, Texas. **Deadline:** Abstracts, 1/15/66. **TO:** G. I. Doering Program Dir., Industrial Nucleonics Corp., 1205 Chesapeake Ave., Columbus, Ohio.

MAY 16-18, 1966: NAECON (Natl. Aerospace Elec. Conf.), IEEE, G-ANE-AIAA, Dayton Section, Dayton, Ohio. **Deadline:** Abstracts, 1/3/66. **TO:** R. E. Henning, c/o Sperry Microwave Co., PO Box 1828, Clearwater, Fla.

JUNE 1-4, 1966: Acoustical Society of America Mtg.; Boston, Mass. **Deadline:** Abstracts, 3/2/66. **TO:** L. Batchelder, Raytheon Co., 20 Seyon St., Waltham, Mass.

JUNE 6-8, 1966: Design & Construction of Large Steerable Aerials for Satellite Communications, Radio Astronomy & Radar Mtg., IEEE, IEE, et al.; IEE, Savoy Place, London, England. **For Deadline Info.:** IEEE Headquarters, Box A, Lenox Hill Station, N.Y., N.Y.

JUNE 13-17, 1966: Soc. for Applied Spectroscopy Mtg.; Chicago, Ill. **Deadline:** Abstracts, 3/1/66. **TO:** J. E. Burroughs, Borg-Warner Corp., Roy C. Ingersoll Res. Ctr., Wolf and Algonquin Rds., Des Plaines, Ill.

JUNE 14-17, 1966: Applied Mechanics Mtg., Amer. Phys. Soc.; Univ. of Minn. **Deadline:** Abstracts, 1/15/66. **TO:** R. Plunkett, 107 Aero Bldg., Univ. of Minnesota, Minneapolis, Minn.

JUNE 15-17, 1966: 1966 IEEE Intl. Communications Conf., IEEE, G-ComTech, et al.; Sheraton Hotel, Phila., Pa. **Deadline:** Abstracts, 3/1/66. **FOR INFO.:** IEEE Headquarters, Box A, Lenox Hill Station, N.Y., N.Y.

JUNE 20-22, 1966: San Diego Symp. for Biomedical Engineering, IEEE, U.S. Naval Hosp.; San Diego, Calif. **For Deadline Info.:** IEEE Headquarters, Box A, Lenox Hill Station, N.Y., N.Y.

JUNE 21-23, 1966: Conf. on Precision Electromagnetic Measurements, IEEE, G-IM NBS; NBS Standards Lab., Boulder, Colo. **For Deadline Info.:** Dr. Kiyo Tomiyasu, Genl. Electric Co., Schenectady, N.Y.

JULY 4-8, 1966: Rarefied Gas Dynamics Mtg., Amer. Phys. Soc.; Oxford, England. **Deadline:** Abstracts, March 1966. **TO:** C. L. Brundin, Dept. of Eng. Science, Univ. of Oxford, Parks Rd., Oxford, England.

AUG. 17-19, 1966: Joint Automatic Control Conf., IEEE, G-AC, et al.; Univ. of Wash. **Deadline:** Abstracts, 1/3/66. **FOR INFO.:** IEEE Headquarters, Box A, Lenox Hill Station, N.Y., N.Y.

AUG. 23-26, 1966: WESCON (Western Electronic Show & Convention), IEEE, WEMA; Sports Arena, Los Angeles. **Deadline:** Abstracts, approx. 5/1/65. **FOR INFO.:** IEEE LA. Office, 3600 Wilshire Blvd., Los Angeles, Calif.

AUG. 29-31, 1966: 2nd Intl. Congress on Instrum. in Aerospace Simulation Facilities, IEEE, G-AED; Stanford Univ., Stanford, Calif. **For Deadline Info.:** IEEE Headquarters, Box A, Lenox Hill Station, N.Y., N.Y.

SEPT. 5-9, 1966: Intl. Organization for Pure and Applied Biophysics Mtg., Amer. Physical Soc.; Vienna, Austria. **Deadline:** Abstracts, 5/15/66. **TO:** E. Weidenahus, Viennese Medical Academy, Alserstr 4, Vienna 9, Austria.

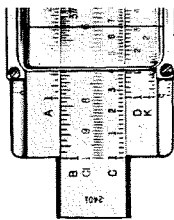
SEPT. 8-13, 1966: Physics of Semiconductors Mtg., Physical Soc. of Japan; Tokyo, Japan. **For Deadline Info.:** G. M. Hatoyama, PSJ, Hongo, PO Box 28, Tokyo, Japan.

SEPT. 12-24, 1966: Eastern Conv. on Aerospace & Electronic Systems, IEEE, G-AED; Wash. Hilton Hotel, Wash., D.C. **For Deadline Info.:** IEEE Headquarters, Box A, Lenox Hill Station, N.Y., N.Y.

SEPT. 21-23, 1966: Physics of Semiconducting Compounds, Inst. of Physics and Physical Soc.; Univ. of Wales. **For Deadline Info.:** R. H. Jones, Dept. of Physics, Univ. College of Swansea, Singleton Park, Swansea, England.

OCT. 3-5, 1966: Natl. Electronics Conf., IEEE, et al.; McCormick Place, Chicago, Ill. **Deadline:** Abstracts, approx. 5/1/66. **FOR INFO.:** Natl. Elec. Conf., 228 N. LaSalle St., Chicago 1, Illinois.

NOV. 14-16, 1966: 19th Ann. Conf. on Eng. in Medicine & Biology, ISA, IEEE; Sheraton-Palace Hotel, San Francisco, Calif. **Deadline:** Abstracts, 7/15/66. **TO:** Dr. Victor Bolie, Genl. Chairman, Autoneutics, 3370 Miraloma Ave., Anaheim, Calif.



## DR. OLSON RECEIVES MICROPHONE AWARD

Dr. Harry F. Olson, Director of the Acoustical & Electromechanical Research Laboratory, RCA Laboratories recently received the *Maker of the Microphone Award* for 1965 for his many developments in electro-acoustic devices, and particularly for the velocity microphone. The award, inaugurated three years ago by the family of the late Emile Berliner, inventor of the microphone, disk record and player, was presented to Dr. Olson by Oliver Berliner, grandson of Emile Berliner, on October 8 at NBC Radio Network headquarters in New York.

## "BEST PAPER" AWARD TO MARYE

Robert Marye has been awarded the 1965 *Scott Helt Award Plaque* for contributing the best paper during 1964 to the *IEEE Transactions on Broadcasting*. Mr. Marye is Manager, Low Power Transmitter Engineering, for the Broadcast and Communications Products Division, Meadow Lands, Pa. His article was entitled "Phase Equalization of TV Transmitters," appeared in the Dec. 1964 issue.

## EIGHT MOORESTOWN ENGINEERS GET TECHNICAL EXCELLENCE AWARDS

The first recipients of the quarterly *Technical Excellence Awards* at the Missile and Surface Radar Division, Moorestown, N. J., have been announced by Chief Engineer R. A. Newell. The award winners are: T. V. Bolger, R. C. Durham, H. M. Finn, L. H. Fulton, T. B. Howard, A. F. Lisicky, R. D. Mitchell, and L. J. Schipper.

## DR. S. CHRISTIAN NAMED VISITING RESEARCH ASSOCIATE AT CORNELL

Dr. Schuyler M. Christian, of the Research Services Laboratory, RCA Laboratories, Princeton, has been appointed a Visiting Research Associate in the Electrical Engineering Department of the Engineering College, Cornell University, Ithaca, N. Y. Dr. Christian, whose appointment is for one year, began his new duties in Ithaca about September 15.

The appointment of Dr. Christian as a Visiting Research Associate will continue the close association between Cornell University and RCA Laboratories in materials research and solid state device work. Professor Lester F. Eastman of Cornell recently completed an assignment at RCA Laboratories as a Visiting Member of the Technical Staff during his sabbatical year.

## DISTAFF CHANGES ON RCA ENGINEER

Mrs. Judy Carter has been promoted to RCA ENGINEER Editorial Secretary, replacing Mrs. Carmella Marchionni, who had held that position on the Editorial Staff for several years. Mrs. Marchionni left RCA to start a family, and our best wishes go with her. Mrs. Carter had been with the RCA ENGINEER and RCA Staff Technical Publications office since 1962. Miss Dottie Ritter has joined the office staff to assume Mrs. Carter's duties on the RCA ENGINEER and on staff activities connected with technical papers and reports.—*The Editors*.

## DR. WATTERS NAMED DIVISION VICE PRESIDENT, DEFENSE ENGINEERING

Appointment of Dr. Harry J. Watters to the newly created position of Division Vice President, Defense Engineering, RCA Defense Electronic Products, has been announced by Arthur L. Malcarney, RCA Group Executive Vice President. Formerly Chief Defense Engineer, Defense Engineering, Dr. Watters will continue to be responsible for Applied Research, SEER, and Defense Microelectronics activities, as well as technical and engineering performance for the five-division Defense Electronic Prod-



Dr. H. J. Watters

ucts organization (Communications Systems Division, Aerospace Systems Division, Astro-Electronics Division, Missile and Surface Radar Division, and West Coast Division).

Dr. Watters joined RCA in 1962. Previously, he had served as assistant to Dr. Edwin H. Land, President of Polaroid Corporation. Before becoming associated with Polaroid, Dr. Watters had been involved in scientific and technical matters of national importance. He served as Technical Assistant to the Science Advisor to the President of the United States for both Dr. James R. Killian, Jr. and Dr. George B. Kistiakowsky. While associated with Polaroid Corporation, Dr. Watters continued to serve as a consultant to the White House Office of Science and Technology. He also was a member of the ad hoc Committee, under the chairmanship of Dr. Jerome B. Wiesner, which reported to the President on U. S. military and civilian space activities. From 1956 to 1958, Dr. Watters was chief of nuclear systems research and development for the Atomic Energy Commission's Division of Military Application.

Dr. Watters received his BS degree from Purdue University in 1949, and did his graduate work at MIT in Physics and Electronics. He received his MS in 1953 and continued his work in Physics to obtain a PhD from MIT in 1955. From 1956 to 1960, Dr. Watters was Professor of Physics at Georgetown University, Washington, D.C.

## LICENSED ENGINEERS

- J. L. Cammarato, DEP-MSR, Moorestown, PE-20388, Mass.
- J. R. Neubauer, DEP-CSD, Camden, PE-14344, N. J.
- H. M. Langley, RCA Home Instruments Div., Indpls., PE-11822-E, Ind.
- C. Hirsch, RCA Research and Engineering, Princeton, PE-18811, N. Y.
- H. Perry, ECD, Lancaster, PE-1144-E, Pa.
- Dr. T. T. N. Bucher, DEP-CSD, Camden, PE-14341, N. J.
- L. C. Linesch, ECD, Cincinnati, PE-30626, Ohio

## SEVEN FROM RCA HOLD OFFICE IN IEEE-GEWS

RCA is strongly represented among national officeholders of the IEEE Group on Engineering Writing and Speech (GEWS) for the 1965-66 term: C. A. Meyer, ECD Harrison, is Chairman of the Group; C. W. Sall, RCA Labs, Princeton, is Secretary; in addition to Sall and Meyer, members of the Administrative Committee include W. B. Dennen, MSR Moorestown, and Dr. J. S. Donal, Jr., RCA Labs, Princeton. Standing Committee Chairmen include: Eleanor M. McElwee, ECD Harrison (Education); R. Samuel, ECD Somerville (Membership); and Dennen (Meetings).

Editor of the *EWS Newsletter* is C. W. Fields who is also Chairman of the Philadelphia Section of GEWS and an Associate Editor of the *Transactions on EWS*.

## RCA LABS TECHNICAL WRITING AND ORAL PRESENTATION COURSE

A course in technical writing and oral presentation began at RCA Laboratories on October 10 under the auspices of Rider College. The course, scheduled to continue until January 10, 1966, consists of ten sessions devoted mainly to technical writing, and five to oral presentations, visual aids, and speech techniques. Emphasis is being given to workshop participation, practice, and class discussion. Classes are conducted on Monday evenings from 5 p.m. to 6:40 p.m. Those who complete the course satisfactorily will qualify for an RCA tuition refund for the fee of \$75 paid to Rider College. Textbooks and other instructional materials are provided free.

The course, in which enrollment has been limited to 25, is being taught by Joseph Chapline, who is currently on special assignment in Technical Writing to RCA-EDP at Cherry Hill, where he also serves as a consultant to the RCA Service Company.

## RECEIVING TUBE AND CONSUMER SEMICONDUCTOR PRODUCT ENGINEERING CONSOLIDATED IN SOMERVILLE

The Commercial Receiving Tube and Semiconductor Division was established a few years ago as part of the realignment of the former Electron Tube Division and Semiconductor Materials Division into RCA Electronic Components and Devices. Prior to this realignment, separate product engineering functions were maintained with receiving tubes at Harrison, New Jersey, and consumer semiconductors at Somerville, New Jersey.

Now, both product engineering groups have been consolidated in the Somerville, New Jersey plant, providing better coordination between tubes and semiconductor product development and a more efficient and objective applications engineering service.—*P. L. Farina*

## MOS SYMPOSIUM

A group of engineers from ECD and Princeton conducted an educational symposium on MOS devices and applications at the Naval Research Labs. (Washington) on June 15-16 and at NASA Langley Field (Virginia) on August 10-11. The topics covered were device physics, equivalent circuit representation, and amplifier and digital applications. The total audience substantially exceeded 200.—*D. H. Wamsley*

### RCA MONOGRAM REVISED

Effective Oct. 1, a revised version of the RCA Monogram was initiated, as shown. The modernized version should be phased into all publications as quickly as possible, (although existing supplies of material like correspondence paper should be used up first).

The following is extracted from a *Standardizing Topics*, Vol. 14, No. 7, Oct. 1965, issued by Product Engineering Standardizing, Cherry Hill, N.J.

"The [revised] RCA monogram standard . . . is the result of careful study and development by the Corporate Identification Committee; it is the first significant change in the monogram in over twenty years.

"The committee's objective was to update the character of the monogram with a number of minor alterations. As a result, to many not familiar with the details of the monogram design, it may not be readily apparent that changes have been made.

"The [revised] monogram illustrated is effective Oct. 1, 1965, and is to be phased into operations in an orderly manner. Existing stocks of monograms, nameplates, blank forms and printed materials are to be used up in the normal course of business.

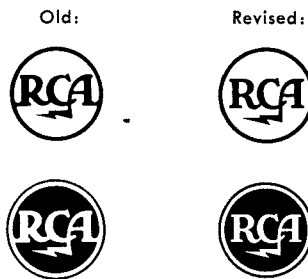
"All new production items, and all replenishments for depleted stocks, which include the RCA monogram in their design, are to incorporate the new monogram standard.

"A new *Corporate Trademark Manual* is in preparation and will become available in the near future. This manual, together with the associated corporate standards, will provide information and guidance on monogram applications.

"Section 31 of the *Corporate Standard Books*, which includes monogram standards, is being reissued with a complete complement of precise secondary masters. These may be used in the preparation of photom-

### RCA COMMUNICATIONS, INC., PLANS AIRLINES SERVICE NETWORK

Plans for an Automated Information and Reservations Combined Operations Network (AIRCON) to service international and foreign-flag airlines has been announced by RCA Communications, Inc., New York. Employing two RCA Spectra 70/45 computers, AIRCON will provide a complete intra- and inter-line message and reservations exchange service for all subscriber airlines. The AIRCON Center—to be installed in RCA Communications Central Telegraph Office in New York—will handle messages over subscribers' existing wire line networks in North America and via their international leased circuits with points abroad.



asters, drawings and other artwork in which the monogram is included.

"The Corporate Identification Committee is responsible for advising and consulting with the major operating units on all matters relative to the Corporation's program of corporate identification. Its members are: **Mort Gaffin**, Chairman, **Charles L. Greiter**, Corporate Trademark Attorney, **John D. Hill**, **Robert M. Jones**, **Tucker P. Madawick**, and **John L. Parvin**."

### EDP BUILDS NEW MULTI-COMPUTER SPECTRA 70 SYSTEMS CENTER AT CHERRY HILL

RCA Electronic Data Processing is establishing a Spectra 70 Systems Center at its headquarters at Cherry Hill, N.J. The first Spectra 70/15 units are installed and operating. By the end of 1965, EDP expects to have three 70/15 computers, two 70/25's and one 70/45—the first computer with integrated circuitry—installed at the Center. Early next year, another 70/45 and two 70/55's will be placed in operation.

The new center, in Building 205, will serve as a demonstration area and as a proving ground for RCA Spectra 70 customers. The Center will give RCA customers an opportunity to develop, refine, and test software on configurations that exactly duplicate what they will eventually use—but months in advance of delivery. In addition, visitors will be able to see the complete product line in a single area. The Center will contain peripheral equipment for the Spectra 70's, including 62 magnetic tape units, random access memories, and Video Data Terminals. The RCA 3301 and 301 Center in Building 202, Cherry Hill, will be continued as a service to customers using those models.

One of the major users of the new Spectra 70 Center will be the EDP Systems Programming Department. Consisting of three design groups—Languages, Operating Systems, and Communications and Utilities—plus a Project Planning and Management activity, Systems Programming is responsible for the Spectra 70 software. At present, RCA has over 200 people working on Spectra 70 software at Cherry Hill. These in-

clude programmers with experience acquired on other RCA computers and projects, including such military programs as BMEWS and AUTODIN, plus some programmers from RCA International licensees in Europe and Japan.

The programmers got a running start by developing simulators on the RCA 601 for every model in the Spectra 70, and were testing Spectra 70 software for months before they had a working piece of the new equipment.

In describing RCA's philosophy on Spectra 70 software, **A. W. Carroll**, Manager, Systems Programming, pointed to several criteria. "We are dedicated to using proven state of the art techniques and we're employing RCA's research resources similar to the way they're used in developing hardware. RCA Laboratories in Princeton are studying advanced theories in languages and software construction. Also, an Applied Research activity is trying to solve problems by utilizing advanced concepts.

"Another premise in our broad philosophy is standardization—standardizing parameters and specifications of those items which interface with the customer and the programmer. Being different doesn't buy us anything . . . and it certainly doesn't buy the user anything. So we're standardizing on the de facto industry standards. However, the software products being designed around these standards employ RCA's own design concepts to obtain greater performance."

### EDP APPOINTS BRADBURN AS DIVISION VICE PRESIDENT

Appointment of **James R. Bradburn** as Division Vice President, RCA Electronic Data Processing, has been announced by **Arnold K. Weber**, Vice President and General Manager of EDP. Mr. Bradburn, who had been Vice President for Engineering and Manufacturing at the Burroughs Corporation, Detroit, Mich., has responsibility for special assignments in electronic data processing. His office is at EDP headquarters, Cherry Hill, N. J.

Mr. Bradburn holds a BSEE from the California Institute of Technology, and an MBA from Harvard. From 1941 to 1945 he served with U. S. Army Ordnance. He is a member of the IEEE and the Association for Computing Machinery. He worked for General Electric and Eastman Kodak before joining Consolidated Electrodynamics Corp., Pasadena, Calif., where he became Vice President of Sales and of Engineering. In 1953 he was named President of ElectroData Corporation, Consolidated's computer affiliate. ElectroData merged with Burroughs in 1956, and Mr. Bradburn subsequently became Vice President for Engineering and Manufacturing, and a Director of that corporation.

### MAGNETIC RECORDING SUBJECT OF CSD ENGINEERING LECTURES

The aerospace and defense magnetic recording reproducing field encompasses many technical disciplines, such as high data rate digital techniques, FM wideband techniques, precision electromechanisms, and DC motor design. Rigorous mission environments and high signal fidelity requirements make it imperative that engineers and technicians know as much as possible about these disciplines and their interdependency. Therefore, according to **Ellis Hudes**, Manager, Magnetic Recording Equipment Engineering, Communications Systems Division, Camden, a series of 11 lectures is being given for engineers and technicians in his activity.

The 2-hour lectures, prepared and presented by key engineering and management personnel within the activity, are scheduled on a one-per-week basis. Selective attendance is based on the mutual needs of the individuals and the section.

The lecture topics are: *Basic Recording Systems; Transport Systems; Functional Parameters Affecting Recorder Design; Electromechanical Elements of Recording Systems; Critical Recorder Subsystems; Digital Recording Systems; Design Criteria for Electrically Variable Delay Lines; Instrumentation for Radar Recording; DC Motors as Servo Members and Modifications for Continuous Video Recording; and Spectrum and Electron Beam Recording.*

### ERRATA

In the previous issue, Vol. 11, No. 3, Oct.-Nov. 1965, there are errors on page 3 of the article by Schnitzer on "Directory of RCA Environmental Test Facilities." At the top of Table 1, on page 3, the *Location Key* items ECD-2 and ECD-3 should be corrected as follows:

**ECD-2** is located in Lancaster, Pa. (not in Harrison) and it is Dept. 922 (not Bldg. 922).

**ECD-3** is located in Somerville, N. J. (not in Harrison) under J. E. Stolpman (not Stoltzman) and it is Dept. 900 (not 916).

## STAFF ANNOUNCEMENTS

**ECD Commercial Rec. Tube and S/C Division, Needham, Mass.:** The organization of Memory Products Engineering, reporting to **H. P. Lemaire**, Manager, Memory Products Eng., is announced as follows: **B. Frackiewicz**, Manager, Test Equipment and Measurements; **B. P. Kane**, Manager, Memory Systems Engineering; **A. C. Knowles**, Manager, Applications and Design Engineering-Devices; **E. A. Schwabe**, Mgr., Cores and Matls. Eng.; and **L. A. Wood**, Mgr., Memory Devices Eng.

**ECD Television Picture Tube Division, Lancaster, Pa.:** The organization of the Engineering Department, reporting to **C. W. Thierfelder**, Mgr., Eng. Department, is announced as follows: **D. D. Van Ormer**, Mgr., Color Picture Tube Eng.; **H. B. Law**, Dir., Matls. and Display Devices Lab., Princeton; **E. K. Madenford**, Admin., Eng. Administration; and **D. J. Ransom**, Mgr., Black and White Picture Tube Eng., Marion.

Reporting to Mr. Van Ormer are: **R. W. Hagmann**, Mgr., Application and Reliability Lab.; **W. J. Harrington**, Mgr., Development Shop; **A. M. Morrell**, Mgr., Design Lab.; and **R. H. Zachariason**, Mgr., Chemical and Physical Lab.

**ECD Industrial Tube and Semiconductor Division, Somerville, N.J.:** The organization of Industrial Semiconductor Eng., reporting to **J. Hilibrand**, Mgr., Eng., is announced as follows: **G. J. Andeskie**, Mgr., Transistor and Special Products Model Shop; **J. Hilibrand**, Acting Mgr., Rectifier Design and Applications; **K. E. Loofbourrow**, Resident Engr., Mountaintop; **C. R. Turner**, Mgr., Transistor Applications; **N. C. Turner**, Mgr., Transistor Design; and **D. Winans**, Admin., Eng. Administration.

**ECD Special Electronics Components Div., Harrison and Somerville, N.J.:** The organization of the Special Electronic Components Division, reporting to **L. R. Day**, General Mgr., Special Electronic Components Div., is announced as follows: **L. R. Day**, Acting Mgr., Direct Energy Conversion Department; **N. S. Freedman**, Mgr., Superconductive Products Operations Department; **B. A. Jacoby**, Mgr., Integrated Circuit Marketing Department; **R. L. Klem**, Mgr., Integrated Circuit Operations Department; and **R. D. Lohman**, Mgr., Advanced Integrated Circuit Applications and Technology.

The organization of the Direct Energy Conversion Department, under Mr. Day, is as follows: **F. G. Block**, Mgr., Thermionic Products Eng.; **L. J. Caprarola**, Mgr., Thermoelectric Products Eng.; and **P. P. Roudakoff**, Mgr., Direct Energy Conversion Marketing.

The organization of the Integrated Circuit Operations Department under Mr. Klem is announced as follows: **J. W. Ritcey**, Mgr., Integrated Circuit Eng.; **R. A. Wissolik**, Admin., Operations Planning; and **E. M. Troy**, Mgr., Integrated Circuit Products Manufacturing.

Reporting to Mr. Ritcey are: **I. H. Kalish**, Mgr., Design; **B. V. Vonderschmitt**, Mgr., Applications; **F. M. Yates**, Admin., Eng. Projects; and **M. Zanakos**, Mgr., Integrated Circuit Model Shop.

Reporting to Mr. Troy are: **H. L. Eberly**, Mgr., Manufacturing; **L. P. Fox**, Mgr., Production Eng.; **L. P. Garner**, Staff Engineer; **R. R. Giordano**, Mgr., Production and Matl. Control; and **P. Greenberg**, Mgr., Quality and Reliability Assurance.

**Corporate Staff, New York:** **H. W. Phillips** is appointed Manager, Special Computer Systems Projects. In this capacity, Mr. Phillips will be responsible for directing the

implementation, programming and operation of special computer systems projects, such as Operation Ballot. Mr. Phillips will report to **A. L. Malcarney**, Group Executive Vice President.

Mr. Phillips staff is: **L. Dinner**, Mgr., Systems Operations and Contrl; **A. A. Katz**, Mgr., Advanced Systems Analysis and Development; **H. K. Land**, Mgr., Integrated Software Systems and Programming; **H. W. Phillips**, Acting Admin., Hardware Systems Eng. and Implementation; and **A. Posner**, Mgr., Administration and Computer Services.

**DEP Defense Engineering, Camden:** **Dr. Leopold Pessel** formerly connected with Central Engineering, DEP, is now on special assignment, reporting to **Dr. H. J. Watters**, Division Vice President, Defense Engineering. His available consulting assistance covers a wide range of materials science and materials engineering. His principal activities in the past have been in the fields of joint formation technology (chemistry and metallurgy of soldering, brazing, welding, etc.) surface phenomena and treatments (films, corrosion, etc.) solid state phenomena, etc. He can be reached at RCA Camden, Bldg. 8-2-2, extension PC 5450.

**DEP Communications Systems Division, Camden:** **C. K. Law** is appointed Manager, Product Engineering, Camden, reporting to **D. Shore**, Chief Engineer, Eng. Department.

**New Business Programs, Princeton, N.J.:** The New Business Programs organization, reporting to **F. H. Erdman**, Division Vice President, New Business Programs, is announced as follows: **N. R. Amberg**, Mgr., Industrial and Automation Products Department (Detroit); **R. W. Horn**, Mgr., New Projects; **L. F. Jones**, Mgr., Eng.; **R. A. Mahler**, Mgr., Business Analysis; and **A. F. McIntyre**, Mgr., Financial Analysis.

## ... PROMOTIONS ...

### to Engineering Leader & Manager

As reported by your Personnel Activity during the past two months. Location and new supervisor appear in parentheses.

#### DEP Astro-Electronics Division

- S. Halpern**: from Sr. Engr. to *Ldr.*, Engrs. (J. Kimmel, AED, Princeton)
- R. R. Scott**: from Engr. to *Ldr.*, Engrs. (G. Barna, AED, Princeton)
- R. D. Wilkes**: from Engr. to *Ldr.*, Engrs. (G. Barna, AED, Princeton)
- W. L. Cable**: from *Ldr.*, Engrs. to *Mgr.*, *Tape Recorders and Electronic Packaging* (R. B. Marsten, AED, Princeton)
- J. J. Dishler**: from Sr. Engr. to *Ldr.*, Engrs. (M. H. Mesner, AED, Princeton)
- A. A. Garman**: from Sr. Engr. to *Mgr.*, *Spacecraft Tests* (A. J. Vaughan, AED, Princeton)
- H. Hamer**: from Sr. Engr. to *Ldr.*, Engrs. (R. T. Callais, AED, Princeton)
- H. C. Lawrence**: from Sr. Engr. to *Mgr.*, *Data Transmission* (R. B. Marsten, AED, Princeton)
- D. J. Mager**: from *Ldr.*, Engrs. to *Mgr.*, *Space Power* (G. Barna, AED, Princeton)
- K. M. Stoll**: from Mgr. Tech. Advisory Staff to *Admin.*, *Value Analysis* (N. M. Brooks, AED, Princeton)
- H. Toegel**: from Engr. to *Ldr.*, Engrs. (W. L. Cable, AED, Princeton)
- L. P. Yermack**: from Assoc. Engr. to *Mgr.*, *OGO/TWTA Equipment Projects* (C. S. Constantino, AED, Princeton)

#### DEP Missile & Surface Radar Division

- L. J. Schipper**: from Engr. to *Ldr.*, *Systems Eng.* (W. V. Goodwin, Moorestown)
- N. M. Some**: from Engr. to *Ldr.*, *D & D Engrs.* (E. T. Hatcher, Moorestown)
- P. J. Dwyer**: from Admin., Program Administration to Mgr. of Engineering Administration (W. Frysztacki, Moorestown)

#### DEP Staff

- I. Maron**: from Engr. to *Ldr.*, *SEER* (S. N. Mills, Moorestown)

#### DEP Aerospace Systems Division

- D. M. Larson**: from Sr. Project Mbr., Tech. Staff to *Ldr.*, *Tech. Staff* (C. E. O'Toole, Eng. Support and Control, Burl.)
- S. V. Piccirillo**: from *Ldr.*, Tech. Staff to *Mgr.*, *Stab. & Cont. Eng.* (S. Kolodkin, Guidance & Control Eng., Burl.)

#### Electronic Components & Devices

- R. H. Godfrey**: from Sr. Engr., Product Dev. to *Eng. Ldr.*, *Product Dev.* (Mgr., Color Picture Tube Design Lab., Lancaster)
- A. M. Morrell**: from Engr. *Ldr.*, Product Dev. to *Mgr.*, *Color Picture Tube Design Lab.* (Mgr., Color Picture Tube Eng., Lancaster)
- F. VanHecken**: from Sr. Engr., Product Dev. to *Eng. Ldr.*, *Product Dev.* (Mgr., Color Picture Tube Design Lab., Lanc.)
- D. D. VanOrmer**: from Mgr., Color Picture Tube Dev. to *Mgr.*, *Color Picture Tube Eng.* (Mgr., Eng. Department, Lanc.)
- L. F. Hopen**: from Mgr., Process and Production Eng. to *Mgr.*, *Tube Manufacturing*

(S. M. Hartman, Mgr., Marion)

- A. M. Trax**: from Sr. Engr., Product Dev. to *Mgr.*, *Process and Production Eng.* (L. F. Hopen, Mgr., Tube Manufacturing, Marion)

#### RCA Communications, Inc.

- I. A. Cohen**: from Design Engr. to *Group Ldr.* (Vice Pres. and Chief Engr., New York)

#### RCA Service Company

- W. A. Bakker**: from Engr., Facilities to *Ldr.*, *Engrs.*, *BMEWS* (J. H. Leitholf, BMEWS, New York)
- G. H. Shuey, Jr.**: from Sys. Service Engr. to *Mgr.*, *AFWR Systems Integration Contract* (E. VanDuyne, Atlantic Fleet Weapons Range)
- J. R. Moore**: from Ship Instrumentation Engr. to *Mgr.*, *Radar-Shipboard* (L. F. Dodson, MTP, Cocoa Beach, Fla.)
- A. F. Penfield**: from Sr. Field Support Engr. to *Ldr.*, *Field Support Engrs.* (G. M. Berube, MTP, Cocoa Beach, Fla.)
- L. E. Marshall**: from Engr., Facilities to *Ldr.*, *Engrs.*, *BMEWS* (R. D. Newton, BMEWS, Site I Tech. Contract)
- C. J. Thompson**: from Engr. to *Ldr.*, *Engrs.* (E. D. VanDuyne, Field Eng., Eastern Area, Government Service)

#### RCA Victor Home Instruments

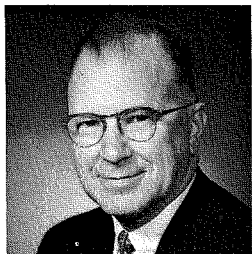
- R. K. Lockhart**: from Mgr., Advanced Digital Techniques, Camden, to *Mgr.*, *New Products Eng.* (R. Rhodes, Indpls.)

**NEW ED REPS: STOCKER FOR SEER,  
AND ELLIS FOR WCD**

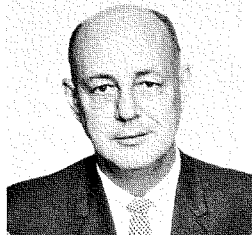
The RCA ENGINEER welcomes two new Editorial Representatives: **A. C. Stocker** has been named as Ed Rep for the DEP Systems Engineering, Evaluation, and Research (SEER) activity located in Moorestown, N. J. He replaces **R. R. Shively**. (The SEER activity is part of DEP Staff Defense Engineering.) **R. J. Ellis** has been named Ed Rep for the DEP West Coast Division, Van Nuys, California. He replaces **S. Hersh**. Both will serve as members of the DEP Editorial Board, of which **Frank Whitmore**, DEP Technical Publications Administrator, is Chairman.

**A. C. Stocker** received his BEE at Ohio State University in 1928, and immediately joined GE at Schenectady. He was transferred to Camden on the formation of RCA's manufacturing division in 1930. He has a long experience in the synthesis of new systems, having been active in television in 1929, frequency synthesis in 1939, air traffic control in 1947, and reconnaissance satellites in 1956. He spent five years on active duty with the Navy during the war, gaining experience in installation at a Navy Yard, in operations with an amphibious force, and in afloat maintenance in the Pacific. After the war he returned to RCA, joining what is now Applied Research. Here he worked on a number of studies, usually in the field of information handling. He now acts as the specialist in display techniques in the Human Factors group in systems Engineering, Evaluation and Research, DEP.

**Robert J. Ellis** received his education as a business administration major at Columbia University and as an English major at Syracuse University. Electronics knowledge was acquired by graduation from Capital Radio Engineering Institute. Additional education has been in the form of various symposiums and present law studies for a LL.B. Mr. Ellis has had more than twenty years experience in all areas of integrated logistic support. These areas include technical publications, provisioning, field support, data management, reproduction and supply support. Mr. Ellis also has extensive value engineering experience. At RCA West Coast Division, Mr. Ellis is Manager of Publications Engineering which includes preparation and production of technical publications, proposals, brochures, presentations, reports, and all similar documentation. He also is responsible for all reproduction services including microfilm, drawing vault files, and drawing distribution.



A. C. Stocker



R. J. Ellis

**PROFESSIONAL ACTIVITIES**

*ECD, Lancaster, Pa.:* **H. R. Krall** attended and presented a paper entitled "New Photomultiplier for Pulse Counting" at the Twelfth Nuclear Science Symposium held Oct. 18-20, 1965, in San Francisco. **R. D. Faulkner** and **D. L. Hanes** attended the American Vacuum Society Symposium on Thin Films held in New York City, Sept. 30-Oct. 1965. **M. N. Slater** attended on Sept. 16, 1965, the National Association of Corrosion Engineers Symp. on High Purity Water, held in Syracuse, N. Y.—*R. Kauffman*

*ECD, Somerville, N. J.:* **Bob Gold**, Industrial Transistor Applications, is teaching an after hour course in Somerville, N. J., entitled "Transistor Applications." The class includes both transistor device design engineers and vacuum tube design and applications engineers. The course uses Volumes 3, 4, and 5 in the MIT SEEC (Semiconductor Engineering Education Committee) series, and is intended to provide a basic understanding of transistor characteristics and circuit applications.—*E. F. Breniak*

*RCA Communications, Inc., N. Y.:* **J. M. Walsh** has been appointed as Meetings Coordinator for the Communications Technology Group for the March 1966 IEEE International Convention in New York City, New York. **Maurice Cha Fong**, RCA Communications, Inc., was awarded a David Sarnoff Fellowship to continue his studies on a full time basis. He will study at Brooklyn Polytechnic Institute. **James C. Hepburn**, RCA Communications, Inc., was named Chairman of the Long Island Chapter of the IEEE Technical Group on Communications Technology.—*C. F. Frost*

*DEP-MSR, Moorestown, N. J.:* **Frank Klawnsnik**, Manager, Advanced Microwave Technology participated as a member of a selected panel of leading authorities on Microwave Component Needs for Communications Systems at a Conference sponsored by NEREM and EIA in Boston on November 4, 1965.

*DEP-AED, Princeton, N. J.:* **H. M. Gurin**, Staff Engineer for the Astro-Electronics Division, was appointed Associate Editor for Engineering Notes, for the *Journal of Spacecraft and Rockets* (AIAA).—*J. Phillips*

*DEP Central Engineering, Camden, N. J.:* **M. S. Gokhale** participated in an educational conference and seminar sponsored jointly by the United Nations and Danish Government at Elsinore near Copenhagen from October 18 to 22, 1965, for the purpose of promoting industrial standardization in the developing countries; 29 countries from Africa, South-East Asia, Middle-East and Latin America participated.—*J. J. Lamb*

*DEP-CSD, Systems Lab., New York:* **Dr. W. Y. Pan**, Manager, Adv. Solid-State Techniques, was elected the President of the Chinese Institute of Engineers. He presided at the 1965 Convention in the Waldorf Astoria Hotel on November 6, 1965. **P. Schneider**, Manager, Adv. Ckt. Switching Systems and Techniques, has been named to the

Communications Switching Committee of the IEEE for the coming year. **Dr. F. A. Assadourian**, Senior Staff Scientist, N. Y. Systems Lab., is teaching a course, "Modulation Theory," at the Graduate School of the Newark College of Engineering. He has been given the title of Adjunct Professor.—*M. P. Rosenthal*

*DEP-CSD, Camden, N. J.:* **P. M. Stallings**, Director of Audio-Visual Photographic Presentations, was elected President of the Society of Cinema Arts and Sciences. The society is composed of film producers from television, industry, commercial houses, government and institutions. The purpose is to advance the state of the art of film production through publication, exhibition, and discussion. **J. Neubauer**, Engineering Mgr., was elected National Chairman for 1965-1966 IEEE Vehicular Communications Group (VCG).

**Franklin H. Fowler** set some sort of a record (in addition to receiving a citation) for the number of reviews in one issue of *Computing Reviews*, a journal of the Association for Computing Machinery. He has five reviews of books and papers in the fields of operations research and switching theory in the March-April issue. He has been an ACM reviewer for one year. **Thomas P. Cunningham** is President, Phila. Chapter Armed Forces Communications and Electronics Association.—*C. W. Fields*

*RCA Service Co., Missile Test Project, Cape Kennedy, Fla.:* Three members of the RCA Service Company's Missile Test Project were featured on the program of the 1965 IEEE International Space Electronics Symp. in Miami Beach Nov. 2-4, 1965. Project Manager **G. Denton Clark** and **C. R. Scott**, Manager of Data Processing, served as Chairman of the Ground Support Equipment and Data Processing Sessions respectively. During the Data Processing session, **T. T. Williams** (of Systems Analysis) presented "Calibration of Radar for Signature Data Processing." Six MTP members were key participants in the First Annual Instrumentation Conference of the Instrument Society of America's (ISA) Canaveral Section on October 27-28, 1965, Cocoa Beach, Florida. **C. R. Scott**, Manager of MTP Data Processing and also Vice President of the ISA Camembers of Data Processing also presented papers during the session: **W. J. Kirklin**, "Process on Demand Computer System"; **C. W. Welch**, "GLAD—The Analytic Data Processing Tool of the Glotrac Tracking System"; and **E. L. Hedman** and **A. L. LeDuc**, "Post-Digitized Processing of TITAN 3 Telemetry." A fourth RCA-authored paper was presented during the Sensor and Instrumentation session by **Eugene Kelsey** of the Precision Measurement Equipment Laboratory, titled "An Accurate Method of Calibrating Audio Frequency Watt Meters."—*T. L. Elliott*

*DEP-ASD, Burlington, Mass.:* **I. Drew** is a member of the EIA Subcommittee MCA2 on "Electrical Characteristics of Microelectronic Circuit Applications," he is also Chairman of a Task Group to define and characterize analog integrated circuits. **E. W. Richter** is Chairman of the IEEE-GMTT Chapter in Boston. **R. C. Miller** is serving as Vice Chairman of the Greater Boston Chapter of the Association for Computing Machinery. **H. Eckhardt** is Director of the New England AIAA Section.—*D. Dobson*

**DEGREES GRANTED**

- P. Goodwin**, DEP-AED .....MSEE, Univ. of Pennsylvania
- Dr. H. Weinstein**, RCA Labs .....Ph.D., EE, Polytechnic Institute of Brooklyn
- A. A. Litwak**, DEP-AppRes .....MSME, Drexel Institute of Technology
- V. J. Nardone**, ECD .....MS, Physics, Wilkes College
- J. V. Yonushka**, ECD .....MSEE, University of Pennsylvania

## Editorial Representatives

The Editorial Representative in your group is the one you should contact in scheduling technical papers and announcements of your professional activities.

### DEFENSE ELECTRONIC PRODUCTS

F. D. WHITMORE\* *Chairman, Editorial Board, Camden, N. J.*

#### Editorial Representatives

##### Aerospace Systems Division

D. B. DOBSON *Engineering, Burlington, Mass.*

##### West Coast Division

R. J. ELLIS *Engineering, Van Nuys, Calif.*

##### Astro-Electronics Division

J. PHILLIPS *Equipment Engineering, Princeton, N. J.*

I. SEIDEMAN *Advanced Development and Research, Princeton, N. J.*

##### Missile & Surface Radar Division

T. G. GREENE *Engineering Dept., Moorestown, N. J.*

##### Communications Systems Division

C. W. FIELDS *Engineering, Camden, N. J.*

H. GOODMAN *Engineering, Camden, N. J.*

M. P. ROSENTHAL *Systems Labs., New York, N. Y.*

##### Defense Engineering

J. J. LAMB *Central Engineering, Camden, N. J.*

M. G. PIETZ *Applied Research, Camden, N. J.*

A. C. STOCKER *Systems Engineering, Evaluation, and Research, Moorestown, N. J.*

### BROADCAST AND COMMUNICATIONS PRODUCTS DIVISION

D. R. PRATT\* *Chairman, Editorial Board, Camden, N. J.*

#### Editorial Representatives

C. E. HITTLE *Closed Circuit TV & Film Recording Dept., Burbank, Calif.*

R. N. HURST *Studio, Recording, & Scientific Equip. Engineering, Camden, N. J.*

D. G. HYMAS *Microwave Engineering, Camden, N. J.*

W. J. SWEGER *Mobile Communications Engineering, Meadow Lands, Pa.*

R. E. WINN *Brdcst. Transmitter & Antenna Eng., Gibbsboro, N. J.*

### NEW BUSINESS PROGRAMS

N. AMBERG *Industrial & Automation Products Engineering, Plymouth, Mich.*

### ELECTRONIC DATA PROCESSING

H. H. SPENCER\* *EDP Engineering, Camden, N. J.*

R. R. HEMP *Palm Beach Engineering, West Palm Beach, Fla.*

B. SINGER *Data Communications Engineering, Camden, N. J.*

### GRAPHIC SYSTEMS DIVISION

DR. H. N. CROOKS *Engineering, Princeton, N. J.*

### RCA LABORATORIES

C. W. SALL\* *Research, Princeton, N. J.*

### RCA VICTOR COMPANY, LTD.

H. J. RUSSELL\* *Research & Eng., Montreal, Canada*

### ELECTRONIC COMPONENTS AND DEVICES

C. A. MEYER\* *Chairman, Editorial Board, Harrison, N. J.*

#### Editorial Representatives

##### Commercial Receiving Tube & Semiconductor Division

P. L. FARINA *Commercial Receiving Tube and Semiconductor Engineering, Somerville, N. J.*

J. KOFF *Receiving Tube Operations, Woodbridge, N. J.*

L. THOMAS *Memory Products Dept., Needham and Natick, Mass.*

R. J. MASON *Receiving Tube Operations, Cincinnati, Ohio*

J. D. YOUNG *Semiconductor Operations, Findlay, Ohio*

##### Television Picture Tube Division

J. H. LIPSCOMBE *Television Picture Tube Operations, Marion, Ind.*

E. K. MADENFORD *Television Picture Tube Operations, Lancaster, Pa.*

##### Industrial Tube & Semiconductor Division

E. F. BRENIAK *Industrial Semiconductor Engineering, Somerville, N. J.*

R. L. KAUFFMAN *Conversion Tube Operations, Lancaster, Pa.*

K. LOOFBURROW *Semiconductor and Conversion Tube Operations, Mountaintop, Pa.*

G. G. THOMAS *Power Tube Operations and Operations Svcs., Lancaster, Pa.*

H. J. WOLKSTEIN *Microwave Tube Operations, Harrison, N. J.*

##### Special Electronic Components Division

R. C. FORTIN *Direct Energy Conversion Dept., Harrison, N. J.*

I. H. KALISH *Integrated Circuit Dept., Somerville, N. J.*

##### Technical Programs

D. H. WAMSLEY *Engineering, Harrison, N. J.*

### RCA VICTOR HOME INSTRUMENTS

K. A. CHITTICK\* *Chairman, Editorial Board, Indianapolis, Ind.*

#### Editorial Representatives

J. J. ARMSTRONG *Resident Eng., Bloomington, Ind.*

D. J. CARLSON *Advanced Devel., Indianapolis, Ind.*

R. C. GRAHAM *Radio "Victrola" Product Eng., Indianapolis, Ind.*

P. G. McCABE *TV Product Eng., Indianapolis, Ind.*

J. OSMAN *Electromech. Product Eng., Indianapolis, Ind.*

L. R. WOLTER *TV Product Eng., Indianapolis, Ind.*

### RCA SERVICE COMPANY

M. G. GANDER\* *Cherry Hill, N. J.*

B. AARONT *EDP Svc. Dept., Cherry Hill, N. J.*

W. W. COOK *Consumer Products Svc. Dept., Cherry Hill, N. J.*

E. STANKO *Tech. Products Svc. Dept., Cherry Hill, N. J.*

T. L. ELLIOTT, JR. *Missile Test Project, Cape Kennedy, Fla.*

L. H. FETTER *Govt. Svc. Dept., Cherry Hill, N. J.*

### RCA COMMUNICATIONS, INC.

C. F. FROST\* *RCA Communications, Inc., New York, N. Y.*

### RCA VICTOR RECORD DIVISION

M. L. WHITEHURST *Record Eng., Indianapolis, Ind.*

### NATIONAL BROADCASTING COMPANY, INC.

W. A. HOWARD\* *Staff Eng., New York, N. Y.*

### RCA INTERNATIONAL DIVISION

L. A. SHOTLIFF\* *New York City, N. Y.*